THE STUDY OF THE EFFECTS OF FLAVANOID DERIVATIVES AS CORROSION INHIBITORS FOR ZINC AND ALUMINIUM METALS IN SULPHURIC AND HYDROCHLORIC ACIDS

TSHEDZA SITHUBA

(15003455)

A dissertation submitted in the fulfilment of the requirements of the Master of science in the

Department of Chemistry

Faculty of Mathematical and Natural Sciences

University of Venda

Supervisor: Dr L.C. Murulana, PhD

Co-Supervisor: S.J. Moema, MSc

February 2021

DECLARATION

I Tshedza Sithuba declare that this dissertation titled ''The study of the effects of flavonoid derivatives as corrosion inhibitors for zinc and aluminium in sulphuric and hydrochloric acids'' is the results of a study carried out originally by me under the guidance and supervision of Dr L.C. Murulana and Mr S.J. Moema as my co-supervisor. This work is being submitted in fulfilment of Master of Science degree in chemistry at the University of Venda and has not been submitted to any university for any degree and examination. Information that I have collected from secondary sources have been properly acknowledged in the reference pages.

Signature: 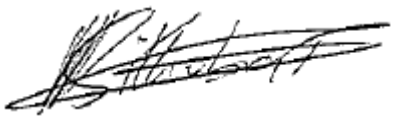 Date: 12/02/2021

Tshedza Sithuba

TABLE OF CONTENTS

ACKNOWLEDGEMENTS

Firstly, I would like to thank God the Almighty whom without His grace it was not going to be possible for me to complete this dissertation.

I extend my heartful thanks and my sincere appreciation to my supervisor Dr L.C. Murulana who was instrumental in introducing me to this research and helping me throughout all the phases of this work as well as providing guidance and insight during the completion of this dissertation.

I would also like to thank my co-supervisor Mr S.J. Moema from MINTEK who helped me a lot with surface characterization using 2D and 3D microscopes. He also made it possible for me to spend some time at MINTEK. I also would like to thank Mrs N.D. Masia for providing me with training on the use of the microscopes.

I also thank the University of Venda community at large, for gracing me with a wonderful lifetime opportunity to pursue my studies with them. Without University of Venda this work was not going to be possible.

Lastly but definitely not the least, I would also like to thank my mom and family for their encouragements and support they showed to me throughout this journey.

ABSTRACT

In this study, the corrosion inhibition potentials of three flavonoid derivatives namely Naringenin (NRNG), Morin hydrate (MNHD) and 6-Hydroxyflavone (6-HFN) for zinc and aluminium metals was investigated using gravimetric analysis, electrochemistry, and surface characterization techniques in three aggressive acidic environments of 0.5 M and 1.5 M hydrochloric acid and 1.5 M sulphuric acid at a temperature range from 30 – 60°C. All the three inhibitors managed to inhibit the corrosion of zinc and aluminium metals from the acid attack by adsorption of their molecules onto the metals surface. The adsorption of the inhibitors onto the zinc metals was found to be both physisorption and chemisorption. However, in the presence of aluminium metals, the inhibitors were found to adsorb through physisorption only. The experimental data obtained from gravimetric analysis obeys Langmuir adsorption isotherms. Atomic Absorption Spectroscopy (AAS) was used to find the concentration of the metal ions leached into the solution after gravimetric analysis in the absence and presence of the inhibitors. The lowest concentration was obtained when the three inhibitors were used in the presence of sulphuric acid in zinc, which suggest that the inhibitors managed to inhibit the metal dissolution to a much greater extent as compared to when the acid was used alone. Fourier Transform Infrared Spectroscopy (FTIR) was utilised to understand the functional groups that disappeared or formed during the adsorption process of the inhibitor's molecules on the metals surface. The Ar - OH functional group was the worst affected since only 6-hydroxyflavone was the only inhibitor to retain it after gravimetric analysis in the presence of hydrochloric acid. The C=C functional group of the aromatic ring was retained by all the inhibitors in all the metals studied. A two-dimensional (2D) and three-dimensional (3D) microscopy was also used to study the extent to which the metals were damaged by the acid and the type of corrosion that resulted thereafter, in the absence and presence of the three inhibitors. The results obtained from Potentiodynamic Polarization (PDP) indicated that the compounds are mixed-type inhibitors. The results from PDP also indicated that the use of three flavonoid derivatives compounds as corrosion inhibitors managed to significantly reduce the corrosion current densities for the cathodic and anodic half reactions, which indicate that, the dissolution and cathodic reduction of the hydrogen ions were inhibited. The order of the inhibition efficiency at $1.8x10^{-3}$ M for the maximum temperature (60°C) was 6-HFN (86.54 and 77.24 %) > MNHD (81.37 and 73.30 %) > NRNG (78.07 and 72.47 %) for zinc metals in sulphuric acid and hydrochloric acid, and NRNG (91.48) > 6-HFN (90.12) > MNHD (81.59) for aluminium metals in hydrochloric acid. In Electrochemical Impedance Spectroscopy (EIS), the charge transfer resistance increased with an increase in inhibitors concentration, while the constant phase element was found to decrease with an increase in inhibitors concentration. This observation is an indication that the inhibitors adsorbed onto the metal surface

and formed a film layer protecting the metal from corrosion. The percentage inhibition efficiency of Electrochemical Impedance Spectroscopy ($\%IE_{EIS}$) was found to correlate with those obtained from PDP, AAS and gravimetric measurements.

LIST OF ABBREVIATIONS

HCl	Hydrochloric acid
H_2SO_4	Sulphuric acid
IUPAC	International Union of Pure and Applied Chemistry
REDOX	Reduction and Oxidation
VLC's	Volatile Corrosion Inhibitors
IMPACT	International Measures of prevention, Application and Economic Corrosion Technology
ASTM	American Society for Testing and Material
TNT	Trinitrotoluene
FTIR	Fourier Transform Infrared Spectroscopy
PDP	Potentiodynamic Polarization
CE	Counter Electrode
RE	Reference Electrode
WE	Working Electrode
AAS	Atomic Absorption Spectroscopy
EIS	Electrochemical Impedance Spectroscopy
2D	Two dimensional
3D	Three dimensional
NRNG	Naringenin
MNHD	Morin hydrate
6-HFN	6-Hydroxyflavone
%IE	Percentage inhibition efficiency
NACE	National Association of Corrosion Engineers

MINTEK	Council for Mineral Technology
SCE	Standard Calomel Electrode
GDP	Gross Domestic Product
RSA	Republic of South Africa
USA	United States of America
UK	United Kingdom
FAAS	Flame Atomic Absorption Spectroscopy
GFAAS	Graphite Furnace Atomic Absorption Spectroscopy

LIST OF FIGURES

No. **DESCRIPTION** **PAGE**

LIST OF TABLES

No. **DESCRIPTION** **PAGE**

CHAPTER 1

INTRODUCTION

1.1 Background of the study

Since metals discovery, the technical progress, the quality of daily lives of people and the time to carry out some tasks was affected by corrosion [1]. A number of corrosion researches have been done in the past to try to combat its lineage. To date, the human generation is still tormented by this old enemy of their progress. Although corrosion is a nightmare to humans, it brings justice to the environment since it happens to return modified substances into their original natural state. Corrosion has been defined in many ways, but it is widely described as the metal deterioration by means of electrochemical and chemicals reaction on its environment [2].

Metals and alloys which are the backbone of industries often act in such a manner that forces a change in them into their more preferred stable or fixed oxidized state such as oxides, hydroxides, or sulphides. This happens because metals in their manufactured free state are thermodynamically unstable as compared to their combined states in which they occur naturally. This behaviour causes these metals and alloys to undergo various chemical reactions in virous environmental conditions (including marine and atmospheric conditions) such as vapour or gases, water, moisture, and electrolytes, amongst others, resulting in their deterioration or corrosion [3]. Therefore, corrosion is an enormous problem for most industries. With its severe damages, corrosion cannot be prevented, but several strategies can be used to control it. Such strategies include coating, painting, and the use of corrosion inhibitors. The choice of the corrosion prevention strategy relies on the environmental conditions and the nature of the metal.

This research project will be focusing on using corrosion inhibitors to minimize or control zinc and aluminium metals corrosion. Based on the National Association of Corrosion Engineers (NACE), corrosion inhibitors are chemicals and materials that retards corrosion after being in coalesce with the environment in small concentrations [4]. The inhibitors utilised to preserve metals must be able to adsorb onto the surface of the metal and delay the corrosion caused by the corrosive environment. The application of chemical substances as corrosion inhibitors is believed to be as early as the Roman civilization. However, a scientific research started relatively late in 1870s. A detailed timeline about the important occasions in the development of corrosion science and inhibitors could be seen in Sastri's work [5]. These corrosion inhibitors are categorised as inorganic or organic chemicals that work by providing a thin film layer of protection on the metal surface. Between the two types of inhibitors, inorganic once such as phosphates, molybdates, and chromate are no longer of high regards since they are toxic and pose environmental threats. Nowadays organic corrosion inhibitors are the most preferred inhibitors because of their minimal environmental effects.

Not every organic compound qualifies as an inhibitor since several requirements such as high efficiency at low concentrations, good thermal stability, low water solubility, effectiveness over a broad pH range, ease of addition, little or no interactions with other components of the coating and the presence of heteroatoms must be met [6]. Heteroatoms on the compounds increase their polarity which then allows the compounds to act as surfactants in aqueous solutions. Organic compounds with a large molecular weight are also effective as corrosion inhibitors. Polymeric coatings are also used as the most widely and common approach for shielding metals from corrosion. These coatings are known to supply an intense barrier against the diffusion of electrolytes, water and oxygen thereby preventing the access of aggressive corrosive species to the surface of the metal. However, the barrier formed by coatings cannot prevent the spreading of corrosion process further in situation when the coating undergoes oxidation with atmospheric oxygen [7].

1.2 Justification of the Study

An uneven surface results when corrosion products on the corroding surface of the metal when the metal reacts with oxygen and water in the air which makes it difficult to regulate atmospheric corrosion process. This later leads to metal growing holes and even metal failure. When such happens, severe problems like environmental disasters, collapse of buildings, fires factory blasts and fires may occur [8,9]. Most corrosion cost studies show that a rapid increase in the cost of corrosion of many nations (e.g. RSA, USA, UK, etc.) has been felt since the beginning of industrialisation. Other studies show that the global direct cost of corrosion every year is between 3.1- 3.5 % of the annual worldwide GDP which is equivalent to 1.3 and 1.4 trillion Euros [10]. The council for mineral technology (MINTEK) embarked on similar study and showed that here in South Africa R130-billion per annum in 2004 was spent dealing with the cost and consequences of corrosion [11]. The ores from which these metals are extracted are being depleted by the continuous mining processes. With an increase in infrastructure development and industrialisation, metals are in very high demand to build, replace or repair damaged metal structures and soon, this could lead to global shortage of metals. Without proper studies about how to circumvent or control corrosion, drastic action cannot be taken to minimize the impact of corrosion. Because of this, lives will continue to be lost, the world economy will continue to be contrarily influenced and natural resources will eventually run out in the near future, all this because of corrosion. The significance of the corrosion process study as well as suitable prevention and control measures, therefore, cannot be undermined or taken for granted.

1.3 Scope of the Research Project

The scope of this research project covers the study of the corrosion inhibition potentials of flavonoids derivatives on aluminium and zinc metals in 1.5 M and 0.5 M of hydrochloric and 1.5 M sulphuric acids. The flavonoids derivatives used were procured from Sigma-Aldrich chemicals. The ability of these derivatives as corrosion inhibitors was studied using the gravimetric weight loss method, whereby the effects of concentration, immersion time, and temperature were determined. Atomic absorption spectroscopy was also used to find the amount of metal concentration left in solution after gravimetric analysis. Surface analysis techniques such as Fourier transform infrared spectroscopy and 2D and, 3D optical microscopy was also applied on the metals after gravimetric analysis was performed. The electrochemical techniques such as PDP and EIS were also applied to help give the insight on the adsorption mechanism of the inhibitors on zinc and aluminium metals.

1.4 Problem Statement

Most of the ores from which most of our famous and preferred metals for industrial activities are produced are obtained through mining activities. When metals are produced from these ores, a very high amount of energy input is required [12], and energy is a very expensive commodity as seen from the power cuts that we sometimes experience in South Africa. Most of the energy (electricity) in South Africa comes from the use of coals obtained through industrial activities. These precious ores from which the metals are extracted, and the coal used for supplying enough energy for metals production are being depleted from the on-going mining processes. Also, a very large amount of carbon dioxide is released onto the atmosphere in the process of metal production, posing environmental health hazard. The problem is that these metals are unable to remain in their metallic manufactured state after being exposed to atmospheric environments. They are unable to withstand acids and bases attacks and as a direct repercussion, they recourse to their metal oxides [13]. As time goes on, with the high demand of metals to replace and repair damaged metal structures, it is most likely that in the near future there will be worldwide shortage of metals.

The only way to minimize the severe corrosion impact is through the proper experimentations and research that will help us to understand more about it. There is an urgent demand to find ways of preserving and protecting these metals from corroding back to their chemical stable state, as once the ores are modified into metals, they become chemically unstable. Below are some of the problems or consequences that can be encountered because of corrosion.

- Corrosion has a great threat to human health and safety. Bridges and building collapse, industrial failures and aircraft malfunctions are some of the corrosion related disasters which

can lead to human death tragedies. Some metals when corroding release rusts which can be dangerous and toxic to human beings, for example, iron release iron oxide when corroded.

- The global economy trembles on the corrosion account. The direct cost of corrosion worldwide which does not include waste of resources, personal injuries by corrosion and environmental damages is estimated to be between 3.1 to 3.5 % of annual worldwide gross domestic products (GDP) approximately 1.3 and 1.4 trillion euros [9].
- This corrosion also has negative impact on the environment, from the study undertaken by MINTEK, most of the steels that are being manufactured are being done so to replace the damaged ones. Normally these metals are made from ores which some are being obtained through the process of mining. Continuous mining of these precious ores might end up in their depletion. The process through which these metals are made release a very huge amount of carbon dioxide in the atmosphere, destroying the ozone layer which can lead to changes in climate conditions resulting in drought.

1.5 Aim and Objectives of the Research Project

The main aim of this research project is to use flavonoid derivatives [6-hydroxyflavone, 2-(2,4-dihydroxyphenyl)-3,5,7-trihydroxy-4H-chromen-4-one hydrate (Morin hydrate) and 5,7-dihydroxy-2-(4-hydroxyphenyl) chroman-4-one (Naringenin)] to investigate their inhibition potential on two metals, namely zinc and aluminium in aqueous hydrochloric and sulphuric acids medium.

The specific objectives of this research project are:

1. To examine the rate of corrosion of two metals, zinc and aluminium, in corrosive acidic environments.
2. To assess the inhibition efficiency of flavonoids derivatives in zinc and aluminium metals in aqueous aggressive environment by gravimetric weight loss analysis at different temperatures, concentration of the inhibitors and the time of exposure.
3. To propose the type of mechanism, adsorption, and adsorption isotherm for corrosion inhibition.
4. To use Atomic Adsorption Spectroscopy (AAS) to find the amount of metal ions left in solution after gravimetric analysis in the absence and presence of the flavonoids inhibitors.
5. To use Fourier Transform Infrared Spectrometry (FTIR) in order to determine the mode of interfacial reactions and the functional groups which interacted between the compound and the metal surface.
6. To use 2D and 3D optical microscopy to find the type of corrosion which took place on the metal and to assess the corrosion damage.

7. To assess the interaction of the inhibitor with the metal surface by electrochemical techniques like Electrochemical Impedance Spectroscopy (EIS) and Potentiodynamic Polarization (PDP).

CHAPTER 2

LITERATURE REVIEW

2.1 Definition of Corrosion

The word corrosion historically was derived from the Latin word 'corrodere' which literally means "gnaw into pieces" and on a general tone the definition of corrosion could be something which eats or wears away gradually [14]. It is generally defined as a gradual deterioration of equipments by chemical or electrochemical reaction with the environment. This process happens to return metals in manufactured states back to their chemically stable natural oxidation states such as oxide, hydroxide, or sulphide. However, corrosion can be defined in several ways and the (IUPAC) international Union of pure and applied Chemistry define corrosion as an irreversible interfacial reaction of materials (which can be metals, polymer and ceremic) with its environment which leads in the dissolution into the materials or deterioration of the materials of a component of the environment. Figure 2.1 below shows the life cycle of metals which involves the corrosion process.

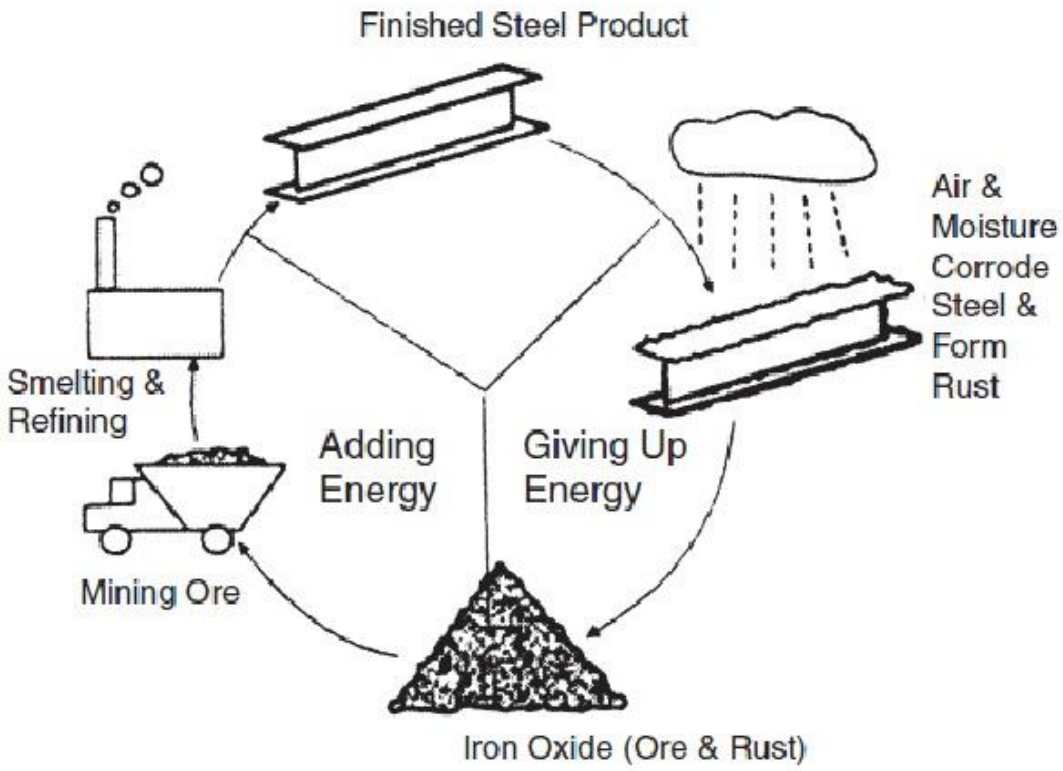

Figure 2.1: Life cycle of metals which involve the corrosion process [15]

Other texts define corrosion as the disintegration of the materials (metals or alloys) surface in a specific environmental condition [16]. Some metals have the ability to withstand aggressive conditions (show corrosion resistance) which may accelerate corrosion rate, there by contributing largely to the enhanced functional lifetime of a metal in use. several factors such as the nature of the electrochemical reactions and chemical constituents among others are attributed to why some metals

exhibits high corrosion resistance compared to others. The definition put forward by ISO 8044-1986 states that corrosion is a physicochemical interaction between a metal and its environment which leads in changes in the properties of the metal and may often lead to the deterioration of the functionality of the metal, the environment, or the technical system of which these form a part [17]. Another definition that virtually includes all materials in engineering and regarded as a very wide open definition support that corrosion can also results from the usage effects of the material considered, especially from physical and mechanical processes such as abrasion or mechanical fracture, melting or evaporation, but these are excluded in the definition of the term corrosion [18].

It is realised that the most commonly used definition of corrosion defines it as a gradual deterioration of equipment by chemical or electrochemical reaction with the environment.

2.1.1 Reactions during Metal Corrosion

Corrosion takes place through the chemical reaction called the reduction-oxidation (REDOX) reaction in which the metal is oxidized by its surrounding environment, which is often oxygen and air. This reaction requires a species of material that is oxidized (the metal), and another that is reduced (the oxidizing agent). In this case the complete reaction is divided into two partial reactions: one, oxidation and the other, reduction. In oxidation, the metal loses electrons and the zone in which this takes place is known as the anode. In reduction reaction, the metal gains electrons that have been shed by the metal and the zone in which this takes place is known as the cathode [19]. All the metals surface is believed to be covered by equal number of small anodes and cathodes sites and these sites are generally developed due to the following factors [20].

- Stress caused by welding or other works.
- irregularities of surface from production, extruding and other working operations of metals.
- Different compositional proportion at the metal surface.

Figure 2.2 below shows the model of electrochemical cell of reaction.

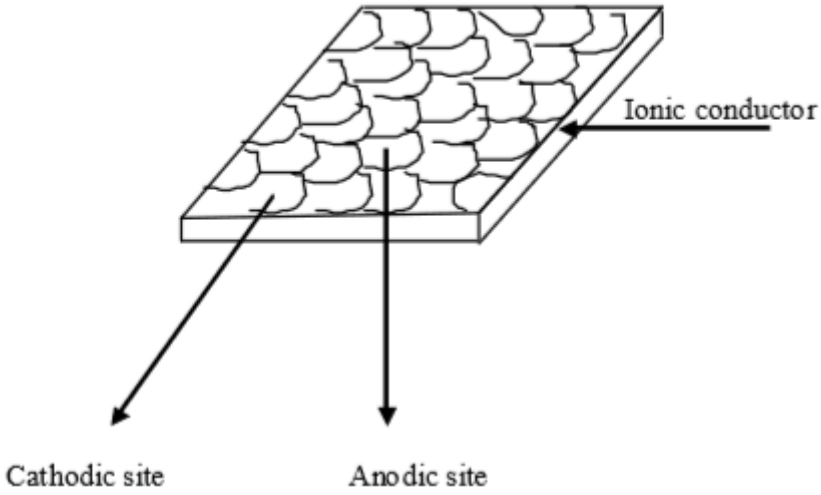

Figure 2.2: A model of electrochemical cell of corrosion [21].

A brief overview on the two partial reactions is provided in the sub-sections below.

2.1.1.1 Anodic Reaction

The anode in the electrochemical reaction, is the site of the electrode at which the metal loses electrons or corroded in the presence of the electrolyte which is the corrosive medium. At the anode, the positively charged ions of the metal, which is being corroded passes through the electrolyte, releasing electrons which take part in the cathodic reaction [22]. The released electrons become deposited on the cathodic electrode, and this process is known as oxidation.

As an example, when iron metal reacts with water and oxygen, a reduction-oxidation reaction takes place producing iron rust. In this reaction, iron metal is the anode which is where the metal gives up electrons thereby corroding in the process.

The anode half reaction can be written in the form of equation (1) bellow.

$$Fe_{(s)} \rightarrow Fe^{2+}{}_{(aq)} + 2e^{-} \quad (1)$$

2.1.1.2 Cathodic Reaction

In electrochemical reaction, the cathode is the site of the electrode where reduction reaction takes place. The cathode reaction plays a very important role in terms of establishment of the equilibrium of a corrosion system, that is to balance the anodic reaction. This causes the electrons that are generated in the oxidation half reaction at the anode to be consumed at the cathode surface [22].

As an example, in the same example of iron metal with oxygen and water, water acts as the cathode.

The cathodic half reaction occurs in the form of equation (2) as follows:

$$\frac{1}{2}O_{2\ (g)} + H_2O_{\ (l)} + 2e^- \rightarrow 2OH^-_{\ (aq)} \quad (2)$$

The overall reaction of the iron metal with water and oxygen which is the combination of the cathodic and anodic half reaction is written as in equation (3) bellow:

$$Fe_{(s)} + \frac{1}{2}O_{2\ (g)} + H_2O_{\ (l)} \rightarrow Fe^{2+}_{\ (aq)} + 2OH^-_{\ (aq)} \quad (3)$$

The above reaction (equation 3) can also be further written as equation (4) below.

$$Fe^{2+}_{\ (aq)} + 2OH^-_{\ (aq)} \rightarrow Fe(OH)_{2\ (aq)} \quad (4)$$

The corrosion processes taking place on iron surface can be detailed further schematically using Figure 2.3.

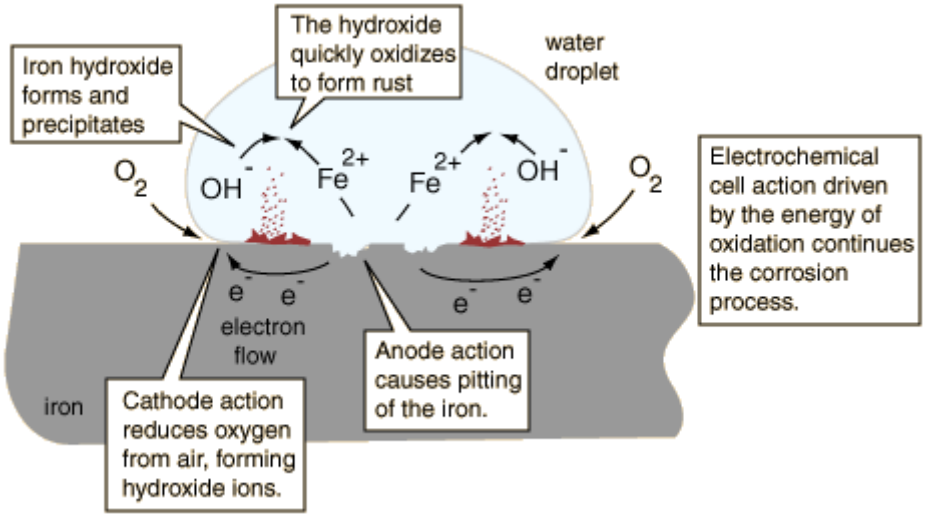

Figure 2.3: The schematic diagram showing electrochemical reaction of iron and water [23].

2.1.2 Corrosive Environment

A more convincing information about corrosion is normally obtained when the metal being corroded, and the environment are considered. The environment is an important influencer in the type of corrosion a material can undergoes. This is also because different types of corrosion are identified by the way in which the metal corrode and the environment in which the metal corrode. These types of corrosion include wet and dry corrosion. Wet corrosion takes place in electrolytic or aqueous environments while dry corrosion takes place in conditions above the dew point of the environment such as in cases when the corrodents are gases and vapours [24]. Therefore, it is very important to

have a clear and better understanding concerning the various types of environments during corrosion of metals studies. The corrosive environments are said to exists in three diffident main groups which are outer space environments e.g., vacuum, atmospheric environment e.g., marine, mining, rural and urban areas and man-made environments which include industrial molten metals and salts. These environments depend on factors such as temperatures and pressures. For instance, environment with high temperatures is associated with high corrosion rate of the metals [25].

2.1.3 Corrosion in different Media

Neutral, alkaline (basic) and acids are the most commonly known media in which corrosion takes advantage of in order to occur. Most materials which are used in different industrial applications are more likely to be exposed to these types of media. The acidic media is the one which possess low pH value ranging from 1-6, alkaline media also known as basic media possess a high pH value ranging from 8-14, while neutral media is at pH value of 7.

Acidic Medium

Literatures have stated that diluted acids are highly corrosive as compared to concentrated acids. This is due to the fact that diluted acids from which metals can be exposed to, contains more amount of water than when metals are exposed to concentrated acids, as a result, large number of hydrogens is given off and this leads in the corrosion of the metal. For example, when zinc is exposed to diluted hydrochloric acid, the results is the zinc chloride, and a large amount of hydrogen gas is given off in the process [25]. The reaction equation of such process is given in equation (5) below.

$$Zn_{\ (s)} + 2HCl_{\ (g)} \rightarrow ZnCl_{2\ (s)} + H_{2\ (g)} \quad (5)$$

Alkaline

Alkaline solutions like sodium hydroxide can also be corrosive towards metals surfaces, especially in the presence of dissolved oxygen. Equation (6) below is the example of the reaction of base sodium hydroxide with zinc metal which results in the corrosion of the zinc metal.

$$Zn_{\ (s)} + 2NaOH_{(s)} \rightarrow Na_2ZnO_{2\ (g)} + H_{2\ (g)} \quad (6)$$

Neutral Media

When oxygen carried by air comes in contact with water, the oxygen dissolve in water and this is normally what causes the formation of corrosion when the surface of the metal comes in contact with water [26]. For example, the reaction of zinc with water is given by equation (7) below.

$$Zn_{(s)} + 2H_2O_{(I)} \rightarrow Zn(OH)_{2\ (s)} + H_{2\ (g)} \quad (7)$$

Acids are very strong corrosive media compared to their counterpart basic media, this is because a higher pH means there are fewer free hydrogen ions, so more hydrogens are given off in the presence of low pH which results in the corrosion of metals. Acids solutions such as hydrochloric and sulphuric acids are normally utilised in the removal of undesirable scale and rust in many industrial processes. These acids are also widely utilised in the pickling process of metals, hence acid media are the most reported corrosion influencer [27].

2.1.4. Kinetics and Thermodynamics of Corrosion

Kinetics of corrosion

The kinetics of corrosion answers the question on how fast the metal will corrode or simply gives us the knowledge of the rate at which the metal will corrode. This is very important when trying to design the system that will slow down or prevent corrosion process especially under different solution conditions and pH.

The Arrhenius law which provides the relation between the reliance of the rate constant of chemical reactions on the temperature, helps us to understand the electrochemical behaviour of metallic materials in corrosive media through the influence of temperature on the kinetic process of corrosion [28,29].

$$K = Ae^{-E_a/RT} \quad (8)$$

where;

k = the rate constant

A = the pre-exponential factor or the pre-factor

E_a = the activation energy

R = gas constant

T = the absolute temperature

From equation (8) above, the rate constant is directly proportional to the temperature and parameter such as E_a. The pre-exponential factor (A) may vary with temperature. The rate constant can be calculated using the above equation.

Thermodynamics of corrosion

Thermodynamics is very helpful in determining the corrosion behaviour of different materials. It shows the spontaneous direction of a chemical reaction and it is utilised to determine whether or not corrosion is theoretically possible. Most of the alloys and metals that are being used are thermodynamically unstable. These metals thus have fundamental thermodynamic tendency to return to a stable state through corrosion processes. Thermodynamics is more based on the energy state of materials. The ores which are used to make metals are said to be in a state of low energy and when external energy (heat) is applied to these ores to convert them to usable metals and alloys, they transform to high energy state. When these metals react with aggressive environment they tend to revert to a lower (more stable) energy state. Even though thermodynamics can predict whether a corrosion reaction will occur or not, it does not provide an indication of the rate of corrosion reactions.

For a reaction to be considered spontaneous, there must be a free energy change, ΔG. In the case of a spontaneous reaction, energy is given out and the free energy change sign is negative [28,29]. The magnitude of the ΔG and its sign are of great importance, since it indicates whether the corrosion reaction will occur or not.

For example, the following reaction (equation 9) of aluminium in hydrochloric acid:

$$Al_{\ (s)} + 3HCl_{\ (g)} \rightarrow AlCl_{3\ (aq)} + \frac{3}{2}H_{2\ (g)} \quad (9)$$

The reaction is thermodynamically favourable, i.e., free energy change ΔG must be negative. This reaction can be divided into anodic half and cathodic half reactions as expressed in equations (10) and (11) as follows:

$$Al_{\ (s)} \rightarrow Al^{3+}{}_{(aq)} + 3e^{-} \quad \text{(Anodic half reaction)} \quad (10)$$

$$3HCl_{\ (g)} + 3e^{-} \rightarrow \frac{3}{2}H_{2\ (g)} + 3Cl^{-}{}_{(aq)} \quad \text{(Cathodic half reaction)} \quad (11)$$

These two half reactions have associated free energy change, thus, overall, the sum of the two free energies change must be negative as expressed in equation (12).

$$\Delta G_{Anodic} + \Delta G_{Cathodic} < 0 \quad (12)$$

where: ΔG_{Anodic} is the free energy change for anodic iron dissolution.

$\Delta G_{Cathodic}$ is the free energy change for cathodic hydrogen evolution.

The electrical potential, can be related to the free energy change by equation (13) bellow:

$$\Delta G = -n\mathrm{FE} \quad (13)$$

where: ΔG is the free energy change.

n is the number of electrons transferred in the half-cell reaction.

F is the charge transported by 1 mole of electrons and has the value of 96494 coulombs per mole.

E is the measured potential in volts (Vs. SHE).

Similarly, equation (14) gives:

$$\Delta G^o = -\mathrm{nFE}^o \quad (14)$$

where: ΔG˚ is the standard free energy change.

n and F are defined as above.

E˚ is the standard electrode potential and can be obtained from thermodynamic tables.

It is believed that the values of ΔG_{ads} around -20 kJ.mol^{-1} or less are in consistent with physisorption, which involves the electrostatic interaction between the charged molecules and the charged metal. Those more negative than -40 kJ.mol^{-1} are consistent with chemisorption, which involves charge transfer or sharing from the inhibitor molecules to the metal surface to form a coordinated bond. One of the important differences between chemisorption and physisorption is that chemisorption reaction is irreversible while physisorption is reversible [30,31].

$$Al \rightarrow Al^{3+} + 3e^- \qquad E^o = 1.7V \quad (15)$$

Under nonstandard conditions i.e., the respective ions not at unit activity, the electrode potential is related to the standard electrode potential by Nernst equation, equation (16).

$$E = E_O + \left(\frac{RT}{nF}\right) In \left(\frac{aOx}{aRed}\right) \quad (16)$$

From the above equation, as the electrode potential (E) becomes more positive, the activity of the oxidised species (aOx) increases.

2.1.5 The Rate of Corrosion

The rate of corrosion can be explained as a tool that tells how fast any metal will deteriorates or loss weight after a certain period in a specific environment. During the process of corrosion by gravimetric analysis, the weight lost by metal that is being corroded in each unit of time is regarded as the rate of corrosion. The rate of corrosion varies for every metal and it relies on the environmental conditions and the kind of the metal considered [32]. Some of the metals show resistance to corrosion, for example, aluminium instantly reacts with oxygen present (in the water, soil, or air) to form aluminium oxide. This formed aluminium oxide layer is chemically bound to the surface of the metal, and it covers the core aluminium from any further reaction. Zinc metals lacks the ability to form such films and because of that, their rates of corrosion are much higher than those of aluminium. Metals like copper also lacks such ability to form this film to some extent, and hence they have high rates of corrosion.

From the gravimetric analysis data, the corrosion rate can be computed according to equation (17) below.

$$\rho = \left(\frac{\Delta w}{st}\right) \tag{17}$$

where: ρ is the corrosion rate ($g.cm^{-2}.h^{-1}$)

w is the average weight loss of the materials (g)

S is the surface area of the materials (cm^2)

T is the immersion time (h)

2.1.6 Factors Affecting the Rate of Corrosion

As long as chemicals and properties of the metal in its manufactured state remains active, the metal is always protected from corrosion [33]. The rate and extent of corrosion of a metal relies on two important factors which are nature of the metal also called primary factor and nature of corroding environment which is also known as secondary factor [34].

2.1.6.1 Nature of the Metal

- **Purity of metal**

Impurities present within the metal increases the rate of corrosion, since they form a very small electrochemical cells under suitable environmental conditions and undergo corrosion [35].

- **Surface state of the metal**

Rough surfaces which contain different types of imperfections such as point defects and dislocations are easily attacked by corrosion. Corrosion cannot easily happen on polished and smooth surface. The rate of corrosion of the metals is affected directly by the surface ratio of anode and cathode. In most cases galvanic corrosion is often prevented by the use of sacrificial anodes. Since the corrosion attack in the simplest case only happen at the metal surface, surface modification can slow down the rate of the reaction process. Methods like painting, electroplating, metal spraying and claddings are used for protecting the surface [36].

- **Position in gravimetric series**

The metals which are found at an elevated or higher position up in the gravimetric series are said to be more reactive and has greater tendency to undergo corrosion. The opposite is the case for metals which are found at lower position in the gravimetric series [35].

- **Protective film**

Metals like aluminium forms oxide film that functions as a physical barrier and causes passivation of the metal thereby protecting it from corrosion caused by any corrosive medium [37]. This oxide layer determines the rate of further corrosion process on the metal. In metals like iron which forms rust as a corrosion product, the oxide film formed on the surface of the metal is soluble, non-stoichiometric, unstable, porous in nature and a good conductor. Therefore, corrosion on the metal surface cannot be prevented by such film. In metals like tantalum, zinc and molybdenum, the oxide film formed on the surface is insoluble, stoichiometric, and non-porous in nature with low ionic and electronic conductivity, then such film functions as protective layer and prevents further corrosion. Not only do these metals develop the protective layer, but also self-repairs it when damaged [36].

- **Physical state of the metal**

The physical state of the metal (orientation of crystals, grain size, stress, etc.) is very important in deciding the rate of corrosion. As the grain size is small, the rate of corrosion increases. This is because solubility of the metal is increased by increasing the size of the metal [35].

- **Reactivity of metals**

Metals such as Nickel, Cobalt, Titanium and Chromium, amongst the others, are regarded as passive and do not undergo corrosion frequently. They form a highly protective and very slim film of oxides on the metal surface. These oxides films are self-healing in nature which means they tend to repair by themselves during any cracking [35].

- **Volatility of corrosion product**

In the case of volatile corrosion product, metal undergoes corrosion very rapidly. This is due to the fact that volatile product is formed, and it escapes the metal, and the inner metal surface becomes exposed for further attack and as a result corrosion takes place very rapidly and continuous [35].

- **Solubility of corrosion products**

When the corrosion products are soluble in the corroding medium, the inner layer of the metal comes in contact with the corroding medium and corrosion of metal takes place fast. Similarly, when the corrosion products are insoluble in the corroding medium, the products of corrosion function as a protective layer and as a result corrosion of the metal takes place slowly [35].

2.1.6.2 Nature of the Corroding Environment

- **The effect of Temperature**

The nature of the corrosion reactions is said to be electrochemical and increasing the temperature of the surrounding environment usually accelerate these reactions. This is due to the increase in temperature with an increase in conductance of the medium and hence an increase in the diffusion rate. It can be concluded that corrosion reactions are faster in warm environments than in cold environments [35]. In certain instances, the rise in temperature decreases passivity, which also results to an increase in the rate of corrosion. According to the thermodynamic considerations, a chemical reaction is normally expected to speed up with an increase in temperature, thereby increasing the corrosion rate [38].

- **The effect of Humidity**

Humidity, time of wetness and the time the material is exposed to moisture play a crucial role in accelerating and promoting corrosion. The time of wetness refers to the length of time an atmospherically exposed material has enough moisture to support the corrosion process. The more the metal is exposed to moisture and wetter environment, the more corrosion is likely to take place [35].

- **The effect of pH**

Acidic media (pH < 7) was noted to be the one where corrosion takes place very often than in neutral media (pH = 7) and alkaline media (pH > 7) [39]. Metals such as zinc, palladium and aluminium tend to form complexes in basic or alkaline media, hence these kinds of metals corrode much faster in alkaline media [35]. Metals like iron tend to form protective iron oxide layer at very high pH which prevents

corrosion. But at very low pH, severe corrosion occurs. Corrosion of every metal depend highly on the pH. The decrease in pH increases the speed at which the metal corrodes, since it facilitates the rate of hydrogen evolution which speed up the process of corrosion. In conditions in which the pH of the corrosive medium is changing, the corroding metal surface may exhibit activity, passivity or immunity [40].

- **Effect of atmospheric gases present in air**

The gases like carbon dioxide, sulphur dioxide, water etc present in the atmosphere or fumes of acids like nitric acid, sulphuric acid etc forms the medium which is more acidic above the metal surface because these gases are soluble in water to form acids. Acids have more conducting power hence it enhances the corrosion rate [35].

- **Effects of the nature of the electrolyte present**

The presence of an electrolyte in the corroding environment plays a significant role in corrosion. Anions like chloride destroy the protective layer on the surface of the metal and the inner surface is exposed for further corrosion, hence corrosion takes place rapidly. On the other hand, anions like sulphite forms an insoluble film on surface of the metal and prevents it from further corrosion [35].

- **Effects of concentration of oxygen**

The rate of corrosion increases in the presence of moisture and oxygen. Corrosion generally occurs in an environment that is oxygen-deficient, but the rate of corrosion is much slower. In situations in which the metal is immersed in an aqueous medium, when one area of the metal containing more oxygen is in contact with an electrolyte than the other area of the metal in contact with the electrolyte, the higher oxygen concentration area is cathodic relative to the remaining surface. As a results differential aeration set up several concentration cells and due to this electrochemical process increases the rate of corrosion [35]. In the presence of dry oxygen corrosion rate decreases.

Other factors that affect the rate of corrosion may include:

- **Availability of corrosion inhibitors:**

Inhibitors are chemical substances that once introduced into the corrosive atmosphere or environment in very small concentrations minimizes the consequences of the corrosive environment on a given metal. Many studies reveal that as the concentration of the inhibitor is inflated, the speed at which corrosion takes place is attenuated. But when the concentration of the inhibitor is attenuated, the opposite is the case as the rate of corrosion is inflated [39, 41, 42].

- **Galvanic effects**

Generally galvanic corrosion occurs when two metals are placed together in a corrosive electrolyte. Lower metals have a high tendency to corrode while the upper metals have the least tendency to corrode in the galvanic series. This series is based on measuring the potentials of metals as compared to a reference electrode. The galvanic corrosion is found to be much rapid If one joins two metals that are very far apart in the galvanic series in the presence of an electrolyte. However, if the two joined metals are carefully selected from the galvanic series such that they are very close to each other, the rate of corrosion may be reduced. From the galvanic series, gold is the least active while magnesium metal is the most active [43].

- **Fluid speed**

The main causes of corrosion by fluids in motion are diffusion effects. Corrosion is firmly experienced by those metals that are protected by chemical coatings as early as they are exposed to fluid carrying particles which are moving very fast. These fast-moving particles are likely to get rid of the chemical coatings and leave the metal exposed to corrosion. High corrosion rates are directly associated with high fluid speeds [44].

2.1.7 Different Types of Corrosion`

Types of corrosion are classified based on the appearance of the corrosion damage, the mechanism of attack and the type of environment the metal is subjected to, these include, amongst others, the following [45]:

- **Galvanic corrosion**

Galvanic or dissimilar metal corrosion takes place when two dissimilar metals are put together in a corrosive electrolyte. A galvanic couple develops between the two metals where the more active metal acts as an anode (the one that will corrode) and the more resistant metal function as a cathode. A potential difference generally exists when two different metals are in contact and in such cases, the less resistant metal corrosion is increased whereas the more resistant metal corrosion is reduced. Under these conditions, the anodic metal would corrode faster while the cathodic metal would corrode slower [46, 1].

- **Fretting Corrosion**

This type of corrosion takes place as a consequence of ongoing repeated vibration, wearing and weight on an uneven, rough surface. Fretting corrosion is normally found in impact machinery and rotation, surfaces subjected to vibration during transportation, and bolted assemblies and bearing [47, 48].

Fretting corrosion is normally experienced when heavy metal equipment's move against each other and this is mainly because when they do so, they create friction, leaving an abrasive wear known as fretting. The protective layer on the metallic surface is removed by this friction process. The metal surface merges with oxygen and forms the metal oxide because of this rubbing action [48]. Fretting corrosion is not driven by an electrolytic reaction, like other types of corrosion do. Amongst others, the best way of minimizing this type of corrosion is by the application of a lubricant; nevertheless, the installation of a fretting-resistant material between the two surfaces can also contribute greatly to minimizing this form of corrosion [1, 36].

- **Intergranular corrosion**

Intergranular corrosion is a type of corrosion that selectively attack at the grain boundaries of alloy or stainless steel because of the presence of secondary phase. It normally occurs due to the impurities within the metal, which tend to be present in higher concentration near the grain boundary. It also results due to chromium depletion which is carried by precipitation of chromium carbides in the grain boundary [49]. Any commercial alloy features a profoundly magnified cross that shows granular structure of the metal. There are individual grains and every one of these grains contain a defined boundary which further contains distinctive chemical characteristics in comparison with that of the metal within the grain. The grain centre can function as an anode while the grain boundary can function as the cathode. When these two becomes in contact with the electrolyte, they begin to react. It is essential that the metals are appropriately treated and handled to prevent intergranular corrosion when they are subjected to aggressive environment. Aluminium metals like 2014 and 7075 are severely affected by this form of corrosion [1, 36].

- **Uniform corrosion**

Uniform corrosion is also referred to as general attack. This type of corrosion describes the corrosion that takes place nearly at equivalent rate over the entire exposed surface of the metal. It leads to a great loss of weight and destruction of the metal. Rusting of steel is a very familiar example of uniform corrosion [48].

- **Crevice corrosion**

Crevice corrosion takes place in confined spaces such as contact areas between two parts, gaps and inside cracks where there is limited access of fluids from the environment [50]. Some other literatures describe crevice corrosion as shielded corrosion [36]. This is because this corrosion takes place where the surface is protected thereby preventing the free and open interactions of oxygen and the metal surface. The passive layers that form in some metals during the corrosion process usually tend to break down in these areas [36].

- **Pitting corrosion**

Pitting is a highly localized form of corrosion that takes place when one area of a metal becomes anodic as compared to the rest of the metal surface producing holes which may be small or large in diameter on the surface of a metal. The pits produced may be close to each other or isolated resembling a roughened surface [48]. Metals like magnesium and aluminum which are able to form protective layer, are found to be the most attacked by this type of corrosion. The corrosion by-products that normally forms due to this type of corrosion is gray or white powder. This by-product powder is generally used as the identification symbol of pitting corrosion. When by-product powder is removed from the metal surface, small pits or holes are then left on the surface of the metal. When these small pits or holes in the metal surface penetrate deep into the metal structure, a great deal of destruction can be seen on the metal. In situations where conditions that give rise to fretting corrosion cannot be changed, materials consisting of high content of alloy usually contribute less to the problem [1, 36].

- **Erosion corrosion**

Erosion is described as the mechanical process, while corrosion is described as the deterioration process of materials which takes place due to chemical or electrochemical action. When these two processes act together in aqueous environment, their conjoint action is known as erosion-corrosion [51]. Erosion corrosion is further described as the process in which the surface of the metal is continuously washed away by corrosive, high- velocity wet steam because of the interaction of mechanical erosion and chemical reaction. Steam temperature, velocity, wetness, pH value, geometry of flow passage and corrosive elements which form part of the steam are some of the parameters that influence the rate of erosion-corrosion. Because of sand, erosion-corrosion is an increasingly significant problem in gas and oil production industries [52, 53]. The combined impact of erosion and corrosion processes (erosion corrosion) is found to be greater than the total impact of the processes acting separately, and this impact is known as synergism. Many researchers believed that this net impact is a result of the enhancement of corrosion by erosion or enhancement of erosion by corrosion [54, 55]. In the past, synergism was not well quantified due to the shortage of detailed knowledge and understanding of the separate kinetics of pure corrosion or pure erosion [56].

- **Exfoliation corrosion**

Exfoliation corrosion is defined as a type of intergranular corrosion that is seen on the surface of aluminum alloys with a stretched grain structure. The hydrated aluminium oxide corrosion product has a higher volume than the alloy matrix from which the product is formed, when intergranular

corrosion continues along intergranular path parallel to the surface. This results to production of relatively large wedging stress, which lifts the surface grains, giving rise to a layered appearance. Exfoliation corrosion is a common source of life-limiting degradation in airframes. It is known to consume load bearing cross section and increases the stress in the remaining intact material, resulting in a loss in mechanical properties of aluminium alloys [57].

- **Microbiological corrosion**

Microbiological corrosion is referred to as a localized aggressive type of corrosion that leads to biodeterioration of material and is frequently referred to as biocorrosion or microbially influenced corrosion [58]. This type of corrosion is started and accelerated by the microorganism's activities. This is because microbiological aerobic bacterium produces highly corrosive species as part of their metabolism. Microbiological corrosion is a serious problem for the ship industry because it minimizes the structural lifetime together with the safety risks for crewmembers or inspection personnel and increases maintenance costs [59].

There are many different types of bacteria genera associated with microbiological corrosion and are categorized by their respiration techniques. The following are some examples,

- Sulfate-reducing bacteria: This include desulfuromonas sp, desulfobacter sp, desulfococus sp [60].
- Sulfur-oxidizing bacteria: These includes thiobacillus. The organisms form sulfuric acid during oxidation and are capable of both oxidizing sulfur and ferrous iron [60].
- Iron bacteria: There are two types of this bacteria which includes stalked (Gllionella sp) and flamentous (Leptothrix sp, Clonothrix sp, Sphaerotilus sp). These bacteria are known to reduce or oxidize iron species during respiration [60].

The prerequisite for microbiologically influenced corrosion is the presence of microorganisms. In cases where the corrosion is influenced by their activities, additional resources or conditions which are needed are:

- A source of energy
- A source of carbon
- Electron donor and acceptor
- Water
- Substrate (host location)
- Presence of nutrients
- Aerobic and anaerobic circumstances

This type of corrosion normally occurs in arctic and deep sea and it applies to materials like plastics, concrete, coating, and adhesives [61].

2.1.8 Classification of Corrosion

Corrosion can be categorised into different techniques. One technique separates corrosion into oxidation (or direct combination) and electrochemical corrosion. Another technique separates corrosion into low temperature and high temperature. The most preferred classification of corrosion is the one that divides it into three factors namely: the nature of the corrodent (wet and dry corrosion), mechanism of corrosion and appearance of the corroded metal [45, 62]. These three factors are further elaborated below.

Nature of the corrodent: This type of categorization depends on wet or dry conditions in which corrosion takes place. For wet corrosion, the presence of moisture is essential and dry corrosion normally involves reaction with gases at high temperature [63, 64, 34].

- **Wet corrosion**

  Wet corrosion takes place in the presence of the liquid. It takes place through the electron transfer, which involves two processes, reduction, and oxidation. In reduction, the surrounding environment gains the electrons lost by the metal atoms in oxidation. The metal where electrons are lost is known as the anode. The other liquid, gas or metal which gain the electrons is known as the cathode. Wet corrosion account for the greatest amount of corrosion by far [65].

- **Dry corrosion**

  Dry corrosion is generally associated with high temperatures and occurs in the absence of liquids or above dew point of the environment. Gases and vapours are often the corrodents. In this process, the metal oxide itself and reacts with the atmosphere alone. In this study we will focus on the corrosion that happens in the presence of liquids (Wet corrosion) [66].

Mechanism of corrosion: This classification state that Corrosion can take place either electrochemically or with direct chemical reactions.

Appearance of the corroded metal: corrosion can be either localized or uniform. In localized corrosion, only minute areas on the metal surface are affected, and the metal corrodes at an equivalent rate over the entire metal surface for uniform corrosion.

Categorization of corrosion by appearance is best understood by the morphology of the corrosion attack and this can be viewed either by magnification or naked eye [67]. The picture displayed in Figure 2.4 shows some of the most common forms of corrosion and appearance.

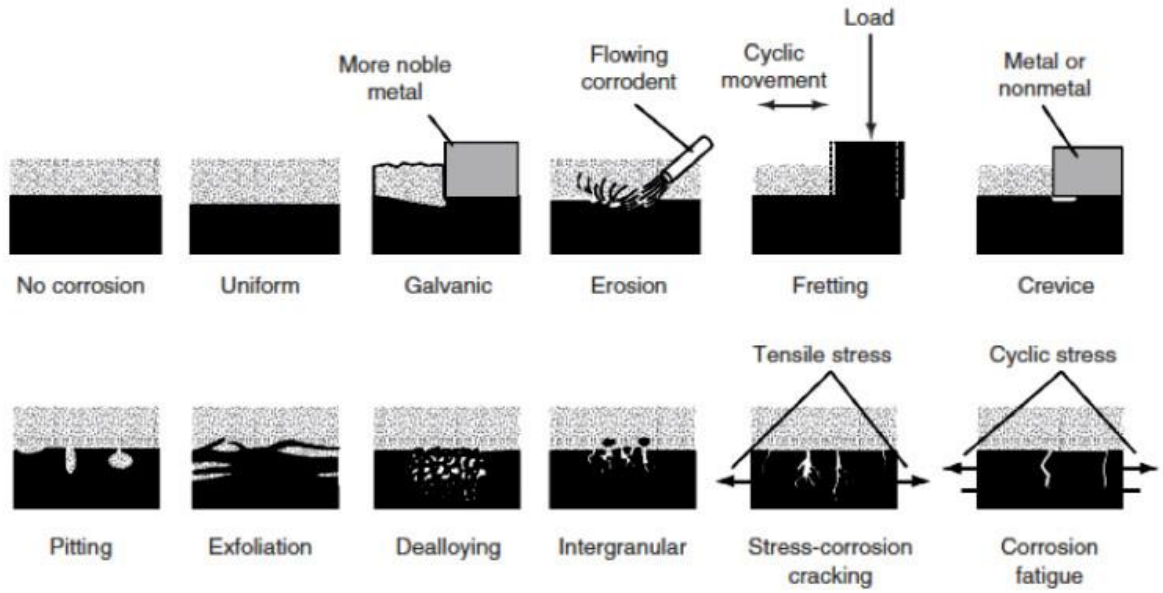

Figure 2.4: Picture illustrating the common forms of corrosion [67].

2.1.9. Consequences of corrosion

Corrosion has numerous serious technological, health, safety, economic, and cultural repercussion to our society. These consequences or repercussions are further explained below.

Technological effects

Corrosion is considered to be the main hindering factor of many advances in technology in our lifetime. Most of the greatest deal of recent technological development is hindered by the corrosion problems since materials are expected to endure very harsh conditions such as high temperatures, very high corrosive environments and pressures. Our progress in the energy sector is compromised due to corrosion problems as the materials used to drill oil in the sea and land become heavily affected by the corrosion. In most cases corrosion is to blame as it is the hindering factor sabotaging the innovation of technological workable systems [68].

Economic effects

Great global challenges in sectors like industries, our personal lives and the nation is due to the economic effects as a consequence of corrosion that has led to enormous loss in terms of properties, resources and productivity in different areas. For instance, in the gas and oil sectors, electrical power

plants, pipelines and plants for chemical processing are affected because of corrosion, which results in their shut down, loss of efficiency and lives, loss of jobs and waste of valuable resources. In addition, the efficiency in hot water heaters decreases because of corrosion and may cause failure to the heater earlier than anticipated and the malfunctioning of plumbed features in the house. This corrosion can also add to bitter taste of water due to highly unalleviated level of toxic metals like copper, zinc and lead, which can result in chronic and acute health problems. The NACE (National Association of corrosion Engineers) released the International Measures of Prevention, Application and Economics of Corrosion Technology (IMPACT) study in March 8 2016, which estimated the global cost of corrosion to be around 3.4 percent of the Global Domestic Product (GDP), equivalent to roughly $2.5trillion U.S [15].

Health effects

The replacement of original body parts with artificial once's (prosthesis) like plates, implants, hip joints and pacemakers have seen an increase in the recent years. The use of recent devices has caused quite a revolutionary change in our health systems. Corrosion keeps on creating problems which has brought numerous restrictions in our health systems despite the development and implementations of new alloys and better technologies. Examples of such problems incudes failures through inflammation because of corrosion products in tissues around implants, broken connections in pacemakers and fracture of weight bearing prosthetic devise. With all these problems, the hope is not lost since the prosthetic devices are constantly improving everyday [15].

Cultural effects

Corrosion is also capable of deteriorating the precious artefacts of our ancestors. Many museums all over the world have even gone to the extent of hiring expects to preserve these treasures of our precious pasts and to get rid of corrosion traces on culturally or artistically important artefacts. Changes in the global climate is one factor that is contributing to the corrosion of the beautiful creatures of our past which has always been essential to humans. The artistic relics have huge effects on our identity and must be protected from corrosion. These effects illustrate the corrosion consequence on our daily lives and preventive measures against corrosion must be applied and implemented [15].

Safety effects

Corrosion put the safety of our morden day structures such as bridges, aircrafts, pipelines and automobile in danger. Accidents that occur as result of corroded structures can cause a tremendous loss of lives, properties, resources, and safety concern. Most of the structures that cannot sustain their

environment have proven to be very dangerous and it can cause serious injuries and possible loss of lives. Catastrophe such as failed pipelines and bridge collapse leads to immense indirect cost like more traffic delays, loss of business and public out-cry. This indirect cost may be as five to ten times that of the direct cost, depending on which market sector e.g., industrial, infrastructures, commercial etc, is being considered. Nevertheless, the corrosion cost is not just financial. Above the huge direct distribution of funds to replace corroded structures are the indirect costs like natural resources, loss of lives and potential hazards. A project which is constructed by building materials that are unable to survive the environment for a long time, consumes natural resources needed to continuously maintain and repair the structure. Therefore, corrosion has deeply affected industries, our daily lives, and the world as a whole [15].

2.2 Metals Often used in Corrosion Studies.

2.2.1 Aluminium Metal

The existence of aluminium was established in 1807 by the British scientist Sir Humphrey Davy whereby he incidentally named it aluminium., the spelling which is still used across the globe. Aluminium is normally found on the surface of the earth and it is third most abundant element. Aluminium has not been used for centuries as has gold and copper because it is never found in its natural form as pure metal as it is always mixed with or locked with other metals. It is normally found in rocks, soil etc., in its combined form as very stable chemical compound such as alumino-silicates. Ancient man used some aluminium-bearing compounds without aluminium knowledge, for example pottery were made by clays containing hydrated aluminium silicate. Babyloanians and Egyptians used aluminium salts for the preparation of dyes and medicines. Low density of approximately 2.7, high mechanical strength achieved by suitable alloying and relatively high corrosion resistance of the pure metal and heat treatments, are the three main properties which makes aluminium to have many applications [69].

Aluminium is considered one of the very active metal because of its nature ability to oxidize quickly. This quality is regarded as the weakness of most metals, but it’s actually the key to aluminium ability to resist corrosion. Aluminium instantly reacts with oxygen present (in the water, soil or air) to form aluminium oxide. This formed aluminium oxide layer is chemically bound to the surface of the metal, and it covers the core aluminium from any further reaction. The aluminium oxide film is hard, tenacious, and instantly self-renewing. This is a very different form of corrosion (oxidation) of steel whereby the rust pile on the surface and later flakes off, exposing the new metal to corrosion. However, when aluminium is exposed to other harsh environmental conditions that destroy the oxide layer, aluminium is no match to corrosion as it gets devoured quickly. According to the US Army Corps

of Engineers, aluminium's protective oxide film is normally stable in the pH range of 3.5 to 8.5. Under extreme pH levels and highly acidic and basic environment, the oxide layer becomes unstable and eventually breakdown (exposing the metal) and its automatic renewal may not be sufficiently quick to prevent corrosion.

Normally the corrosion of aluminium metal is by the chloride and fluoride ions which have the capability to destroy the oxide film causing corrosion. Aluminium metals are known to undergo pitting corrosion when chloride ions are present in the system [70]. The chemical reactions that are involved during the process of pitting corrosion of aluminium metal are described below.

Firstly, aluminium metal is oxidized to Al^{3+} ion as expressed by equation (18) bellow.

$$Al_{(s)} \rightarrow Al^{3+}{}_{(aq)} + 3e^{-} \quad (18)$$

This is followed by the reaction between the aluminium 3+ ion and water to produce aluminium hydroxide as expressed in equation (19).

$$Al^{3+}{}_{(aq)} + 3H_2O_{(l)} \rightarrow Al(OH)_{3\ (l)} + 3H^{+}{}_{(aq)} \quad (19)$$

The reaction involving hydrogen evolution takes place at the intermediate cathode as shown in reaction equation (20).

$$2H^{+}{}_{(aq)} + 2e^{-} \rightarrow H_{2\ (g)} \quad (20)$$

Lastly, the reaction involving oxygen reduction takes place according to reaction equation (21).

$$O_{2\ (g)} + 2H_2O_{(l)} + 4e^{-} \rightarrow 4OH^{-}{}_{(aq)} \quad (21)$$

The exact processes involved can be further explained schematically using Figure 2.5. This figure shows how reactions (18) to (21) take place.

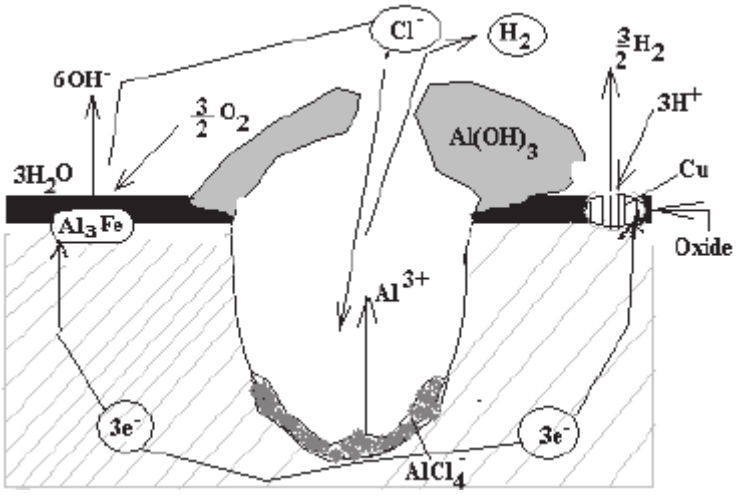

Figure 2.5: Schematic diagram of the pitting corrosion of aluminium [71].

2.2.2 Zinc Metal

Zinc is considered to be the 24th most abundant element in earth's crust. It is found in the form of an ore and the most common of such ores are sphalerite and zinc sulphide mineral. Zinc is regarded as one of the most significant non-ferrous metals and it is widely utilised in metallic coatings. Zinc is amphoteric in its behaviour towards acids and alkalides just like aluminium [72]. Zinc alloys man made products have been reliably dated as far back as 500 BC. It was first deliberately added to copper to form brass in the late 200 – 300 BC. During the Roman empire, brass supplemented bronze was used in the manufacturing of weapons, coins and art, and it remained the main use of zinc until 1746 when Andreas Sigismund Marggraf knowingly isolated the pure zinc element. Andreas was also able to describe the isolation process and how it works, which made zinc to be commercially available [73].

Zinc generally has the capability to form insoluble basic carbonate film that is able to hold firmly to its surface, minimizing the corrosion rate. With this regard, zinc still suffers corrosion the most compared to aluminium and suffers the least compared to mild steel. Environment plays the important role in the corrosion of zinc. For instance, environments with a pH of around 6.5 – 12 have been found to have the lowest corrosion rates of zinc. Conditions such as acid solutions and marine makes the corrosion of zinc unbearable and for such conditions zinc is not a suitable candidate for use and therefore its protection is needed. When zinc comes in contact with sulphate ions, corrosion happens, and the behaviour follows the half reactions below [74].

Firstly, zinc is oxidized to zinc 2+ ions as shown in reaction equation (22).

$$Zn_{(s)} \rightarrow Zn^{2+}{}_{(aq)} + 2e^{-} \qquad (22)$$

This is followed by the reduction of hydrogen ion to hydrogen gas by taking up the two electrons of the oxidized zinc as articulated in equation (23) bellow.

$$2H^{+}{}_{(aq)} + 2e^{-} \rightarrow H_{2\,(g)} \tag{23}$$

The two reactions can be combined to form the final reaction as indicated in reaction equation (24).

$$Zn_{\,(s)} + H_2SO_{4\,(l)} \rightarrow ZnSO_{4\,(aq)} \tag{24}$$

2.2.3 Copper Metal

Metallic copper deposits have been mined in several parts of the world. Nowadays, however copper is found naturally as a simple or complex sulphide, or as compounds such as hydroxides or carbonates produced from sulphides by weathering [75]. Because of its extreme atmospheric corrosion resistance and its good thermal and electrical conductivity, copper is a broadly utilised material. Even when the copper corrosion is low, it can still have negative impact on the correct functioning of electronic equipment's like printed circuits [76]. Although corrosion of metal is a curse to human settlement, corrosion product film formed on copper known as patina, forms part of nature attraction, since this material has been utilised for ages in architectural applications like roofing, domes and frontages on churches, castles, and other monumental buildings [77-83]. Patinas are formed on the atmosphere polluted with sulphur dioxide and other atmospheric compounds [84]. The colour of the cuprite patina changes from an initial appearance of metallic luster into a dull brown, depending on the exposure conditions [76].

Example of copper corrosion is the formation of cuprite layer on the copper surface. The exact moment that copper is exposed to air, it turns out to be quickly coated with a nanometric thin layer of cuprite by means of a direct oxidation mechanism [85]. When the cuprite thickness reaches 5 nm, the oxidation rate decreases with time and practically comes to a stop [86, 87].

Once the aqueous layer has formed on the copper metal surface because of condensed humidity or rainfall, the electrochemical corrosion of copper takes place in the atmosphere. The possible anodic reaction would be:

$$Cu_{\,(s)} \rightarrow Cu^{+}{}_{(aq)} + e^{-} \tag{25}$$

$$Cu_{\,(s)} \rightarrow Cu^{2+}{}_{(aq)} + 2e^{-} \tag{26}$$

And the common cathodic reaction in neutral aerated solutions would be given by equation (27) bellow:

$$O_{2\,(g)} + 2H_2O_{\,(l)} + 4e^- \rightarrow 4OH_{\,(aq)} \quad (27)$$

The formation of the cuprite will occur according to the overall reaction as expressed by equation (28):

$$2Cu^+_{\,(aq)} + 2OH^-_{\,(aq)} \rightarrow Cu_2O_{\,(s)} + H_2O_{\,(aq)} \quad (28)$$

As indicated by Graedel, the passive cuprite film may have a sequential structure of Cu_2O, CuO and $Cu(OH)_2$ or $CuO.XH_2O$, depending on its depth. Cu^+ and Cu^{2+} ions can form stable complexes in the presence of Cl^- ions and for this reason the concentration of copper decreases noticeably [88]. This also supports that in marine atmosphere, the oxidation of Cu and Cu^{2+} is the only possible reaction [89]. It is unanimously agreed that the cuprite (CuO) is the initial corrosion product to form in the atmospheric conditions.

The aqueous deposit on the surface of the cuprite may produce an oxidation process based on the following reaction (equation 29):

$$Cu_2O_{\,(s)} + 2H^+_{\,(aq)} \rightarrow 2Cu^{2+}_{\,(aq)} + H_2O_{\,(l)} + 2e^- \quad (29)$$

The figure below illustrates the copper corrosion when oxygen and water are the corrosive environment.

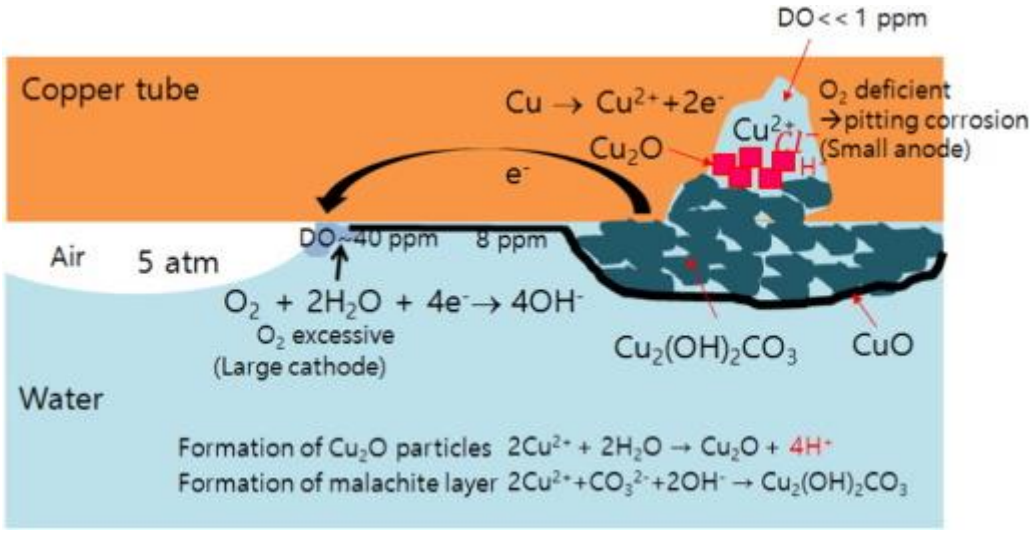

Figure 2.6: Schematic diagram for the formation of cuprite or copper corrosion [90].

2.2.4 Mild Steel Metal

Mild steel is generated from steel, which is extracted from pig iron and it is readily available and cheap to produce. It is well known for its high carbon content of about 0.2% to 2.1%, copper 0.6%, silicon 0.6%, manganese 1.65% and iron is the balance of these percentage composition. Its outstanding

weldability, toughness and high machinability, makes it to be the preferred metal for use in various engineering applications for the manufacturing of certain structural shapes such as I-beam and angle iron, automobile components and sheets that are utilised in plants, pipelines, building, tin cans and bridges [91]. Even though it has many applications, the production or development of mild steel does not involve corrosion resistance as a primary consideration, which is the basic property related to the ease with which the metal reacts with a given environment. With this short come, when this metal is exposed to hash environment, its binding energy start to decrease which leads to corrosion, with the end product involving the metal being oxidized as the bulk metal loses one or more electrons. The lost electrons are then conducted through the bulk metal to another site where they are reduced [92]. Most of the steels that are produced are subjected to outdoor conditions, usually in highly polluted environment where corrosion is considerably much severe than in clean rural environment. The sketch below shows the corrosion of steel with brine water.

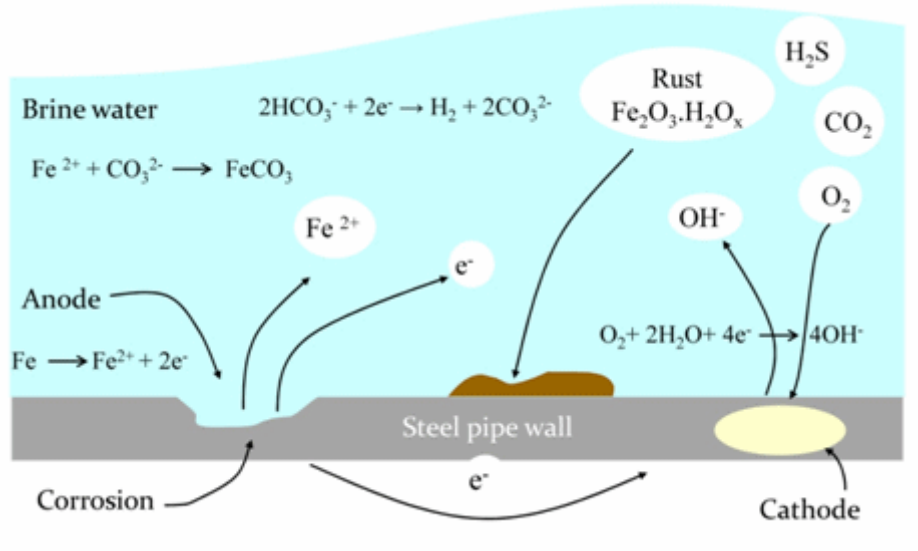

Figure 2.7: Internal corrosion of a crude oil pipeline made of mild steel [93].

Another example of mild steel reaction with H_2SO_4 can be well represented with iron Using the following two half reaction expressed by equations (30) and (31):

$$Fe_{(s)} \rightarrow Fe^{2+}{}_{(aq)} + 2e^- \quad \text{(oxidation)} \tag{30}$$

$$2H^+{}_{(aq)} + 2e^- \rightarrow H_{2\,(g)} \quad \text{(reduction)} \tag{31}$$

Even though the overall rate of corrosion of mild steel in concentrated sulphuric acid is low, a small amount of corrosion can still take place. Iron sulphate and hydrogen gas are the reaction products from such corrosion process as expressed in equation (32) below.

$$Fe_{(s)} + H_2SO_{4\ (I)} \rightarrow FeSO_{4\ (s)} + H_{2\ (g)} \quad (32)$$

High acid velocities or other disturbances in the liquid can disturb the relatively weak iron sulphate film. Hydrogen is known to be a problem with mild steel in sulphuric acid environments because it can literally scrub off the mechanically weak iron sulphate layer, which is the only thin layer preserving the steel from attack.

2.3 Corrosion Prevention methods

Metals like copper and aluminium always strive to return to their chemically natural stable state such as oxide and hydrides which makes them vulnerable to corrosion. Certain procedures can be employed to try to delay the process of corrosion and minimizing its effects. This procedure makes the metals to perform their assigned duties for a prolonged period of time. Coating, painting, the use of inhibitors, cathodic and ionic protection, surface cleaning and inspection are some of the useful procedures for controlling corrosion. Regardless of that, it must be known that the principle of corrosion prevention methods depends on corrosion resistant materials, modification of environment and electrochemical approaches [94]. Coating is the general term that includes most of the corrosion prevention and control methods like modification of environment (barrier effects and inhibition), cathodic protection (sacrificial) and materials selection (development of corrosion resistant materials like conducting polymers) therefore its importance cannot be over- emphasized. In this study corrosion inhibitors will be utilised to control corrosion of aluminium and zinc using hydrochloric and sulphuric acids as corrosive medium and its concept is represented in the following section.

2.4 Inhibitors and Inhibition

2.4.1 Definition of Corrosion Inhibitors

American Society for Testing and Material (ASTM-G15-08) defines corrosion inhibitors as a chemical substance or a combination of chemical substances that when present in appropriate concentration and form in the corrosive environment, reduces or prevent corrosion [95]. Inhibitors are inorganic or organic compounds that are soluble in the medium and eventually form a protective film either on the cathodic or anodic area of the metal [96]. Compounds that can function as corrosion inhibitors need to have functional groups and centres in their molecules with high electron density from which electrons can be donated to the metal surface to cause coordination or adsorption of the inhibitor to

the surface of the metal. This is the reason why organic compounds which contain π-electrons in conjugated double or triple bonds and electronegative functional groups are usually regarded as good corrosion inhibitors.

Various kinds of organic compounds that contain multiple bonds and hetero atoms like oxygen, sulphur and nitrogen in their molecule have adsorption centres of great significance due to their high electron density. They provide a better inhibition efficiency because they are adsorbed on the surface of the metal by chemisorption the process forming a protective layer by conjugation with metallic ions. Inhibitors also cause a metal to form its own protective layer of metal oxides which increases its efficiency [97]. The molecular weight of the molecule is also a crucial element in determining the efficiency of the inhibitor, with those compounds having higher molecular weight showing high inhibition efficiency [98, 99]. There are other factors which form part of what influences the adsorption of the inhibitors onto the metal surface. They include: the metal surface nature, the bonding strength of the metal, the size of the organic molecule and the electrochemical potential at the interface [36, 98]. The mechanisms of action that inhibitors usually adapt are [100]:

- Adsorption, which involves forming a layer that is adsorbed onto the surface of the metal.
- Inducing the formation of corrosion products like iron sulphide, which is a passivizing species.
- Altering media characteristics, forming precipitates that can be protective and eliminating or inactivating an aggressive constituent.

2.4.2 Classification of Corrosion Inhibitors

Corrosion inhibitors can be categorised into two unique types which are, interface inhibitors and environmental conditioners. Environmental conditioners decrease corrosion of the medium by scavenging the aggressive corrosive substances on the medium. In alkaline solutions where oxygen reduction is a common cathodic reaction, scavengers can be used to control corrosion by decreasing the oxygen content [101, 102]. Interface inhibitors control corrosion by forming a layer at the surface of the metal. Interface inhibitors can also be categorized into two subcategories which are, liquid and vapor phase inhibitors, where the vapor phase inhibitors are also known as volatile corrosion inhibitors, which are compounds that can be transported into a closed environment to the site of corrosion by volatilization from a source [102]. They are also utilised in boilers where they are transported with steam to forestall corrosion in the condenser tubes. The liquid phase inhibitor is further categorised into cathodic, anodic, and mixed corrosion inhibitors relying upon electrochemical reactions they inhibit [45]. The following subsections present some the corrosion inhibitors.

2.4.2.1 Organic Inhibitors

Organic compounds utilised as inhibitors function through a process of surface adsorption, also known as film-forming. They can also function as cathodic, anodic, or together as cathodic and anodic inhibitors generally called mixed inhibitors. The most desired organic inhibitors are those which show good inhibition efficiency and minimal environmental hazard or impact [103]. These types of inhibitors are known to develop a protective hydrophobic layer which consist of adsorbed molecules on the surface of the metal, which gives a boundary to the dissolution of the electrolyte and they must be soluble in the medium surrounding the metal [104]. The presence of the polar functional groups such as S, O and N atoms in the molecule, pi electrons and heterocyclic compounds, are related to the good efficiency of organic compounds used as corrosion inhibitors because they generally have hydrophobic parts ionizable. The reaction centre to trigger the adsorption process is provided by this polar functionality. Organic compounds with pi bonds are very effective as corrosion inhibitors as compared to organic acids inhibitors that contain sulphur, oxygen, and nitrogen. Even though with their effectiveness, they present biological toxicity and environmental harmful characteristics which makes then less favourable to be used [105]. The efficiency of an organic inhibitor also relies on the following factors:

- Chemical structure. e.g., the dimension of the organic molecule
- Aromaticity and conjugated bonding. e.g., as the carbon chain length
- The number and type of bonding atoms or groups in the molecule (either π or σ)
- Nature and the charges of the metal surface of adsorption mode like bonding strength to metal substrate
- The ability for the organic layer to become compact or cross-linked
- Ability or capability to form a complex with the atom as a solid within the metal lattice
- kind of the electrolyte solution like adequate solubility in the environment [106].

2.4.2.2 Anodic (Passivating) Corrosion Inhibitors

Anodic inhibitors are mostly utilised in near-neutral solutions where soluble corrosion products, like hydroxides, or oxides are formed [45]. They work by facilitating the formation of passivating layers that inhibit the anodic metal dissolution reaction. Anodic inhibitors are usually called passivating inhibitors. The corrosion may be accelerated rather than being inhabited when the concentration of the anodic inhibitor is not sufficient. The critical concentration above which inhibitors are effective

depends upon nature and concentration of the aggressive ions [97, 102]. Anodic inhibitors are responsible for enormous anodic shift of the corrosion potential, forcing the metallic surface into the passivation range. There are two kinds of passivating inhibitors which are oxidizing anions and non-oxidizing ions. Oxidizing anions passivate the steel in the absence of oxygen, and they include species or compounds like nitrite, nitrate, and chromate, while non-oxidizing ions require the presence of oxygen to passivate steel, and they involve species like tungstate, molybdate and phosphate. These inhibitors are the most widely used because of their effectiveness. Chromate inhibitors have been used recently in variety of applications such as refrigeration units and rectifiers because of its affordability.

2.4.2.3 Cathodic Corrosion Inhibitors

Cathodic inhibitors control corrosion by slowing down the reduction rate (cathodic poisons) or by specifically precipitating on the cathodic areas (cathodic precipitators) to increase the surface impedance and limit the diffusion of reducible species to these areas. Cathodic inhibitors can provide inhibition by three various mechanisms which are: as cathodic poisons, as cathodic precipitates, and as oxygen scavengers. Cathodic toxin, like sulphides and selenides, are adsorbed on the surface of the metal; whereas compounds of arsenic, bismuth, and antimony are reduced at the cathode and form a metallic film. In near-neutral and alkaline solutions, inorganic anions, such as phosphates, silicates, and borates, form protective layers that decrease the cathodic reaction rate by restricting the diffusion of oxygen to the surface of the metal. Cathodic precipitators such as ions of zinc, magnesium and calcium protect the metal by being precipitated as oxides thereby forming an extra protective film on the metal. Oxygen scavengers are known to inhibit corrosion by forestalling the cathodic depolarization brought about by oxygen. Sodium sulphate is the most regularly utilised oxygen scavenger at ambient temperatures [102].

2.4.2.4 Mixed Corrosion Inhibitors

Mixed inhibitors function by suppressing both the cathodic and anodic corrosion reactions. They do this by adsorption on the whole metal surface, thereby forming a thin protecting film [107]. The film formed causes the formation of precipitates on the surface of the metal, blocking indirectly both cathodic and anodic sites. Mixed inhibitors are often referred to as film-forming inhibitors or adsorption inhibitors. Nowadays they are amongst the most used inhibitors for concrete. Phosphates and silicates are the most used mixed corrosion inhibitors. Sodium silicate is utilised in domestic water softeners to prevent the occurrence of rust water. Mixed inhibitors minimize the corrosion rate

without a significant change in the corrosion potential. The total effects on the corrosion potential are negligible but may shift towards either the cathodic or the anodic site [102, 108].

2.4.2.5 Precipitation Inhibitors

These are known as film-forming compounds that have a general action over the metal surface, thereby blocking both anodic and cathodic sites directly on the metal surface. Precipitation inhibitors are compounds that provide protective film by forming precipitates on the surface of the metal. Hard water that is very high in calcium and magnesium is known to have high level of salt which precipitate on the metal surface and form a protective film; therefore, this hard water is less corrosive than soft water with normal nutrients level. Phosphates and silicates are the most widely known inhibitors of this category. For example, sodium silicate is utilised in numerous domestic water softeners to forestall the occurrence of rust water. This sodium silicates also protects metals such as steel, brass, and copper in aerated hot water system. However, the protection of the metal is not always reliable since it relies on the pH and a saturation index that depends on water composition and temperature. Chromates and nitrates provide a very high degree of protection compared to silicates and sulphates; however, they are very important in circumstances where nontoxic additives are required [109].

2.4.2.6 Volatile Organic Inhibitors

Volatile corrosion inhibitors (VCIs) are compounds that are transported in a closed environment to the site of corrosion by volatilization from a source. This kind of inhibitors are additionally known vapor phase inhibitors (VPIs) [110]. Example of these inhibitors are found in boilers, where steam transport the volatile basic compounds like hydrazine or morpholine to forestall corrosion in condenser tubes by shifting the surface pH or neutralizing acidic dioxide towards less acidic and corrosive values. Volatile solids like salts of cyclohexylamine, hexamethylene-amine and dicyclohexylamine are utilised in closed vapor spaces such as shipping containers [111]. The vapor of these salts condenses on contact with the metal and is hydrolysed by any dampness to free defensive ions. An efficient volatile corrosion inhibitor is desired to provide inhibition quickly and to keep going for a lengthy period. These characteristics rely upon the volatility of these compounds, quick action requiring high volatility, while enduring protection requires low volatility.

2.5 Flavonoids

Flavonoids are a group of plant metabolites found in different fruits and vegetables which are thought to give health benefits through cell signalling pathway and antioxidant effects. They are polyphenolic molecules which dissolve in water and contains 15 carbon atoms and are normally used medicinally

because of their anti-allergic, anti-cancer, anti-inflammatory, and anti-viral activities [112, 113]. They contain two benzene rings connected by a three-carbon chain. One of the carbons in this chain is connected to a carbon in one of the benzene rings, either directly or through an oxygen bridge, which gives a third middle ring. Flavonoids are all good candidates for corrosion inhibitors since they contain benzene rings with π-electrons in conjugated double and electronegative functional group oxygen which is a characteristic of a good corrosion inhibitors [36, 100].

Flavonoids can be subdivided into various subgroups depending on the carbon of the C ring which the B ring is attached and the oxidation state and degree of unsaturation of the C ring. Flavonoids in which the B ring is connected in position 4 are called neoflavonoids. Those in which the B ring is connected in position 3 of the C ring are called isoflavones, while those in which the B ring is connected in position 2 can be further subdivided into several subgroups on the basis of the structural features of the C ring. These subgroups are: flavonols, flavanones, flavanonols, flavanols or catehins, anthocyanins and chalcones (figure. 1) [114]. Below is the figure showing the different types of flavonoids subgroups and examples.

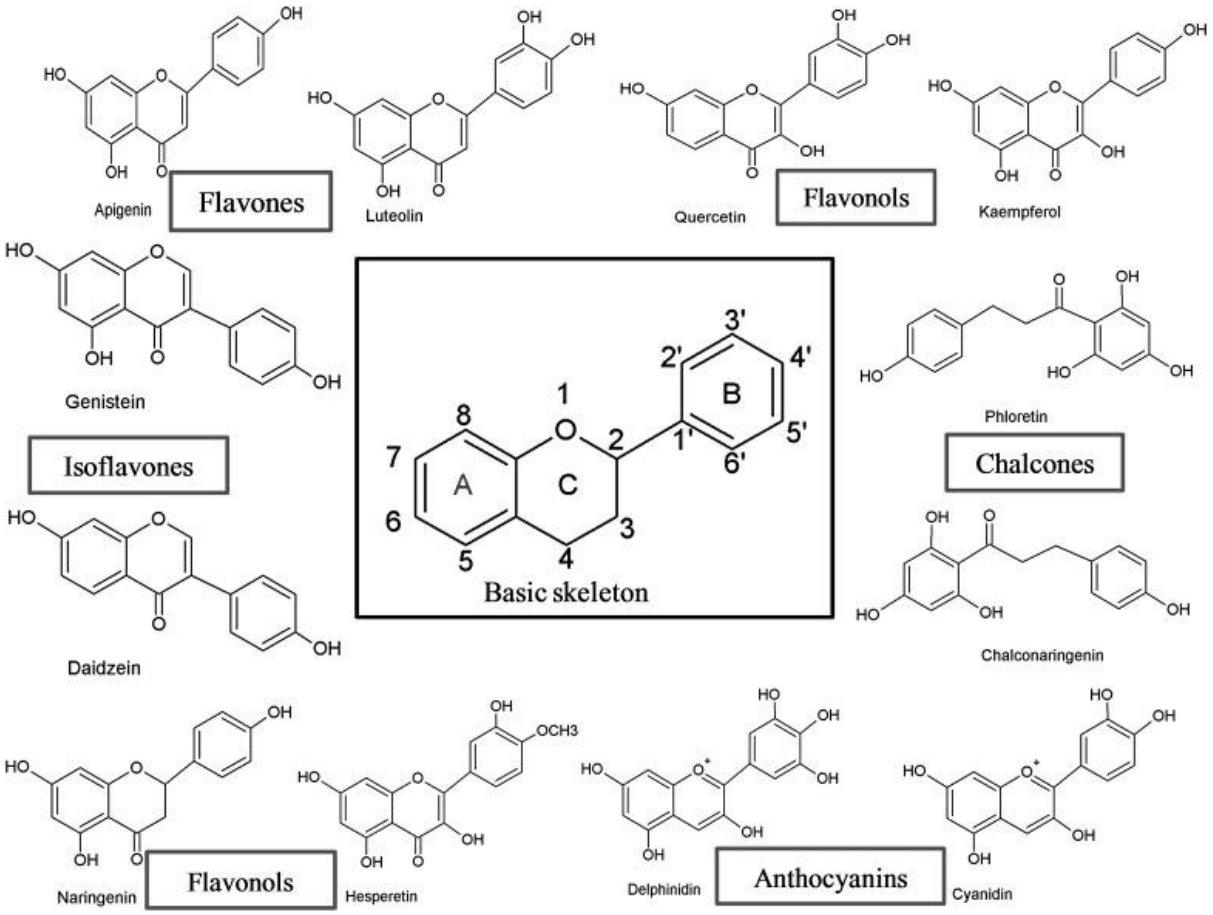

Figure 2.8: different types of flavonoids subgroups and examples [114].

2.5.1 Development of Flavonoids

Flavonoids are a diverse group of secondary plant substances and because of their strong pigments, they are responsible for the bright colours of numerous kinds of vegetables, flowers and fruits and also for the colours in autumn leaves. Flavonoids are also referred to as bioflavonoids. They were discovered by Albert Szent-Györgyi, one of the few successful chemist in the twentieth century. He discovered the flavonoids while working on the isolation of vitamin C. Because of his hard work, he was awarded the noble prize in 1937 for his discovery and description of vitamin C [115]. The term flavonoid was first utilised in 1952 by the German research scientists Geissmann and Hinreiner. These scientists were also responsible for the classification system based on the structure of the core of the basic flavonoids structure which is the oxygen-containing pyran ring. Today flavonoids are the largest group of polyphenols and up to date more than 8000 polyphenols are known. In addition, more than 5,000 naturally occurring flavonoids have been isolated from various plants [116].

2.5.2 Flavonoids as Corrosion Inhibitors

Flavanones are a group of natural substances with variable phenolic structures found in fruits, vegetables, balk,roots, grain, sterm, flowers, wine and tea [114]. Since flavonoids are original plants products, they contain organic compounds such as alkaloids, tannis, pigment, amino and organic acids, and are mostly known to have the inhibitive action. Heterocyclic compounds that contain N, O and S atoms, like pyrans and their derivatives, have drawn much attention because of their efficient inhibition capabilities on the metal. Heteroatoms like N, O and S usually becomes the dynamic focal point of inhibition. These atoms donate lone pairs of electrons to the vacant orbitals of the metal atom, when a metal is immersed in inhibiting solution. Thereafter strong and stable bonds are formed between the inhibitor and the surface of the metal during the self -assembling process [26].

Corrosion inhibition characteristics of numerous substances are directly related to adsorption phenomena, which can follow various types of isotherms like those of Langmuir, Temkin, Freundlich and Frumkin that have been utilised to help adsorption phenomena over the steel electrode. The adsorption of organic inhibitors at the electrode or electrolyte interface may occur through displacement of adsorbed water molecules at the inner Helmholtz plane of the electrode, likely in concurrence with the accompanying reaction scheme [26];

$$Org_{(sol)} + nH_2O_{(ads)} \rightarrow Org_{(ads)} + nH_2O_{(sol)} \quad (33)$$

2.5.3. Plant Extracts as Corrosion Inhibitors

Naturally produced compounds like plant extracts can be utilised as corrosion inhibitors because of their eco-friendly nature. These compounds normally contain oxygen and are widely studied and reported [95]. Amongst others this includes compounds that falls under the flavonoids group.

AL-Qudah investigated the effects of some substituted flavonoids compounds (apigenin, luteolin-3-methyl ether, quercetin-3,3-dimethyl ether and jaceidine) on copper corrosion in 2.0 M HNO_3 for 4 hours at various temperatures by gravimetric analysis. It was found that the percentage inhibition efficiency (%IE) increases as concentration of the flavonoids increases and reaches optimum value because of the formation of a monolayer film on the metal surface. In some of the flavonoids studied, the inhibition efficiency of 92 % was observed. It was also observed that as the temperature increases, the percentage inhibition decreases. The %IE of quercetin-3,3-dimethylether and jaceidine are very high even at low concentrations, indicating that both compounds adsorbed strongly at the surface of copper metal due to a decrease in steric effect. The activation energy (E_a) was found to be 114.1, 123.8, 127.3 and 132.9 kJ/mol for all the compounds, respectively. The E_a for copper in 2.0 M HNO_3 without the presence of the inhibitor was found to be equal to 73.4 kJ/mol, which is in accordance with literature value. The author found this results in accordance with the strength of adsorption on the surface of copper metal [113].

Ikeuba et al. reported the inhibitive properties of flavonoids extracted from Gongronema latifolium (FEGL) and the crude extracts from Gongronema latifolium (EEGL) on the corrosion of mild steel in H_2SO_4 solutions using hydrogen evolution method at 30 – 60° C. According to the authors the results revealed that the extracts function as good inhibitors for the corrosion of mild steel in 5.0 M H_2SO_4 solutions. It was observed that the inhibition efficiency increases with increase in EEGL and FEGL concentration from 1.0 g/L to 10 g/L, attaining a maximum of 86.7 and 94.2 at 10.0 g/L for FEGL and EEGL respectively. The order of efficiency was found to be EEGL > FEGL. The authors proposed that the adsorption mechanism of the extracts was physical adsorption on the surface of mild steel. They also reported that, the negative values of ΔG; -9.88 to -9.12 KJ/mol for FEGL and -10.69 to -13.97 KJ/mol for EEGL indicate spontaneity and stability of the adsorption layer [117].

Olubunmi and Nwaugbo studied the corrosion of mild steel in sulphuric acid by flavonoids, separated from Nypa fruticans Wurmb (catechin) leaves extracts using gravimetric analysis at 303 – 353 K. The constituents were separated by fractionation using Soxhelt apparatus after room temperature extraction with 70% acetone. The constituents were said to be identified using standard functional group analysis method also known as (phytochemical screening). Five inhibitors concentrations of 0.1 g/L, 0.2 g/L, 0.3 g/L, 0.4 g/L and 0.5 g/L were used in 0.1 M, 0.5 M, 1 M and 2 M concentrations of acid

solutions. The authors found that the inhibition efficiency increased with increase in temperature and inhibitors concentration. A maximum efficiency of 74.48% was obtained at 323 K and 0.5 g/L of the flavonoid's constituent. The authors concluded that the flavonoid – catechin, separated from Nypa fruticans Wurmb leaves extract by differential extraction, can be used as a pure, safe, environment friendly and efficient corrosion inhibitor of mild steel in sulphuric acid at 303 - 353 K [118].

Gopiraman and co-workers investigated the inhibition effects of 2,3-dihydroxyflavone on the corrosion of mild steel in 100 – 600 ppm aqueous hydrochloric acid solution by electrochemical impedance spectroscopy and weight loss. The authors found that the corrosion inhibition efficiency increases with increasing concentration of the inhibitor and the time the mild steel was immersed in the hydrochloric acid solution. For example, it was clear that the inhibitor shows maximum inhibition of 96.45% at 600 ppm concentration. The effect of temperature on the corrosion behaviour of mild steel in 1 M HCl solution with the addition of the inhibitor was also studied and found that the corrosion of mild steel increases as the temperature increases even when the inhibitor is added but this happens at a very slow rate compared to the case without the inhibitor. The authors also reported that the adsorption mechanism of the inhibitor was due to physisorption. The free energy of adsorption (G_{ads}) for the inhibitor was found to be around -30 kJ/mol and it was categorised as mixed type inhibitor [119].

2.6. Acids Normally used as Corrosive Medium

Hydrochloric acid is the most used acid to evaluate the corrosion inhibition effects of various compounds because of its clear and simple corrosion mechanism. Sulphuric acid is the second most used acid to study corrosion inhibition. Nitric acid is normally used for nonferrous metal and alloys. Nitric acid is rarely used in the test related to steel because it is not only an acid but also an oxidizing agent. More details about these acids are given below.

2.6.1. Hydrochloric Acid

Hydrochloric (HCl) acid which is also called muriatic acid is a colourless corrosive acid which has a destructive pungent smell. It was discovered in 800 AD by the alchemist Jabir Ibn Hayyan. It was called acidum salis and spirirts salt because it was produced from iron (II) sulfate (green vitriol) and rock salts. HCl is regarded as a very strong acid with plenty industrial application among which, when it reacts with an organic base, it forms a hydrochloric salt. It is also used industrially in hydrometallurgical processing, activation of petroleum walls and miscellaneous cleaning which includes metal cleaning [120]. This acid is being used in industries despite its strong corrosive capability, especially in metals.

Therefore, there is a need to find organic compounds that will be used as inhibitors to effectively protect the metals from being attacked by this acid. In recent years hydrochloric acid was being produced from the reaction of sodium chloride and sulphuric acid.

$$2NaCl_{(s)} + H_2SO_{4\ (l)} \rightarrow 2HCl_{(g)} + Na_2SO_{4\ (s)} \quad (34)$$

2.6.2. Sulphuric Acid

Sulphuric acid also referred to as vitriol is a mineral acid which is colourless, odourless, and sweet fluid that dissolves in water. It is synthesized by reactions which are profoundly exothermic. Sulphuric is an essential raw material utilized in various mechanical (industrial) procedures and assembling (manufacturing) activities. A huge amount of sulphuric acid fabricated is utilised in the production of phosphate fertilizers. Other utilizations incorporate copper leaching, inorganic pigment production, petroleum refining and industrial organic production. It is produced from elemental sulfur in three phase process [120].

$$S_{(s)} + O_{2\ (g)} \rightarrow SO_{2\ (g)} \quad (35)$$

$$2SO_{2\ (g)} + O_{2\ (g)} \rightarrow 2SO_{3\ (g)} \quad (36)$$

$$SO_{3\ (g)} + H_2O_{(l)} \rightarrow H_2SO_{4\ (l)} \quad (37)$$

The corrosiveness of sulphuric acid can be attributed to its strong acidic nature. At high concentration its corrosiveness is ascribed to its oxidizing and dehydrating properties. Because of its corrosiveness, it is important to find more effective ways to protect the metals that it comes into contact with.

2.6.3. Nitric Acid

Nitric acid widely referred to as spirit of inter and as aqua Fortis is a very corrosive mineral acid which is colourless. It is the primary reagent used for nitration (the addition of -NO_2) to an organic molecule. Nitric acid is also utilised in the manufacturing of explosives like trinitrotoluene (TNT) derivatives, nitro-benzene derivatives and dinitrotolune derivatives and for the production of other chemicals intermediate. Nitric acid is made by the reaction of nitrogen dioxide and water [121].

$$4NO_{2\ (g)} + 2H_2O_{(l)} \rightarrow 2HNO_{3\ (l)} + NO_{(g)} + NO_{2\ (g)} + H_2O_{(l)} \quad (38)$$

CHAPTER 3

EXPERIMENTAL PROCEDURE

3.1 Metal Specimens

All the experimental procedures were performed using aluminium specimens of approximately 99 wt % and Zinc sheets with 99.09 wt % purity. The gravimetric test was conducted on aluminium and zinc metal sheets. The metals used in gravimetric test were having the surface area of 12 cm^2, with zinc metals weighing approximately 2.500 g and aluminium metals weighing approximately 1.000 g. For electrochemical studies, only 1 cm^2 surface of the metal coupon was exposed on the epoxy resin. Before each measurement, the aluminium and zinc metals attached to the epoxy resin were mechanically abraded on the Struers Labosystem instrument to remove traces of epoxy resin on the surface for clear measurements.

3.2 Solutions

The destructive solutions of 1.5 M H_2SO_4, 1.5 and 0.5 M HCl were carefully prepared in 1000 ml volumetric flasks by dilution of the analytical reagent 98 % sulphuric acid and 32 % hydrochloric acid, respectively by the addition of exact amounts of distilled water. These acids were purchased from Sigma-Aldrich. A stock solution of 5.2 x 10^{-3} M of corrosion inhibitors was prepared by the addition of exact amount of distilled water. To ensure complete dissolution of the flavonoid derivatives used as inhibitors, a small amount of 1-methyl-2-pyrrolidinone and 2-pyrrolidinone was first used to dissolve the compounds before adding distilled water to make stock solution. From the stock solution, a series of concentrations (2.0 x 10^{-4} – 1.8 x 10^{-3} M) were prepared through the usage of appropriate amounts of distilled water.

3.3 Corrosion Inhibitors

All the flavonoids corrosion inhibitors, namely, 5,7-trihydroxy-4H-chromen-4-one hydrate (Morin hydrate (MNHD)), 6-hydroxyflavone (6-HFN) and 5,7-dihydroxy-2-(4-hydroxyphenyl) chroman-4-one (Naringenin (NRNG)) were sourced from Sigma-Aldrich Chemicals and were used in as-received condition. The working solutions in the concentration range of 2.0 x 10^{-4} M to 1.8 x 10^{-3} M were prepared for each flavonoid derivative from the stock solution of 5.2 x 10^{-3} M. The names and structures of the flavonoid derivatives used in this study are shown in Figure 3.1.

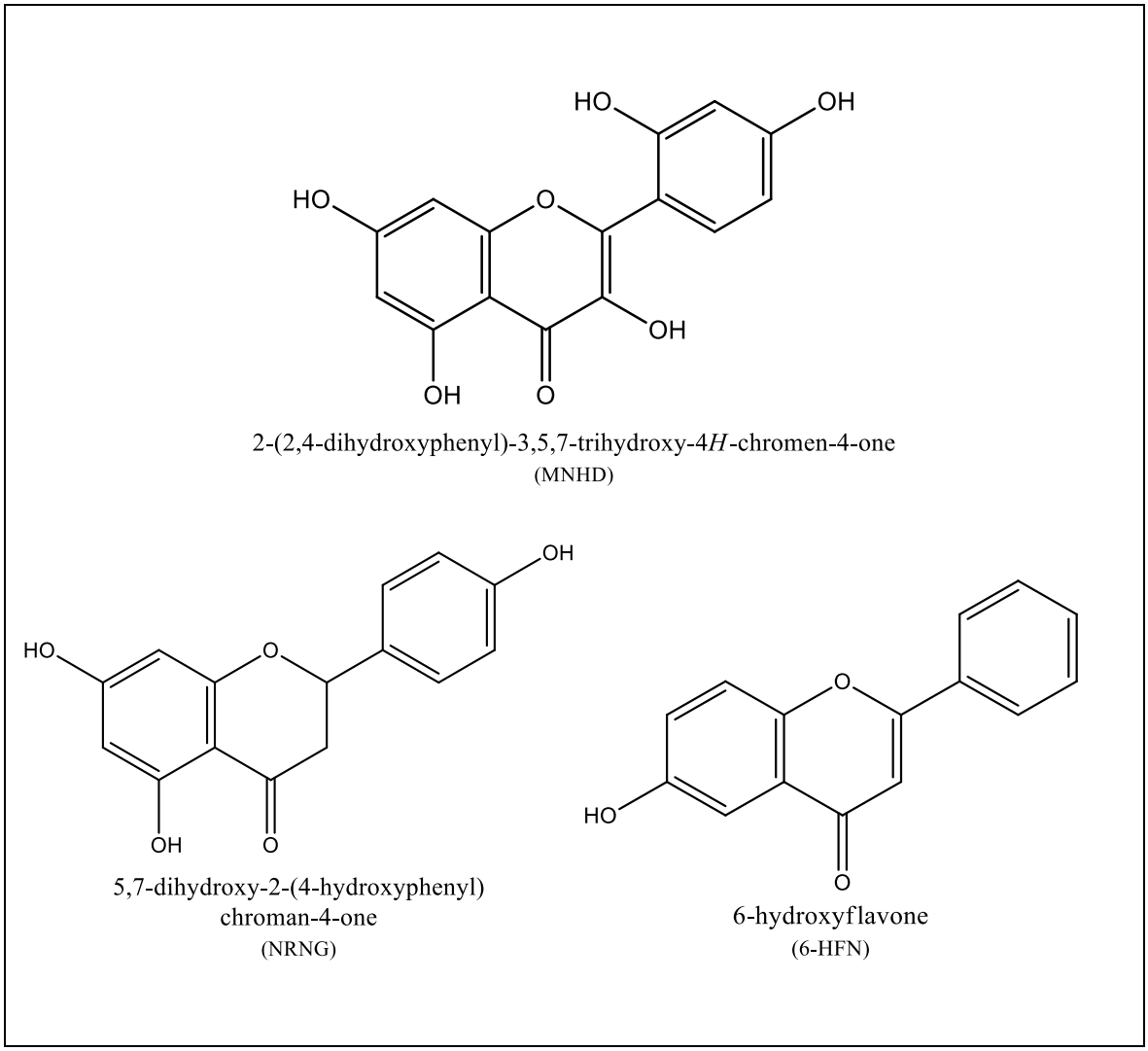

Figure 3.1: Molecular structures of the flavonoid derivatives used as corrosion inhibitors in this study.

3.4 Fourier Transform Infrared Spectrometer (FTIR)

Amongst other molecular vibrational spectroscopic techniques, FTIR is the most widely utilised technique for the identification of organic functional groups and for structural elucidation. The wavenumber region 1.3 x 10^4 – 3.3 x 10^1 cm^{-1} (which is between microwave and UV visible light) in the electromagnetic spectrum is where the infrared band is found [122]. The layer of the inhibitor that was adsorbed on the surface of zinc and aluminium metals in 0.5 and 1.5 M hydrochloric and sulphuric acids at 30 °C were removed off with a knife and the powder obtained was analysed using the FTIR. The procedure was also done on the metals in the absence of the inhibitors at 30°C, this time the corroded layer due to acid was the one removed off the metals and analysed. The pure compounds were also analysed under the FTIR.

The analysis method of FTIR is regarded as both quantitative and qualitative. In the quantitative method, the area under the FTIR adsorption bands is used to determine the concentration of the compound for the selected spectrum region. This concentration is obtained using the Beer-Lambert law by establishing a standard curve from the spectra for known concentration. The law states that for a given layer thickness (I), the temperature, T(λ), (i.e.), ratio of the transmitted and the incident radiation) is directly proportional to the concentration (C) as given by equation (39) below:

$$A(\lambda) = -\log_{10} T(\lambda) = -\log_{10} \frac{I}{I_o} = \varepsilon(\lambda) \mathrm{IC} \tag{39}$$

where A(λ) is the absorbance and Ɛ(λ) is the absorptivity at wavelength λ.

In the qualitative analysis, the infrared spectrum of the material being investigated is collected and compared against that of the reference sample. The specificity of the FTIR bands allows the computerised data searches within reference libraries to identify the material [123].

3.5 2D and 3D (Dimension) Microscope

The 2D and 3D surface analysis on zinc and aluminium metals in the presence of the highest concentration used of each of the three inhibitors (NRNG, MNHG and 6-HFD) and the highest concentration used of the two acids (HCl and H_2SO_4) were evaluated using the OLYMPUS DSX – CB Microscope fitted with DSX software. The images were taken in the lowest magnification range of 139x. The zinc metals where immersed in the mixture of the inhibitors and H_2SO_4 for 5 hours, and HCl for 8 hours, while the aluminium metals were immersed in the mixture of inhibitors and HCl solution for 3 hours.

3.6 Gravimetric Analysis

The gravimetric weight loss method is one of the most precise and accurate technique of macro quantitative analysis. This method is cost effective and simple to conduct. The weight loss method was performed by first weighing all the metals that were going to be used with the ACCULAB electronic top loading balance. The weighed metals were suspended by means of glass rod and hook in 100 ml beakers containing different concentrations of acid and inhibitors solutions. The different concentrations used were 0.1 M, 0.3 M, 0.5 M, 1.0 M and 1.5 M. The beaker together with the metal was placed inside a water bath at various temperatures of 30° C, 40° C, 50° C and 60° C for 3 and 8 hours in hydrochloric acid and 5 hours in sulphuric acid. After the mentioned hours, the metals were removed, cleaned with a brushed and rinsed in distilled water. The metals were then dried for 10 minutes and reweighed again to get the mass difference, and this is normally called a blank test.

Another gravimetric method for one inhibitor was conducted with 50% of each of the five different concentrations of the inhibitor (i.e., 2.0 x 10^{-4} M, 6.0 x 10^{-4} M, 1.0 x 10^{-3} M, 1.4 x 10^{-3} M and 1.8 x 10^{-4} M) and 50 % of 1.5 M and 0.5 M acids solutions, and when the experiment was done, the metals were removed and dried. This method was repeated but this time around after the above-mentioned hours, the metals were removed, cleaned with a brush in distilled water and then desiccated for about 10 minutes before being weighed to get the mass different. This method was conducted for the other inhibitors in the same way.

From the change in the mass of the metals, the rate of corrosion was calculated using equation (17). [124]

$$\rho = \left(\frac{\Delta w}{st}\right) \tag{17}$$

The degree of surface coverage was also calculated using the following equation:

$$\theta = \left(1 - \frac{\rho 1}{\rho 2}\right) \tag{40}$$

where: θ = The degree of surface coverage

ρ_1 = The corrosion rate of metal in the presence of inhibitor

ρ_2 = The corrosion rate of metal in the absence of inhibitor

The percentage inhibition efficiency was also calculated using the following expression [125 – 129]:

$$\%IE = \left(1 - \frac{\rho 1}{\rho 2}\right) \times 100\% \tag{41}$$

where: IE = Inhibition efficiency

ρ_1 = The corrosion rate of metal in the presence of inhibitor

ρ_2 = The corrosion rate of metal in the absence of inhibitor.

3.7 Electrochemical Studies

Electrochemical studies were performed using a three-electrode cell SP-150 Biologic instrument. The three electrodes were: working electrode (WE), reference electrode (RE) which is Ag/AgCl and counter electrode (CE) which is graphite. The working electrode is the metal under investigation (aluminium and zinc). The reference electrode is used as a reference when measuring the potential of the working

electrode and hence no current flows through the reference electrode. The purpose of the counter electrode is to provide an electron source for the working electrode. The electrochemical analysis that was used in this study were Potentiodynamic Polarization (PDP) and Electrochemical Impedance Spectroscopy (EIS). The metals were also allowed to corrode in Open Circuit Voltage (OCV) freely for a period of 30 minutes for reliable results.

3.8 Electrochemical Impedance Spectroscopy (EIS)

The EIS was utilised to evaluate the corrosion of aluminium and zinc in 1.5 M hydrochloric, 1.5 and 0.5 M sulphuric acids and the data was utilised to calculate the percentage inhibition efficiency. This procedure was performed on a scan rate with final frequency of 100,000 KHz and initial frequency of 0.100 Hz and sinus amplitude of 10.0 mV.

The percentage inhibition efficiency in the EIS was calculated by using equation (42):

$$\%IE_{EIS} = \left(1 - \frac{R^0 ct}{Rct}\right) \times 100 \quad (42)$$

where R°_{ct} and R_{ct} are the charge transfer resistance in the absence and presence of the inhibitor.

3.9 Potentiodynamic Polarization (PDP)

Electrochemical parameters like the corrosion potential, corrosion current density, anodic and cathodic Tafel slopes were obtained by using PDP. This procedure was performed in scan (E_{WE}) of 50.0 mV/s. The potential (E) was run from -0.600 to 0.600 V. The corrosion current density values measured were utilised to calculate the inhibition efficiency by using the equation (43) given below:

$$\%IE_{PDP} = \left(\frac{i^0_{corr} - i^i_{corr}}{i^i_{corr}}\right) X100 \quad (43)$$

where i^0_{corr} and i^i_{corr} are values of corrosion current density in absence and presence of inhibitor, respectively.

3.10 Atomic Absorption Spectroscopy (AAS)

Atomic absorption spectroscopy is an analytical technique that measures the concentrations of the elements in which free gaseous atoms absorb electromagnetic radiation at a specific wavelength to produce a measurable signal [130]. This technique utilises wavelengths of light that are absorbed specifically by an element. These wavelengths are equivalent to the energies needed to promote electrons from one energy level to another, higher or lower energy level. AAS is very sensitive that it

can measure down to parts per billion of a gram. It is the most frequently used technique for the quantitative determination of elements in different materials at ultra-trace and trace level [131]. In terms of corrosion studies, the AAS will be used to analyse the concentration of the metals that would have remained in the solution after the gravimetric analysis at different concentrations of the flavonoids compounds and acids while varying the temperature. This procedure will help to understand the effect of flavonoids compounds as corrosion inhibitors for zinc and aluminium metals in the presence of H_2SO_4 and HCl at various temperatures.

CHAPTER 4

RESULTS AND DISCUSSION

4.1 Flavonoid Derivatives

In this section, the results of flavonoid derivatives compounds [Naringenin (NRNG), Morin hydrate (MNHD) and 6-hydroxyflavone (6-HFN)] will be displayed and discussed for zinc and aluminium metals in sulphuric and hydrochloric acids.

4.1.1 Gravimetric Test

The weight loss method was performed for zinc and aluminium metals, whereby the metals were first weighed before being immersed in the acidic solution. After the chosen immersion time elapsed, the metals were taken out of the solution and re-weighed to get the mass difference. The weight loss method was performed at various concentrations of the acid and varying temperatures (30 – 60°C) and this is called the blank test. This method was also performed using equal proportion of various concentrations of the inhibitors and a fixed 0.5 and 1.5 M HCl and 1.5 M H_2SO_4 solution at the same temperatures as those of the blank test. Generally, corrosion of metals increases with increasing corrodent concentration and temperature. This has been strongly attributed to the fact that reaction rates increase with an increase in temperature and concentration [132]. The results obtained are presented in Tables 4.1 – 4.3 and graphically presented in Figures 4.1 – 4.3.

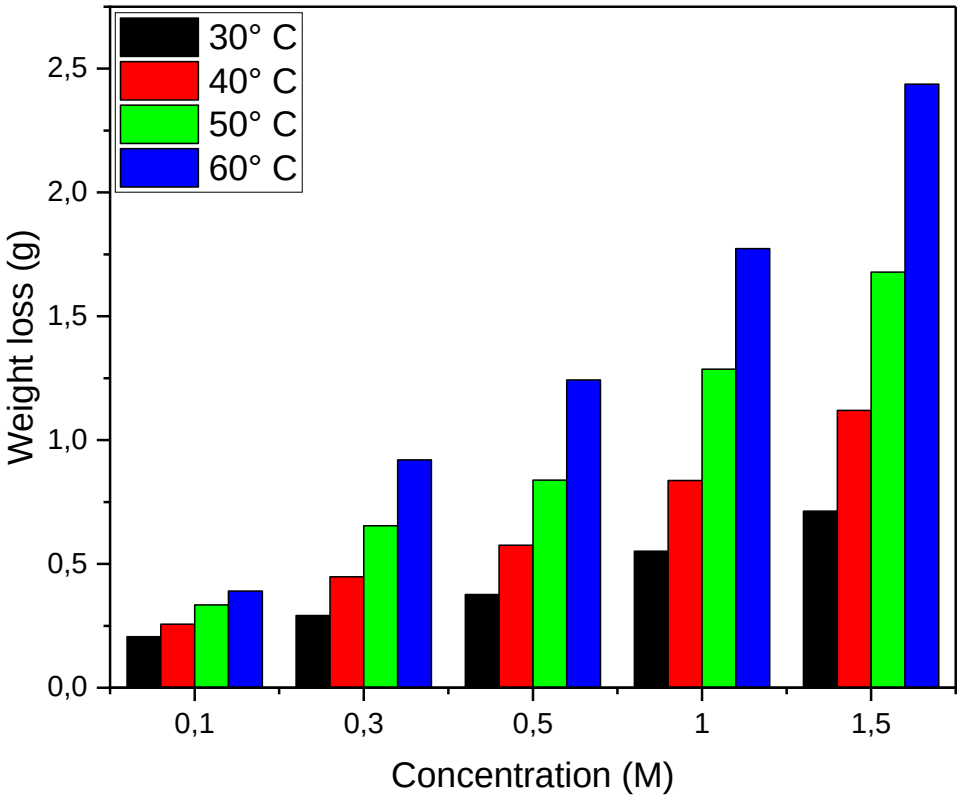

Figure 4.1: Weight loss graph for zinc in five different concentrations of sulphuric acid.

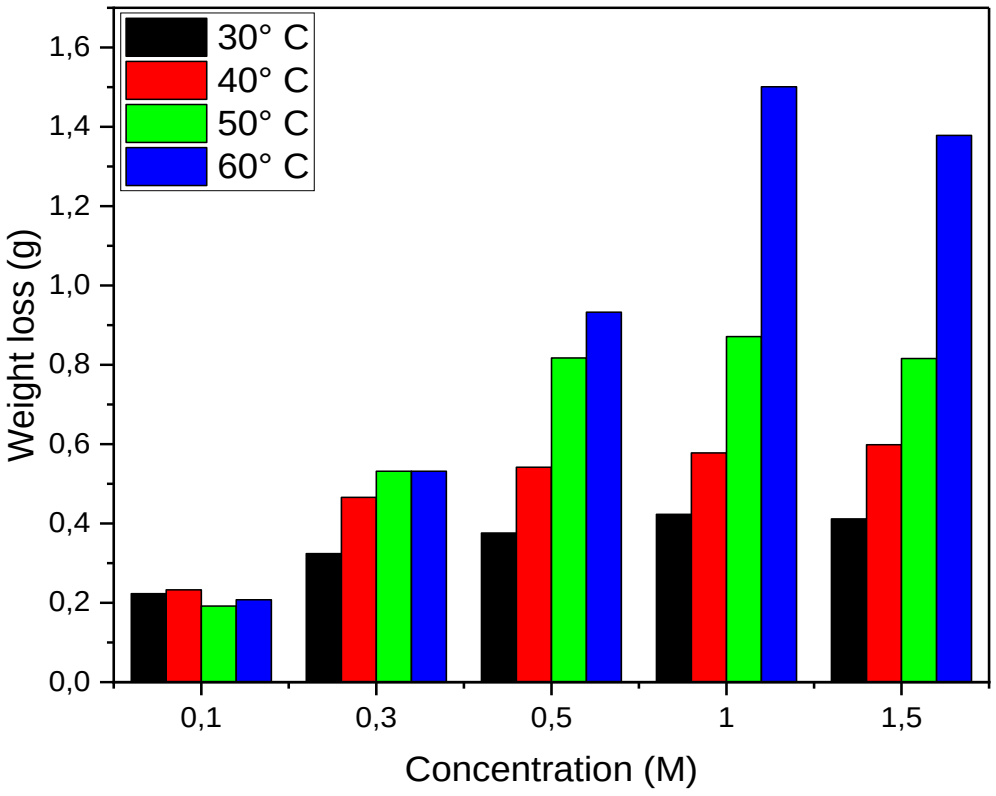

Figure 4.2: Weight loss graph for zinc in five different concentrations of hydrochloric acid.

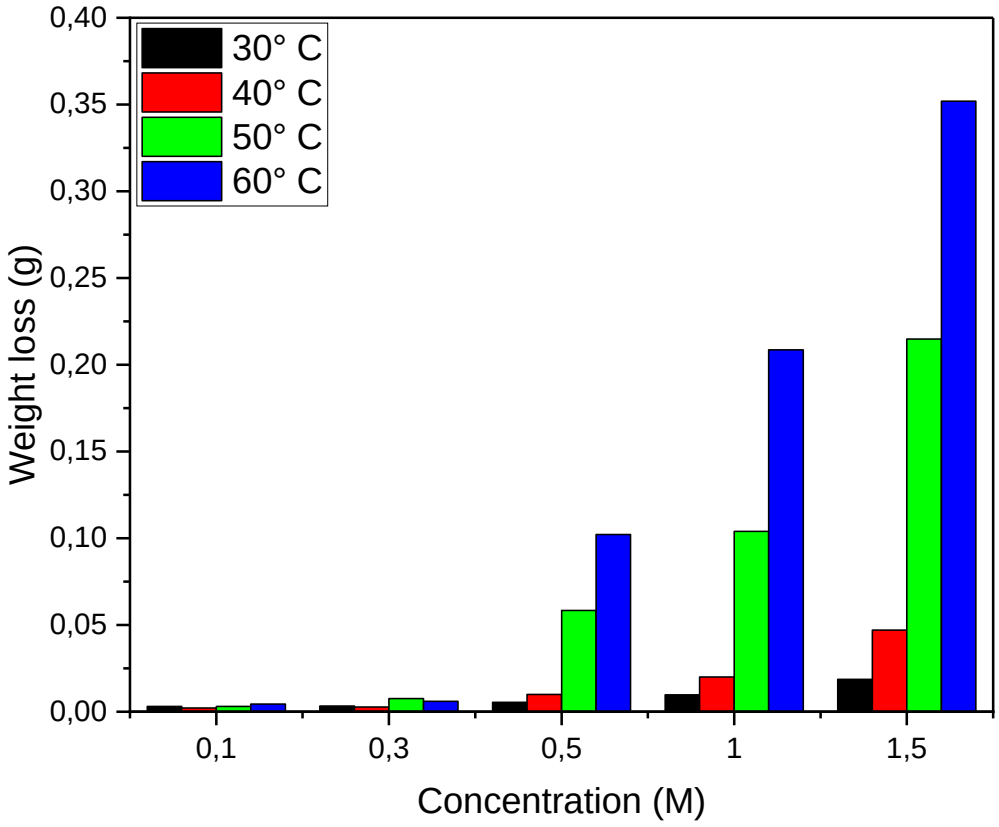

Figure 4.3: Weight loss graph for aluminium in five different concentrations of hydrochloric acid.

Figures 4.1 – 4.3 show the weight loss of zinc and aluminium metals in five different concentrations of hydrochloric and sulphuric acids solutions at 30 – 60° C. A smooth trend is observed in the figures whereby there is an increase in the weight loss as the concentration of the acid is increased. It can also be observed that the weight loss of the metals is directly proportional to the increase in temperature. However, in Tables 4.1 and 4.3, at 0.1 M concentration, it can be seen that there is no proper trend, which could be because of the minimal concentration used with its significant close to that of a solution with no acid (water).

Table 4.1: Weight loss measurements and corrosion rate of zinc metal in H_2SO_4 from 0.1 – 1.5 M, in the absence of the corrosion inhibitors.

Acid	Temperature (° C)	Acid concentration (M)	Weight loss (g)	Corrosion rate ($g.cm^{-2}.h^{-1}$)
Sulphuric acid	30	0.1	0.2062	0.006873
		0.3	0.2920	0.009733
		0.5	0.3764	0.012547
		1.0	0.5514	0.018380
		1.5	0.7134	0.023780
	40	0.1	0.2566	0.008553
		0.3	0.4480	0.014933
		0.5	0.5758	0.019193
		1.0	0.8368	0.027893
		1.5	1.1201	0.037337
	50	0.1	0.3342	0.011140
		0.3	0.6537	0.021790
		0.5	0.8385	0.027950
		1.0	1.2865	0.042883
		1.5	1.6780	0.055933
	60	0.1	0.3908	0.013027
		0.3	0.9204	0.030680
		0.5	1.2427	0.041423
		1.0	1.7733	0.059110
		1.5	2.4370	0.081233

Table 4.2: Weight loss measurements and corrosion rate of zinc metal in HCl from 0.1 – 1.5 M, in the absence of the corrosion inhibitors.

Acid	Temperature (° C)	Acid concentration (M)	Weight loss (g)	Corrosion rate ($g.cm^{-2}.h^{-1}$)
Hydrochloric acid	30	0.1	0.2233	0.004652
		0.3	0.3239	0.006748
		0.5	0.3761	0.007835
		1.0	0.4233	0.008819
		1.5	0.4115	0.008573
	40	0.1	0.2325	0.004844
		0.3	0.4660	0.009708
		0.5	0.5420	0.011292
		1.0	0.5778	0.012038
		1.5	0.5985	0.012469
		0.1	0.1918	0.003996
		0.3	0.5315	0.011073
		0.5	0.8172	0.017025
		1.0	0.8712	0.018150
		1.5	0.8159	0.169979
	60	0.1	0.2075	0.004323
		0.3	0.5318	0.011079
		0.5	0.9325	0.019427
		1.0	1.5008	0.031267
		1.5	1.3782	0.028713

Table 4.3: Weight loss measurements and corrosion rate of aluminium metal in HCl from 0.1 - 1.5 M, in the absence of the corrosion inhibitors.

Acid	Temperature (° C)	Acid concentration (M)	Weight loss (g)	Corrosion rate ($g.cm^{-2}.h^{-1}$)
	30	0.1	0.0031	0.000172
		0.2	0.0033	0.000183
		0.3	0.0054	0.000300
		0.4	0.0097	0.000539
		0.5	0.0187	0.001039
	40	0.1	0.0022	0.000122
		0.2	0.0027	0.000150
		0.3	0.0100	0.000556
		0.4	0.0200	0.001111
		0.5	0.0471	0.002617

Hydrochloric acid				
	50	0.1	0.0031	0.000172
		0.2	0.0076	0.000422
		0.3	0.0584	0.003244
		0.4	0.1040	0.005778
		0.5	0.2148	0.011933
	60	0.1	0.0044	0.000244
		0.2	0.0060	0.000333
		0.3	0.1022	0.005678
		0.4	0.2086	0.011589
		0.5	0.3519	0.019550

From Tables 4.1 - 4.3, it is evident that the weight loss increases with an increase in the concentration of the acid and temperature. Between the two acids used in zinc, sulphuric acid was found to be the most destructive one, with the weight loss of 2.4370 g at maximum concentration and temperature compared to 1.3782 g for hydrochloric acid. For aluminium in hydrochloric acid, the maximum weight loss observed was also at the highest temperature and concentration with a value of 0.3519 g. From the tables, it can be observed that the corrosion rate is found to increase with an increase in the concentration of the acids and the temperature. For instance, the corrosion rate of zinc in sulphuric acid at 60°C was found to be 0.013027, 0.030680, 0.041423, 0.059110 and 0.81233 $g.cm^{-2}.h^{-1}$ at 0.1, 0.3, 0.5, 1.0 and 1.5 M respectively. Through a careful observation of Tables 4.1 – 4.3 above, it can be seen that similar trend is obtained for all the acids and metals studied. The high corrosion rate of zinc in HCl even though it has more positive reduction potential compared to aluminium might be because of the ability of aluminium to form an oxide layer which resist to some point corrosion to further takes place on the metal and because of the small acid concentration used in aluminium metal.

4.1.2 Weight loss in the presence of inhibitors

The effects of introducing the inhibitor compounds, NRNG, MNHD and 6-HFN on the weight loss of zinc and aluminium metals, in 0.5 and 1.5 M HCl, and 1.5 M H_2SO_4 was studied at four different temperatures (30°C,40°C,50°C and 60°C) and in the absence and presence of five various concentrations ($2.0x10^{-4}$ M, $6.0x10^{-4}$ M, $1.0x10^{-3}$ M, $1.4x10^{-3}$ M and $1.8x10^{-3}$ M) of the inhibitors. The data obtained is shown in Table 4.4 – 4.6 and graphically represented in Figures 4.4 and 4.12. From these Figures, it can be seen that as the concentration of the inhibitors increases, the weight loss of the metals decreases. However, when the temperature of the corrosive environment was increased, the weight loss also increased specifically at the maximum temperature. The weight loss also increases with an increase in the time of immersion in acid solution, which is a period of 5 hours for H_2SO_4 and, 3 and 8 hours for HCl, as well as upon the increase in the acidic medium concentration. This is normally

attributed to the presence of air, water, and H^+ ions which speed up the corrosion process. Increase in concentration of the inhibitors and temperature of the surrounding often leads to an increase in the ionization and diffusion of active species in the corrosion process. Some authors reported that, above certain critical concentrations, the compounds used as inhibitors start to act as corrosion accelerators instead of inhibitors [132].

4.1.2.1 Zinc in 1.5 M sulphuric acid.

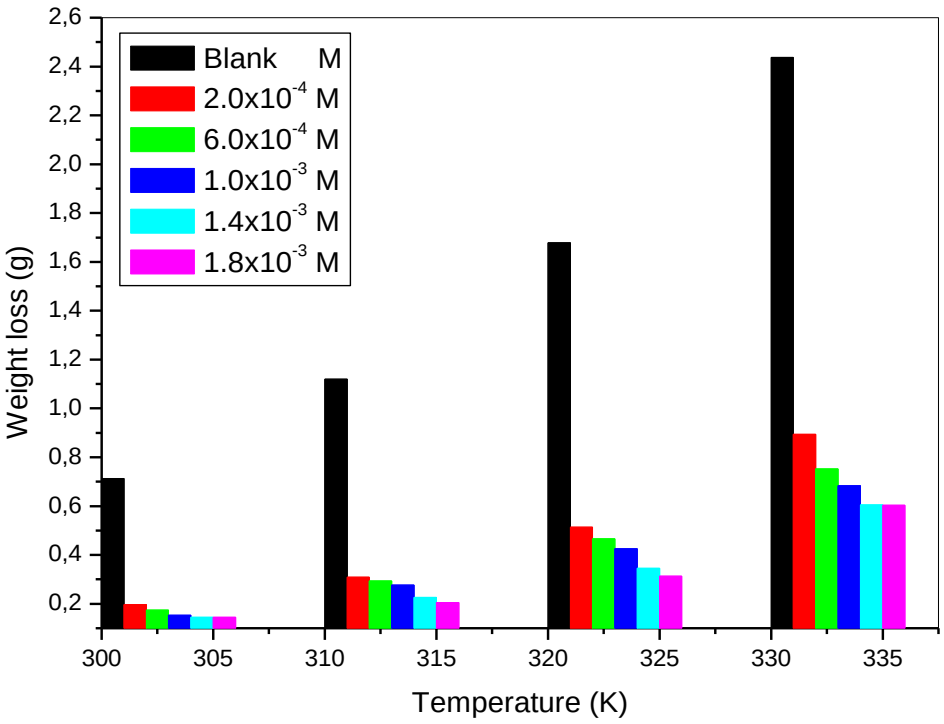

Figure 4.4: The graph showing the weight loss measurements of zinc metal in absence and the presence of NRNG in 1.5 M H_2SO_4 at different temperatures.

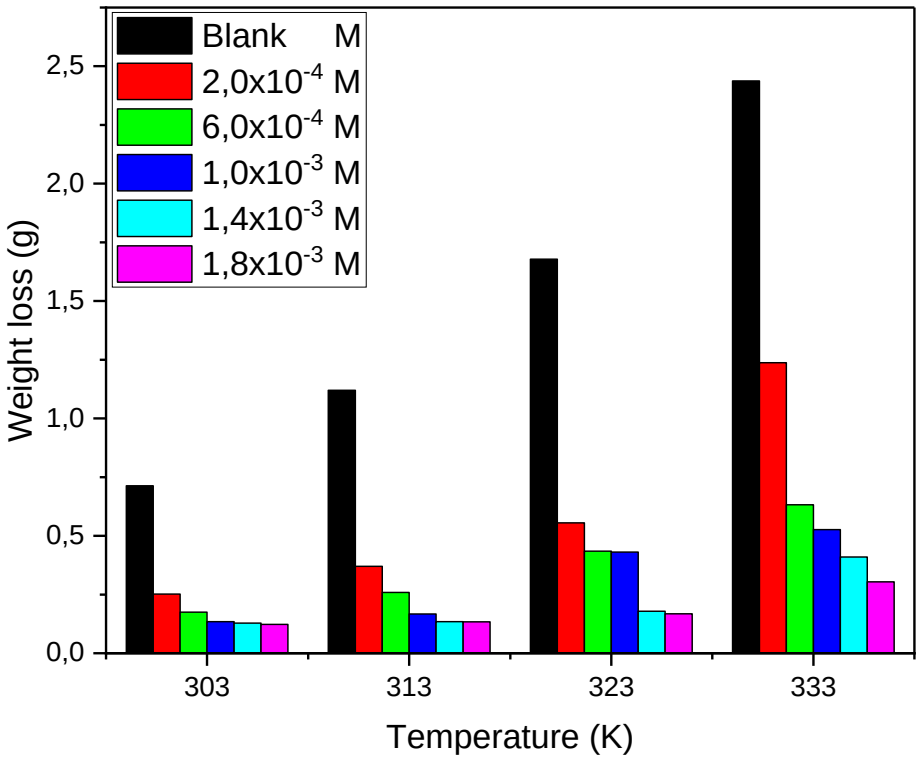

Figure 4.5: The graph showing the weight loss measurements of zinc metal in the absence and presence of MNHD in 1.5 M H_2SO_4 at different temperatures.

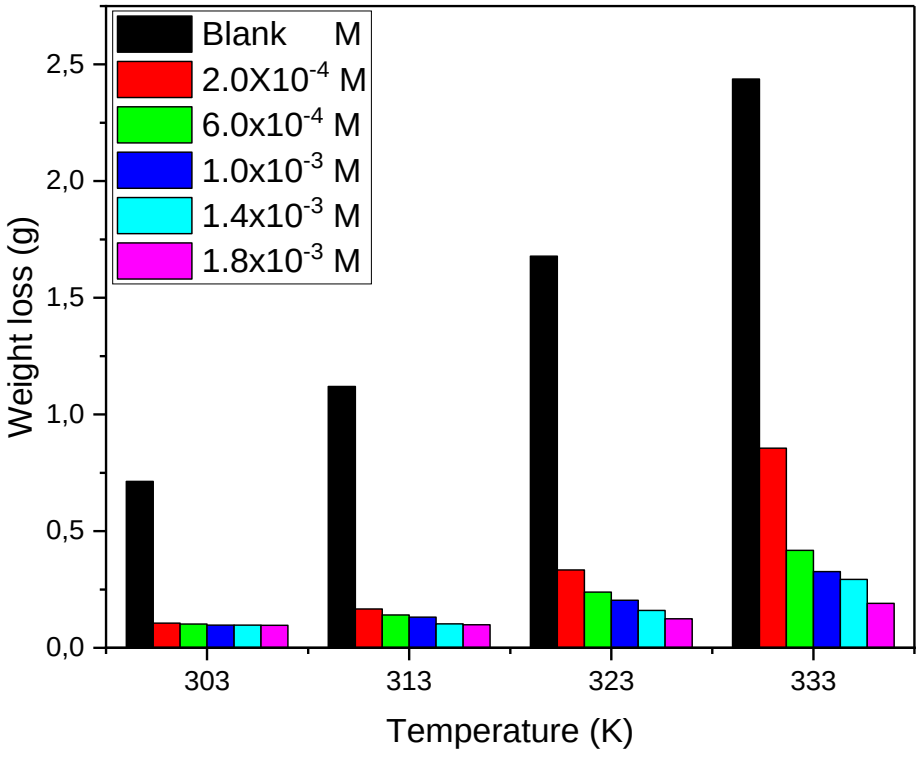

Figure 4.6: The graph showing the weight loss measurements of zinc metal in the absence and presence of 6-HFN in 1.5 M H_2SO_4 at different temperatures.

4.1.2.2 Zinc in 1.5 M hydrochloric acid.

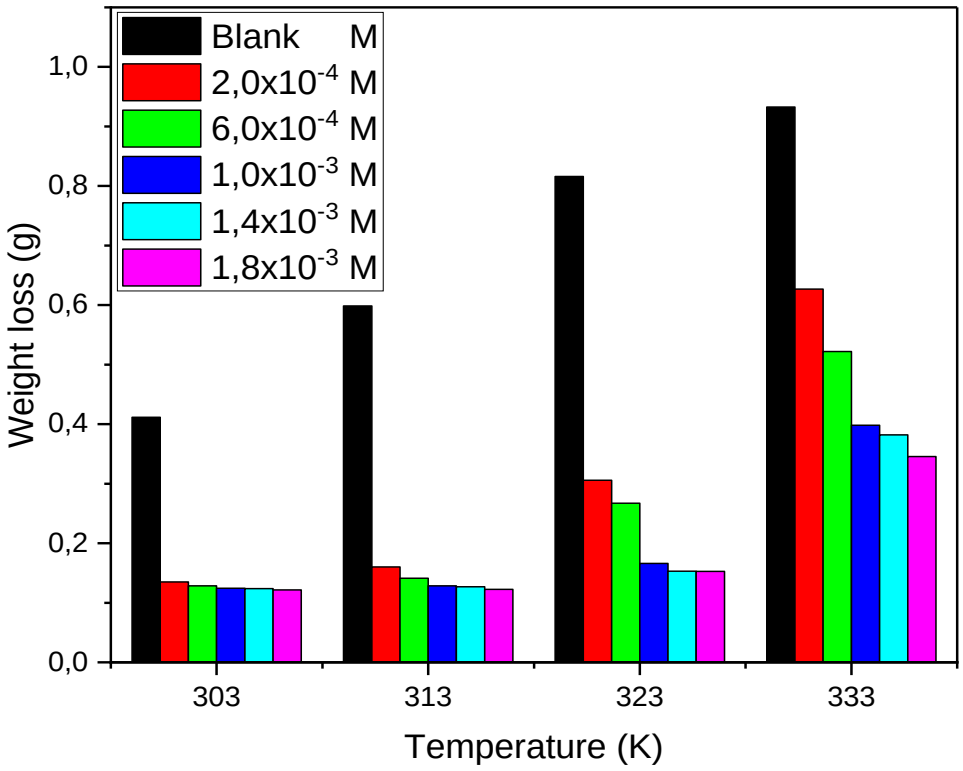

Figure 4.7: The graph showing the weight loss measurements of zinc metal in the absence and presence of NRNG in 1.5 M HCl at different temperatures.

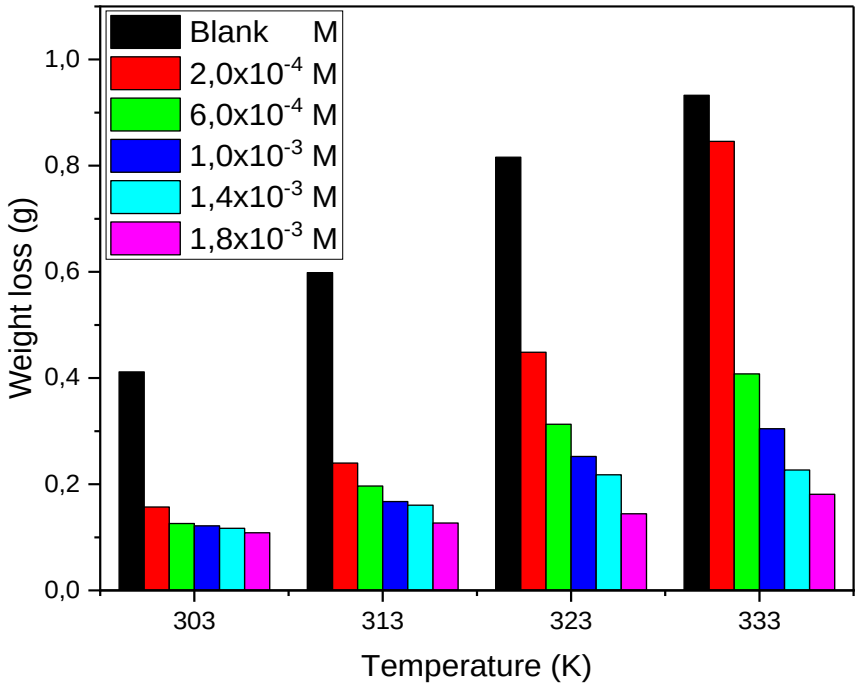

Figure 4.8: The graph showing the weight loss measurements of zinc metal in the absence and presence of MNHD 1.5 M HCl at different temperatures.

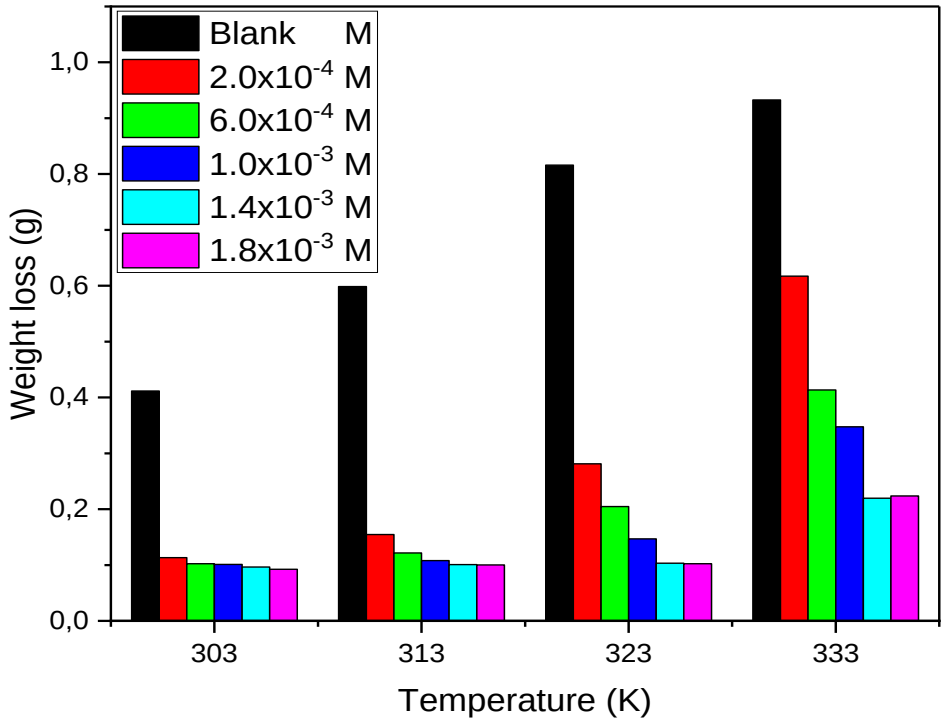

Figure 4.9: The graph showing the weight loss measurements of zinc metal in the absence and presence of 6-HFN in 1.5 M HCl at different temperatures.

4.1.2.3 Aluminium in 0.5 M hydrochloric acid.

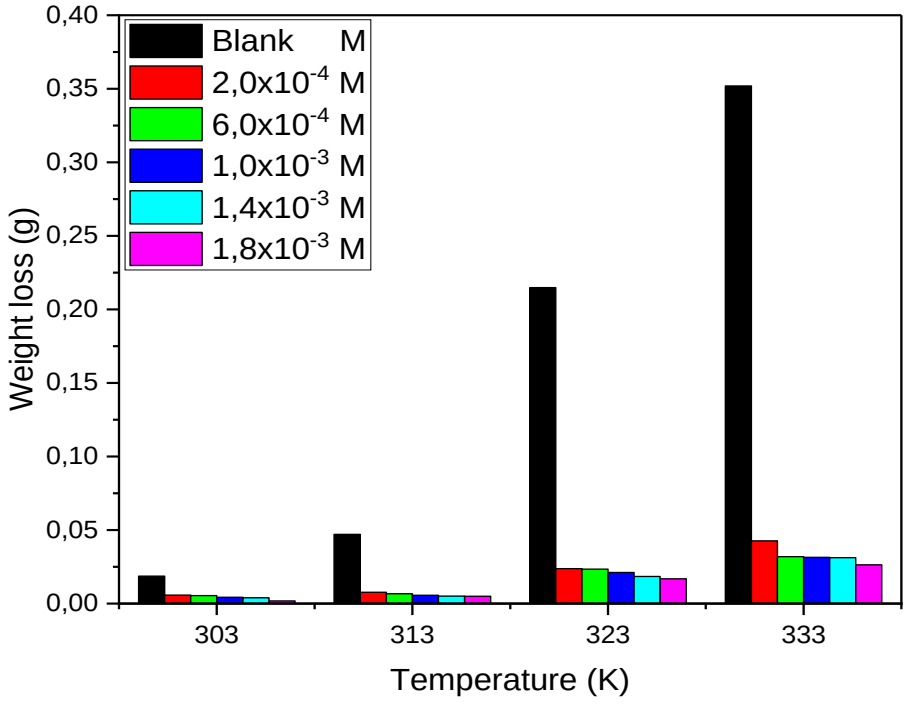

Figure 4.10: The graph showing the weight loss measurements of aluminium metal in the absence and presence of NRNG in 0.5 M HCl at different temperatures.

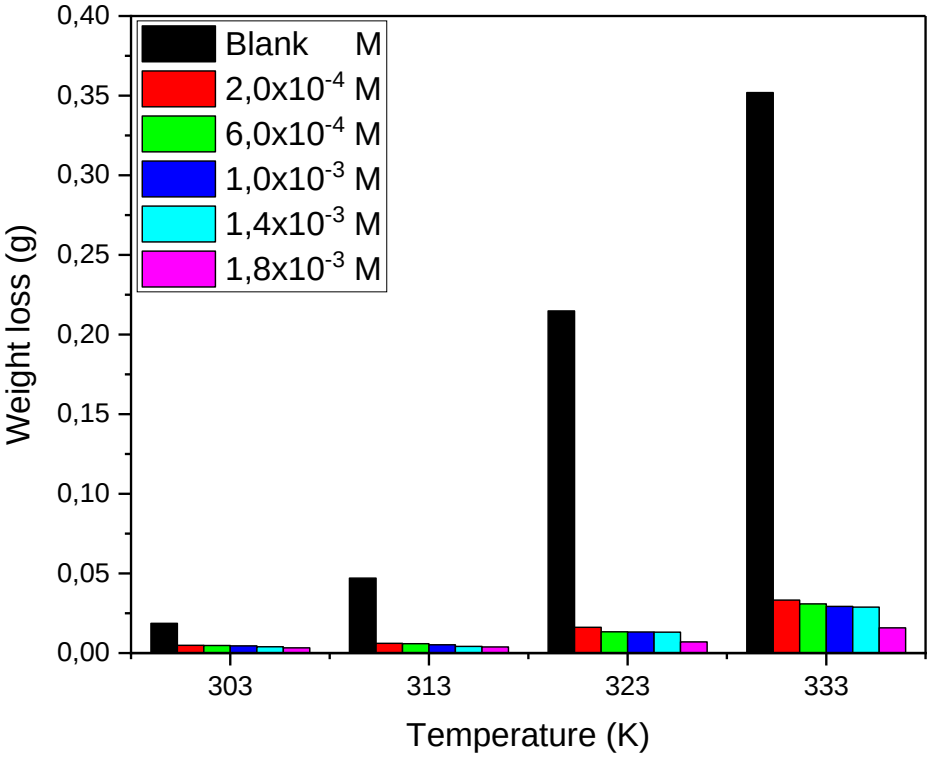

Figure 4.11: The graph showing the weight loss measurements of aluminium metal in the absence and presence of MNHD 0.5 M HCl at different temperatures.

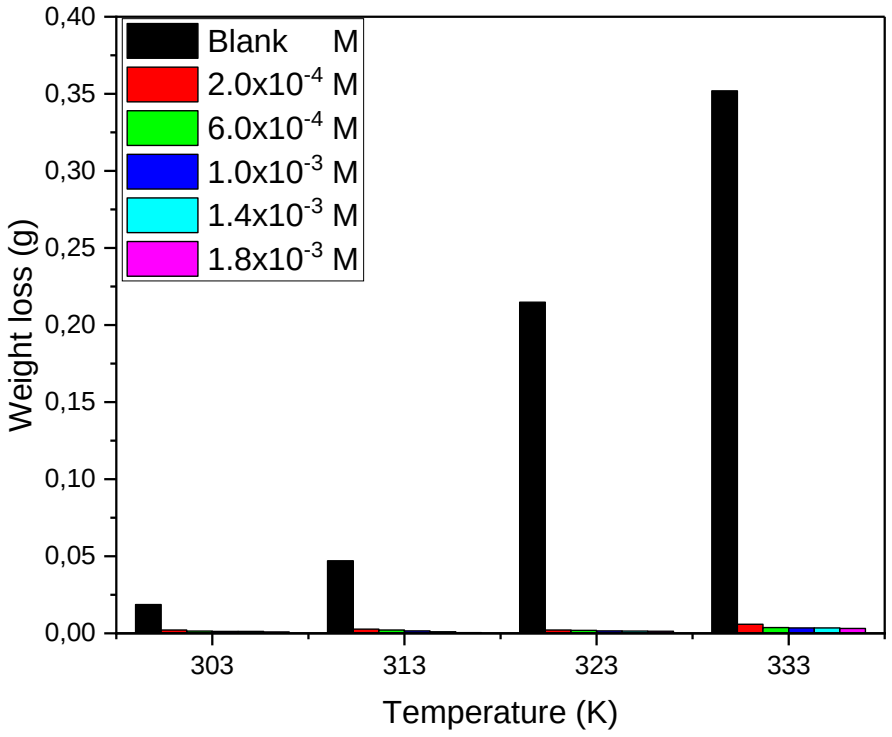

Figure 4.12: The graph showing the weight loss measurements of aluminium metal in the absence and presence of 6-HFN in 0.5 M HCl at different temperatures.

A number of research done have articulated that the rate of metal dissolution is strongly hindered by increasing the inhibitors concentration [133, 134]. With that said, looking at the results obtained in this study, it can be observed that they concur with what other studies have found based on the statement above. For instance, looking at Table 4.4 for NRNG in H_2SO_4, the weight loss of the metal for $2.0x10^{-4}$ M is 0.1975 g, 0.3095 g, 0.5142 g and 0.8939 g for 30°C, 40°C, 50°C and 60°C temperatures respectively as compared to 0.1447 g, 0.2047 g, 0.3139 g and 0.6043 g for $1.8x10^{-3}$ M at 30°C, 40°C, 50°C and 60°C temperatures respectively. Similar trend was also observed in Table 4.5 of NRNG in HCl whereby the weight loss of the metal is 0.1350 g, 0.1601 g, 0.3058 g and 0.6268 g for $2.0x10^{-4}$ M at 30°C, 40°C,50°C and 60°C respectively. But for $1.8x10^{-3}$ M at 30°C, 40°C, 50°C and 60°C the weight loss is 0.1215 g, 0.1227 g, 0.1526 g and 0.3457 g. MNHD and 6-HFN inhibitors also showed similar trend demonstrated by NRNG inhibitor in all the metals and acids used. Through this observation, it can be said that the corrosion rate of zinc and aluminium is a function of the acidic media concentration. This observation is in agreement with the fact that the rate of a chemical reaction increases with increasing concentration of the acid and probably because of the increase in the rate of diffusion and ionization of active species in the corrosion reaction [135]. This observation supports the findings by Omoduda and Oforka [136]. Table 4.6 for aluminium metal registered the lowest weight loss when compared to Tables 4.4 and 4.5 for zinc. When zinc metal was used irrespective of the acid used a little difference in the weight loss is obtained and this is evident by comparing the weight loss obtained in Table 4.4 for sulphuric acid and Table 4.5 for hydrochloric acid.

Table 4.4: Weight loss of measurements of zinc metal in the absence and presence of NRNG, MNHD and 6-HFN in 1.5 M H_2SO_4.

Inhibitor	Concentration (M)	Weight loss (g)			
		30° C	40° C	50° C	60° C
	0.00	0.7134	1.1201	1.6780	2.4370
NRNG	$2.0x10^{-4}$	0.1975	0.3095	0.5142	0.8939
	$6.0x10^{-4}$	0.1743	0.2943	0.4660	0.7529
	$1.0x10^{-3}$	0.1539	0.2762	0.4254	0.6837
	$1.4x10^{-3}$	0.1448	0.2269	0.3451	0.6047
	$1.8x10^{-3}$	0.1447	0.2047	0.3139	0.6043
MNHD	$2.0x10^{-4}$	0.2522	0.3701	0.5555	1.2372
	$6.0x10^{-4}$	0.1750	0.2586	0.4348	0.6325
	$1.0x10^{-3}$	0.1349	0.1671	0.4307	0.5264
	$1.4x10^{-3}$	0.1286	0.1349	0.1790	0.4101
	$1.8x10^{-3}$	0.1232	0.1338	0.1677	0.3041

6-HFN	$2.0x10^{-4}$	0.1059	0.1666	0.3334	0.8553
	$6.0x10^{-4}$	0.1019	0.1407	0.2391	0.4176
	$1.0x10^{-3}$	0.0972	0.1315	0.2039	0.3267
	$1.4x10^{-3}$	0.0970	0.1025	0.1599	0.2931
	$1.8x10^{-3}$	0.0961	0.0986	0.1248	0.1905

Table 4.5: Weight loss measurements of zinc metal in the absence and presence of NRNG, MNHD and 6-HFN in 1.5 M HCl.

Inhibitor	**Concentration (M)**	**Weight loss (g)**			
		30° C	40° C	50° C	60° C
	0.00	0.4115	0.5985	0.8159	0.9325
NRNG	$2.0x10^{-4}$	0.1350	0.1601	0.3058	0.6268
	$6.0x10^{-4}$	0.1286	0.1412	0.2671	0.5220
	$1.0x10^{-3}$	0.1245	0.1285	0.1660	0.3983
	$1.4x10^{-3}$	0.1238	0.1270	0.1532	0.3820
	$1.8x10^{-3}$	0.1215	0.1227	0.1526	0.3457
MNHD	$2.0x10^{-4}$	0.1570	0.2399	0.4486	0.8459
	$6.0x10^{-4}$	0.1261	0.1967	0.3128	0.4077
	$1.0x10^{-3}$	0.1216	0.1674	0.2523	0.3047
	$1.4x10^{-3}$	0.1170	0.1604	0.2178	0.2268
	$1.8x10^{-3}$	0.1087	0.1270	0.1443	0.1811
6-HFN	$2.0x10^{-4}$	0.1132	0.1547	0.2812	0.6171
	$6.0x10^{-4}$	0.1023	0.1215	0.2046	0.4134
	$1.0x10^{-3}$	0.1012	0.1081	0.1469	0.3474
	$1.4x10^{-3}$	0.0963	0.1009	0.1032	0.2195
	$1.8x10^{-3}$	0.0924	0.1002	0.1025	0.2236

Table 4.6: Weight loss measurements of aluminium metal in the absence and presence of NRNG, MNHD and 6-HFN in 0.5 M HCl.

Inhibitor	**Concentration (M)**	**Weight loss (g)**			
		30° C	40° C	50° C	60° C
	0.00	0.0187	0.0471	0.2148	0.3519
NRNG	$2.0x10^{-4}$	0.0058	0.0077	0.0238	0.0427
	$6.0x10^{-4}$	0.0054	0.0067	0.0234	0.0319
	$1.0x10^{-3}$	0.0043	0.0056	0.0212	0.0314
	$1.4x10^{-3}$	0.0040	0.0051	0.0184	0.0312
	$1.8x10^{-3}$	0.0018	0.0050	0.0169	0.0264

MNHD	$2.0x10^{-4}$	0.0049	0.0061	0.0162	0.0333
	$6.0x10^{-4}$	0.0047	0.0059	0.0133	0.0309
	$1.0x10^{-3}$	0.0045	0.0052	0.0132	0.0293
	$1.4x10^{-3}$	0.0040	0.0042	0.0131	0.0289
	$1.8x10^{-3}$	0.0033	0.0039	0.0070	0.0158
6-HFN	$2.0x10^{-4}$	0.0022	0.0027	0.0022	0.0059
	$6.0x10^{-4}$	0.0015	0.0022	0.0019	0.0037
	$1.0x10^{-3}$	0.0013	0.0016	0.0016	0.0035
	$1.4x10^{-3}$	0.0012	0.0010	0.0015	0.0035
	$1.8x10^{-3}$	0.0009	0.0004	0.0014	0.0032

4.1.3 Corrosion rate and inhibition efficiency

The percentage inhibition efficiency was calculated from the results obtained in gravimetric analysis and they are represented by Figures 4.13 – 4.21. It can be observed that the %IE is directly proportional to the concentration of the inhibitors since in most cases it increased with an increase in the concentration of the inhibitors. The trend of the %IE versus inhibitor concentration is almost similar for all the three-inhibitors utilized at 30 – 60° C. In all the metals used, the highest inhibition was obtained at $1.8x10^{-3}$ M and the main course of this can be said to be the fact that there are many inhibitors molecules available in $1.8x10^{-3}$ M than in $2.0x10^{-4}$ M to cause necessary interaction with the metal surface to reduce its dissolution.

4.1.3.1 Zinc in 1.5 M sulphuric acid.

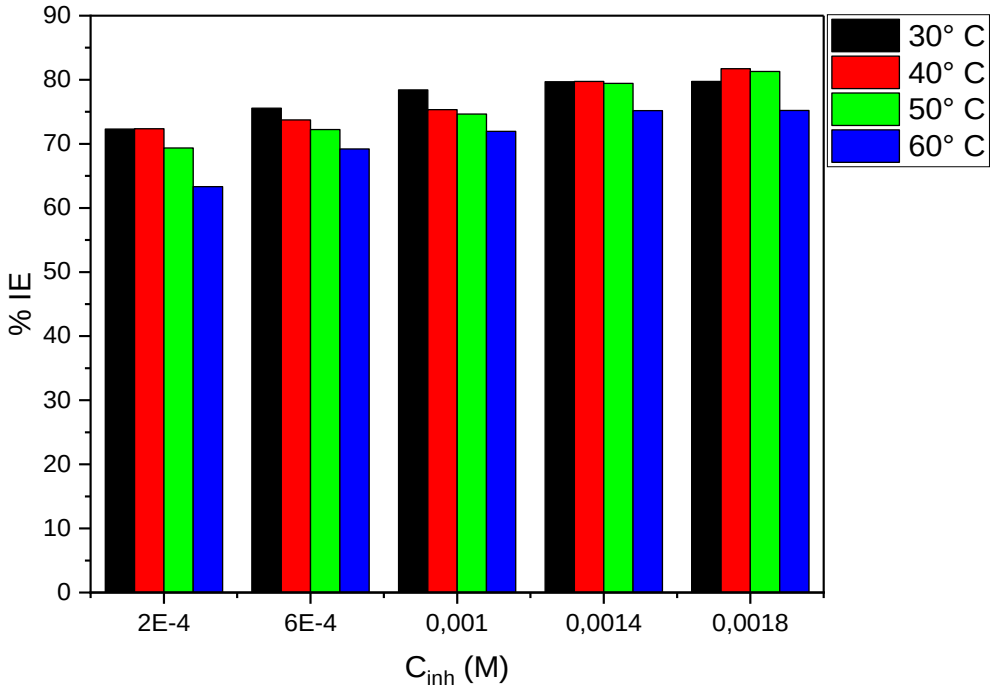

Figure 4.13: The graph of inhibition efficiency using NRNG in 1.5 M H_2SO_4 at different temperature.

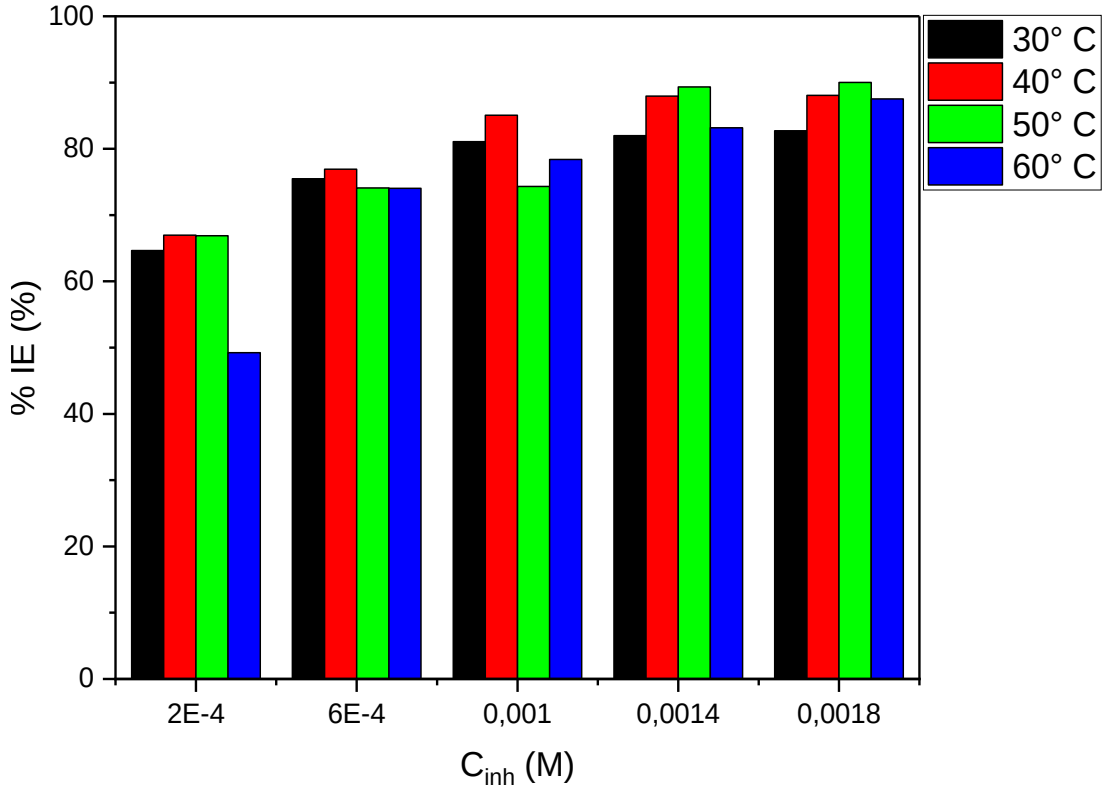

Figure 4.14: The graph of inhibition efficiency using MNHD in 1.5 M H_2SO_4 at different temperature.

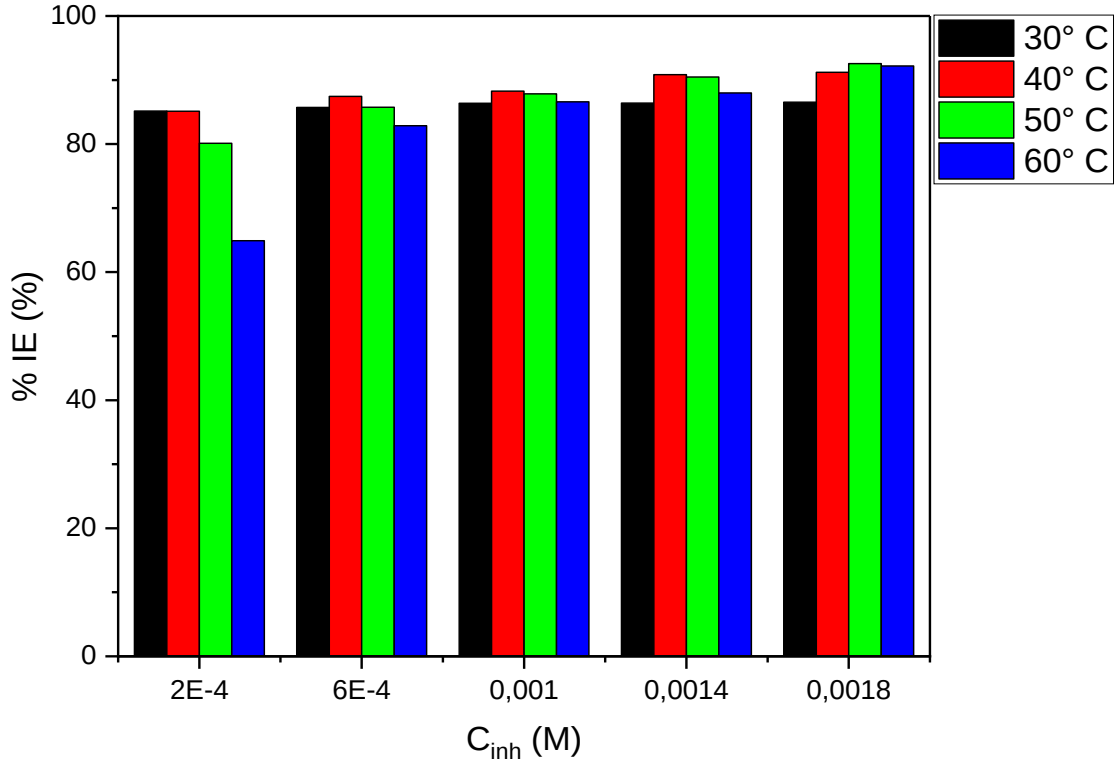

Figure 4.15: The graph of inhibition efficiency using 6-HFN in 1.5 M H_2SO_4 at different temperature.

4.1.3.2 Zinc in 1.5 M hydrochloric acid.

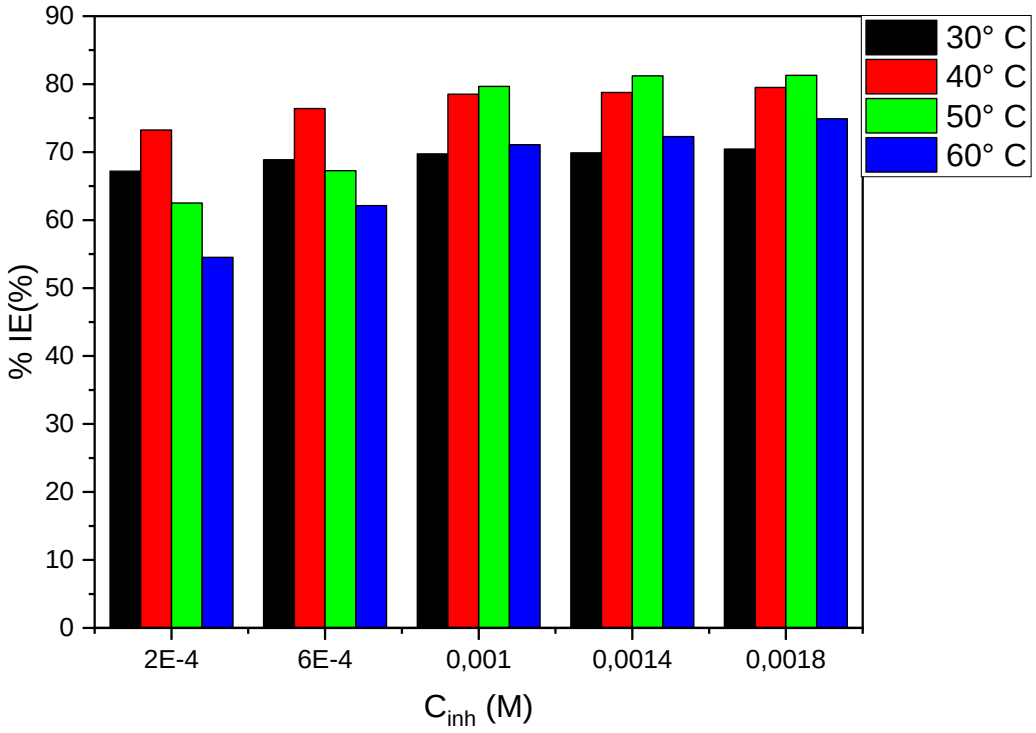

Figure 4.16: The graph of inhibition efficiency using NRNG in 1.5 M HCl at different temperature.

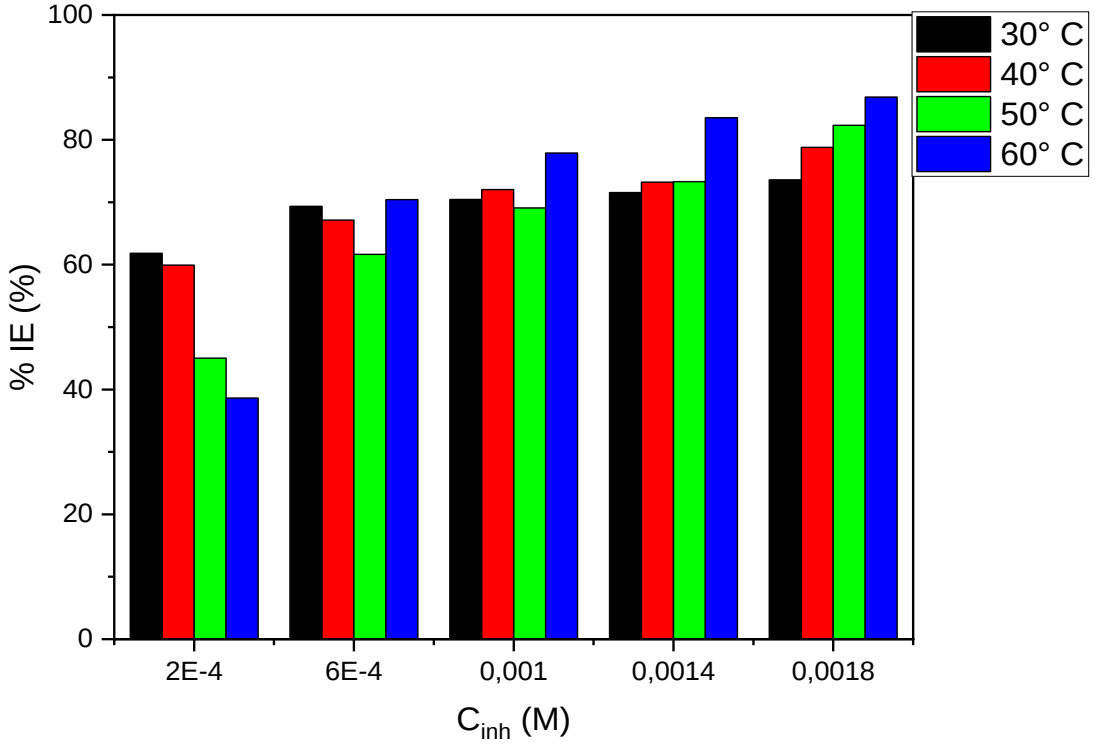

Figure 4.17: The graph of inhibition efficiency using MNHD in 1.5 M HCl at different temperature.

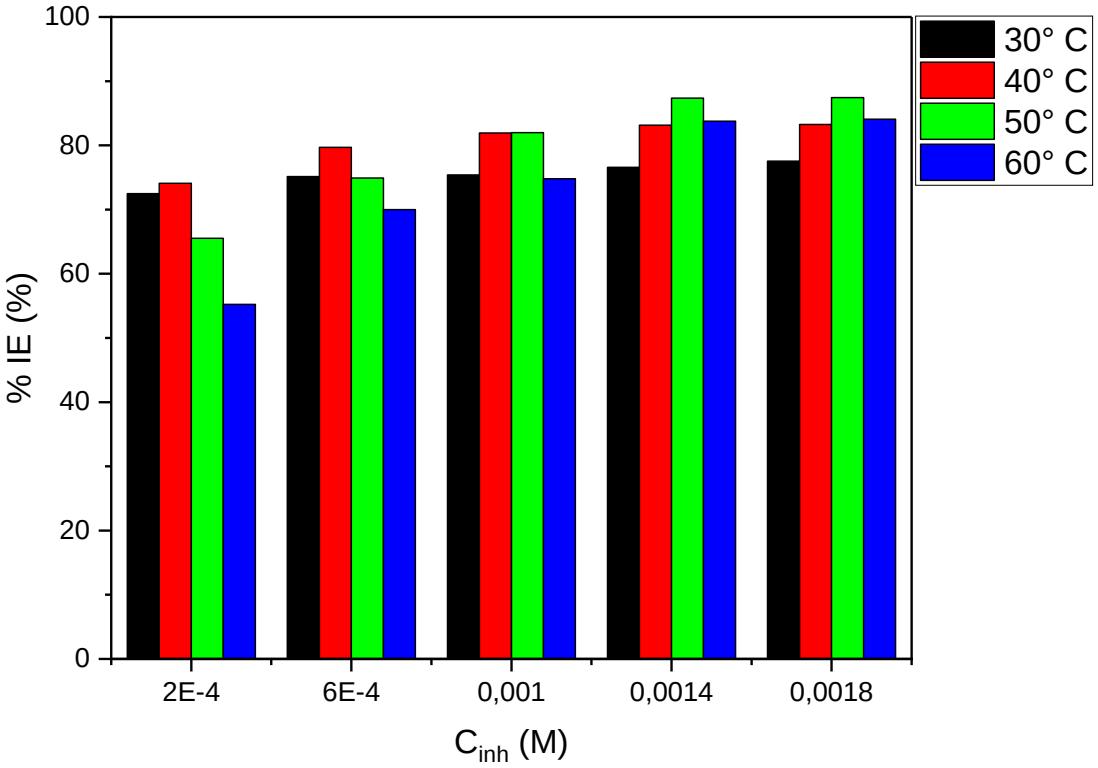

Figure 4.18: The graph of inhibition efficiency using 6-HFN in 1.5 M HCl at different temperature.

4.1.3.3 Aluminium in 0.5 M hydrochloric acid.

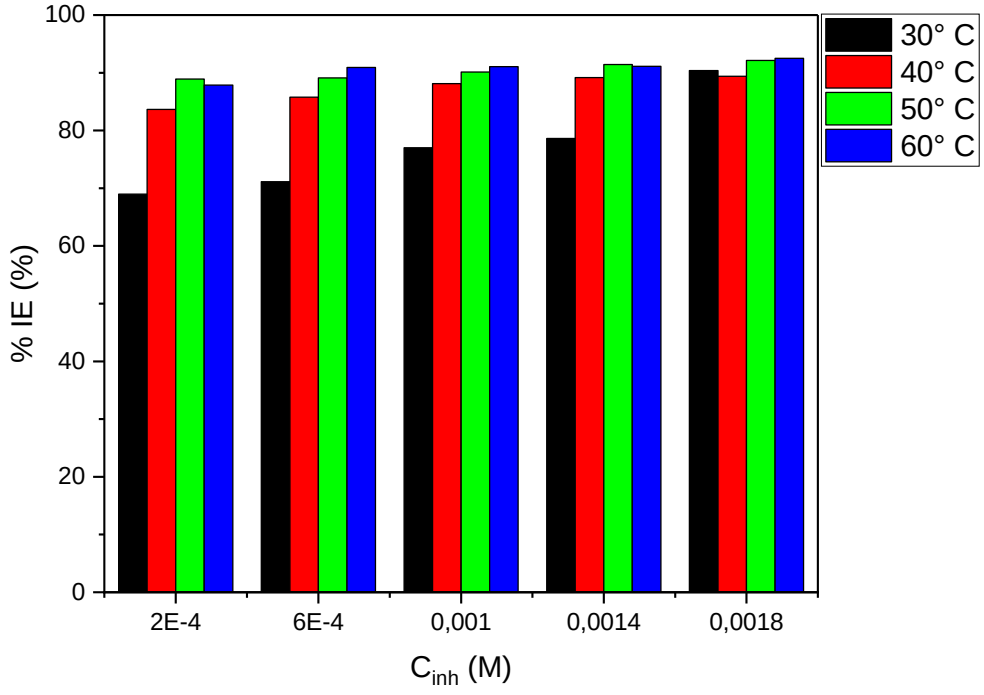

Figure 4.19: The graph of inhibition efficiency using NRNG in 0.5 M HCl at different temperature.

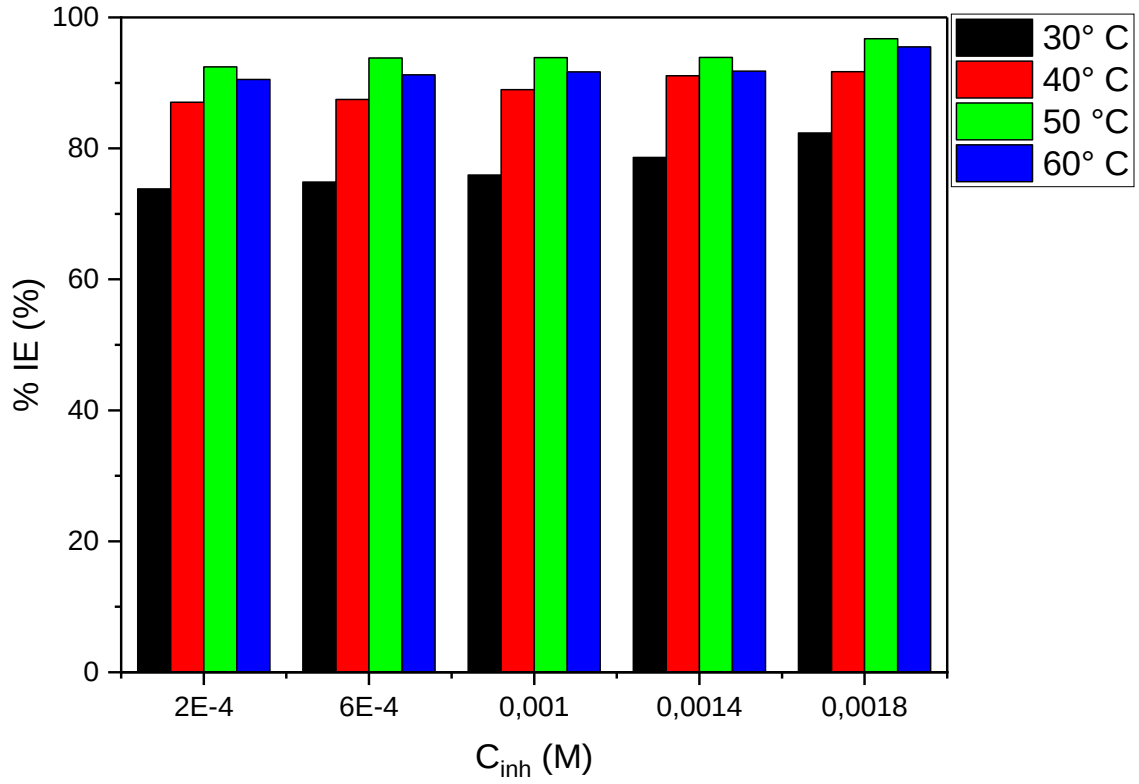

Figure 4.20: The graph of inhibition efficiency using MNHD in 0.5 M HCL at different temperatures.

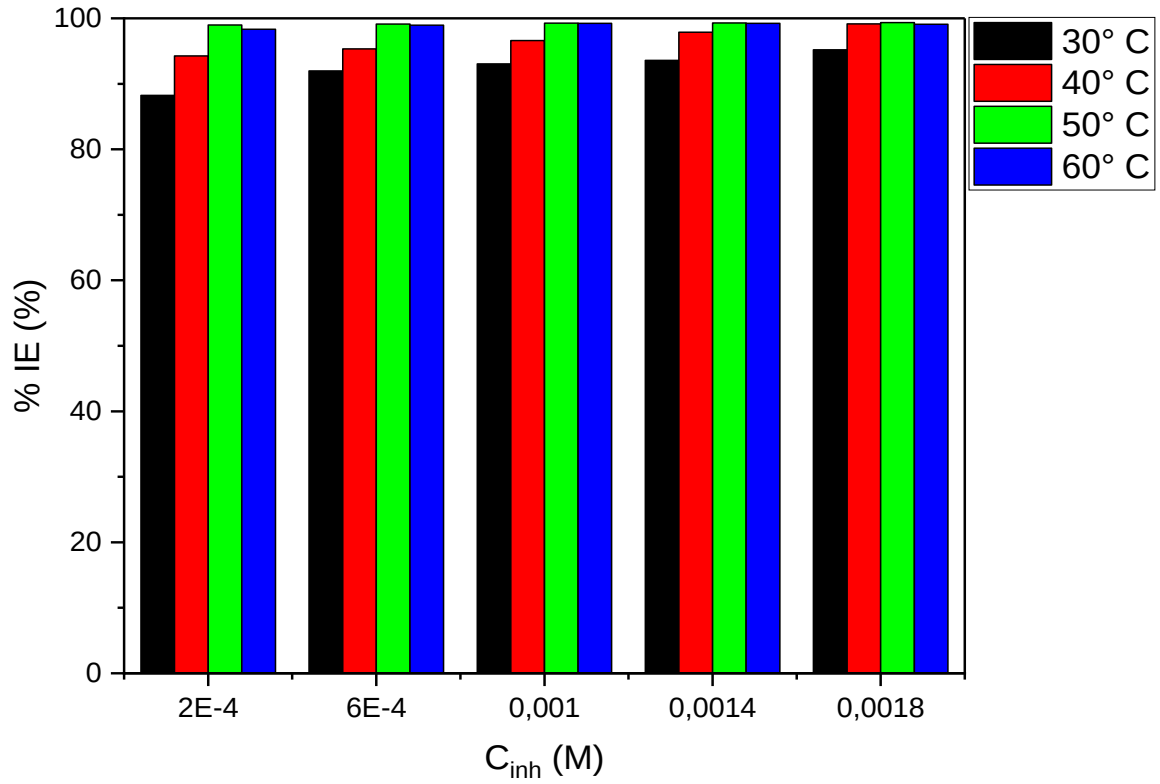

Figure 4.21: The graph of inhibition efficiency using 6-HFN in 0.5 M HCl at different temperature.

The effects of concentration on the corrosion rate of zinc and aluminium metal have been studied in the absence and presence of different concentrations of the inhibitors at 30 – 60° C. The data obtained is recorded in Tables 4.7- 4.9 below. From the tables, it is observed that the rate of corrosion decreases with an increase in the concentration of the inhibitor. This behaviour can be attributed to the increase in the number of molecules available for adsorption on the metal surface, when the concentration of the inhibitors is increased. The molecules adsorb on the metal surface thereby forming a protective film protecting the metal from further corrosion. The corrosion rate obtained in the presence of the inhibitors is less than that obtained in the presence of the corrosive acid medium. In the presence of naringenin inhibitor in sulphuric acid at 30°C, the corrosion rates obtained were 0.00658, 0.00581, 0.00513, 0.00483 and 0.00482 $g.cm^{-2}.h^{-1}$ at $2.0x10^{-4}$, $6.0x10^{-4}$, $1.0x10^{-3}$, $1.4x10^{-3}$ and $1.8x10^{-3}$ M, respectively, compared to 0.02378 $g.cm^{-2}.h^{-1}$ of blank solution. The similar trend was obtained in the presence of the other two inhibitors studied at all the temperatures.

The surface coverage which is the extent to which the inhibitor covers the surface of the metal is given by equation (40) and its values are also recorded in Tables 4.7, 4.8 and 4.9.

$$\theta = \left(1 - \frac{\rho 1}{\rho 2}\right) \tag{40}$$

where:

θ is the degree of surface coverage, ρ_1 is the corrosion rate of metal in the presence of inhibitor and ρ_2 is the corrosion rate of metal in the absence of inhibitor.

Inspection Form these tables shows that the surface coverage increases with an increase in temperature from 30 – 50° C but drops at 60° C. This indicate the formation of a monolayer adsorbate film on zinc and aluminium surface until 50° C was reached. The direct proportionality of the number of molecules and the increase in concentration of the inhibitor can be said to be responsible for the increase in the surface coverage until 50° C was reached. The drop in the surface coverage at the maximum temperature was very small which suggest almost the whole surface of the metal was covered by the inhibitor molecules. The protective action of the inhibitor in the course of metal corrosion is based on the absorbability of their molecules, in which the resulting adsorption layer isolates the metal surface from the corrosive medium. The surface coverage of Naringenin at 30° C was found to be 0.72317, 0.75568, 0.78427, 0.79731 and 0.79689 at $2.0x10^{-4}$, $6.0x10^{-4}$, $1.0x10^{-3}$, $1.4x10^{-3}$ and $1.8x10^{-3}$ M, respectively. Similar trend is also observed for all the inhibitors studied.

Table 4.7: The corrosion parameters for zinc in aqueous solution of 1.5 M H_2SO_4 in the absence and presence of different concentration of NRNG, MNHD and 6-HFN from weight loss measurements at four different temperatures (30 – 60° C).

Inhibitor	Temperature (° C)	Inhibior Concentration (M)	Corrosion rate ($g.cm^{-2}.h^{-1}$)	Inhibition Efficiency (%)	Surface coverage (θ)
NRNG	30	0.00	0.02378	-	-
		$2.0x10^{-4}$	0.00658	72.317	0.72317
		$6.0x10^{-4}$	0.00581	75.568	0.75568
		$1.0x10^{-3}$	0.00513	78.427	0.78427
		$1.4x10^{-3}$	0.00483	79.689	0.79731
		$1.8x10^{-3}$	0.00482	79.731	0.79689
	40	0.00	0.03734	-	-
		$2.0x10^{-4}$	0.01032	72.362	0.72362
		$6.0x10^{-4}$	0.00981	73.728	0.73728
		$1.0x10^{-3}$	0.00921	75.335	0.75335
		$1.4x10^{-3}$	0.00756	79.754	0.79754
		$1.8x10^{-3}$	0.00682	81.735	0.81735
	50	0.00	0.05593	-	-
		$2.0x10^{-4}$	0.01714	69.355	0.69355
		$6.0x10^{-4}$	0.01553	72.233	0.72233
		$1.0x10^{-3}$	0.01418	74.647	0.74647
		$1.4x10^{-3}$	0.01150	79.439	0.79439
		$1.8x10^{-3}$	0.01046	81.298	0.81298
	60	0.00	0.08123	-	-
		$2.0x10^{-4}$	0.02980	63.318	0.63318
		$6.0x10^{-4}$	0.02501	69.211	0.69211
		$1.0x10^{-3}$	0.02279	71.944	0.71944
		$1.4x10^{-3}$	0.02016	75.182	0.75182
		$1.8x10^{-3}$	0.02014	75.206	0.75206
	30	0.00	0.02378	-	-
		$2.0x10^{-4}$	0.00840	64.648	0.64648
		$6.0x10^{-4}$	0.00583	75.471	0.75471
		$1.0x10^{-3}$	0.00450	81.090	0.81090
		$1.4x10^{-3}$	0.00429	81.974	0.81974
		$1.8x10^{-3}$	0.00411	82.730	0.82730
	40	0.00	0.03734	-	-
		$2.0x10^{-4}$	0.01234	66.961	0.66961
		$6.0x10^{-4}$	0.00862	76.915	0.76915
		$1.0x10^{-3}$	0.00557	85.082	0.85082
		$1.4x10^{-3}$	0.00450	87.957	0.87957
		$1.8x10^{-3}$	0.00446	88.056	0.88056

MNHD	50	0.00	0.05593	-	-
		$2.0x10^{-4}$	0.01852	66.893	0.66893
		$6.0x10^{-4}$	0.01449	74.087	0.74087
		$1.0x10^{-3}$	0.01436	74.331	0.74331
		$1.4x10^{-3}$	0.00597	89.332	0.89332
		$1.8x10^{-3}$	0.00559	90.005	0.90005
	60	0.00	0.08123	-	-
		$2.0x10^{-4}$	0.04124	49.232	0.49232
		$6.0x10^{-4}$	0.02108	74.043	0.74043
		$1.0x10^{-3}$	0.01755	78.398	0.78398
		$1.4x10^{-3}$	0.01367	83.171	0.83171
		$1.8x10^{-3}$	0.01014	87.521	0.87521
6-HFN	30	0.00	0.02378	-	-
		$2.0x10^{-4}$	0.00353	85.156	0.85155
		$6.0x10^{-4}$	0.00340	85.715	0.85715
		$1.0x10^{-3}$	0.00324	86.375	0.86375
		$1.4x10^{-3}$	0.00323	86.405	0.86405
		$1.8x10^{-3}$	0.00320	86.531	0.86331
	40	0.00	0.03734	-	-
		$2.0x10^{-4}$	0.00555	85.130	0.85130
		$6.0x10^{-4}$	0.00469	87.440	0.87440
		$1.0x10^{-3}$	0.00438	88.259	0.88259
		$1.4x10^{-3}$	0.00342	90.849	0.90849
		$1.8x10^{-3}$	0.00329	91.200	0.91200
	50	0.00	0.05593	-	-
		$2.0x10^{-4}$	0.01111	80.131	0.80131
		$6.0x10^{-4}$	0.00797	85.750	0.85750
		$1.0x10^{-3}$	0.00680	87.848	0.87848
		$1.4x10^{-3}$	0.00533	90.472	0.90472
		$1.8x10^{-3}$	0.00416	92.561	0.92561
	60	0.00	0.08123	-	-
		$2.0x10^{-4}$	0.02851	64.902	0.64902
		$6.0x10^{-4}$	0.01392	82.863	0.82863
		$1.0x10^{-3}$	0.01089	86.594	0.86594
		$1.4x10^{-3}$	0.00977	87.972	0.87974
		$1.8x10^{-3}$	0.00635	92.183	0.92183

Table 4.8: The corrosion parameters for zinc in aqueous solution of 1.5 M HCl in absence and presence of different concentration of NRNG, MNHD and 6-HFN from weight loss measurements at four different temperatures (30 – 60° C).

Inhibitor	Temperature (° C)	Inhibior Concentration (M)	Corrosion rate ($g.cm^{-2}.h^{-1}$)	Inhibition Effeciency (%)	Surface coverage (θ)
NRNG	30	0.00	0.00857	-	-
		$2.0x10^{-4}$	0.00281	67.182	0.67182
		$6.0x10^{-4}$	0.00268	68.874	0.68874
		$1.0x10^{-3}$	0.00259	69.734	0.69734
		$1.4x10^{-3}$	0.00258	69.904	0.69904
		$1.8x10^{-3}$	0.00253	70.463	0.70463
	40	0.00	0.01247	-	-
		$2.0x10^{-4}$	0.00334	73.253	0.73253
		$6.0x10^{-4}$	0.00294	76.410	0.76410
		$1.0x10^{-3}$	0.00268	78.532	0.78532
		$1.4x10^{-3}$	0.00265	78.783	0.78783
		$1.8x10^{-3}$	0.00256	79.508	0.79508
	50	0.00	0.01700	-	-
		$2.0x10^{-4}$	0.00637	62.520	0.62520
		$6.0x10^{-4}$	0.00557	67.263	0.67263
		$1.0x10^{-3}$	0.00346	79.655	0.79655
		$1.4x10^{-3}$	0.00319	81.223	0.81223
		$1.8x10^{-3}$	0.00318	81.297	0.81297
	60	0.00	0.02871	-	-
		$2.0x10^{-4}$	0.01351	54.517	0.54517
		$6.0x10^{-4}$	0.01088	62.121	0.62121
		$1.0x10^{-3}$	0.00830	71.098	0.71098
		$1.4x10^{-3}$	0.00796	72.280	0.72280
		$1.8x10^{-3}$	0.00720	74.914	0.74914
	30	0.00	0.00857	-	-
		$2.0x10^{-4}$	0.00323	61.834	0.61834
		$6.0x10^{-4}$	0.00263	69.346	0.69346
		$1.0x10^{-3}$	0.00253	70.440	0.70440
		$1.4x10^{-3}$	0.00244	71.558	0.71558
		$1.8x10^{-3}$	0.00226	73.576	0.73576
	40	0.00	0.01247	-	-
		$2.0x10^{-4}$	0.00500	59.913	0.59913
		$6.0x10^{-4}$	0.00410	67.135	0.67135
		$1.0x10^{-3}$	0.00349	72.029	0.72029
		$1.4x10^{-3}$	0.00334	73.205	0.73205
		$1.8x10^{-3}$	0.00265	78.782	0.78782

MNHD	50	0.00	0.01700	-	-
		$2.0x10^{-4}$	0.00935	45.020	0.45020
		$6.0x10^{-4}$	0.00652	61.660	0.61660
		$1.0x10^{-3}$	0.00526	69.083	0.69083
		$1.4x10^{-3}$	0.00454	73.302	0.73302
		$1.8x10^{-3}$	0.00300	82.314	0.82314
	60	0.00	0.02871	-	-
		$2.0x10^{-4}$	0.01762	38.621	0.38621
		$6.0x10^{-4}$	0.00849	70.414	0.70414
		$1.0x10^{-3}$	0.00635	77.891	0.77891
		$1.4x10^{-3}$	0.00473	83.539	0.83539
		$1.8x10^{-3}$	0.00377	86.859	0.86859
6-HFN	30	0.00	0.00857	-	-
		$2.0x10^{-4}$	0.00236	72.482	0.72482
		$6.0x10^{-4}$	0.00213	75.131	0.75131
		$1.0x10^{-3}$	0.00211	75.399	0.75398
		$1.4x10^{-3}$	0.00201	76.590	0.76590
		$1.8x10^{-3}$	0.00193	77.538	0.77538
	40	0.00	0.01247	-	-
		$2.0x10^{-4}$	0.00322	74.106	0.74106
		$6.0x10^{-4}$	0.00253	79.701	0.79701
		$1.0x10^{-3}$	0.00225	81.940	0.81940
		$1.4x10^{-3}$	0.00209	83.143	0.83143
		$1.8x10^{-3}$	0.00210	83.260	0.83260
	50	0.00	0.016998	-	-
		$2.0x10^{-4}$	0.00586	65.535	0.65535
		$6.0x10^{-4}$	0.00426	74.924	0.74924
		$1.0x10^{-3}$	0.00306	81.996	0.81996
		$1.4x10^{-3}$	0.00215	87.351	0.87351
		$1.8x10^{-3}$	0.00214	87.437	0.87437
	60	0.00	0.02871	-	-
		$2.0x10^{-4}$	0.01287	55.220	0.55220
		$6.0x10^{-4}$	0.00861	70.002	0.70002
		$1.0x10^{-3}$	0.00724	74.791	0.74791
		$1.4x10^{-3}$	0.00466	83.775	0.83775
		$1.8x10^{-3}$	0.00457	84.072	0.84072

Table 4.9: The corrosion parameters for aluminium in aqueous solution of 0.5 M HCl in absence and presence of different concentration of NRNG, MNHD and 6-HFN from weight loss measurements at four different concentrations (30 – 60° C).

Inhibitor	Temperature (° C)	Inhibior Concentration (M)	Corrosion rate ($g.cm^{-2}.h^{-1}$)	Inhibition Effeciency (%)	Surface coverage (θ)
NRNG	30	0.00	0.00104	-	-
		$2.0x10^{-4}$	0.00032	68.984	0.68984
		$6.0x10^{-4}$	0.00030	71.123	0.71123
		$1.0x10^{-3}$	0.00024	77.005	0.77005
		$1.4x10^{-3}$	0.00022	78.610	0.78610
		$1.8x10^{-3}$	0.00010	90.374	0.90374
	40	0.00	0.002617	-	-
		$2.0x10^{-4}$	0.000428	83.652	0.83652
		$6.0x10^{-4}$	0.000372	85.775	0.85775
		$1.0x10^{-3}$	0.000311	88.110	0.88110
		$1.4x10^{-3}$	0.000283	89.172	0.89172
		$1.8x10^{-3}$	0.000278	89.384	0.89384
	50	0.00	0.119333	-	-
		$2.0x10^{-4}$	0.001322	88.920	0.88920
		$6.0x10^{-4}$	0.001300	89.106	0.89106
		$1.0x10^{-3}$	0.001178	90.130	0.90130
		$1.4x10^{-3}$	0.001022	91.434	0.91434
		$1.8x10^{-3}$	0.000939	92.132	0.92132
	60	0.00	0.019550	-	-
		$2.0x10^{-4}$	0.002372	87.866	0.87866
		$6.0x10^{-4}$	0.001772	90.935	0.90935
		$1.0x10^{-3}$	0.001744	91.077	0.91077
		$1.4x10^{-3}$	0.001733	91.134	0.91134
		$1.8x10^{-3}$	0.001467	92.498	0.92498
	30	0.00	0.001039	-	-
		$2.0x10^{-4}$	0.000272	73.800	0.73800
		$6.0x10^{-4}$	0.000261	74.866	0.74866
		$1.0x10^{-3}$	0.000250	75.936	0.75936
		$1.4x10^{-3}$	0.000222	78.610	0.78610
		$1.8x10^{-3}$	0.000183	82.353	0.82353
	40	0.00	0.002617	-	-
		$2.0x10^{-4}$	0.000339	87.049	0.87049
		$6.0x10^{-4}$	0.000328	87.473	0.87473
		$1.0x10^{-3}$	0.000289	88.960	0.88960
		$1.4x10^{-3}$	0.000233	91.083	0.91083
		$1.8x10^{-3}$	0.000217	91.720	0.91720

MNHD	50	0.00	0.011933	-	-
		$2.0x10^{-4}$	0.000900	92.458	0.92458
		$6.0x10^{-4}$	0.000739	93.808	0.93808
		$1.0x10^{-3}$	0.000733	93.855	0.93855
		$1.4x10^{-3}$	0.000728	93.901	0.93901
		$1.8x10^{-3}$	0.000389	96.741	0.96741
	60	0.00	0.019550	-	-
		$2.0x10^{-4}$	0.001850	90.537	0.90537
		$6.0x10^{-4}$	0.001717	91.219	0.91219
		$1.0x10^{-3}$	0.001628	91.674	0.91674
		$1.4x10^{-3}$	0.001606	91.787	0.91787
		$1.8x10^{-3}$	0.000878	95.510	0.95510
6-HFN	30	0.00	0.001039	-	-
		$2.0x10^{-4}$	0.000122	88.238	0.88238
		$6.0x10^{-4}$	0.000083	91.979	0.91979
		$1.0x10^{-3}$	0.000072	93.048	0.93048
		$1.4x10^{-3}$	0.000067	93.583	0.93583
		$1.8x10^{-3}$	0.000050	95.187	0.95187
	40	0.00	0.002617	-	-
		$2.0x10^{-4}$	0.000150	94.266	0.94266
		$6.0x10^{-4}$	0.000122	95.329	0.95329
		$1.0x10^{-3}$	0.000089	96.602	0.96602
		$1.4x10^{-3}$	0.000056	97.875	0.97875
		$1.8x10^{-3}$	0.000063	99.151	0.99151
	50	0.00	0.011933	-	-
		$2.0x10^{-4}$	0.000122	98.976	0.98976
		$6.0x10^{-4}$	0.000106	99.116	0.99116
		$1.0x10^{-3}$	0.000089	99.255	0.99255
		$1.4x10^{-3}$	0.000083	99.302	0.99302
		$1.8x10^{-3}$	0.000078	99.348	0.99348
	60	0.00	0.019550	-	-
		$2.0x10^{-4}$	0.000328	98.323	0.98323
		$6.0x10^{-4}$	0.000106	98.949	0.98949
		$1.0x10^{-3}$	0.000089	99.236	0.99236
		$1.4x10^{-3}$	0.000083	99.236	0.99236
		$1.8x10^{-3}$	0.000078	99.091	0.99091

The percentage inhibition efficiency (%IE) was calculated using equation (41) and its values are recorded in Tables 4.7 – 4.9 above and graphically presented in Figures 4.13 – 4.21. From the tables, it can be seen that the inhibition efficiency of corrosion rate for zinc and aluminium metals does not follow a proper trend but in most cases are found to be increasing with an increase in temperature and concentration of the inhibitors but drops at the maximum temperature. The %IE of NRNG, MNHD

and 6-HFN is due to the adsorption of their molecules on the zinc and aluminium metal surface and the influence of lone pairs of heteroatoms on the zinc and aluminium metals surface. The %IE rely on the mode of interaction between the inhibitors and metal, number of active sites in the molecules and molecular size of the inhibitors. The optimum working condition of NRNG, MNHD and 6-HFN in 1.5 M H_2SO_4 for zinc metals in terms of %IE are 81.735, 90.051 and 92.561 % respectively at 50°C. However, for zinc and aluminium metals in 1.5 M and 0.5 M HCl, the optimum working conditions for NRNG, MNHD and 6-HFN were found to be 81.297, 82.314 and 87.437 %, and 99.348, 96.741 and 92.498 % respectively at 50°C. based on this observation, it can be said that 6-HFN compound used as inhibitor showed to be an outstanding inhibitor amongst the other two inhibitors (NRNG and MNHD) used. The lowest %IE was obtained when MNHD was used in the presence of zinc in hydrochloric acid with a value of 38.621%. overall, NRNG can be said to be the least performing inhibitor amongst the three inhibitors investigated in this study, by looking at the %IE.

4.1.4 Thermodynamic Parameters: Adsorption Isotherms

The raw step in the action of the inhibitors is generally believed to be the adsorption on the metal surface [137]. Adsorption isotherms are utilised to determine the mechanism of any electrochemical reaction. The adsorption of an organic compound on the metal surface is generally regarded as a substitution adsorption between the water molecules absorbed on the metallic surface and the organic molecules in the aqueous solution, as given by the equation below.

$$Org_{\ (sol)} + nH_2O_{\ (ads)} \rightarrow Org_{\ (ads)} + nH_2O_{\ (sol)} \tag{33}$$

where n is regarded as the size ratio which represent the number of water molecules replaced by one molecule of organic compound. The adsorption of organic compounds can be described by two main types of interaction, which are physical adsorption and chemisorption [138]. These are influenced by the nature and charge of the metal, the chemical structure of the inhibitor and the type of electrolyte. The interaction between the inhibitor and the metal surface can be provided by the adsorption isotherm. Adsorption isotherm shows the relationship between the absorbed species with the surface coverage and the concentration of the inhibitors [139]. This surface coverage of the adsorbed molecules is also directly proportional to the percentage inhibition efficiency (%IE). The values of the inhibitor's concentration over surface coverage at different concentrations of the inhibitors and 0.5 and 1.5 M HCl and 1.5 M H_2SO_4 was fit to the adsorption isotherms against the different concentrations of the inhibitors. Of all the isotherms fitted the Langmuir adsorption isotherm was found to fit the experimental data much better compared to other isotherms like Temkin and Frumkin adsorption isotherms. Equation (44) is the one utilised to fit the experimental data.

$$\frac{C_{inh}}{\theta} = \frac{1}{K_{ads}} + C_{inh} \quad (44)$$

where C_{inh} is the concentration of the inhibitors, θ is the surface coverage and K_{ads} is the adsorption equilibrium constant which is the intercept of the straight line. The Langmuir adsorption isotherms are plotted as shown in Figures 4.22 – 4.30. The confidence of Langmuir plots is supported by the values of r^2 that are close to unity, signifying that a monolayer type of film was formed between the surface of the metal and the inhibitor.

The values of r^2, slope, calculated adsorption equilibrium constant (K_{ads}) and the standard free energy of adsorption (ΔG^o_{ads}) are recorded in Tables 4.10 – 4.12. The slope values indicate the amount of films adsorbed on metal surface. From these figures, it is observed that a straight line was obtained which indicate that the adsorption of the three inhibitors obeys the Langmuir adsorption isotherm. Since the Langmuir adsorption isotherm is based on the fact that each site of the metal is responsible for holding one adsorbed species, this means that one adsorbed H_2O molecule is substituted by one molecule of the inhibitor compound on the surface of the metal. Therefore, no interaction between the adsorbed inhibitors constituents on the zinc and aluminium surface. K_{ads} is related to the Gibbs free energy of adsorption (ΔG^o_{ads}) by the equation below.

$$K_{ads} = \frac{1}{55.55} exp(-\frac{\Delta G^0_{ads}}{RT}) \quad (45)$$

where R is the universal gas constant, T is the time in temperature and the value of 55.5 is the molar concentration of water in solution expressed in units of M.

4.1.4.1 Zinc in 1.5 M sulphuric acid.

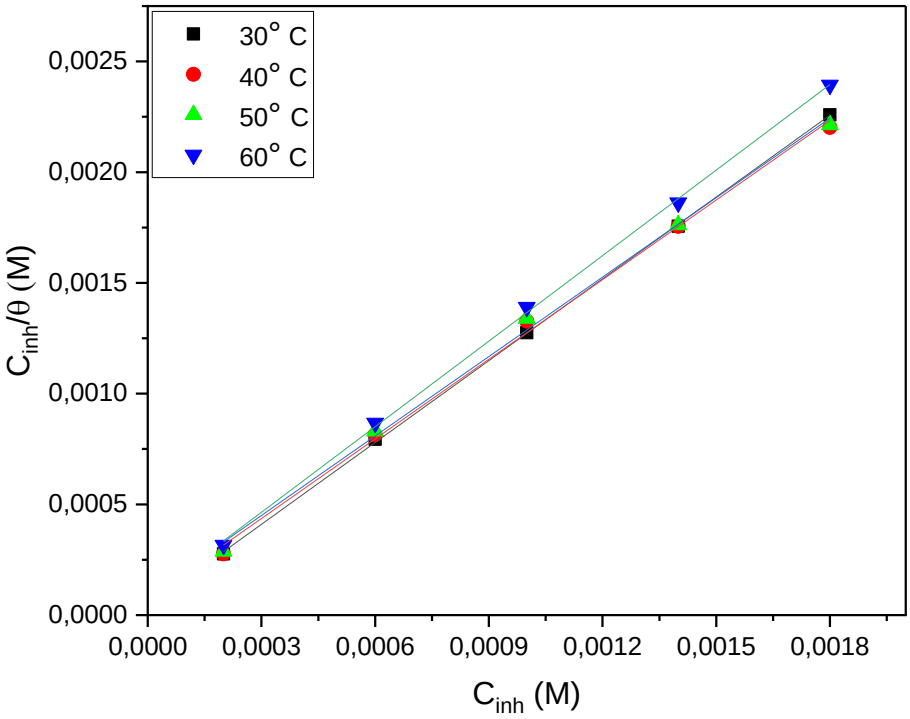

Figure 4.22: Langmuir adsorption isotherm for the adsorption of NRNG on zinc metal in 1.5 M H_2SO_4 at 30, 40, 50 and 60°C.

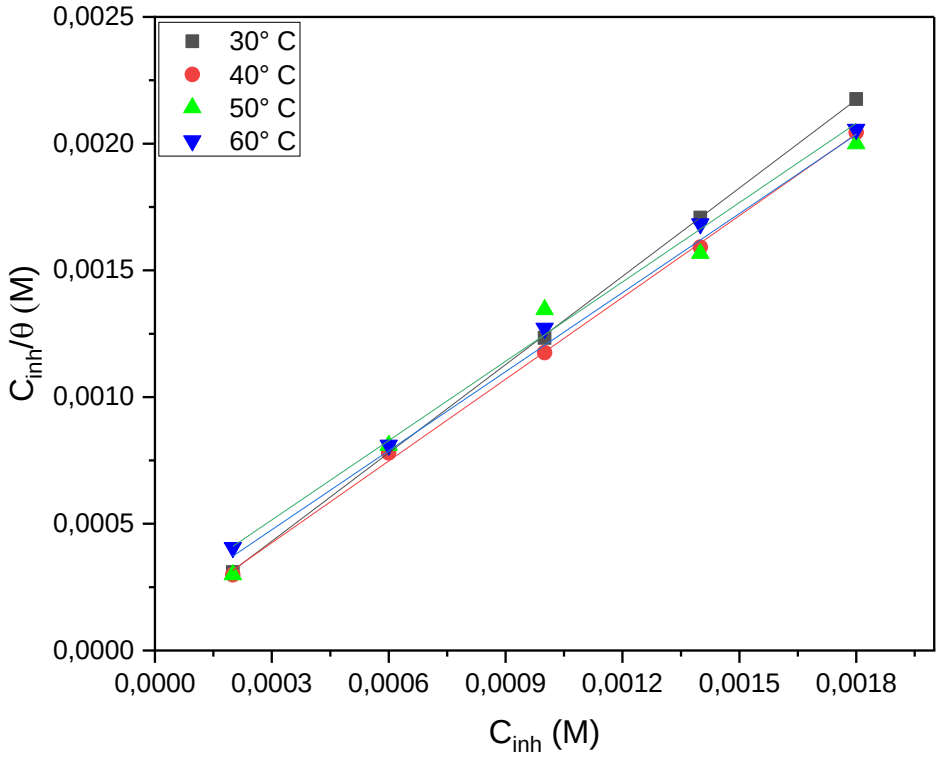

Figure 4.23: Langmuir adsorption isotherm for the adsorption of MNHD on zinc metal in 1.5 M H_2SO_4 at 30, 40, 50 and 60°C.

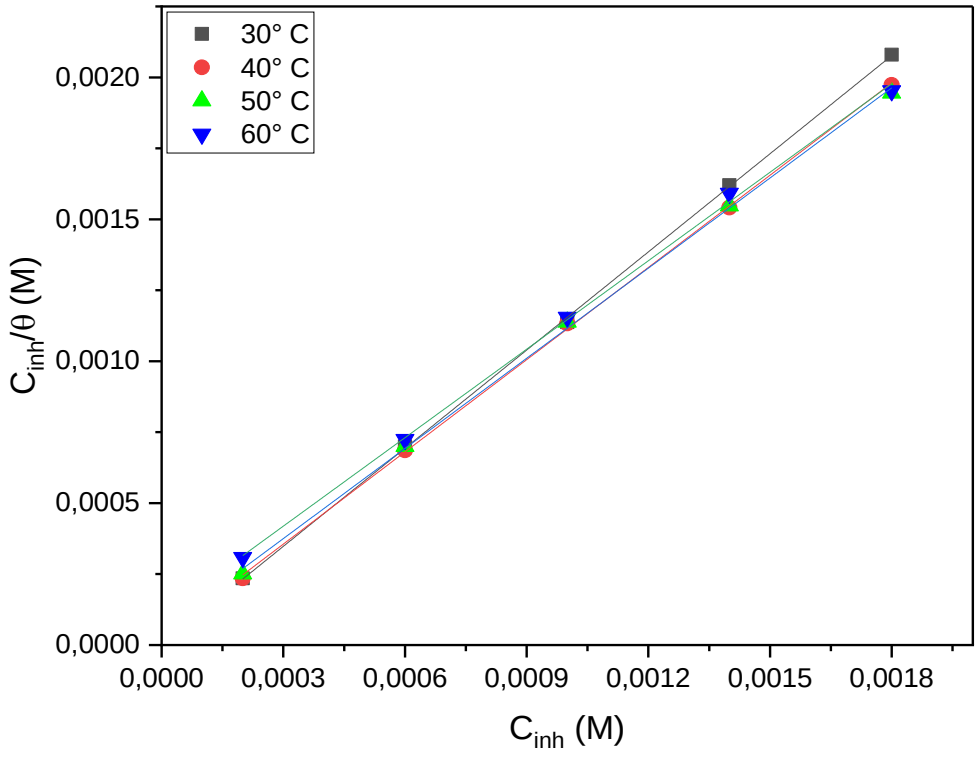

Figure 4.24: Langmuir adsorption isotherm for the adsorption of 6-HFN on zinc metal in 1.5 M H_2SO_4 at 30, 40, 50 and 60°C.

4.1.4.2 Zinc in 1.5 M hydrochloric acid.

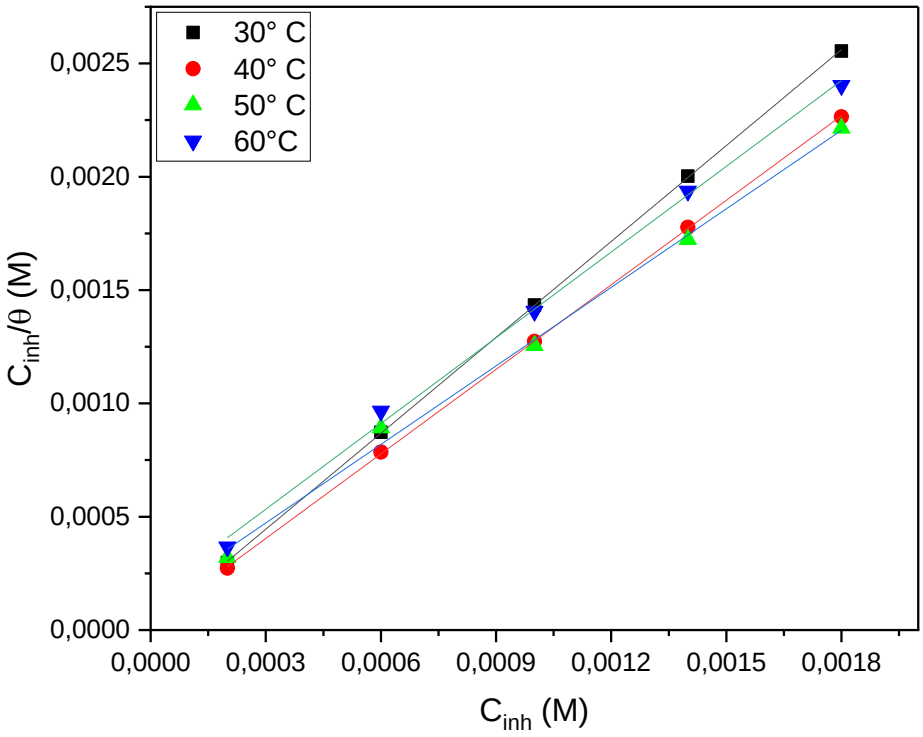

Figure 4.25: Langmuir adsorption isotherm for the adsorption of NRNG on zinc metal in 1.5 M HCl at 30, 40, 50 and 60°C.

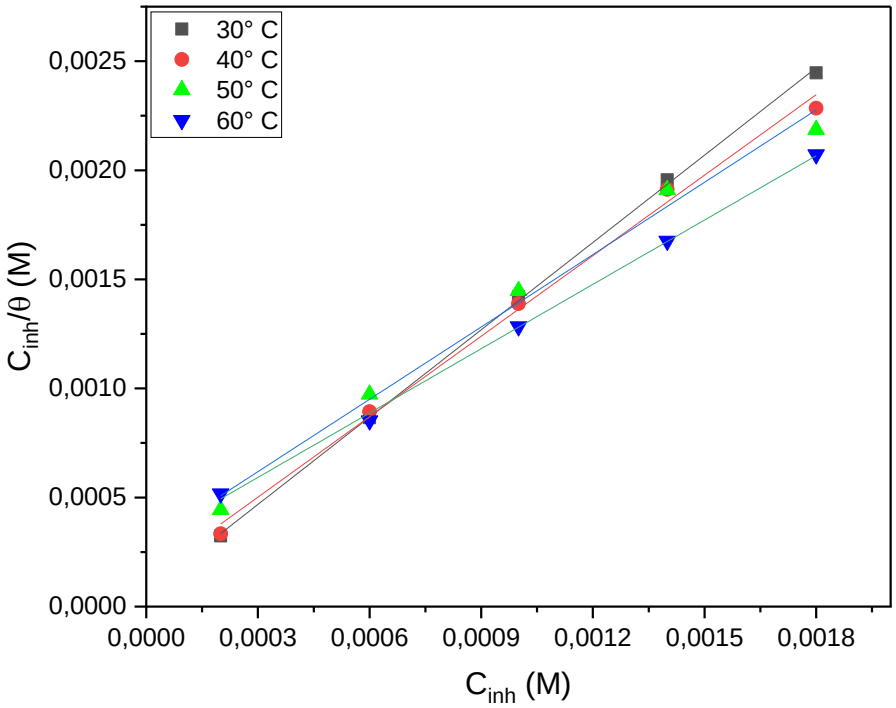

Figure 4.26: Langmuir adsorption isotherm for the adsorption of MNHD on zinc metal in 1.5 M HCl at 30, 40, 50 and 60°C.

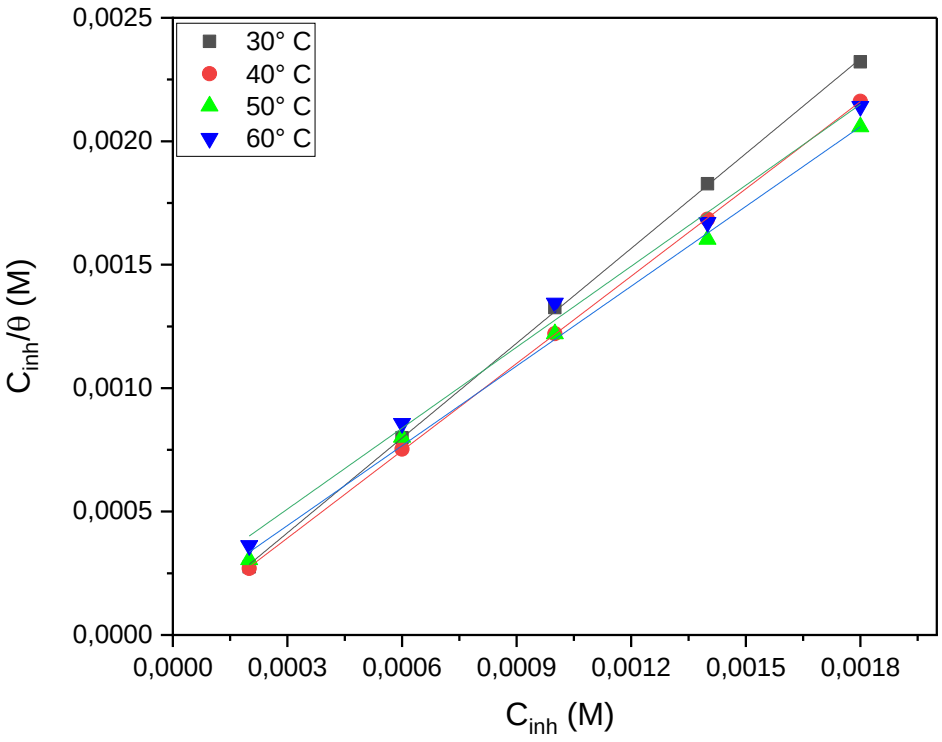

Figure 4.27: Langmuir adsorption isotherm for the adsorption of 6-HFN on zinc metal in 1.5 M HCl at 30, 40, 50 and 60°C.

4.1.4.3 Aluminium in 0.5 M hydrochloric acid

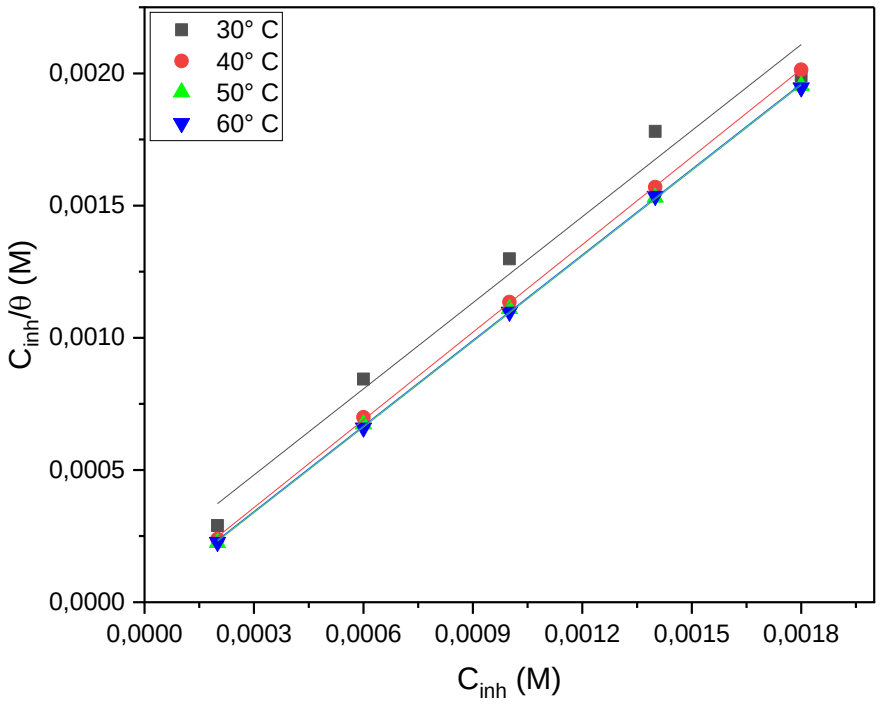

Figure 4.28: Langmuir adsorption isotherm for the adsorption of NRNG on aluminium metal in 0.5 M HCl at 30, 40, 50 and 60°C.

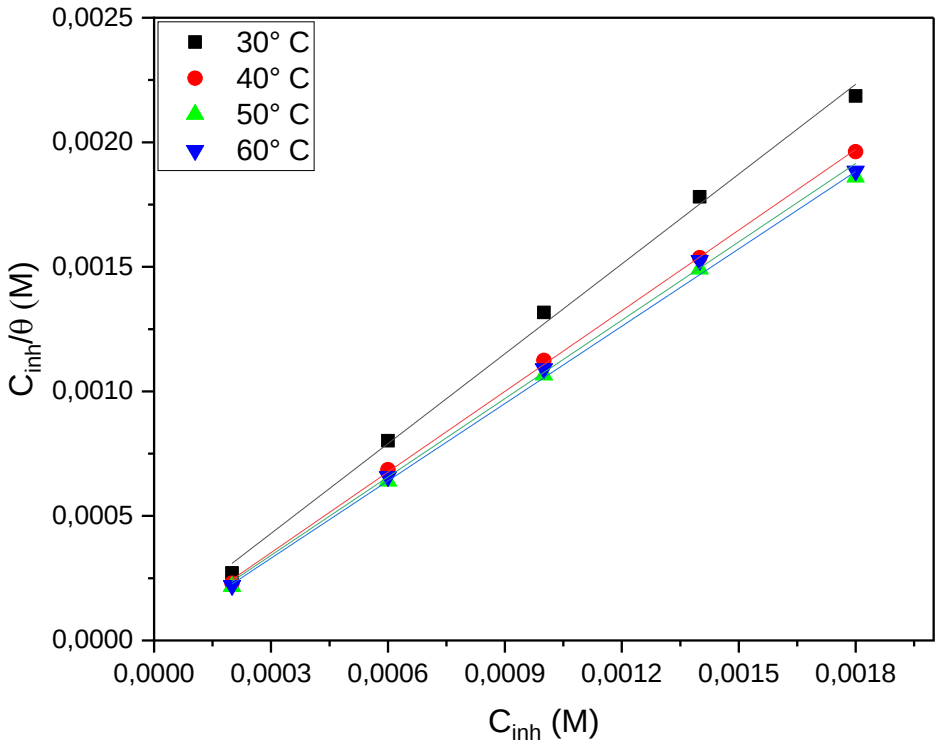

Figure 4.29: Langmuir adsorption isotherm for the adsorption of MNHD on aluminium metal in 0.5 M HCl at 30, 40, 50 and 60°C.

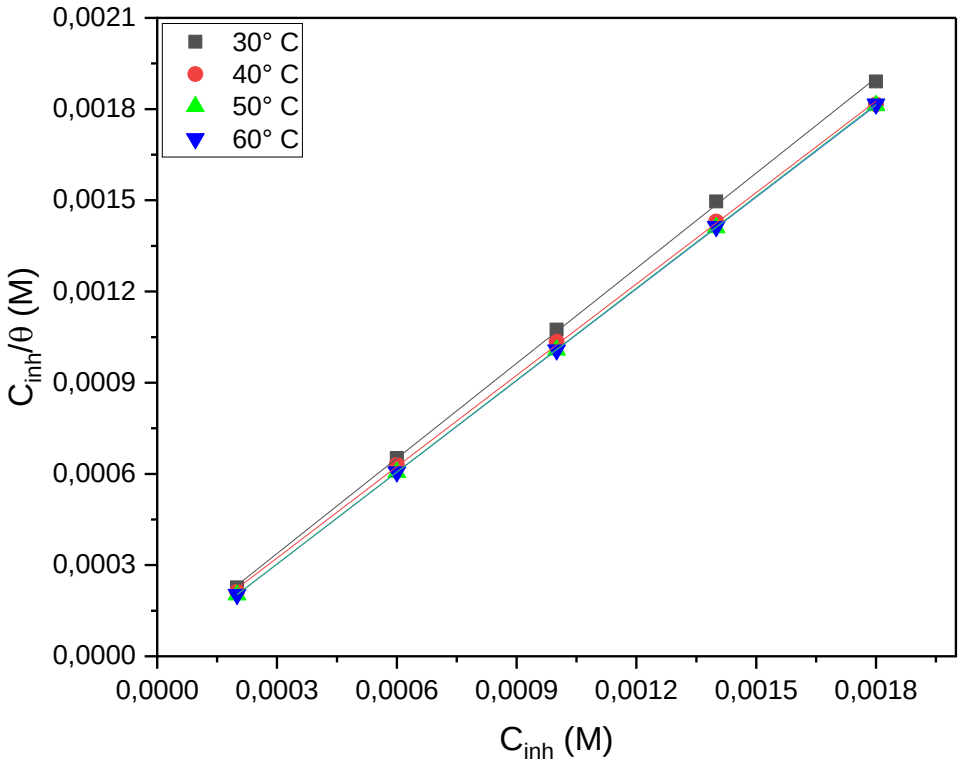

Figure 4.30: Langmuir adsorption isotherm for the adsorption of 6-HFN on aluminium metal in 0.5 M HCl at 30, 40, 50 and 60°C.

Table 4.10: Adsorption parameters from Langmuir Adsorption Isotherm plots for NRNG, MNHD and 6-HFN in 1.5 M H_2SO_4.

Inhibitor	Temperature (° C)	r^2	Slope	K_{ads} (L/mol)	$-\Delta G^{o}_{ads}$ (KJ.mol^{-1})
NRNG	30	0.9999	1.2316	24.7081	18.1982
	40	0.9988	1.1983	13.0332	17.1342
	50	0.9987	1.1958	10.9610	17.2165
	60	0.9997	1.2876	12.8080	18.1807
MNHD	30	0.9999	1.1614	12.0722	16.3938
	40	0.9995	1.0756	9.77049	16.3843
	50	0.9915	1.0398	6.08025	15.6339
	60	0.9908	1.0334	4.94626	15.5465
6-HFN	30	0.9998	1.1527	528.901	25.0000
	40	0.9996	1.0831	32.5880	19.5191
	50	0.9991	1.0588	17.4364	18.4630
	60	0.9987	1.0391	9.33245	17.3042

Table 4.11: Adsorption parameters from Langmuir Adsorption Isotherm plots for NRNG, MNHD and 6-HFN in 1.5 M HCl.

Inhibitor	Temperature (° C)	r^2	Slope	K_{ads} (L/mol)	$-\Delta G^{o}_{ads}$ (KJ.mol^{-1})
NRNG	30	0.9999	1.4109	46.5099	19.7917
	40	0.9991	1.2434	32.1316	19.4824
	50	0.9951	1.1550	7.93544	16.3491
	60	0.9971	1.2607	6.44874	16.2809
MNHD	30	0.9996	1.3343	14.7173	16.8929
	40	0.9998	1.2303	7.54956	15.7132
	50	0.8148	1.1370	3.48623	14.1401
	60	0.9896	0.9709	3.36449	14.4795
6-HFN	30	0.9997	1.2801	33.4134	18.9585
	40	0.9999	1.1788	25.6459	18.8957
	50	0.9977	1.0772	8.32085	16.4745
	60	0.9940	1.0929	5.48014	15.8302

Table 4.12: Adsorption parameters from Langmuir Adsorption Isotherm plots for NRNG, MNHD and 6-HFN in 0.5 M HCl.

Inhibitor	Temperature (° C)	r^2	Slope	K_{ads} (L/mol)	$-\Delta G^{o}_{ads}$ (KJ.mol^{-1})
NRNG	30	0.9746	1.0835	6.42141	10.3245
	40	0.9999	1.1050	37.7441	10.7121
	50	0.9998	1.0789	50.8047	10.9902
	60	0.9998	1.0782	65.5867	11.3289
MNHD	30	0.9961	1.0792	14.4993	10.5824
	40	0.9995	1.0792	34.8259	10.6507
	50	0.9991	1.0350	50.9975	10.8786
	60	0.9983	1.0487	36.8338	11.2520
6-HFN	30	0.9997	1.0431	39.9136	19.4064
	40	0.9996	1.0060	44.1679	20.3104
	50	1.0000	1.0060	755.784	28.5857
	60	1.0000	1.0083	856.421	29.8168

The values of the adsorptive equilibrium constant K_{ads} represent the degree of adsorption and the type of adsorption mechanism. From Tables 4.10 and 4.11, the values of K_{ads} decrease with an increase in temperature, which indicates that, the inhibitor is strongly and easily adsorbed onto the zinc surface

at relatively low temperature. But tend to desorb from the zinc surface at relatively high temperatures. At the maximum temperature for NRNG in zinc in H_2SO_4 in Table 4.10 a slight increase is observed. In Table 4.12 for aluminium in 0.5 M HCl, the opposite tend to be the case since the K_{ads} values are increasing with an increase in temperature. The values of ΔG^o_{ads} were obtained as negative which means that the adsorption of the three inhibitors on the zinc and aluminium metals surface is a spontaneous process which also entails the strong interaction of the inhibitor molecules onto the zinc and aluminium metal surface [140, 141]. It is believed that the values of ΔG^o_{ads} around -20 $kJ.mol^{-1}$ or less are in consistent with physisorption, which involves the electrostatic interaction between the charged inhibitors molecules and the charged metal, which results in the inhibitors adsorption onto the metal surface. It is also generally known that inhibitors which adsorbs through physisorption interact rapidly and can also be removed from the metal surface easily [138]. Those more negative than -40 $kJ.mol^{-1}$ are consistent with chemisorption, which involves charge transfer or sharing from the inhibitor molecules to the metal surface to form a coordinated bond. In this case, the adsorption and inhibition increase with an increase in temperature [142, 143]. The values calculated for ΔG^o_{ads} in this study are less than -20 $kJ.mol^{-1}$ for all the three inhibitors as observed in the tables above. This suggests that the adsorption mechanism of the three inhibitors on zinc and aluminium metals in 0.5 and 1.5 M HCl, and 1.5 M H_2SO_4 solution occurs through physisorption. However, in Table 4.12 for 6-HFN in aluminium metal, all the ΔG^o_{ads} are above -20 $kJ.mol^{-1}$, except at the minimum temperature. This suggest that that this inhibitor was adsorbed physically and chemically in aluminium metal. Since chemisorption is responsible for the increase in the adsorption and inhibition with an increase in temperature, it can be concluded that all the three inhibitors absorb through both physisorption and chemisorption looking at the trend in the values of ΔG^o_{ads} and %IE.

4.1.5 Kinetic Parameters: Effect of Temperature

To have an insight about the nature of inhibitor adsorption, thermodynamic model was used to illuminate the adsorption process. This model looks precisely at the effect of temperature on the inhibition efficiency and corrosion behaviour of zinc and aluminium metals in H_2SO_4 and HCl solutions in the absence and presence of various concentrations of the inhibitors. This was made possible by using the data from weight loss method. Another useful tool used to explain the mechanism of corrosion inhibition for the inhibitors was the kinetic model. By studying the thermodynamics of the

adsorption process, a better understanding of the adsorption behaviour of an inhibition can be achieved.

The mathematical expression between the corrosion rate and the temperature which generally enable the evaluation of the activation energy (E_a) is expressed by the Arrhenius equation (46).

$$log\ C_R = log\ A - \frac{E_a}{2.303RT} \quad (46)$$

where C_R is the corrosion rate in ($g.cm^{-2}.h^{-1}$), A is the Arrhenius pre-exponential factor (frequency factor), E_a is the corrosion activation energy, R is the gas constant (8.3145 $JK^{-1}mol^{-1}$) and T is the absolute temperature. Best fit lines were constructed after plotting the logarithm of the corrosion rate of zinc and aluminium in H_2SO_4 and HCl in the absence and presence of the inhibitors concentrations, against the reciprocal of the studied absolute temperatures, with $E_a/2.303R$ being the slope of the lines. This are represented from figures 4.31 – 4.39.

4.1.5.1 Zinc in 1.5 M sulphuric acid.

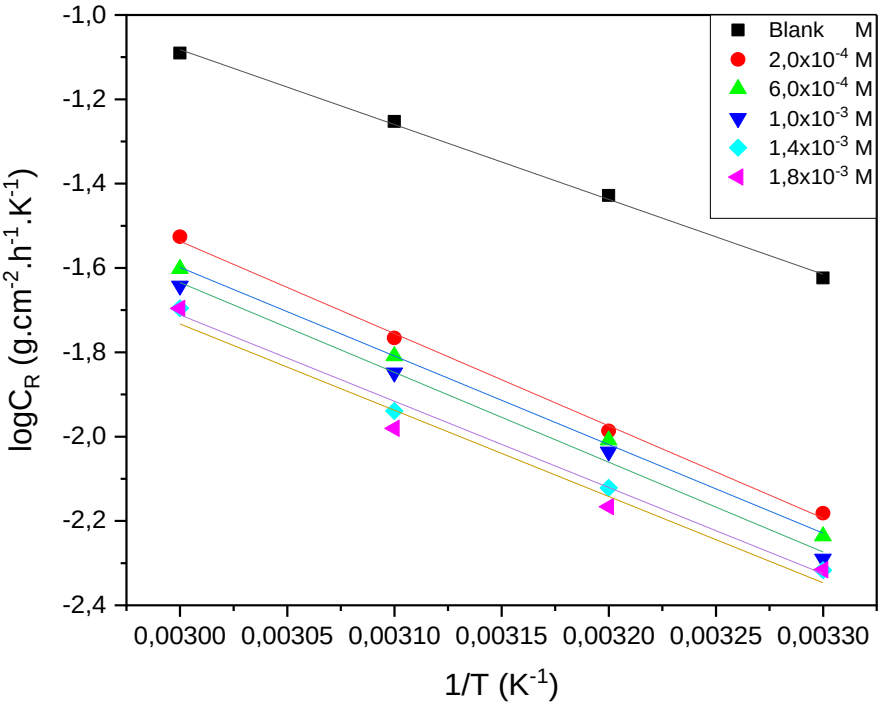

Figure 4.31: Arrhenius plots for zinc metal corrosion in 1.5 M H_2SO_4 solution in the absence and presence of different concentrations of NRNG as the inhibitor.

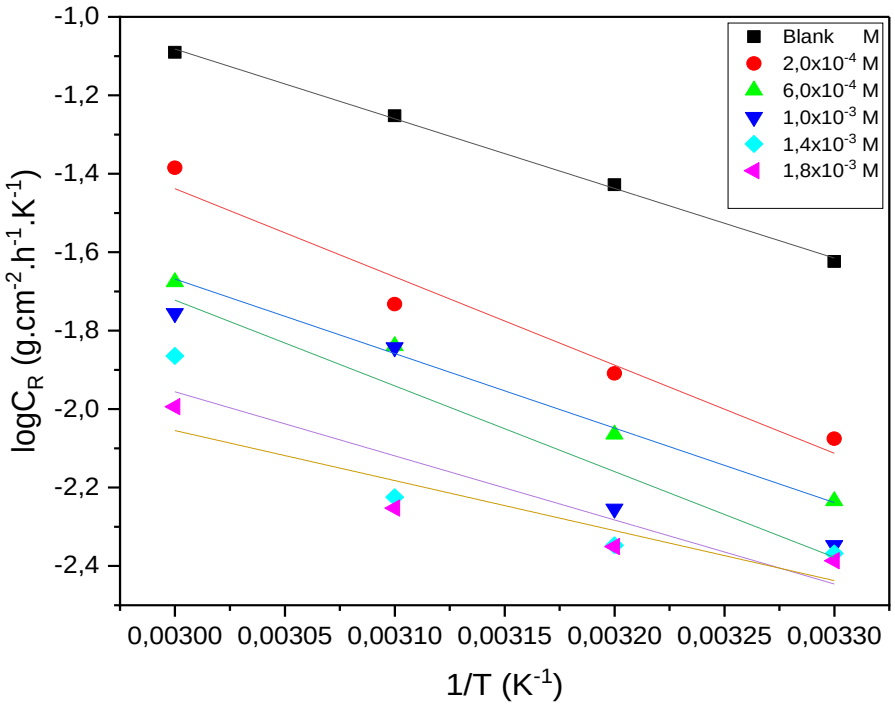

Figure 4.32: Arrhenius plots for zinc metal corrosion in 1.5 M H_2SO_4 solution in the absence and presence of different concentrations of MNHD as the inhibitor.

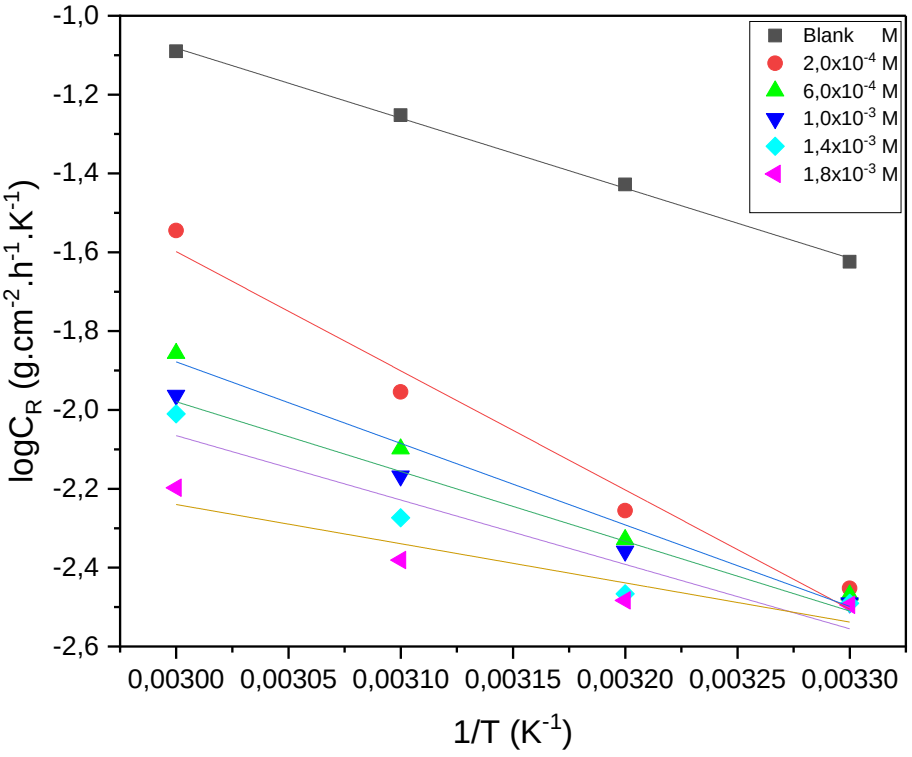

Figure 4.33: Arrhenius plots for zinc metal corrosion in 1.5 M H_2SO_4 solution in the absence and presence of different concentrations of 6-HFN as the inhibitor.

4.1.5.2 Zinc in 1.5 M hydrochloric acid.

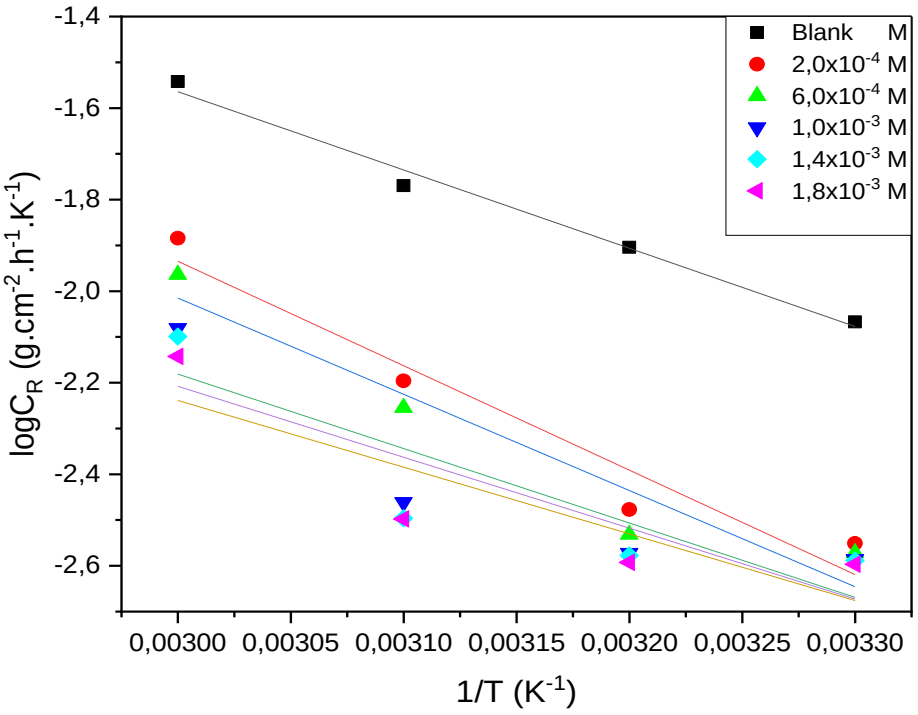

Figure 4.34: Arrhenius plots for zinc metal corrosion in 1.5 M HCl solution in the absence and presence of different concentrations of NRNG as the inhibitor.

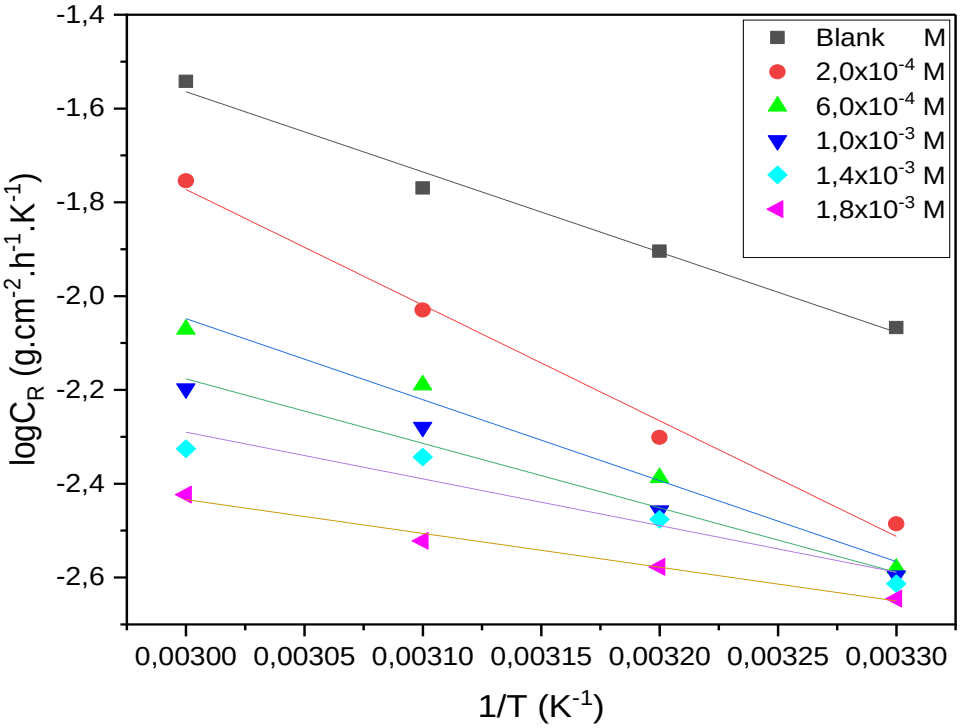

Figure 4.35: Arrhenius plots for zinc metal corrosion in 1.5 M HCl solution in the absence and presence of different concentrations of MNHD as the inhibitor.

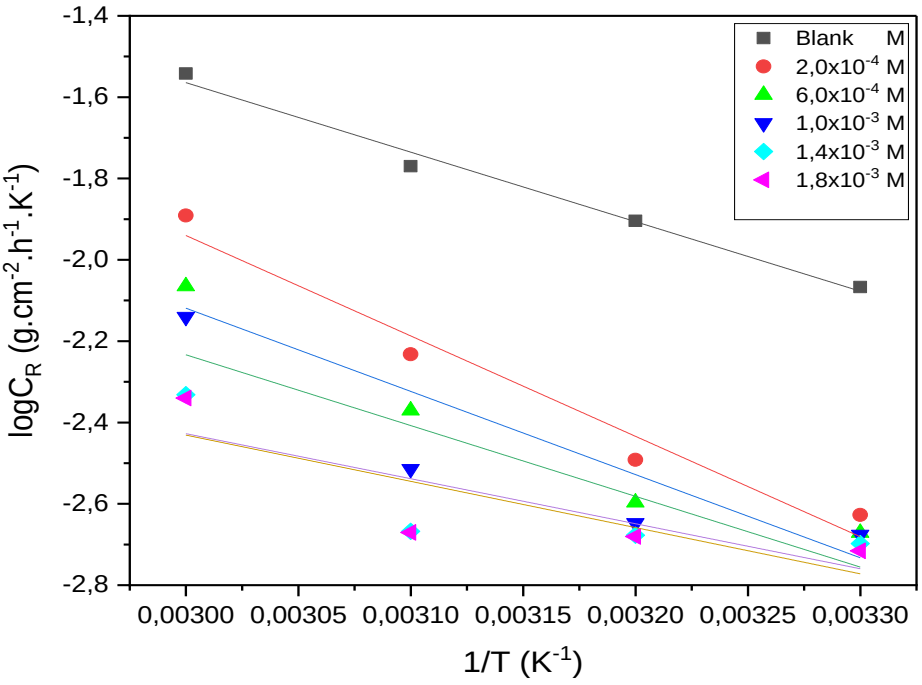

Figure 4.36: Arrhenius plots for zinc metal corrosion in 1.5 M HCl solution in the absence and presence of different concentrations of 6-HFN as the inhibitor.

4.1.5.3 Aluminium in 0.5 M hydrochloric acid.

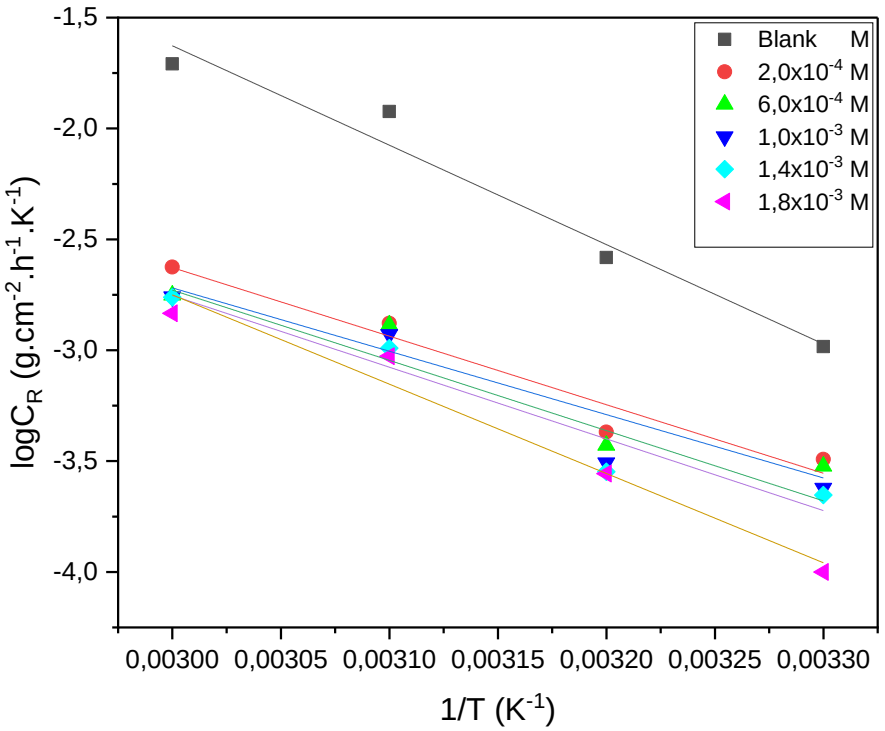

Figure 4.37: Arrhenius plots for aluminium metal corrosion in 0.5 M HCl solution in the absence and presence of different concentrations of NRNG as the inhibitor.

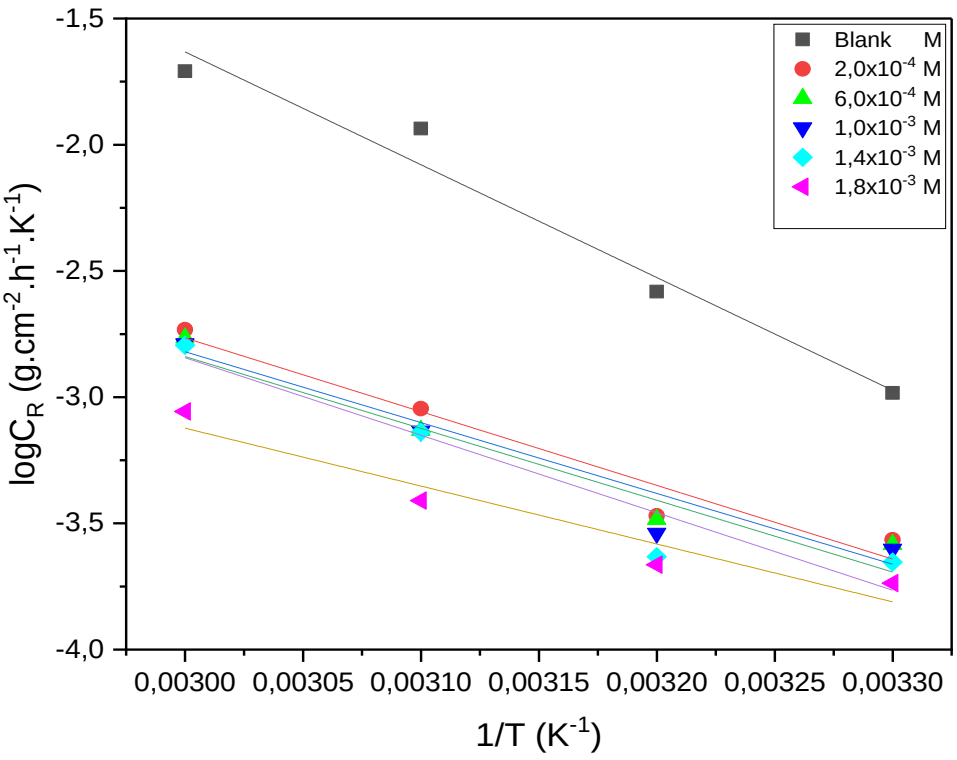

Figure 4.38: Arrhenius plots for aluminium metal corrosion in 0.5 M HCl solution in the absence and presence of different concentrations of MNHD as the inhibitor.

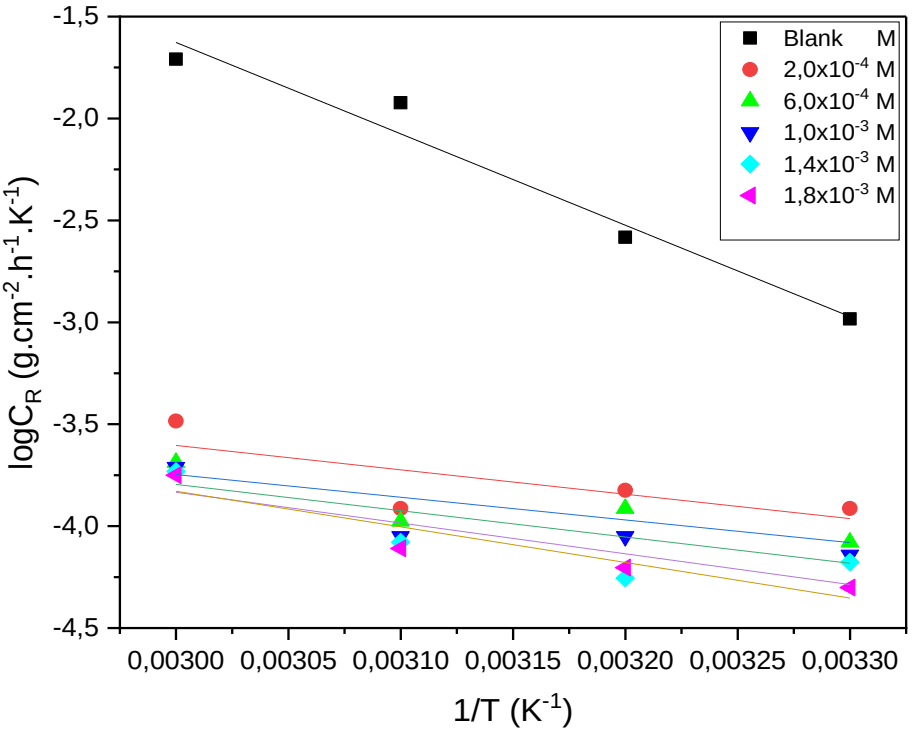

Figure 4.39: Arrhenius plots for aluminium metal corrosion in 0.5 M HCl solution in the absence and presence of different concentrations of 6-HFN as the inhibitor.

The values of the change in enthalpy of activation (ΔH*) and change in entropy of activation (ΔS*) were calculated from the transition state equation below:

$$In\left(\frac{C_R}{T}\right) = \left[In\left(\frac{C_R}{h}\right) + \left(\frac{\Delta S^*}{2.303R}\right)\right] + \left(\frac{-\Delta H^*}{2.303R}\right)\left(\frac{1}{T}\right) \quad (47)$$

where h is the Planck's constant, ΔH* and ΔS* are the activation enthalpy and entropy change, respectively. Figures 4.40 – 4.48, represent plots of ln (C_R/T) against 1/T with the data best fitted having a slope of -ΔH*/R and an intercept of ln(C_R/h)+(ΔS*/2.303R). Tables 4.13 – 4.15, show the values of the E_a , ΔH* and ΔS*.

4.1.5.4 Zinc in 1.5 M sulphuric acid.

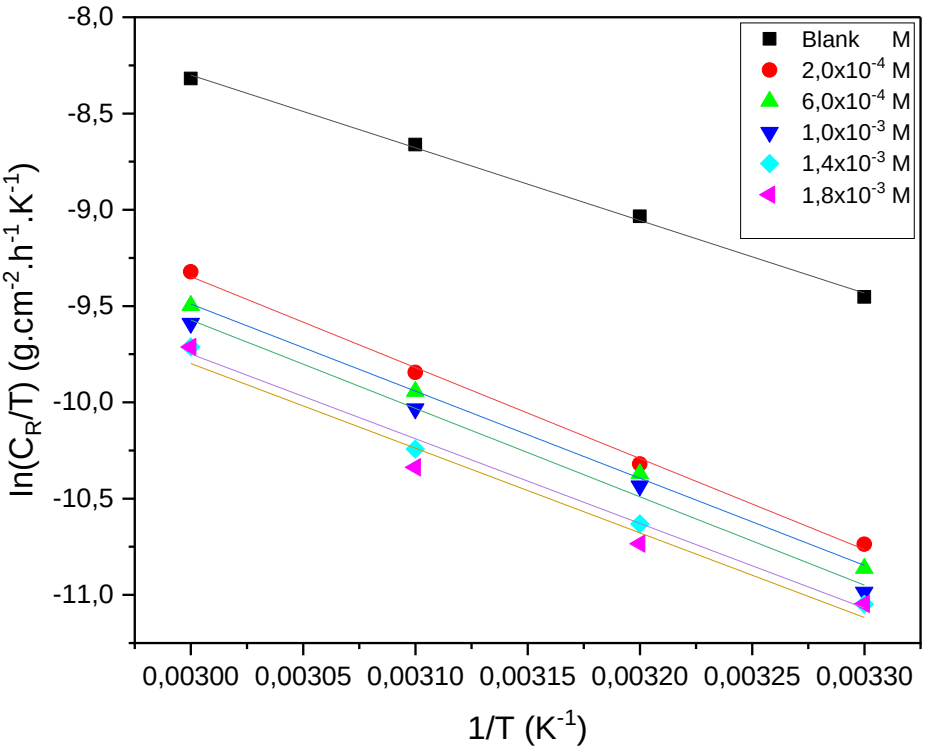

Figure 4.40: Transition state plots for zinc metal corrosion in 1.5 M H_2SO_4 solution in the absence and presence of different concentrations of NRNG as the inhibitor.

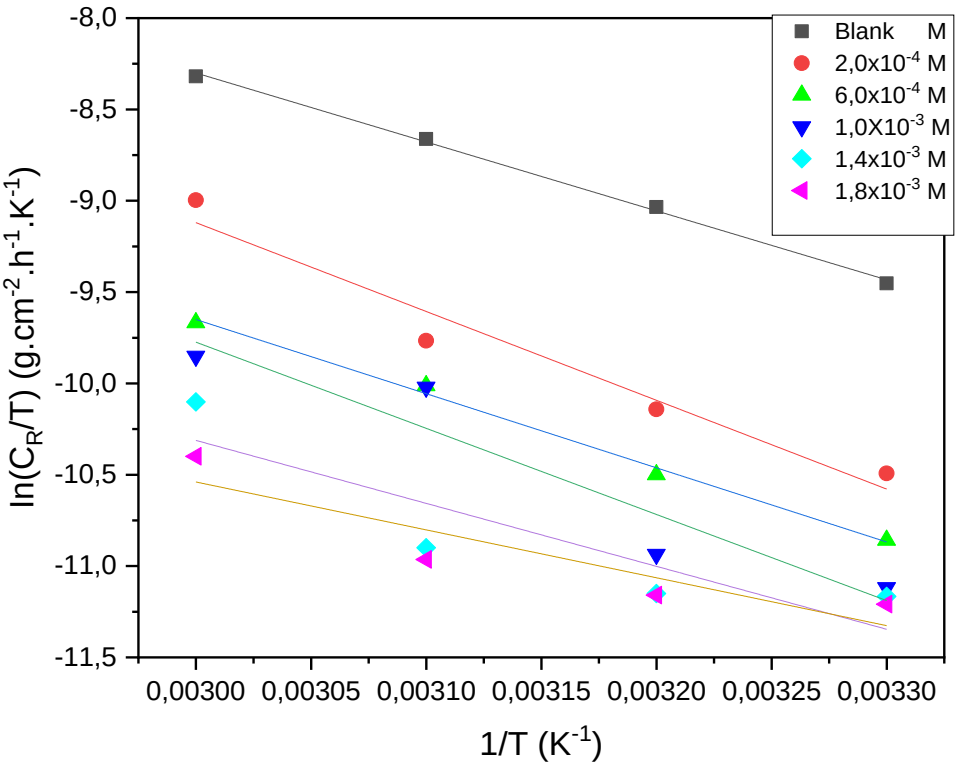

Figure 4.41: Transition state plots for zinc metal corrosion in 1.5 M H_2SO_4 solution in the absence and presence of different concentrations of MNHD as the inhibitor.

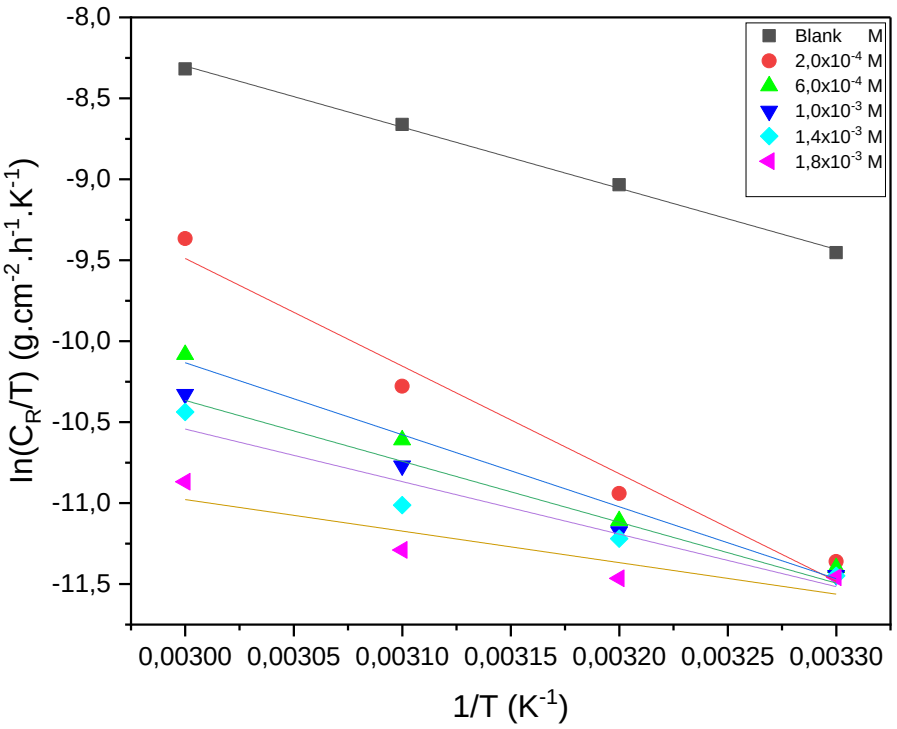

Figure 4.42: Transition state plots for zinc metal corrosion in 1.5 M H_2SO_4 solution in the absence and presence of different concentrations of 6-HFN as the inhibitor.

4.1.5.5 Zinc in 1.5 M hydrochloric acid.

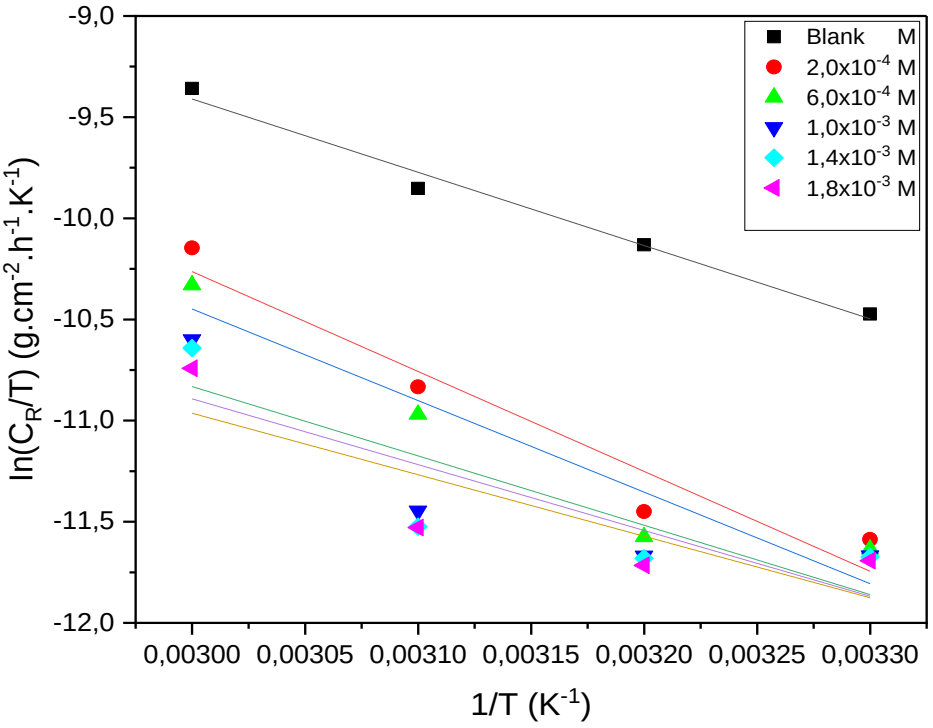

Figure 4.43: Transition plots for zinc metal corrosion in 1.5 M HCl solution in the absence and presence of different concentrations of NRNG as the inhibitor.

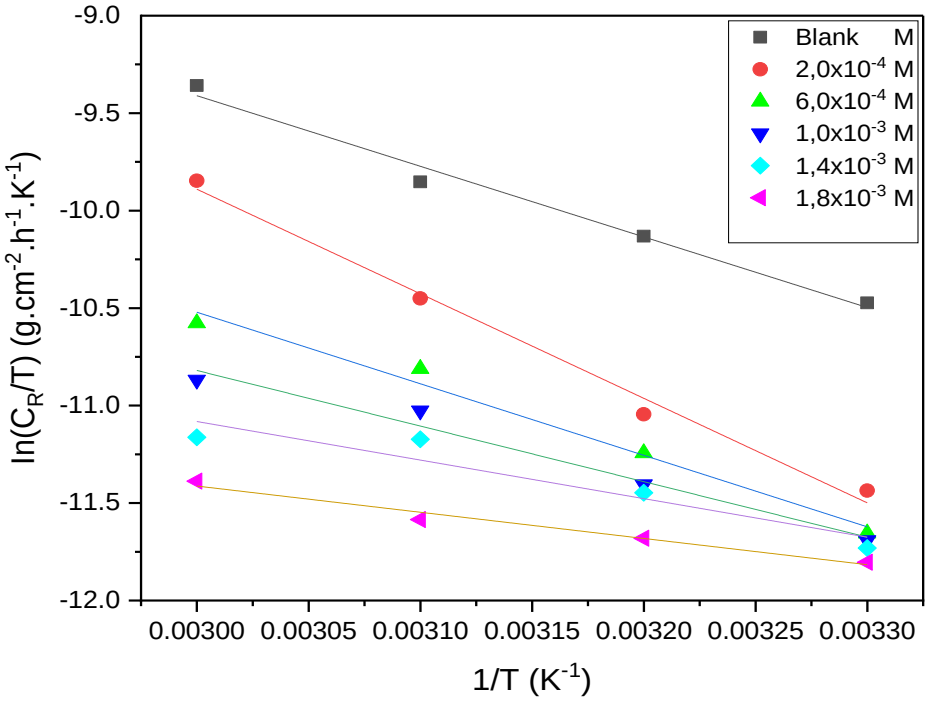

Figure 4.44: Transition state plots for zinc metal corrosion in 1.5 M HCl solution in the absence and presence of different concentrations of MNHD as the inhibitor.

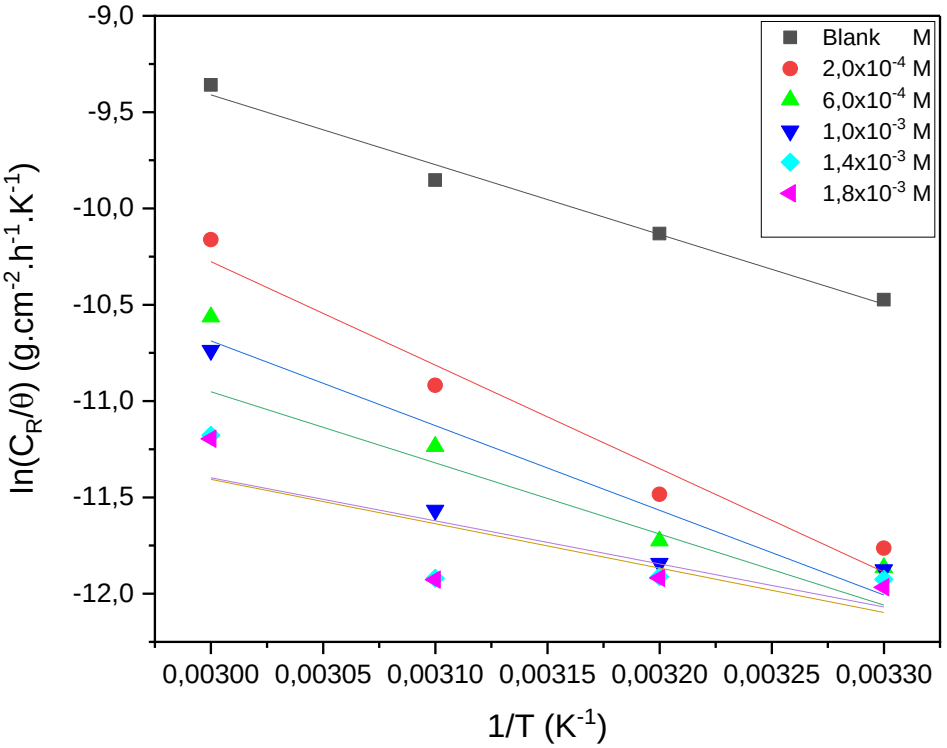

Figure 4.45: Transition state plots for zinc metal corrosion in 1.5 M HCl solution in the absence and presence of different concentrations of 6-HFN as the inhibitor.

4.1.5.6 Aluminium in 0.5 M hydrochloric acid.

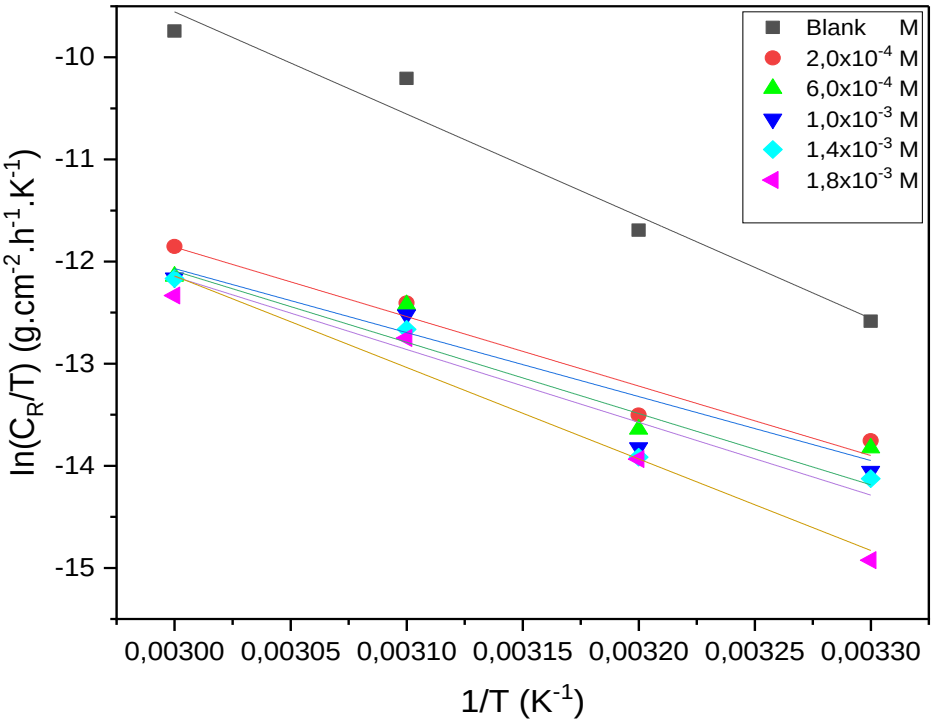

Figure 4.46: Transition state plots for aluminium metal corrosion in 0.5 M HCl solution in the absence and presence of different concentrations of NRNG as the inhibitor.

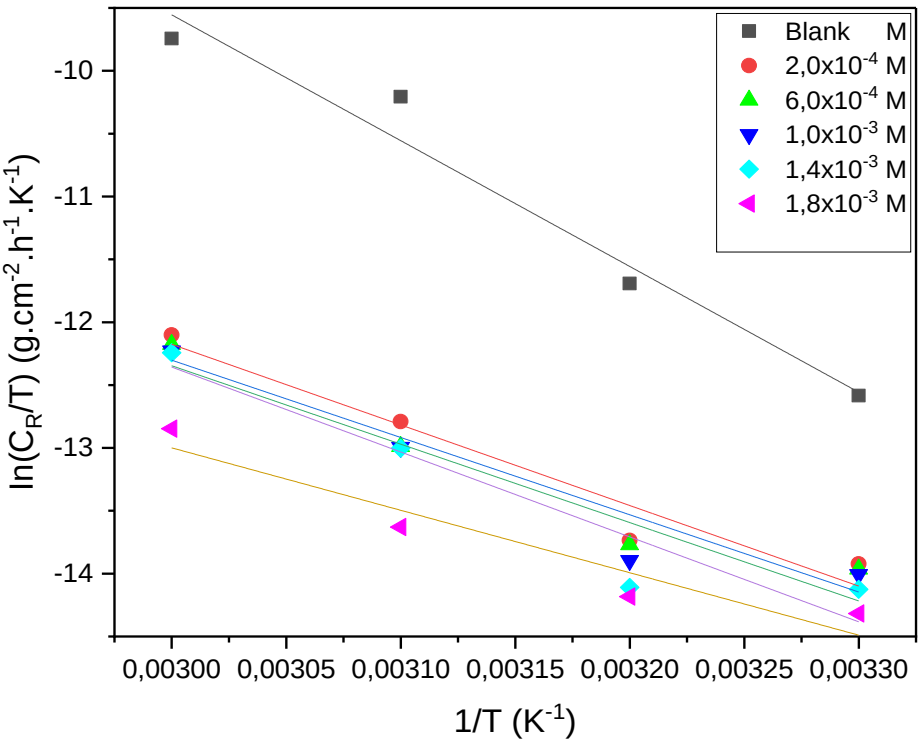

Figure 4.47: Transition state plots for aluminium metal corrosion in 0.5 M HCl solution in the absence and presence of different concentrations of MNHD as the inhibitor.

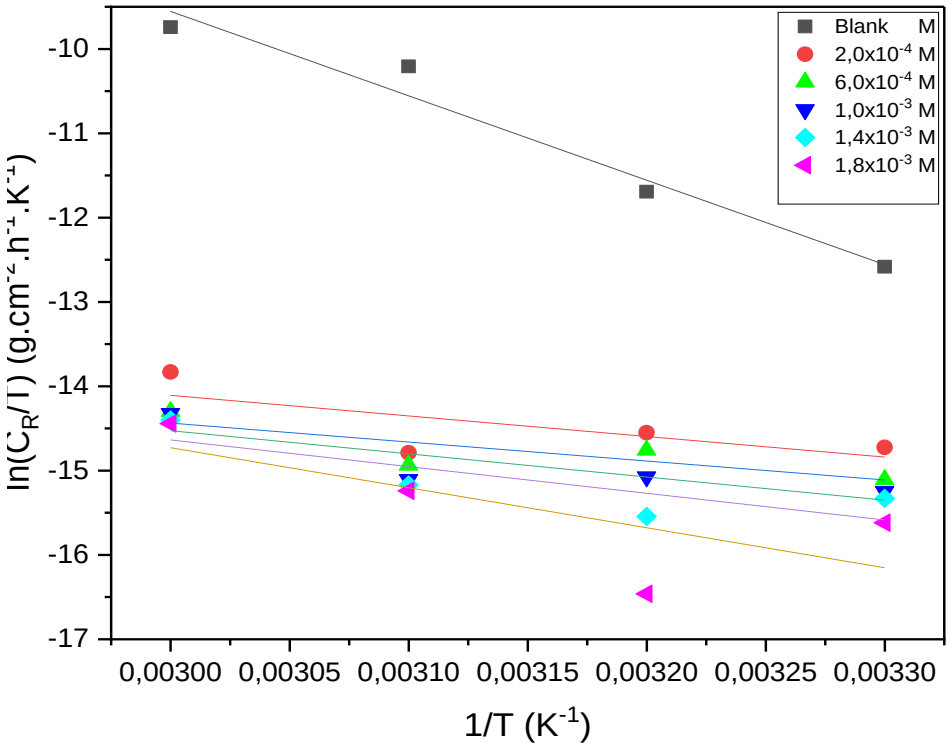

Figure 4.48: Transition state plots for aluminium metal corrosion in 0.5 M HCl solution in the absence and presence of different concentrations of 6-HFN as the inhibitor.

According to the temperature effects, Nasser and company [144], classified the relationships between the E_a and the temperature dependence of %IE of an inhibitor into three groups which are as follows:

- Inhibitors whose inhibition efficiency (IE) decreases with an increase in temperature. The value of apparent activation energy (E_a) found is greater than that in the uninhibited solution.
- Inhibitors whose IE does not change with variation in temperature. The apparent activation energy is found not to change with the absence and presence of inhibitors.
- Inhibitors in which the IE increases with an increase in temperature, the value of E_a for the corrosion process is found to be smaller than that obtained in the uninhibited solution. This according to the author is an indication for a specific type of adsorption of the inhibitors [145].

According to Machu [146], the corrosion process which occurs in the presence of a powerful inhibitor is characterized by an activation energy whose value is smaller than that of the uninhibited process. The lower value of the activation energy of the corrosion process in an inhibitors presence when compared to that in its absence is attributed to its chemisorption, while the opposite is the case with physical adsorption [147, 148].

From Tables 4.13 and 4.14, it is evident that the apparent activation energy decreases with increase in the concentration of the inhibitors. When the inhibitor concentration is between $1.0x10^{-3}$ and $1.8x10^{-3}$ M the apparent activation energy values are lower than that of the blank, except for NRNG in Table 4.13, where the E_a values are all greater than that of the blank. However, when the inhibitor concentration was between $2.0x10^{-4}$ and $6.0x10^{-4}$ M, the E_a values are greater than that of the blank solution. Hence an increase in E_a values with respect to the uninhibited solution at lower concentrations of the acid. Similar results were also reported on the synergistic inhibition between o-phenanthroline and chloride ion cold rolled steel corrosion in phosphoric acid [149]. The higher values of apparent activation energy E_a at low inhibitor concentration may be explained as physical adsorption that takes place in the first stage. The lower values of E_a with reference to the uninhibited solution, observed at higher concentrations of the inhibitor indicates chemisorption [150]. This kind of behaviour observed in E_a for 1.5 M HCl and H_2SO_4 can be considered to be in line with the suggestion that chemisorption at higher concentrations of the inhibitor and physisorption at lower concentrations of the inhibitors. It can be further said that the three inhibitors in the presence of zinc in HCl and H_2SO_4 have a mixture absorption mechanism. This conclusion can be supported by the trend obtained in %IE, where it was increasing with temperature up to 50°C (Chemisorption) and start to decrease at 60°C (Physisorption). In Table 4.15 for aluminium in 0.5 M HCl, an opposite trend was observed compared to that in Tables 4.13 and 4.14, since the apparent activation energy is found to

be increasing with an increase in the concentrations of the inhibitors, and the values are all less than that of the corresponding blank solution. This suggest that the three inhibitors used adsorbs physically in the presence of aluminium metal.

Table 4.13: Arrhenius and transition parameters for the adsorption of different concentrations of NRNG, MNHD and 6-HFN in 1.5 M H_2SO_4 on zinc metal.

Inhibitor	Concentration of inhibitors (M)	E_a (kJ.mol^{-1})	ΔH^* (kJ.mol^{-1})	ΔS^* (J.mol^{-1}.K^{-1})
	0.00	34.007	31.383	-172.418
NRNG	$2.0x10^{-4}$	41.899	39.266	-157.472
	$6.0x10^{-4}$	40.236	37.613	-163.615
	$1.0x10^{-3}$	40.791	38.168	-162.639
	$1.4x10^{-3}$	39.187	36.564	-168.922
	$1.8x10^{-3}$	39.179	36.556	-169.357
MNHD	$2.0x10^{-4}$	43.053	40.429	-152.095
	$6.0x10^{-4}$	36.379	33.756	-176.525
	$1.0x10^{-3}$	41.842	39.217	-161.173
	$1.4x10^{-3}$	31.284	28.662	-197.308
	$1.8x10^{-3}$	24.420	21.799	-219.791
6-HFN	$2.0x10^{-4}$	58.0594	55.258	-110.676
	$6.0x10^{-4}$	39.5970	36.974	-170.883
	$1.0x10^{-3}$	33.8900	27.942	-189.937
	$1.4x10^{-3}$	32.2854	26.971	-204.297
	$1.8x10^{-3}$	19.0355	16.190	-240.260

Table 4.14: Arrhenius and transition parameters for the adsorption of different concentrations of NRNG, MNHD and 6-HFN in 1.5 M HCl on zinc metal.

Inhibitor	Concentration of inhibitors (M)	E_a (kJ.mol^{-1})	ΔH^* (kJ.mol^{-1})	ΔS^* (J.mol^{-1}.K^{-1})
	0.00	32.7376	30.117	-185.44
NRNG	$2.0x10^{-4}$	43.6856	41.061	-159.707
	$6.0x10^{-4}$	40.2515	37.628	-171.544
	$1.0x10^{-3}$	31.1407	28.503	-202.100
	$1.4x10^{-3}$	29.6694	27.048	-206.976
	$1.8x10^{-3}$	27.9033	25.282	-212.867

MNHD	$2.0x10^{-4}$	47.2182	44.593	-146.006
	$6.0x10^{-4}$	33.0662	30.512	-193.505
	$1.0x10^{-3}$	26.3246	23.703	-216.407
	$1.4x10^{-3}$	19.0639	16.444	-240.362
	$1.8x10^{-3}$	13.7912	11.178	-258.912
6-HFN	$2.0x10^{-4}$	47.2785	44.655	-149.031
	$6.0x10^{-4}$	39.1739	36.550	-176.766
	$1.0x10^{-3}$	33.3209	30.698	-196.515
	$1.4x10^{-3}$	21.2015	18.641	-236.407
	$1.8x10^{-3}$	21.7741	19.096	-234.098

Table 4.15: Arrhenius and transition parameters for the adsorption of different concentrations of NRNG, MNHD and 6-HFN in 0.5 M HCl on aluminium metal.

Inhibitor	**Concentration of inhibitors (M)**	**E_a (kJ.mol^{-1})**	**ΔH^* (kJ.mol^{-1})**	**ΔS^* (J.mol^{-1}.K^{-1})**
	0.00	85.8370	83.205	-27.384
NRNG	$2.0x10^{-4}$	59.1892	56.562	-126.465
	$6.0x10^{-4}$	54.7130	52.087	-141.642
	$1.0x10^{-3}$	60.6720	58.044	-123.960
	$1.4x10^{-3}$	61.9190	59.289	-120.691
	$1.8x10^{-3}$	77.1473	74.498	-75.0080
MNHD	$2.0x10^{-4}$	55.9310	53.305	-138.877
	$6.0x10^{-4}$	53.7413	51.115	-146.495
	$1.0x10^{-3}$	54.4871	51.860	-144.625
	$1.4x10^{-3}$	58.7959	56.169	-131.862
	$1.8x10^{-3}$	43.9354	41.300	-181.739
6-HFN	$2.0x10^{-4}$	22.9112	20.291	-253.978
	$6.0x10^{-4}$	21.3090	18.698	-261.493
	$1.0x10^{-3}$	24.7036	22.083	-252.260
	$1.4x10^{-3}$	28.9139	26.303	-240.339
	$1.8x10^{-3}$	33.4522	39.452	-201.657

The values of change in enthalpy (ΔH^*) and entropy (ΔS^*) were calculated from the slope $-\Delta H^*/R$ and intercept $\ln(C_R/h+\Delta S^*/R)$ of the transition state plot. The adsorption process which occurred between zinc, aluminium and the inhibitor molecules can be classified as either endothermic or exothermic. Expanding on this, endothermic process absorbs heat and it entirely suggests chemisorption, while exothermic process gives off heat and may either suggest physisorption or chemisorption [25]. Physisorption involves the electrostatic interaction between the charged molecules and the charged

metal. On the other hand, chemisorption involves charge transfer or sharing from the inhibitor molecules to the metal surface to form a coordinated bond. From Tables 4.13 – 4.15, the values of the change in enthalpy of activation are positive which entails the fact that, the dissolution process of zinc and aluminium is endothermic in nature which entails chemisorption kind of adsorption. Comparison of the value of the change in enthalpy of activation for the inhibited process to that of the uninhibited process for zinc shows that at lower concentration of the inhibitor ($2.0x10^{-4}$ and $6.0x10^{-4}$) the values of ΔH^* are high as opposed to those of the uninhibited process, but at higher concentration ($1.0x10^{-3}$-$1.8x10^{-3}$) it was found to be lower than that of the uninhibited process. When NRNG was used in H_2SO_4, the ΔH^* values are found to be higher than that of the inhibited solution. However, in Table 4.15 for aluminium, the values of ΔH^* for the inhibited solution are found to be lower than those of the uninhibited solution. Through this observation it can be said that there is an adsorption process between zinc metal surface and the inhibitor molecules, and aluminium metal surface and the inhibitor molecules. Studies reveals that the numerical values of enthalpy of activation ranging up to 41.86 $kJ.mol^{-1}$ are associated with physisorption type of adsorption whereas those around 100 $kJ.mol^{-1}$ or higher are associated with chemisorption [151].

In the case of this study, Tables 4.13 and 4.14 shows that the values of change in enthalpy of activation form $6.0x^{-4}$ – $1.8x10^{-3}$ M are below 41.86 $kJ.mol^{-1}$. But at the lowest concentration of $2.0x10^{-4}$ M, the values of ΔH^* are higher than 41.86 $kJ.mol^{-1}$. It can be said that this behaviour is attributed to physisorption and chemisorption kind of adsorption between the zinc, surface, and the inhibitor molecules. NRNG in Table 4.13 adsorbs through physisorption only, since its ΔH^* values are all lower than 41.86 $kJ.mol^{-1}$. In Table 4.15, for aluminium metal, the values of change in enthalpy in the inhibited process are less than that of their respective change in enthalpy for the uninhibited process and are higher than 41.86 $KJ.mol^{-1}$, and this suggest a chemisorption kind of adsorption process. In the presence of 6-HFN in Table 4.15 for aluminium, the values of ΔH^* are less than 41.86 $kJ.mol^{-1}$ and this suggest a physisorption kind of behaviour.

The values of the change in entropy (ΔS^*) are large and negative in absence and presence of the inhibitors solutions and this shows that the activated complex in the rate determining step represent association rather than dissociation, which means a decrease in disordering occurs on going from reactants to activated complex [152]. The negative values of ΔS^* can be explained in the following manner: before the inhibitors are adsorbed onto the zinc and aluminium surfaces, the inhibitors molecules might have been freely moving in the bulk solution, in other words the inhibitors molecules

were very chaotic. With the progress in the adsorption, the inhibitor molecules where orderly adsorbed onto the zinc and aluminium surface and as a result, a decrease in entropy [153].

4.2 Atomic Absorption Spectroscopy

Atomic Absorption Spectroscopy is regarded as an optical atomic spectrometric technique which is focused on the specific absorption measurements originating from the free nonionized atoms in the gas phase. Different types of atomizer, like flame and graphite furnace are used to transfer the analyte to free atoms. Flame has the order of 1 – 100 μgL^{-1} detection limits, making it the most suitable tool for the determination of minor and trace elements for contaminated samples. On the other hand, graphite furnace has detection limits which are 20 – 200 μgL^{-1} lower than that of flame (FAAS). It is normally used for background values and for the unpolluted samples such as biological materials and fresh water and it is regarded as a standard method for many trace elements [131]. In this study, Graphite Furnace Atomic Absorption Spectroscopy (GFAAS) was utilised to get information that is very helpful in explaining the corrosion phenomenon of the materials involved. The results obtained are recorded in Tables 4.16 – 4.19 below and the calibration curve for zinc and aluminium metals are graphically represented in Figures 4.49 and 4.50.

Table 4.16: Absorbance and the concentration for zinc and aluminium metal used in constructing the calibration curve.

Zinc		Aluminium	
Concentration ($mg.L^{-1}$)	**Absorbance**	**Concentration ($mg.L^{-1}$)**	**Absorbance**
0.0	0.000	0.0	0.000
0.2	0.394	0.2	0.308
0.4	0.721	0.4	0.628
1.0	1.305	2.8	1.844
2.0	1.982	8.0	3.760
3.0	3.806	10.0	4.651

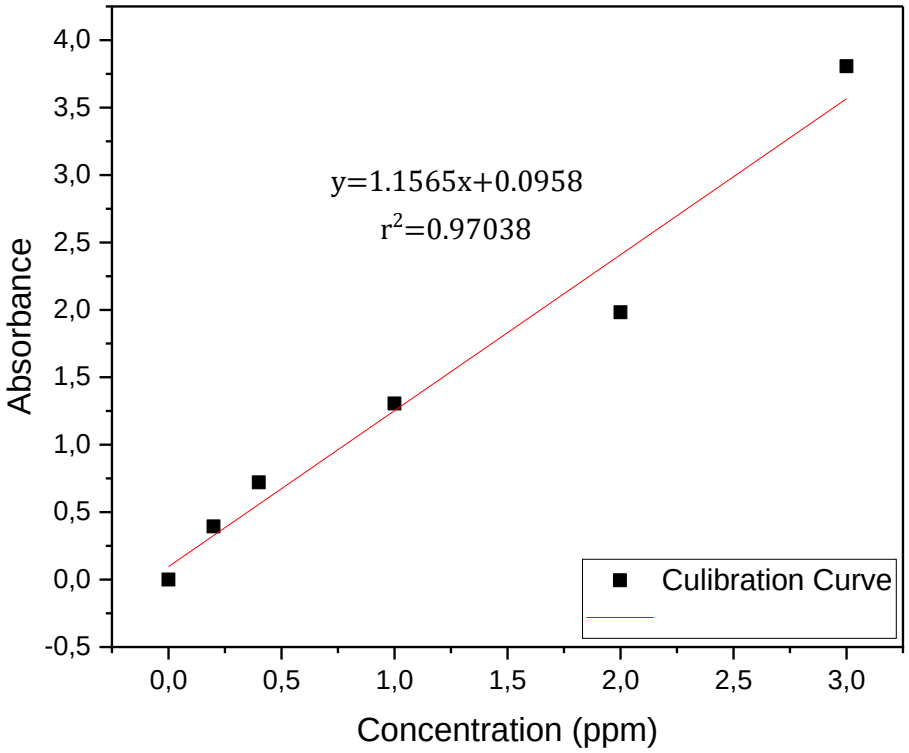

Figure 4.49: Calibration curve for zinc.

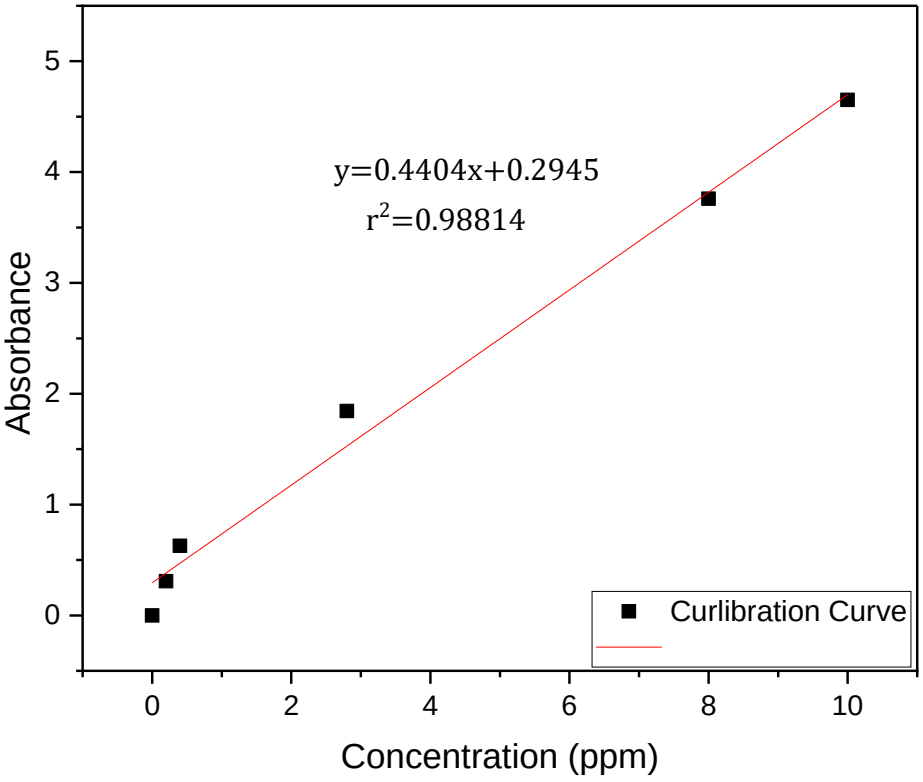

Figure 4.50: Calibration curve for aluminium.

Figures 4.49 and 4.50 show the standardization or calibration curve for zinc and aluminium metals, respectively. The curves were obtained by preparing the zinc and aluminium solutions, which were then analysed by AAS. The curves are very much helpful in terms of generating an equation that assist in calculating the concentration of the metals left in solution due to corrosion after gravimetric analysis, given the absorbance.

Table 4.17: Absorbance and concentration of NRNG, MNHD and 6-HFN in zinc in 1.5 M H_2SO_4

Inhibitors	Absorbance	Concentration (M)	$\%IE_{AAS}$
Blank	8.3203	7.1115	-
NRNG	4.5283	3.8343	46.083
MNHD	1.5228	1.2344	82.642
6-HFN	1.6128	1.3123	81.548

Table 4.18: Absorbance and concentration of NRNG, MNHD and 6-HFN in zinc in 1.5 M HCl

Inhibitors	Absorbance	Concentration (M)	$\%IE_{AAS}$
Blank	7.9396	6.7823	-
NRNG	2.9667	2.4824	63.399
MNHD	2.7235	2.2721	66.500
6-HFN	2.1357	1.7638	73.994

Table 4.19: Absorbance and concentration of NRNG, MNHD and 6-HFN in aluminium in 0.5 M HCl.

Inhibitors	Absorbance	Concentration (M)	$\%IE_{AAS}$
Blank	5.0046	10.6950	-
NRNG	2.2707	4.4873	58.043
MNHD	2.4258	4.8395	54.750
6-HFN	1.4765	2.6839	74.905

Since the metals were confirmed to have halt the corrosion process to some extent in section 4.1, it must be expected that the concentration of the ions of the metals left in solution after gravimetric analysis for the blank solution to be greater than those left in solution after gravimetric analysis for the inhibited solutions. This can be further supported by looking at the weight loss of the metals after gravimetric analysis for both the inhibited solutions and the uninhibited solutions. From the gravimetric results, it was found that the weight loss of the uninhibited solutions was much higher compared to those of the inhibited solutions. From Tables 4.17 – 4.19, it is evident that the

concentrations of the uninhibited solutions are higher than those of the inhibited solutions as expected. Table 4.19 showed the largest difference in concentration between the uninhibited and inhibited solutions, with the concentration of the uninhibited (blank) solution being 10.695 ppm as compared to 4.4873, 4.8395 and 2.6839 ppm for NRNG, MNHD and 6-HFN, respectively. In Table 4.17 for zinc in sulphuric acid, the high percentage inhibition efficiency obtained (82.642 % for MNHD and 81.548 % for 6-HFN) strongly suggest that the inhibitors used managed to reduce the amount of metals specimens or ions left in solution after gravimetric analysis. The lowest inhibition efficiency was obtained for NRNG in Table 4.17 for zinc in sulphuric acid amounting to 46.083 %. The inhibition efficiency was calculated using equation (48).

$$\%IE_{AAS} = \left(1 - \frac{C_{inh}}{C_{blnk}}\right) \times 100 \quad (48)$$

where C_{blnk} and C_{inh} are zinc and aluminium ions concentrations in absence and presence of the inhibitors.

4.3 Fourier Transform Infrared Spectroscopy.

Fourier transform infrared is a type of infrared spectroscopy which is used to Identify functional groups of different compounds. It does this by passing an IR bean on sample positioned on its way. The FTIR spectra of the three inhibitors studied are shown in Figures 4.51 – 4.59. Tables 4.20 – 4.22 show the absorption wavelengths for different important functional groups present on the inhibitor compounds. Three spectra of blank solution, pure compound, and the (compound + acid) at 30° C were drawn in one graph for clear comparisons between the shift and disappearance of the functional groups on the (compound + acid) at 30° C solution after gravimetry as compared to the other two spectra.

4.3.1 Zinc in 1.5 M sulphuric acid.

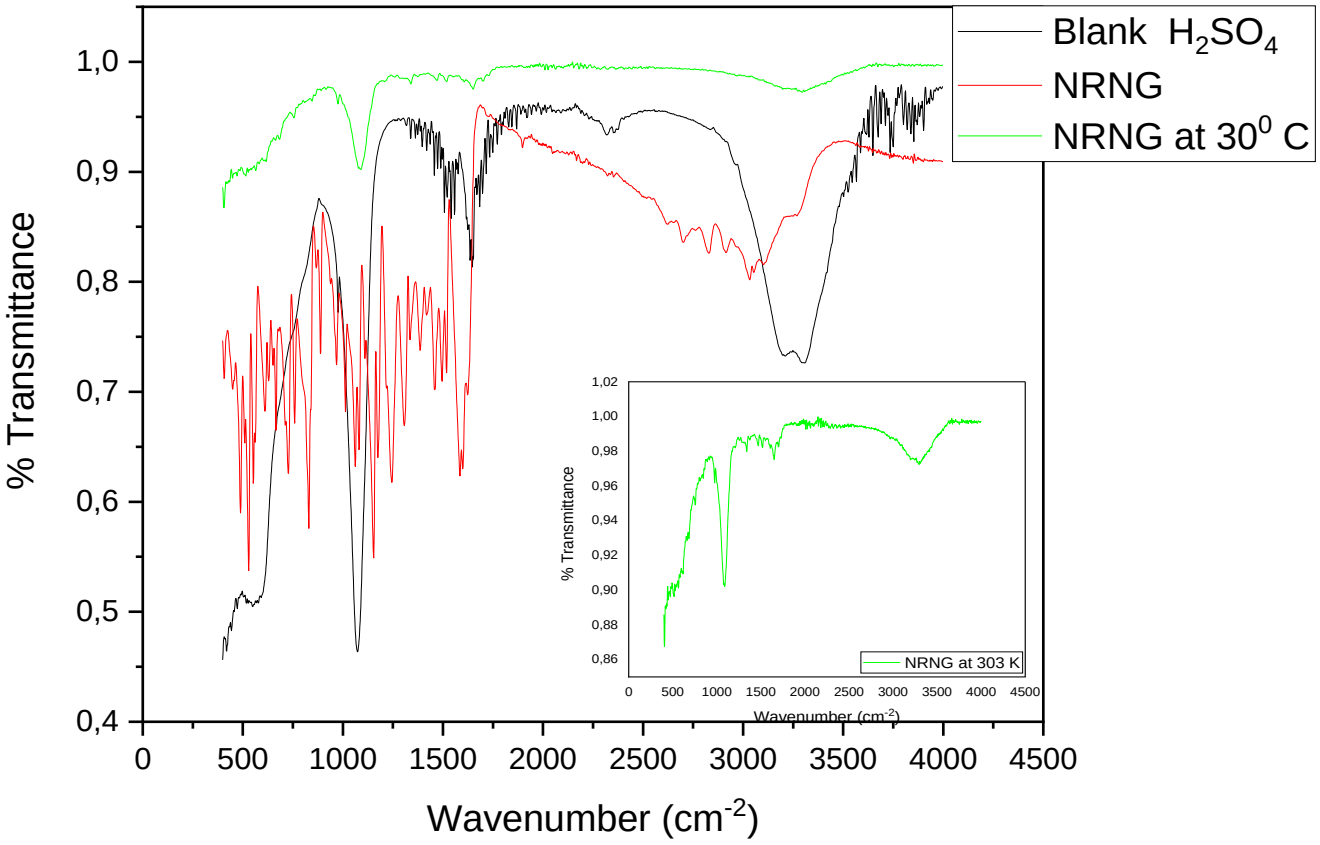

Figure 4.51: FT-IR spectrum of 1.5 M H_2SO_4 blank and NRNG solution for zinc metal from gravimetric analysis at 30° C and NRNG pure compound.

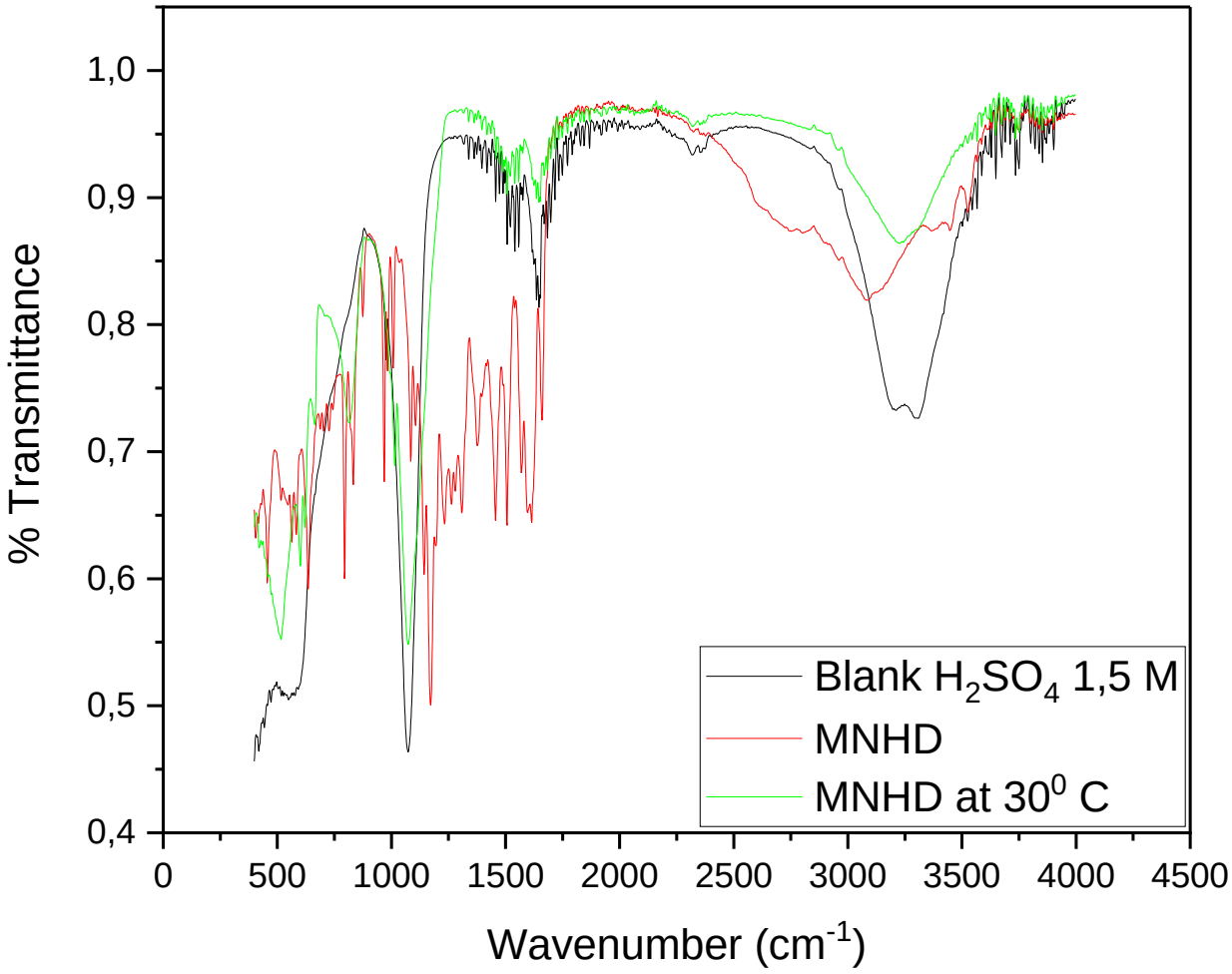

Figure 4.52: FT-IR spectrum of 1.5 M H_2SO_4 blank and MNHD solution for zinc metal from gravimetric analysis at 30° C and MNHD pure compound.

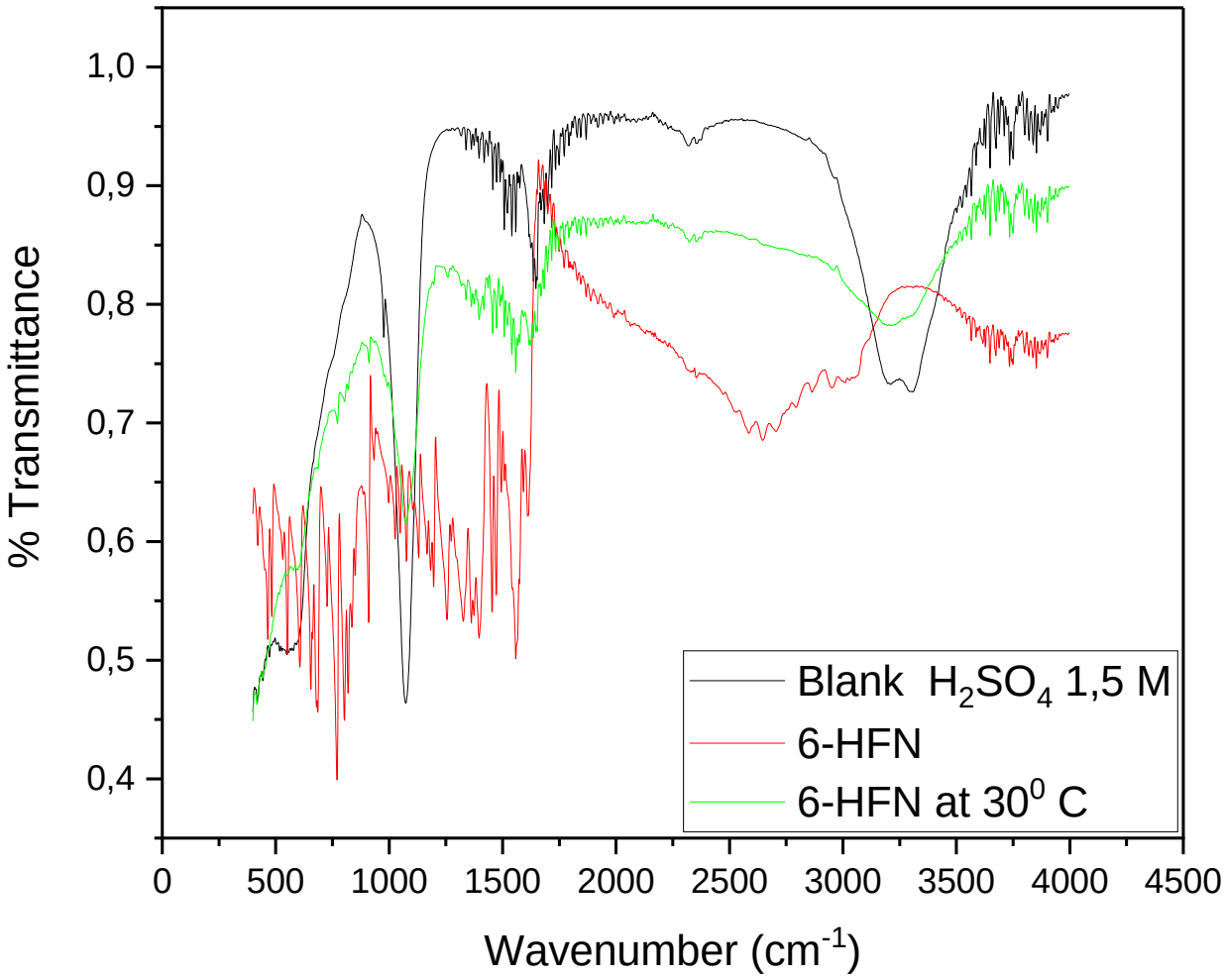

Figure 4.53: FT-IR spectrum of 1.5 M H_2SO_4 blank and 6-HFN solution for zinc metal from gravimetric analysis at 30° C and 6-HFN pure compound.

Figures 4.51 – 4.53 above show the FTIR spectra of the three pure inhibitors (NRNG, MNHD and 6-HFN) represented by red colour, blank solution of sulphuric acid in zinc represented by black colour and that of the inhibitors in the presence of zinc and sulphuric acid represented by green colour. In figure 4.51, a small spectrum of the 6-HFN inhibitor at 30° C was included for clear version of absorption peak, since the bigger spectra did not show the absorption peaks clearly which is due the variation of the % Transmittance scale. A clear shift can be seen in the inhibited spectra at 30° C as compared to that of the pure compound showing a change or disturbance in the absorption wavelength, which can be attributed to the adsorption of the inhibitors on the metal surface.

Table 4.20: Peaks and their identification, from FTIR spectra of the studied corrosion inhibitors and adsorption films formed on the zinc in 1.5 M H_2SO_4.

Inhibitor Zinc in sulphuric acid	Functional groups Peaks form FTIR Spectra (cm^{-1})					
	Ar-OH	Ar-O-R	C=C (Ar)	C=C	C-H (Ar)	Ar-(CO)-R
NRNG	-	-	1470.46	1651.19	-	-
MNHD	-	1073.42	1473.39	1646.80	-	1683.33
6-HFN	-	1074.02	1473.11		-	1683.24

NRNG, MNHD and 6-HFN did not show any signal for OH attached to aromatic ring in the region 1180 – 1260 cm^{-1}. MNHD and 6-HFN showed medium strong intensity peak at 1073.42 and 1074.02 respectively for Ar-O-R, whereas NRNG did not show any signal for this functional group. All the three inhibitors retained their medium strong intensity peak for C=C in the aromatic region but did not retain their strong C-H intensity peak in the aromatic region. NRNG and MNHD retained their very weak medium intensity peak for C=C alkene functional group. 6-HFN do not have an alkene C=C bond in its structure expect the aromatic C=C bond, hence, the reason it was not accounted for it. For AR-(C=O)-R functional group a strong intensity peak was observed for 6-HFN and MNHD at 1683.24 and 1683.33 cm^{-1} respectively, while NRNG did not show any signal for this functional group.

4.3.2 Zinc in 1.5 M hydrochloric acid

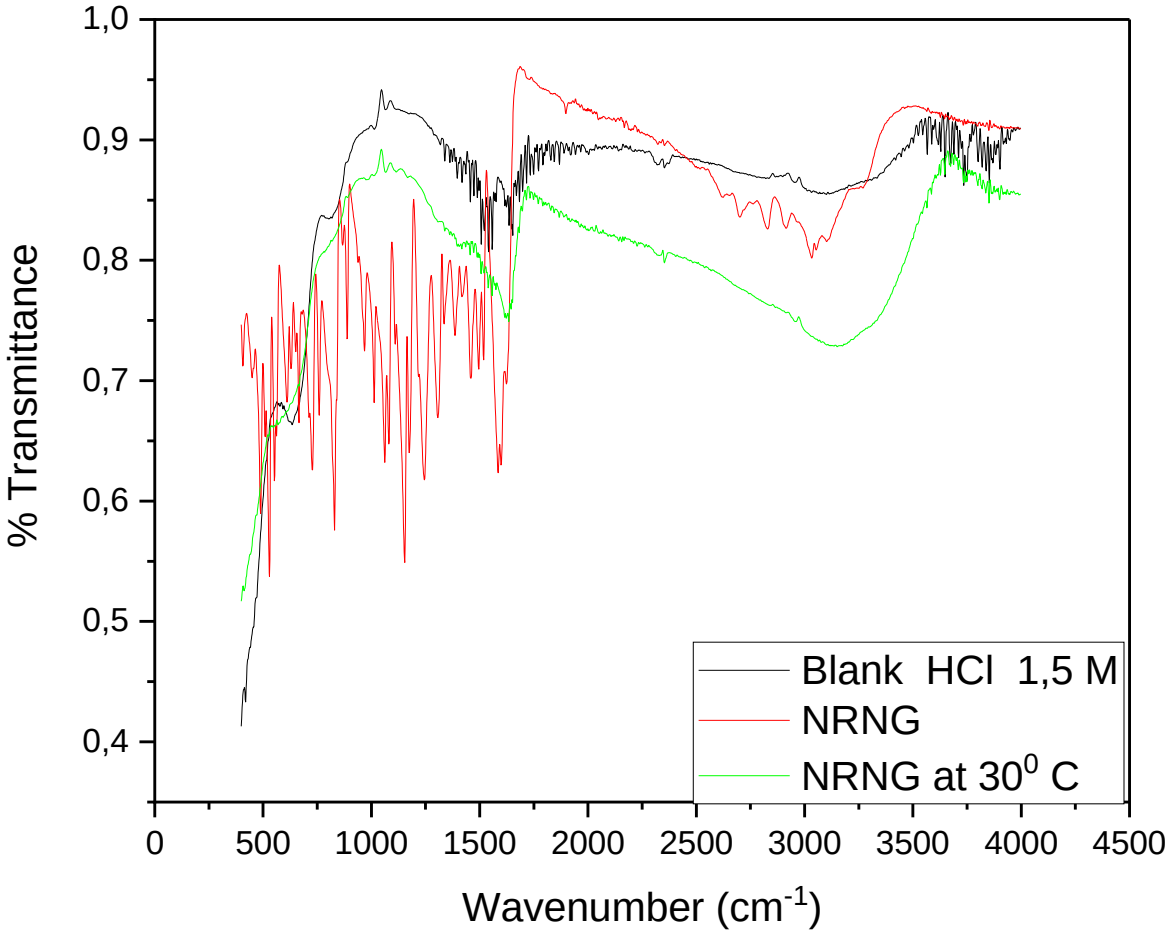

Figure 4.54: FT-IR spectrum of 1.5 M HCl blank and NRNG solution for zinc metal from gravimetric analysis at 30° C and NRNG pure compound.

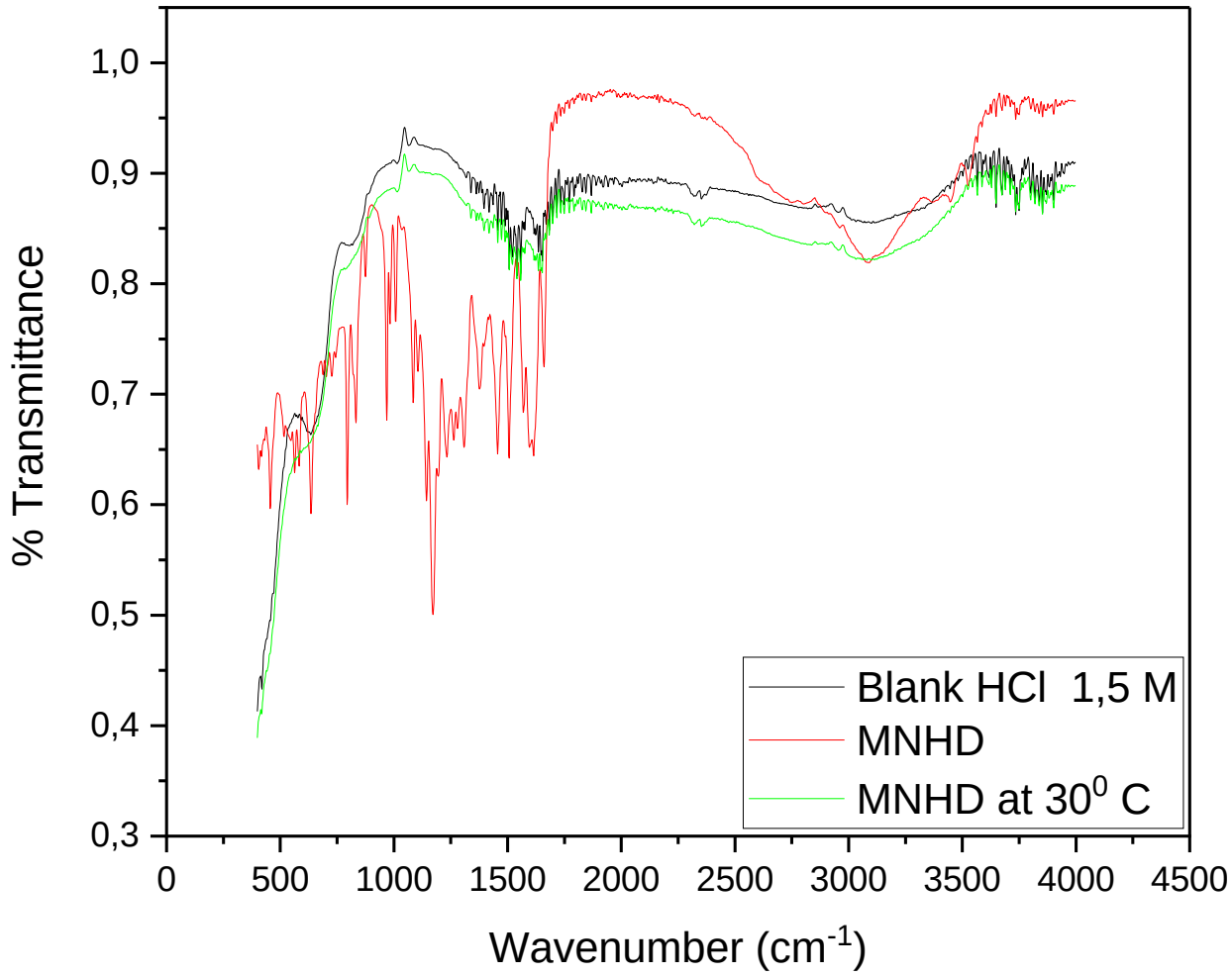

Figure 4.55: FT-IR spectrum of 1.5 M HCl blank and MNHD solution for zinc metal from gravimetric analysis at 30° C and MNHD pure compound.

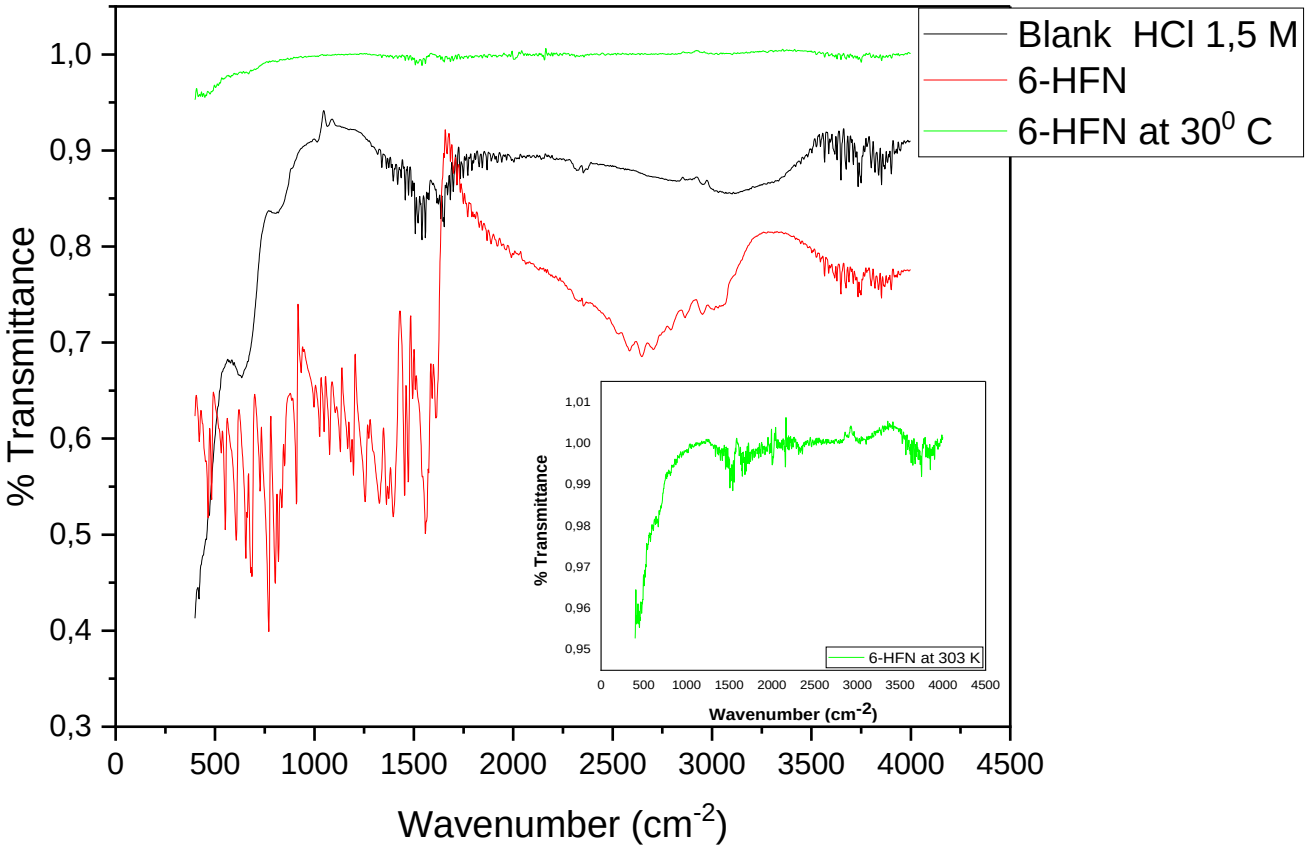

Figure 4.56: FT-IR spectrum of 1.5 M HCl blank and 6-HFN solution for zinc metal from gravimetric analysis at 30° C and 6-HFN pure compound.

Figures 4.54 – 4.56 above shows the FTIR spectra of the three pure inhibitors (NRNG, MNHD and 6-HFN), blank solution of hydrochloric acid in zinc and that of the inhibitors in the presence of zinc and hydrochloric acid. Just like in figure 4.51 above, figure 4.56 also contain a small spectrum of the 6-HFN inhibitor at 303 K for clear version of absorption peak, since the bigger spectra did not show the absorption peaks clearly which is due the variation of the % Transmittance scale. The fact that there is a change in the spectrum of the inhibitor at 303 K as compared to that of the pure inhibitor, indicate the change and adsorption of certain functional group of the compound onto the metal surface.

Table 4.21: Peaks and their identification, from FTIR spectra of the studied corrosion inhibitors and adsorption films formed on the zinc in 1.5 M HCl.

Inhibitor Zinc in sulphuric acid	Functional groups Peaks form FTIR Spectra (cm^{-1})					
	Ar-OH	Ar-O-R	C=C (Ar)	C=C	C-H (Ar)	Ar-(CO)-R
NRNG	-	1065.89	1472.26	-	-	-
MNHD	-	-	1473.07	1652.17	3079.93	1683.18
6-HFN	-	-	1473.13		3064.40	1683.35

When hydrochloric acid was used in zinc as a corrosive medium in the presence of the three inhibitors being studied, Ar-OH functional group was not peaked which means that after gravimetric analysis the compounds lost the O-H bonds. The -O-R attached to the aromatic ring (Ar-O-C) functional group peak for NRNG with a medium strong intensity was spotted at 1065.89 cm^{-1} wavelength, while MNHD and 6-HFN spectra did not show any peak for Ar-O-R functional group. The medium strong intensity peak of C=C functional group in the aromatic ring was retained by the three inhibitors. A very weak medium intensity peak for C=C alkene functional group was only peaked by MNHD inhibitor. 6-HFN does not contain such functional group in its structure, hence the reason it was not considered. MNHD and 6-HFN showed a strong intensity for C-H functional group in the aromatic ring (3079.93 and 3064.40 cm^{-1}) and a medium strong intensity peak for Ar-(CO)-R functional group with 1683.18 and 1683.35 cm^{-1} respectively.

4.3.3 Aluminium in 0.5 M hydrochloric acid.

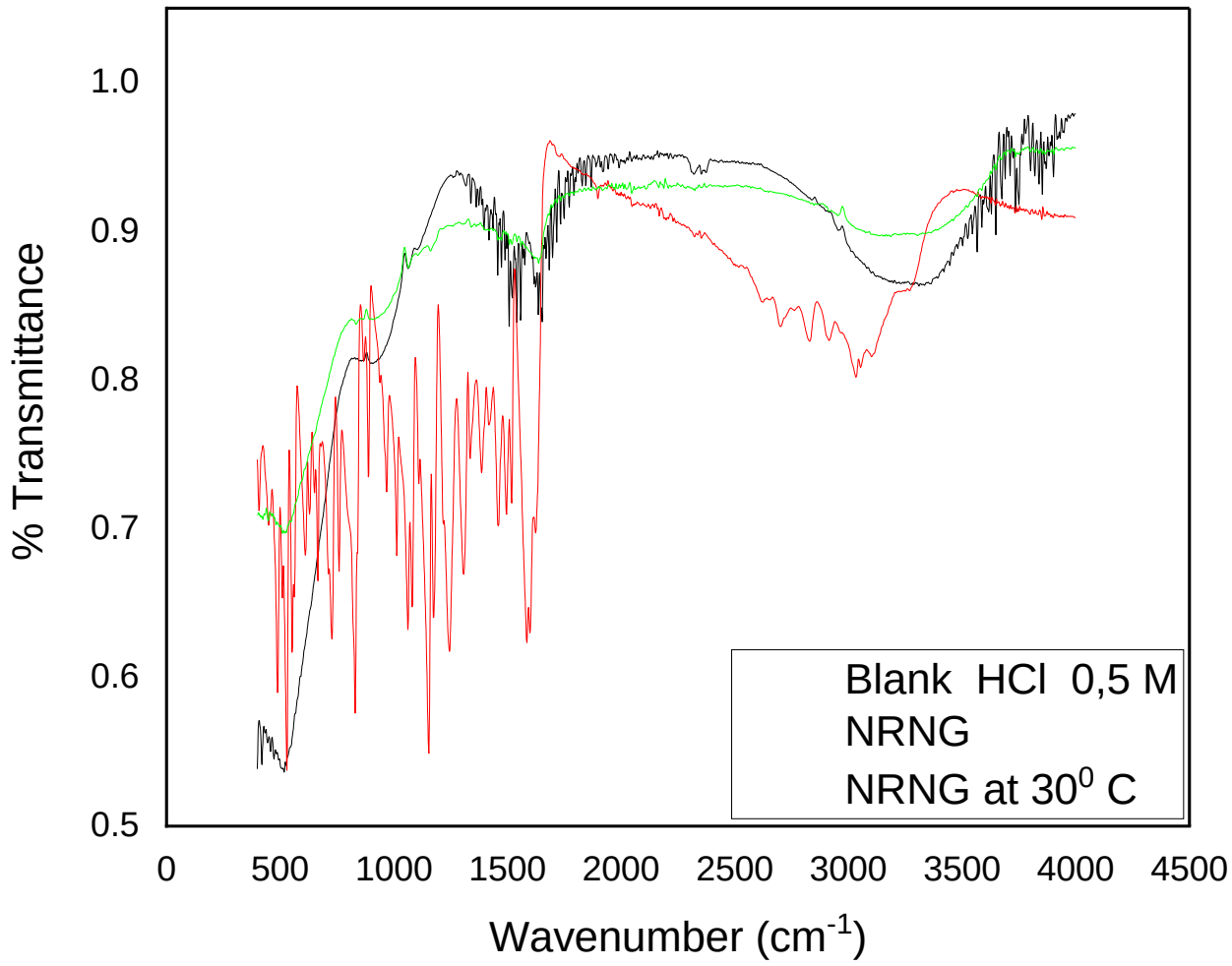

Figure 4.57: FT-IR spectrum of 0.5 M HCl acid blank, NRNG pure compound and NRNG solution for aluminium from gravimetric analysis at 30° C.

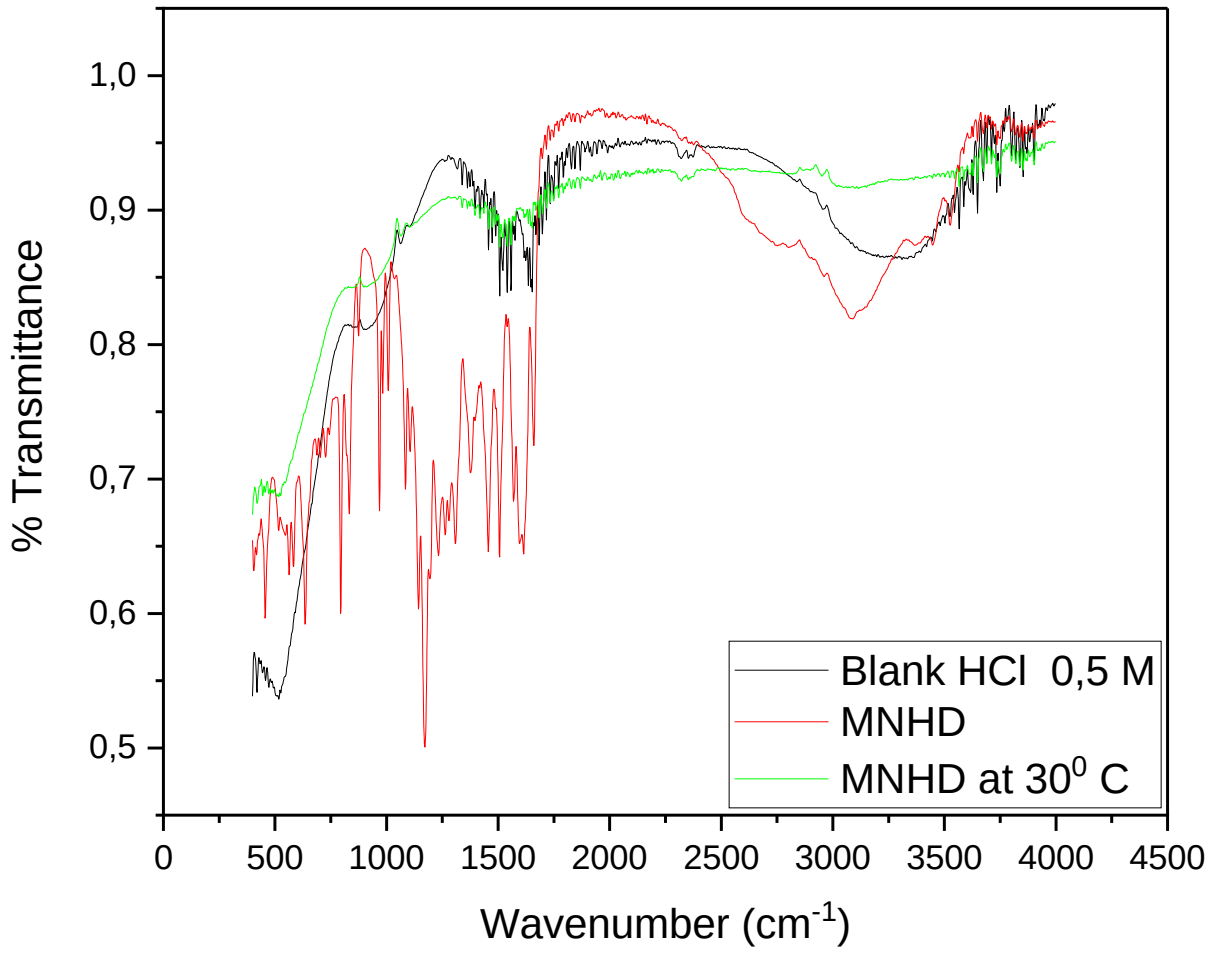

Figure 4.58: FT-IR spectrum of 0.5 M HCl acid blank, MNHD pure compound and MNHD solution for aluminium from gravimetric analysis at 30° C.

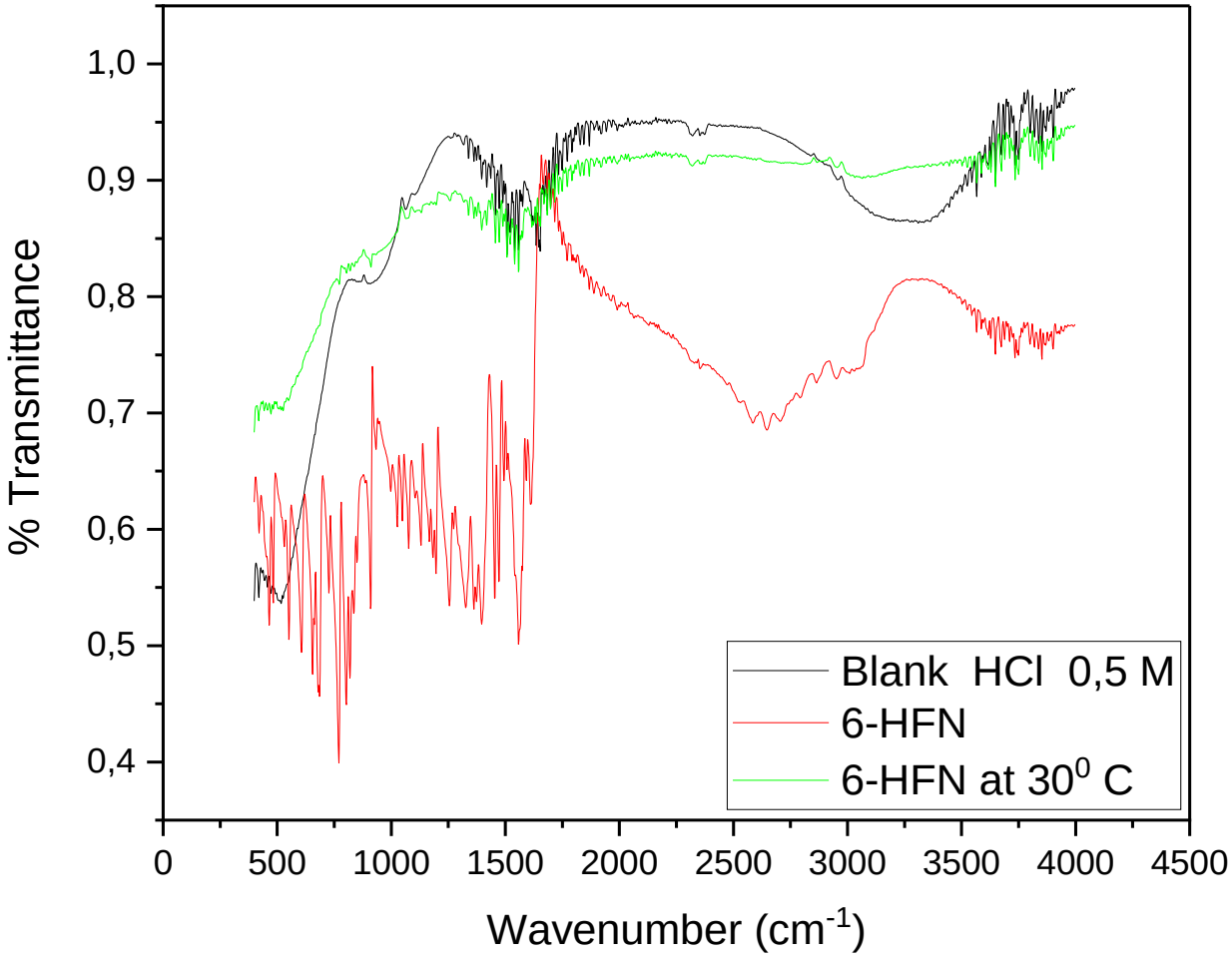

Figure 4.59: FT-IR spectrum of 0.5 M HCl acid blank, 6-HFN pure compound and 6-HFN solution for aluminium from gravimetric analysis at 30° C.

The variation of the absorption peaks of the pure NRNG, MNHD and 6-HFN inhibitors (red colour), inhibitors at 30° C (green colour) and the blank solution of hydrochloric acid (black colour) are shown in the form of spectra in figures 4.57 – 4.59 for zinc and aluminium metals. The variation in the absorption peaks or spectra particularly of the pure inhibitors (red) and the inhibitors at 30° C was due to the adsorption of the inhibitors at 30° C onto the metals surface as the compound will only absorb through active functional groups.

Table 4.22: Peaks and their identification, from FTIR spectra of the studied corrosion inhibitors and adsorption films formed on the zinc in 0.5 M HCl.

Inhibitor Zinc in sulphuric acid	Functional groups Peaks form FTIR Spectra (cm^{-1})					
	Ar-OH	Ar-O-R	C=C (Ar)	C=C	C-H (Ar)	Ar-(CO)-R
NRNG	-	1064.03	1473.11	-	-	-
MNHD	-	1063.85	1473.23	1652.70	-	1683.68
6-HFN	1257.71	1065.68	1473.22		3064.62	1983.68

Just like in Table 4.20 above when sulphuric acid was used in zinc as corrosive medium, NRNG and MNHD did not adsorb a peak of O-H functional group. The same was obtained this time around when aluminium in hydrochloric acid was used instead of zinc. Only 6-HFN showed a medium intensity peak of Ar-OH with a wavelength of 1257.71 cm^{-1}. NRNG, MNHD and 6-HFN retained their medium strong intensity peak for Ar-O-R and C=C (Ar) functional groups after gravimetric analysis. Only MNHD inhibitor showed a very weak medium intensity peak of C=C for alkene functional group just like in table 4.21 above for hydrochloric acid in zinc metal. 6-HFN showed a strong intensity peak of C-H in the aromatic ring with a wavelength of 3064.62 cm^{-1}, whereas NRNG and MNHD did not show any signal. At around 1683.68 cm^{-1} a medium strong intensity Ar-(C=O)-R peak was adsorbed by both MNHD and 6-HFN.

4.4 2D and 3D microscope

A microscope is an instrument that is used to view materials or areas of materials that are not within the resolution range of the normal human eye [154]. There are several types of images that can be obtained from a microscope, which include amongst others 2D, 3D and 4D images. For this study, 3D and 2D microscope images of zinc and aluminium metals will be studied. Figures 4.62 – 4.79 shows the 2D and 3D images of pure aluminium and zinc metals, zinc and aluminium metals in the presence of NRNG, MNHD and 6-HF inhibitors, and in the presence of HCl and H_2SO_4 acids as a corrosive media. For this study, Micro Olympus DSX – CB (DSX – HRSU) microscope connected to Eizo screen fitted with DSX software with a 139x magnification scale was used to obtain all the 2D and 3D images. The main reason to include 3D images was for a clear view of the type of corrosion that took place like in case where a pitting type of corrosion occurred, a deep pit was going to be seen in the metal. The depth of the pit was also going to be easily measured in a 3D format just like in the four images below.

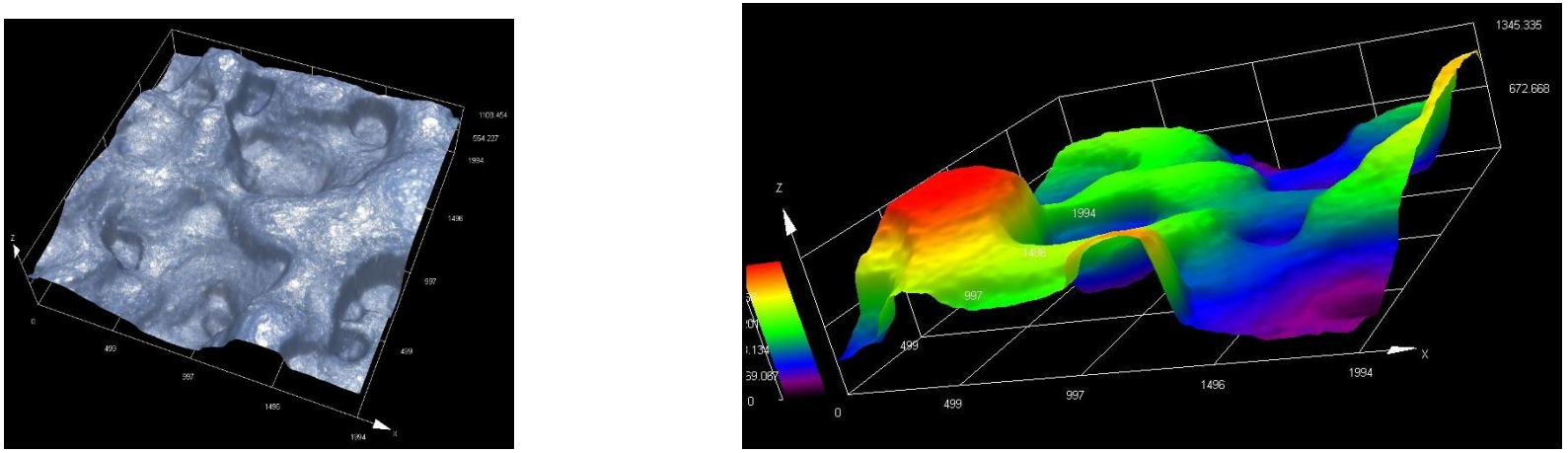

Figure 4.60: 3D pictures of stainless-steel pitting corrosion.

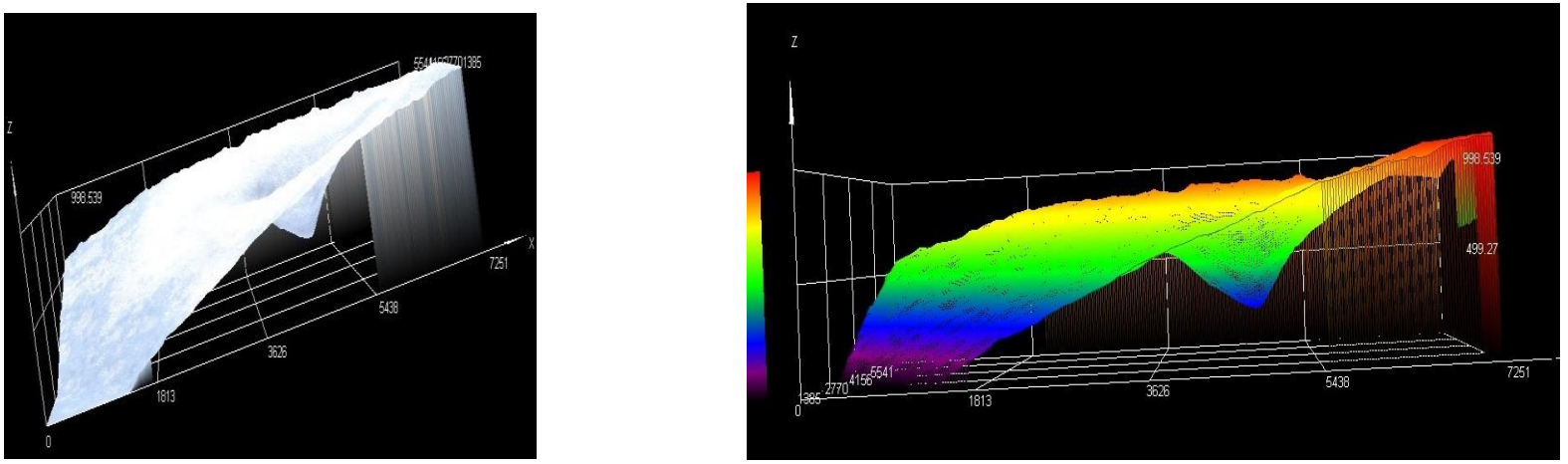

Figure 4.61: 3D pictures of mild steel pitting corrosion

By just looking at the 2D and 3D microscope images, it can be easily spotted what kind of corrosion took place on that particular material. For instance, Figures 4.60 and 4.61 can be said to have suffered pitting kind of corrosion, and this is evident by the deep pits that can be seen on the metal surface. With this regard, microscope images are very useful in terms of identifying the different kinds of corrosion that different metals undergo when exposed to different corrosive media. Not only that, but can also show the extent of corrosion that has taken place on the metal.

4.4.1 Zinc in 1.5 M sulphuric acid

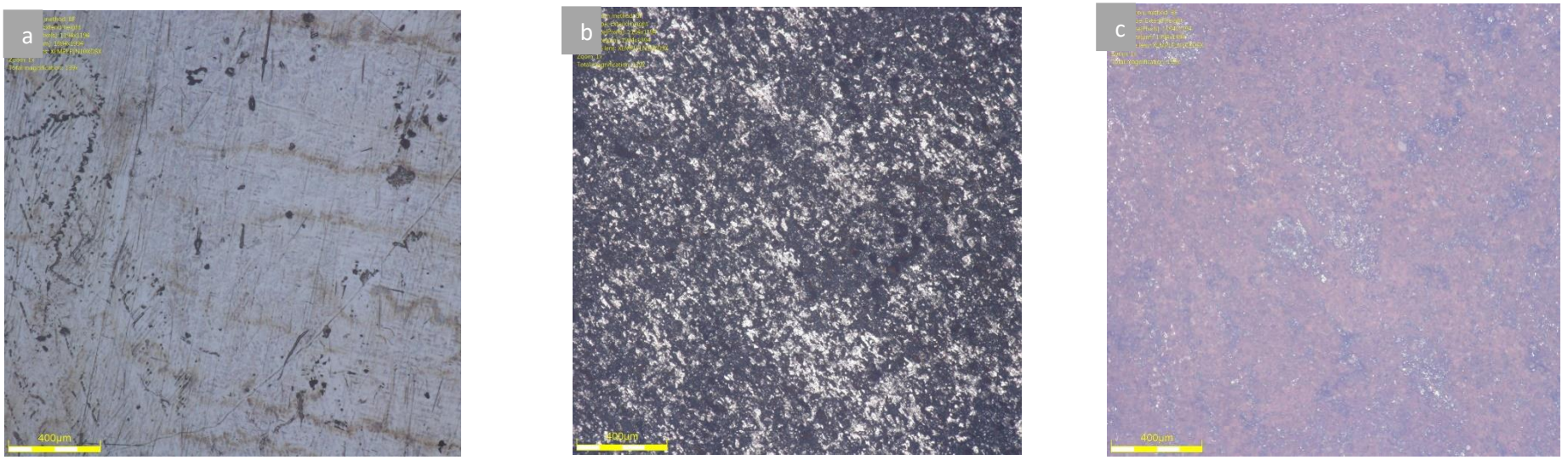

Figure 4.62: Microscope images of (a) pure zinc metal, (b) zinc metal inhibited with NRNG and (c) zinc metal in the presence of hydrochloric acid.

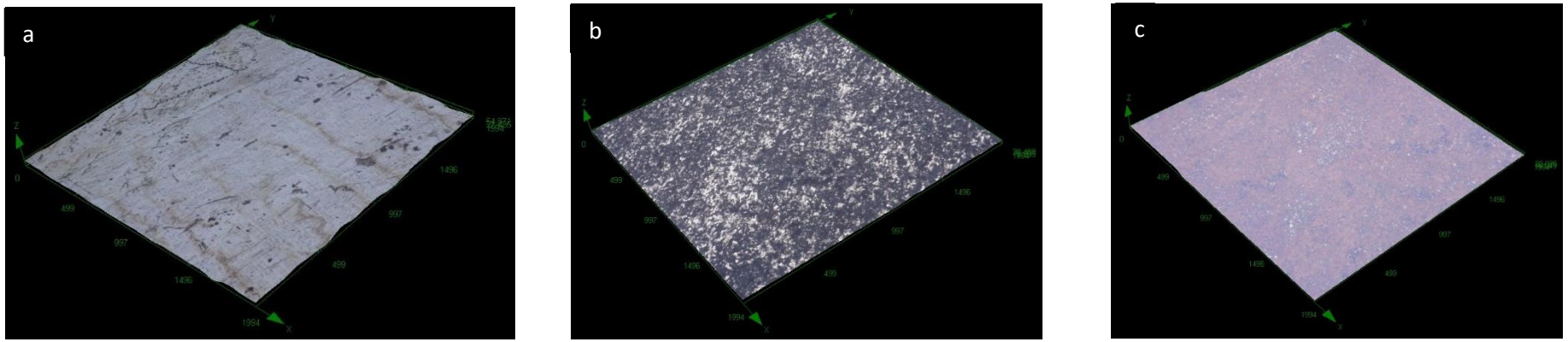

Figure 4.63: 3D microscope images of (a) pure zinc metal, (b) zinc metal inhibited with NRNG and (c) zinc metal in the presence of hydrochloric acid.

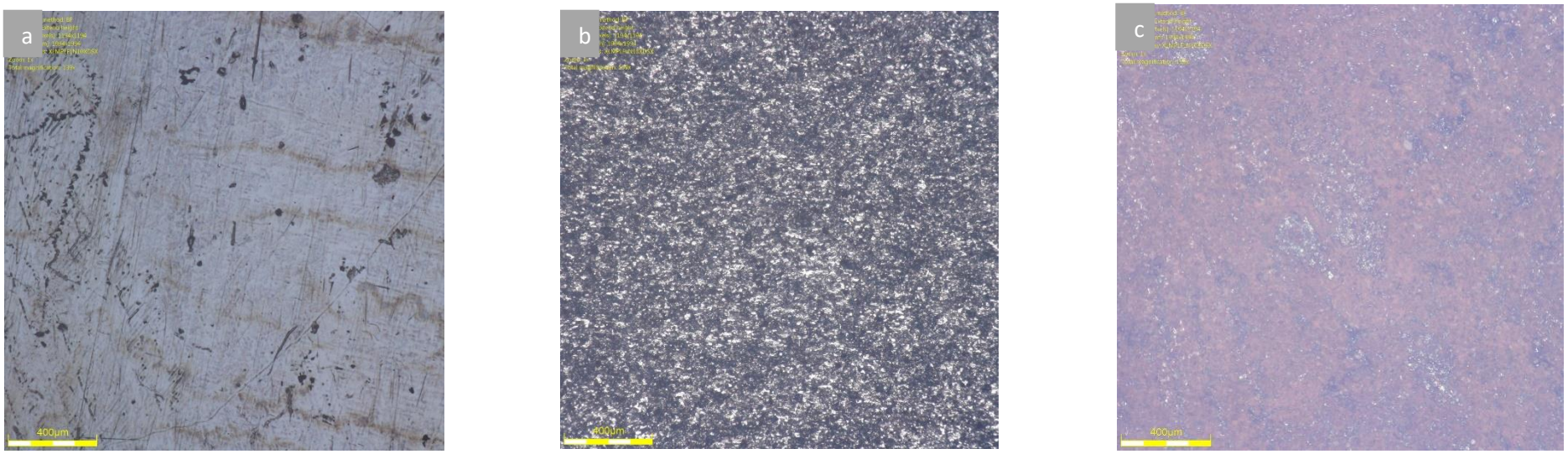

Figure 4.64: Microscope images of (a) pure zinc metal, (b) zinc metal inhibited with MNHD and (c) zinc metal in the presence of hydrochloric acid.

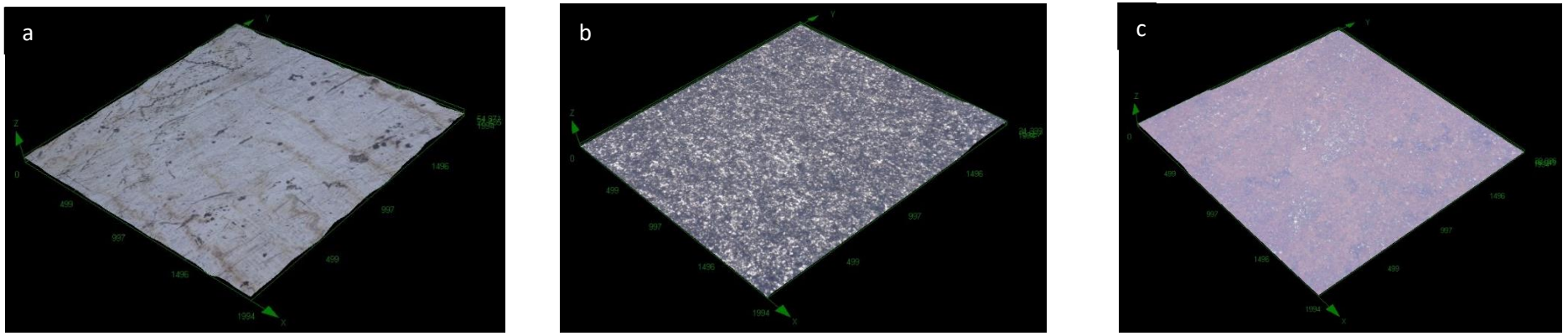

Figure 4.65: 3D microscope images of (a) pure zinc metal, (b) zinc metal inhibited with MNHD and (c) zinc metal in the presence of hydrochloric acid.

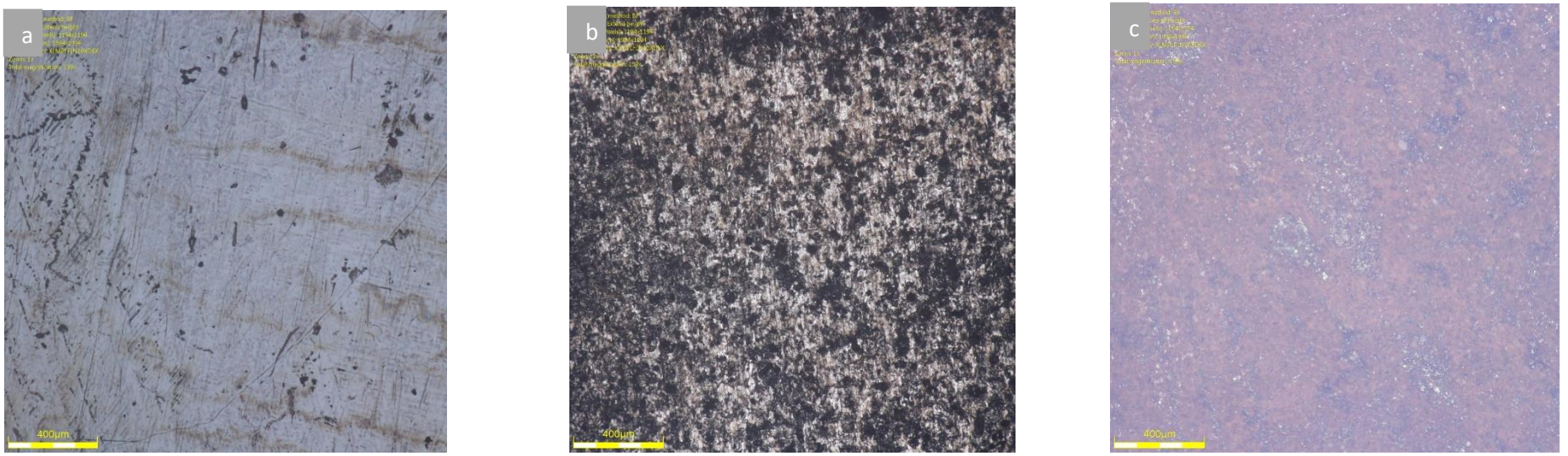

Figure 4.66: Microscope images of (a) pure zinc metal, (b) zinc metal inhibited with 6-HFN and (c) zinc metal in the presence of hydrochloric acid.

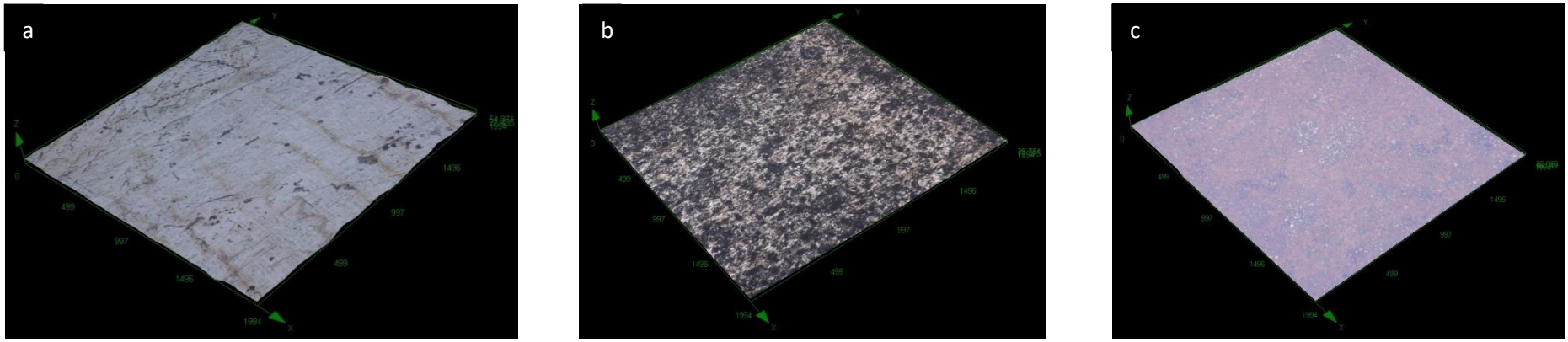

Figure 4.67: 3D microscope images of (a) pure zinc metal, (b) zinc metal inhibited with 6-HFN and (c) zinc metal in the presence of hydrochloric acid.

In the presence of sulphuric acid, NRNG, MNHD and 6-HFD showed some resistance in the corrosion of zinc metal as it can be seen by the white spots on images (b) in Figures 4.62 – 4.67. The white spots can be said to represent the portion of the metal that was protected from the acid corrosion attack. 6-HFN showed the best protection compared to NRNG and MNHD, with MNHD showing the lowest protection against the acid attack amongst the three inhibitors. Overall, it can be said that, in the presence of sulphuric acid, zinc metal was worst affected even in the inhibited solution compared to when hydrochloric acid was used. From images (c) in Figures 4.62 – 4.67 above, it can be observed that a uniform type of corrosion took place. However, in images (b) of the inhibited solution, a localised type of corrosion was observed. It can be concluded that the introduction of an inhibitor in the acid solution, did not only reduce the corrosion attack on the metals, but also altered the type of corrosion that took place.

4.4.2 Zinc in 1.5 M hydrochloric acid

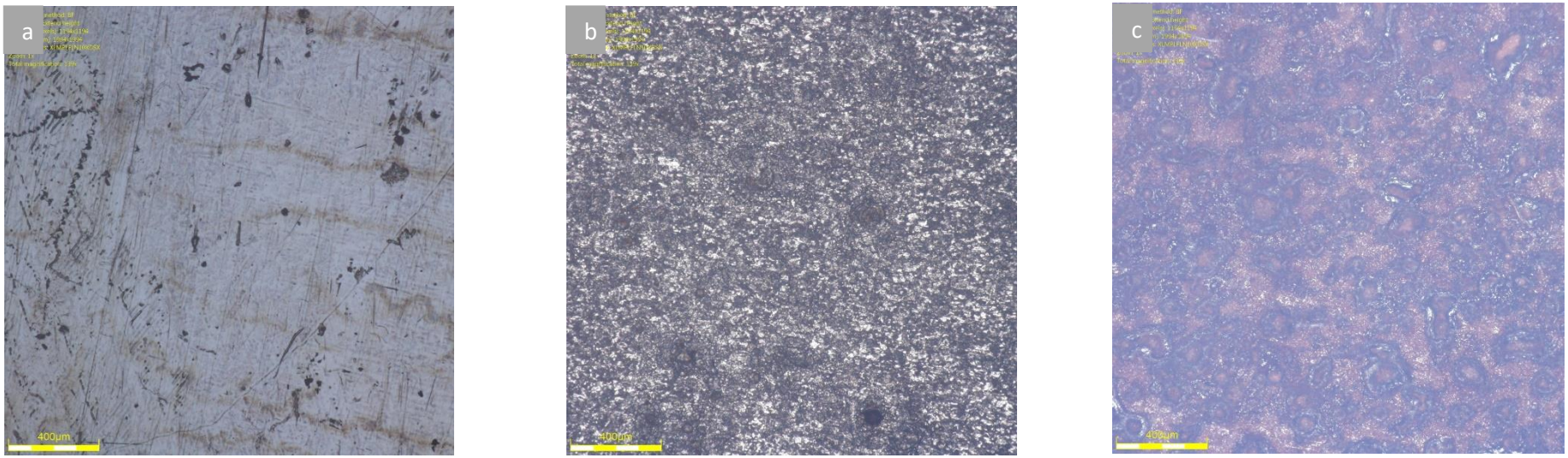

Figure 4.68: Microscope images of (a) pure zinc metal, (b) zinc metal inhibited with NRNG and (c) zinc metal in the presence of hydrochloric acid.

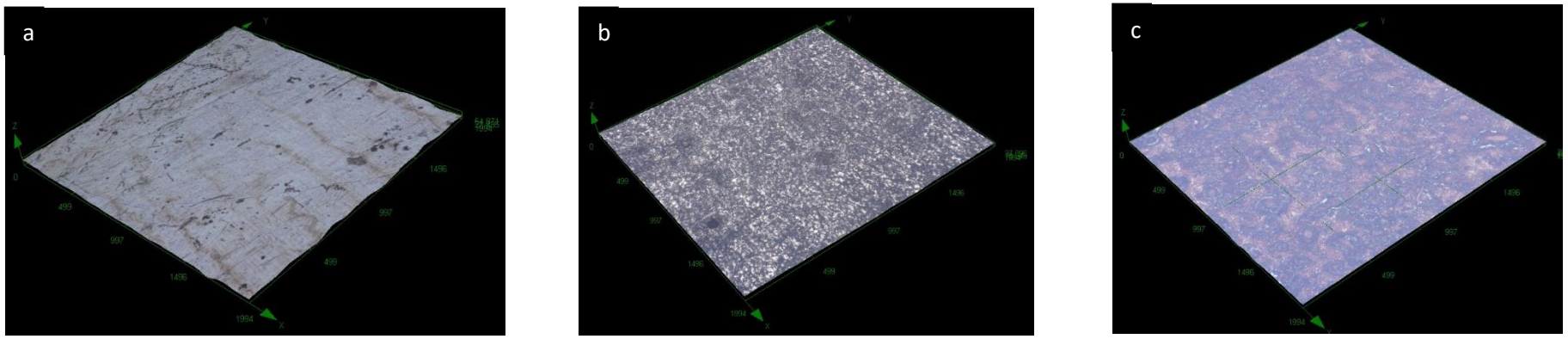

Figure 4.69: 3D microscope images of (a) pure zinc metal, (b) zinc metal inhibited with NRNG and (c) zinc metal in the presence of hydrochloric acid.

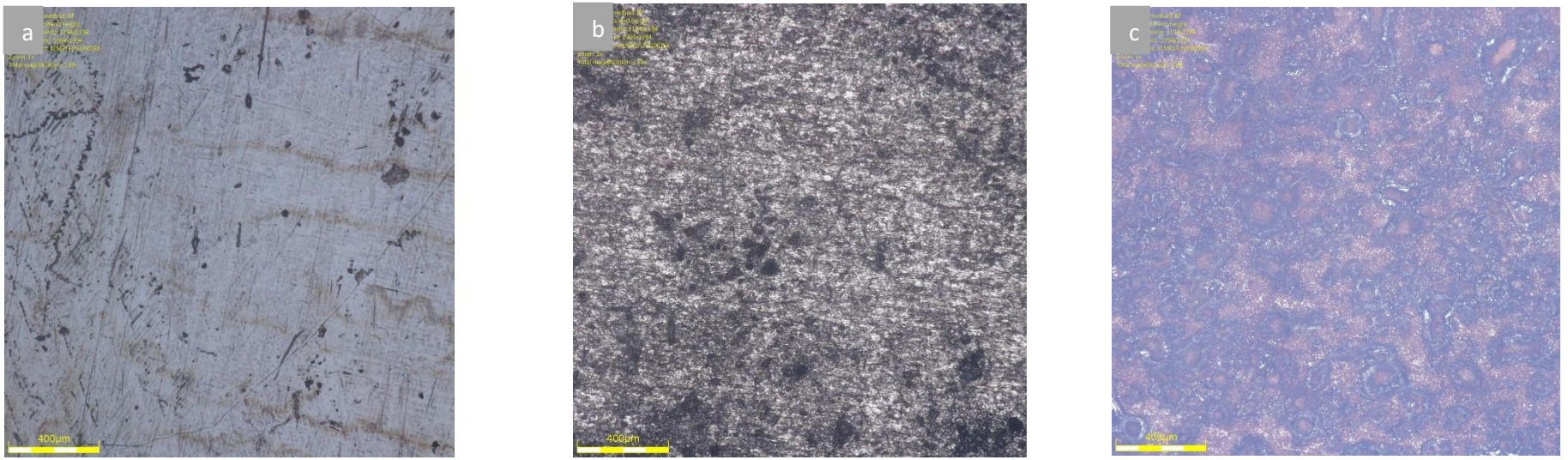

Figure 4.70: Microscope images of (a) pure zinc metal, (b) zinc metal inhibited with MNHD and (c) zinc metal in the presence of hydrochloric acid.

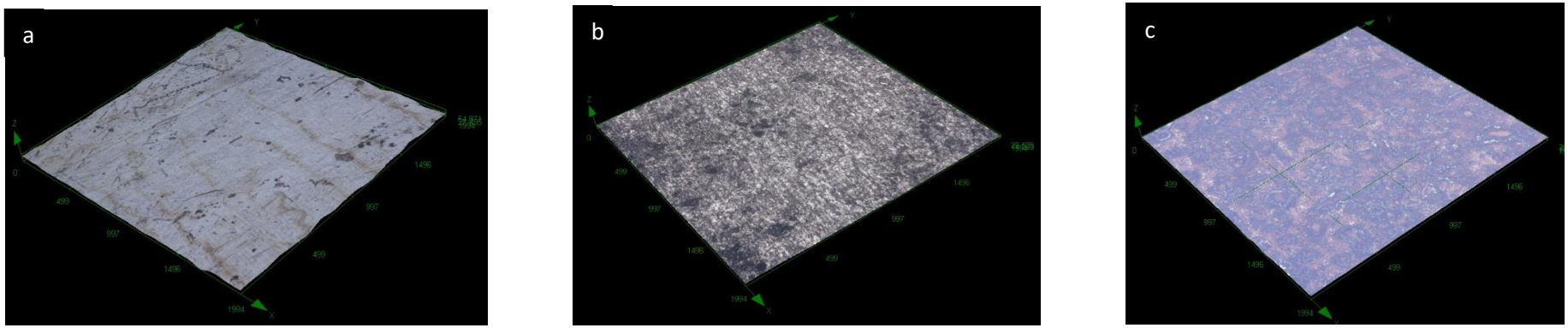

Figure 4.71: 3D microscope images of (a) pure zinc metal, (b) zinc metal inhibited with MNHD and (c) zinc metal in the presence of hydrochloric acid.

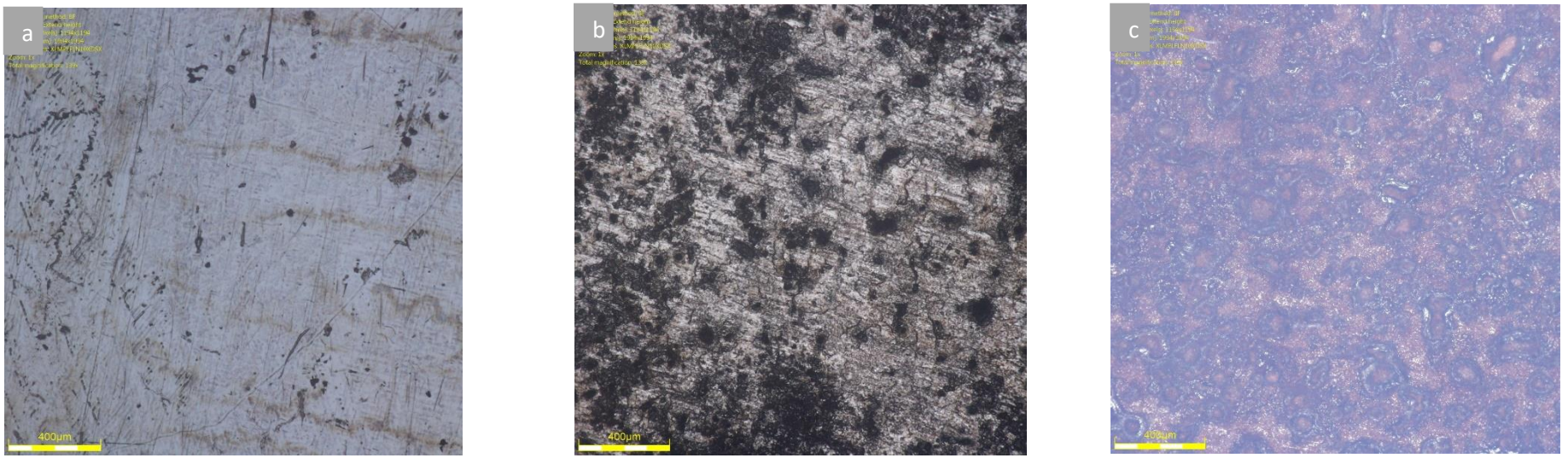

Figure 4.72: Microscope images of (a) pure zinc metal, (b) zinc metal inhibited with 6-HFN and (c) zinc metal in the presence of hydrochloric acid.

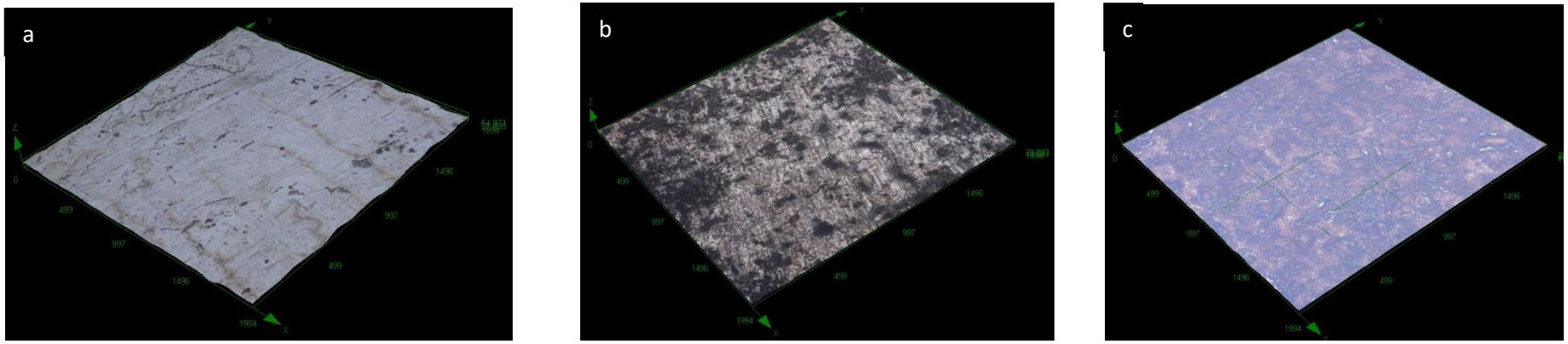

Figure 4.73: 3D microscope images of (a) pure zinc metal, (b) zinc metal inhibited with 6-HFN and (c) zinc metal in the presence of hydrochloric acid.

With its numerous applications in industries, hydrochloric acid is known to have a very intensive effect on metals such as zinc and mild steel. This can be seen by the kind of damage (corrosion) it does to such metals when exposed to it. MNHD inhibitor showed the strongest resistant to hydrochloric acid corrosion as can be observed from images (b) in Figures 4.70 and 4.71 as compared to 6-HFN and NRNG inhibitors. This can be seen by the largest part of whiteness on the metals which is similar to that on the pure metal (a). NRNG showed the lowest resistance to hydrochloric acid corrosion as compared to the other two inhibitors, because of the lowest number of white spots in the inhibited metal. From Figures 4.68 – 4.73 above, images (c) which represent the uninhibited solution and images (b) which represent the inhibited solution showed a localised type of corrosion.

4.4.3 Aluminium in 0.5 M hydrochloric acid

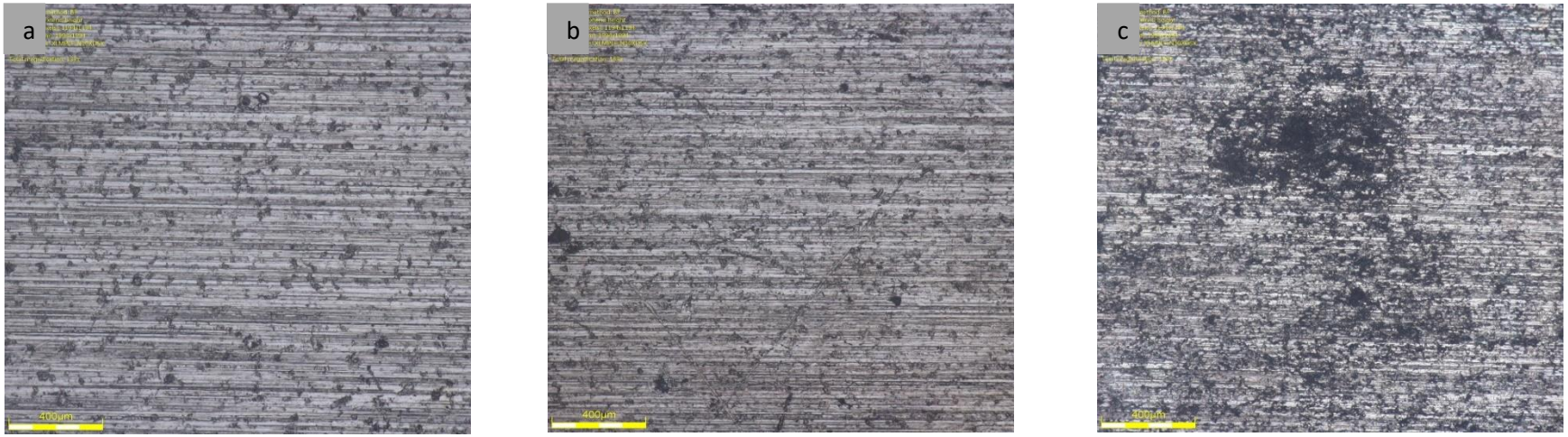

Figure 4.74: Microscope images of (a) pure aluminium metal, (b) aluminium metal inhibited with NRNG and (c) aluminium metal in the presence of hydrochloric acid.

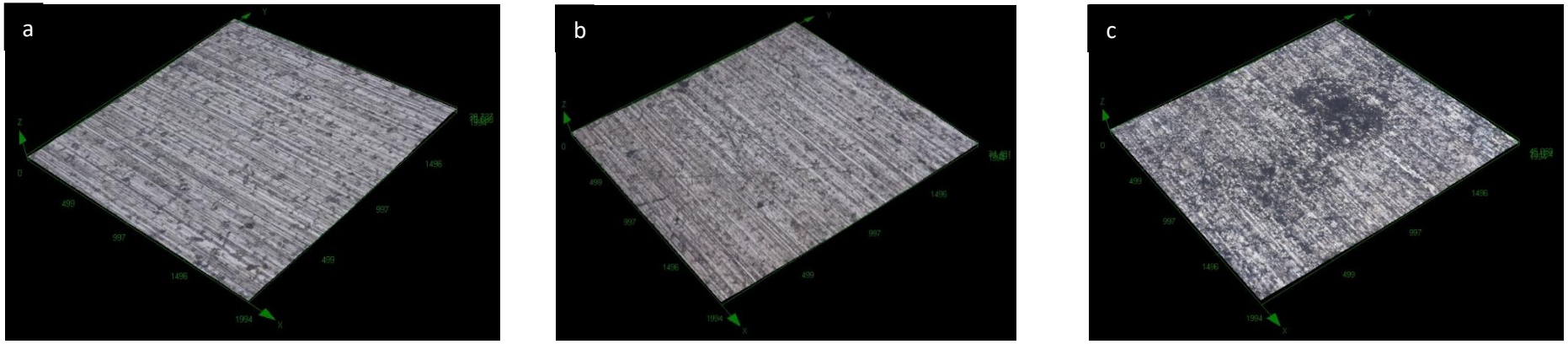

Figure 4.75: 3D microscope images of (a) pure aluminium metal, (b) aluminium metal inhibited with NRNG and (c) aluminium metal in the presence of hydrochloric acid.

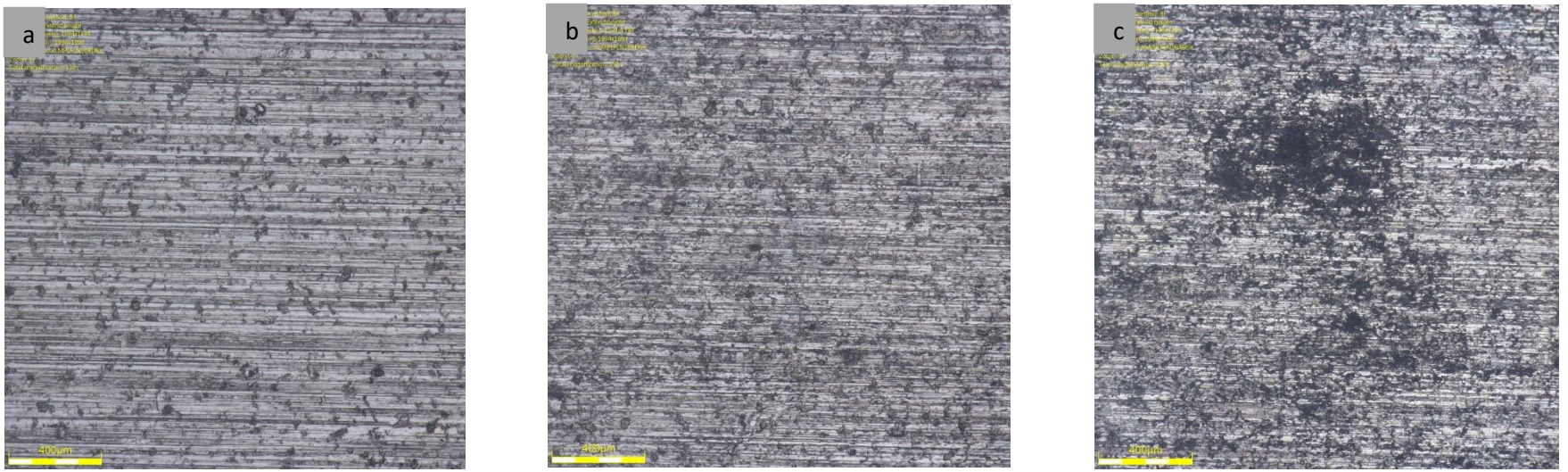

Figure 4.76: Microscope images of (a) pure aluminium metal, (b) aluminium metal inhibited with MNHD and (c) aluminium metal in the presence of hydrochloric acid.

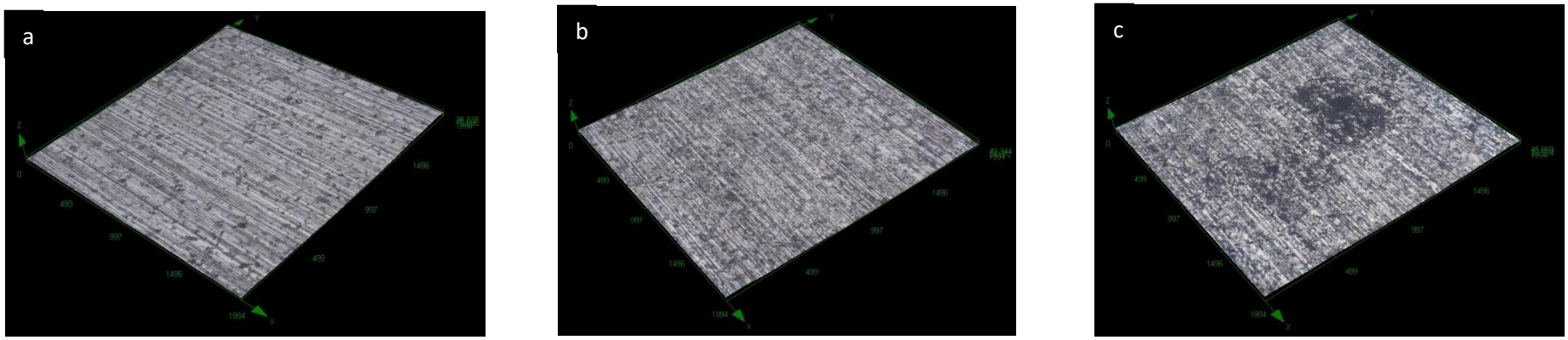

Figure 4.77: 3D microscope images of (a) pure aluminium metal, (b) aluminium metal inhibited with MNHD and (c) aluminium metal in the presence of hydrochloric acid.

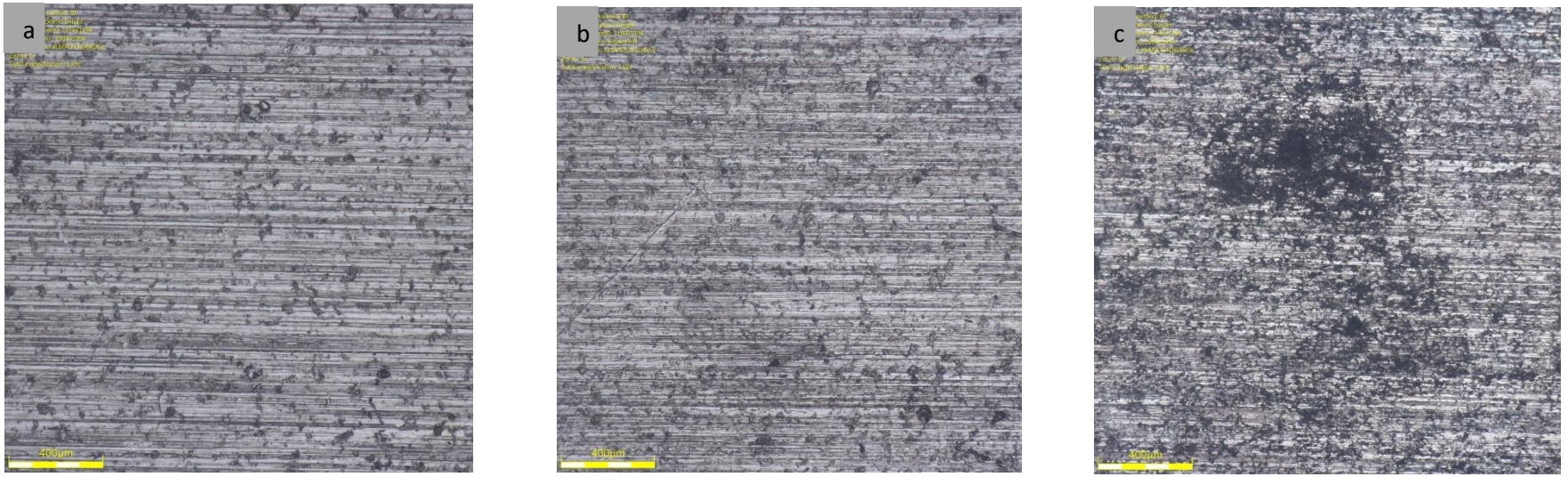

Figure 4.78: Microscope images of (a) pure aluminium metal, (b) aluminium metal inhibited with 6-HFN and (c) aluminium metal in the presence of hydrochloric acid.

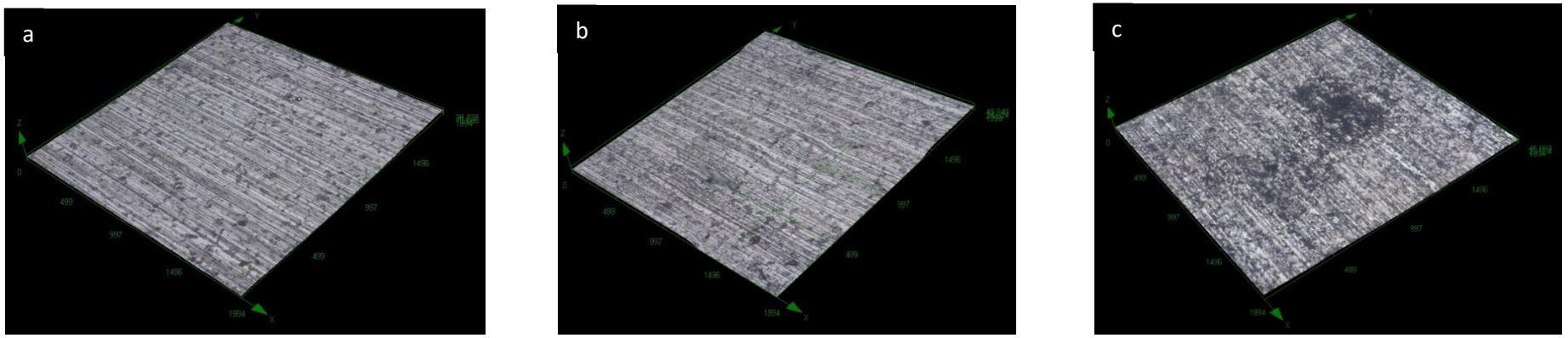

Figure 4.79: 3D microscope images of (a) pure aluminium metal, (b) aluminium metal inhibited with 6-HFN and (c) aluminium metal in the presence of hydrochloric acid.

Figures 4.74 – 4.79, represent the 2D and 3D images of different aluminium metals, with (a) representing the pure aluminium metal, (b) representing the inhibited aluminium metal and (c) representing the aluminium metal treated with a 0.5 M hydrochloric acid. Images (c) looks much damaged compared to images (a) and (b) as expected due to the acid attack. Images (a) and (b) looks very much similar with a very little difference and from this observation, it can be concluded that the three flavonoids compounds used as corrosion inhibitors were able to prevent the acid attack on the metal which was going to cause the metal corrosion. This observation can also be supported by the % inhibition efficiency obtained from gravimetric analysis, which was the highest compared to those of the zinc metals, which is the reason the inhibited metals (b) look similar to the pure aluminium metal (a). Careful examination of images (c) in Figures 4.74 – 4.79 above show that a localised type of corrosion took place on the metals. However, when the inhibitors were introduced images (b) showed a uniform type of corrosion.

4.5 Potentiodynamic Polarization

Potentiodynamic Polarization (PDP) is a widely used technique in electrochemistry to measure the current that arises from varying the electrode potential between a selected range. It is capable of detecting regions where there might be electrode activity [138]. Many literatures have reported that Potentiodynamic Polarization curves are very useful in monitoring the corrosion protecting properties of a film or coat [155]. The Potentiodynamic Polarization studies was conducted at room temperature using the SP-150 Biologic instrument in 1.5 M H_2SO_4 and HCl, and 0.5 M HCl solution with Ag/AgCl reference electrode in the absence and presence of three inhibitors namely NRNG, MNHD and 6-HFN. Figures 4.80 – 4.88 show both the anodic and cathodic Potentiodynamic Polarization curves half reactions (Tafel plots) of zinc and aluminium corrosion in H_2SO_4 and HCl acids.

4.5.1 Zinc in 1.5 M sulphuric acid

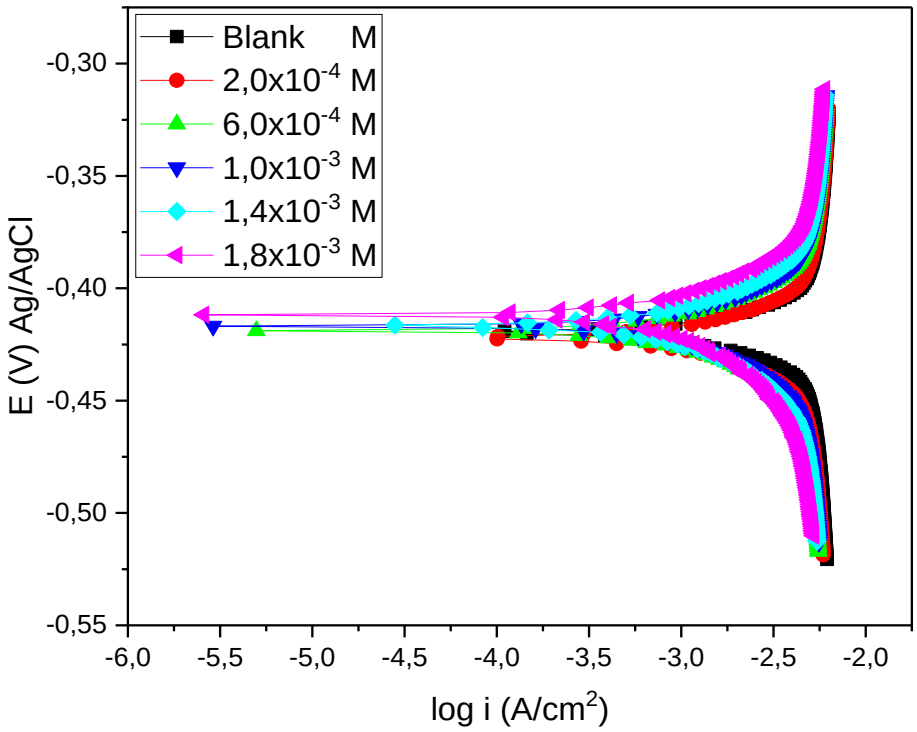

Figure 4.80: Tafel plots for zinc in 1.5 M H_2SO_4 in the absence and presence of different concentrations of NRNG inhibitor compound.

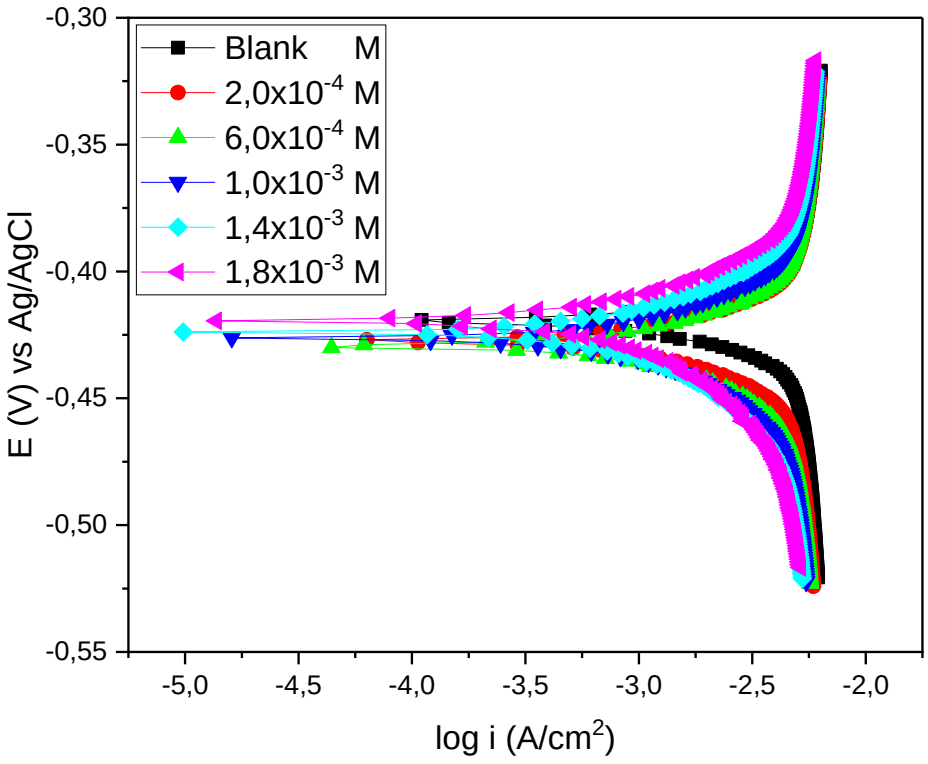

Figure 4.81: Tafel plots for zinc in 1.5 M H_2SO_4 in the absence and presence of different concentrations of MNHD inhibitor compound.

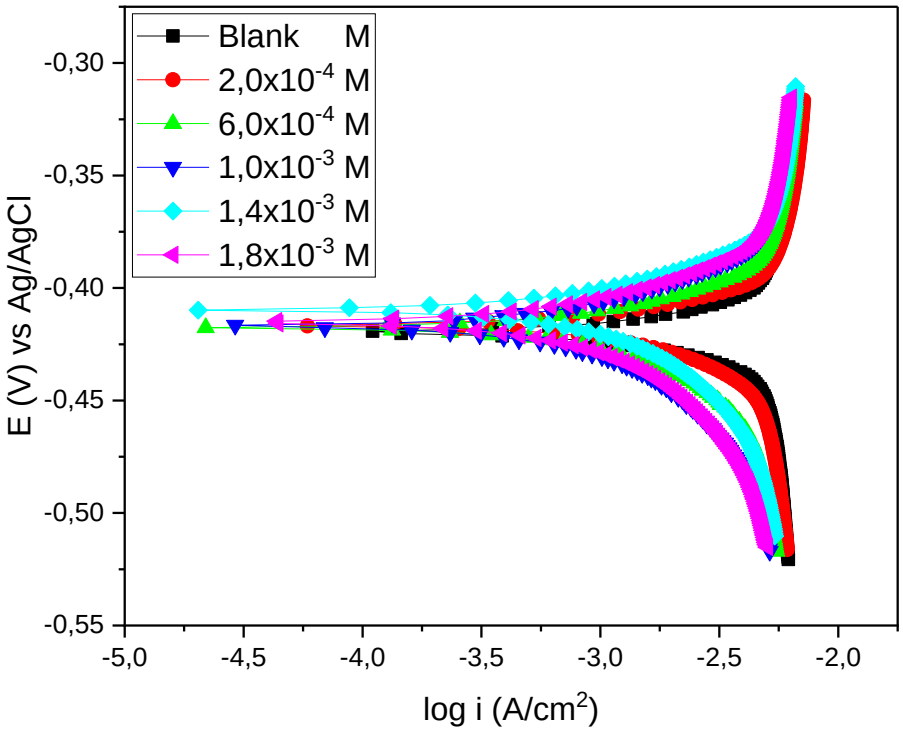

Figure 4.82: Tafel plots for zinc in 1.5 M H_2SO_4 in the absence and presence of different concentrations of 6-HFN inhibitor compound.

4.5.2 Zinc in 1.5 M hydrochloric acid

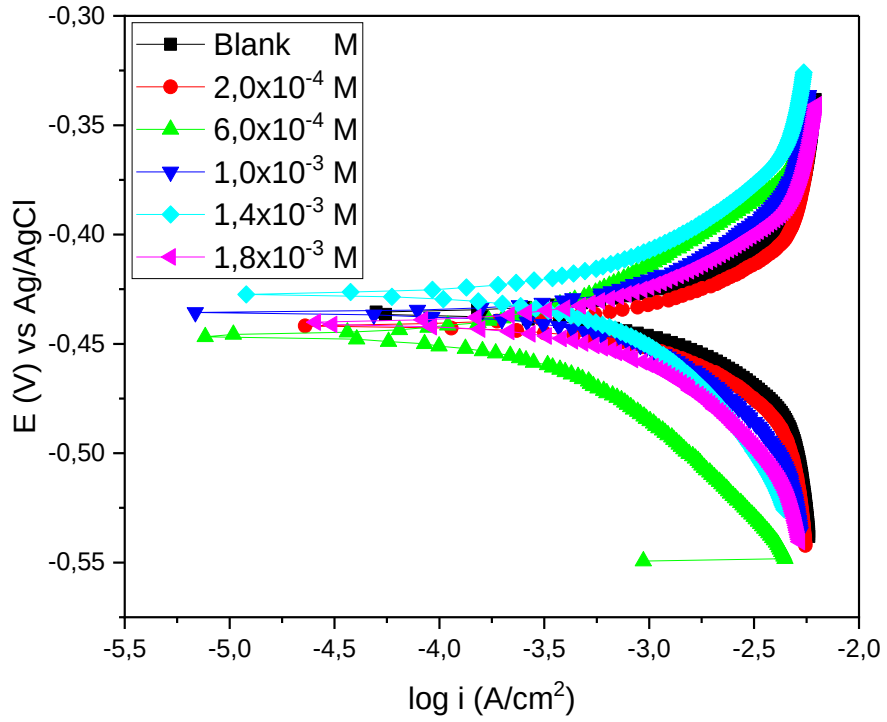

Figure 4.83: Tafel plots for zinc in 1.5 M HCl in the absence and presence of different concentrations of NRNG inhibitor compound.

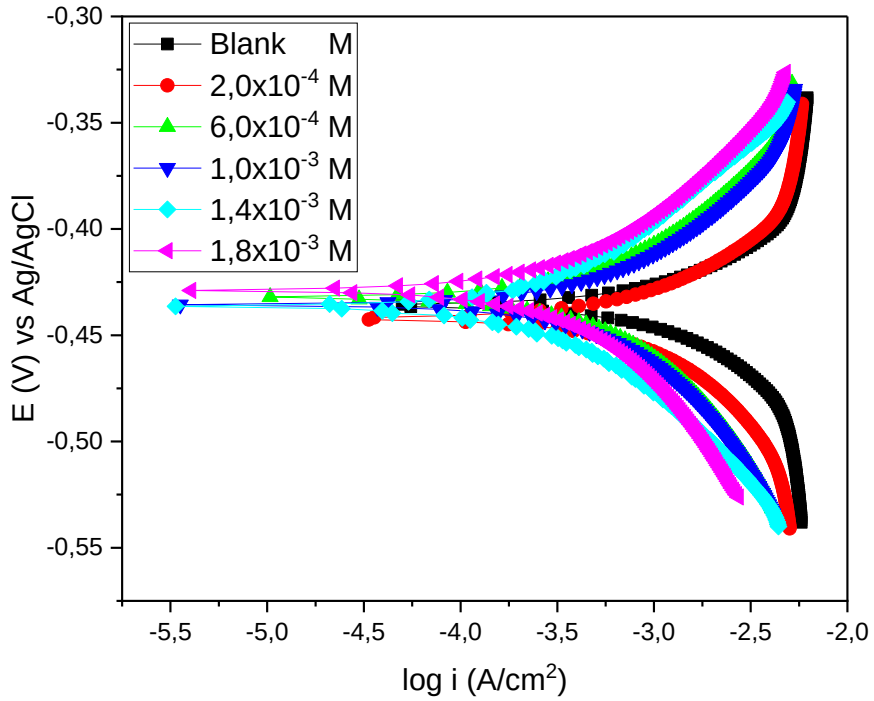

Figure 4.84: Tafel plots for zinc in 1.5 M HCl in the absence and presence of different concentrations of MNHD inhibitor compound.

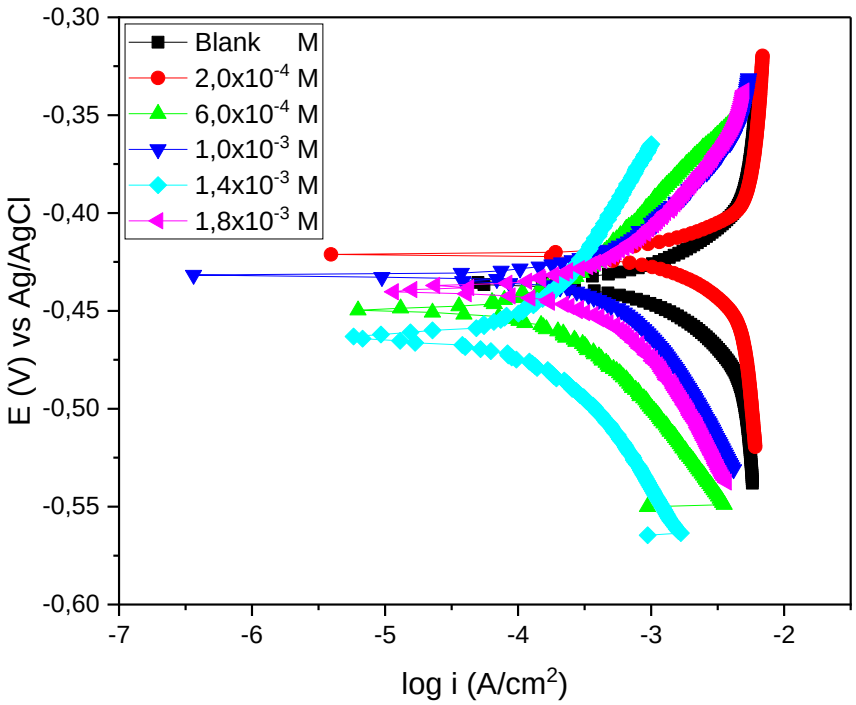

Figure 4.85: Tafel plots for zinc in 1.5 M HCl in the absence and presence of different concentrations of 6-HFN inhibitor compound.

4.5.3 Aluminium in 0.5 M hydrochloric acid

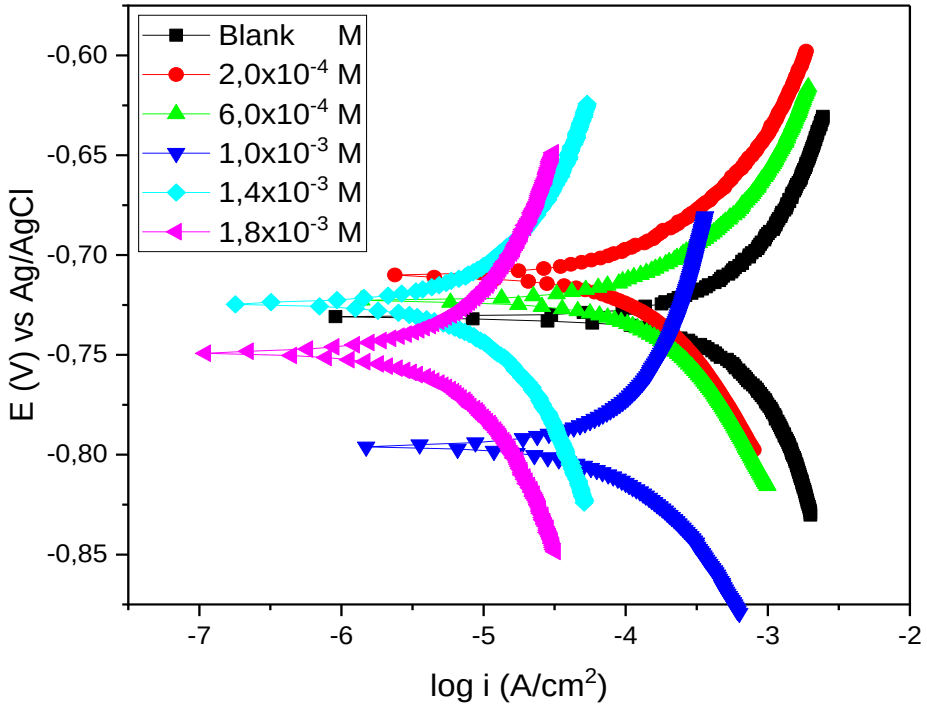

Figure 4.86: Tafel plots for aluminium in 0.5 M HCl in the absence and presence of different concentrations of NRNG inhibitor compound.

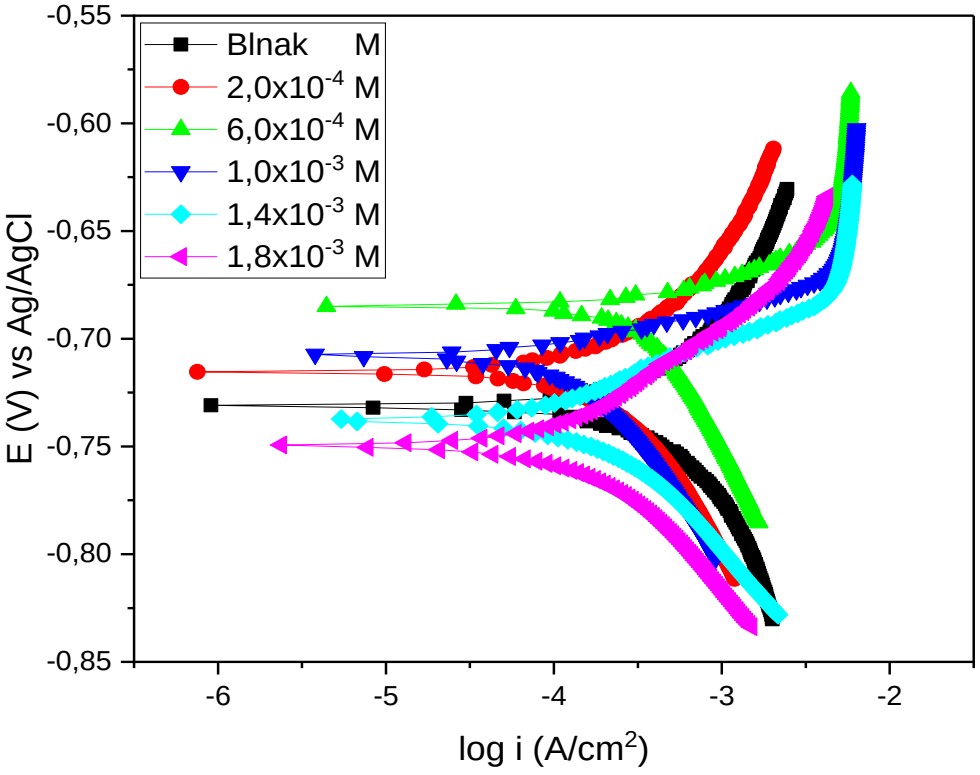

Figure 4.87: Tafel plots for aluminium in 0.5 M HCl in the absence and presence of different concentrations of MNHD inhibitor compound.

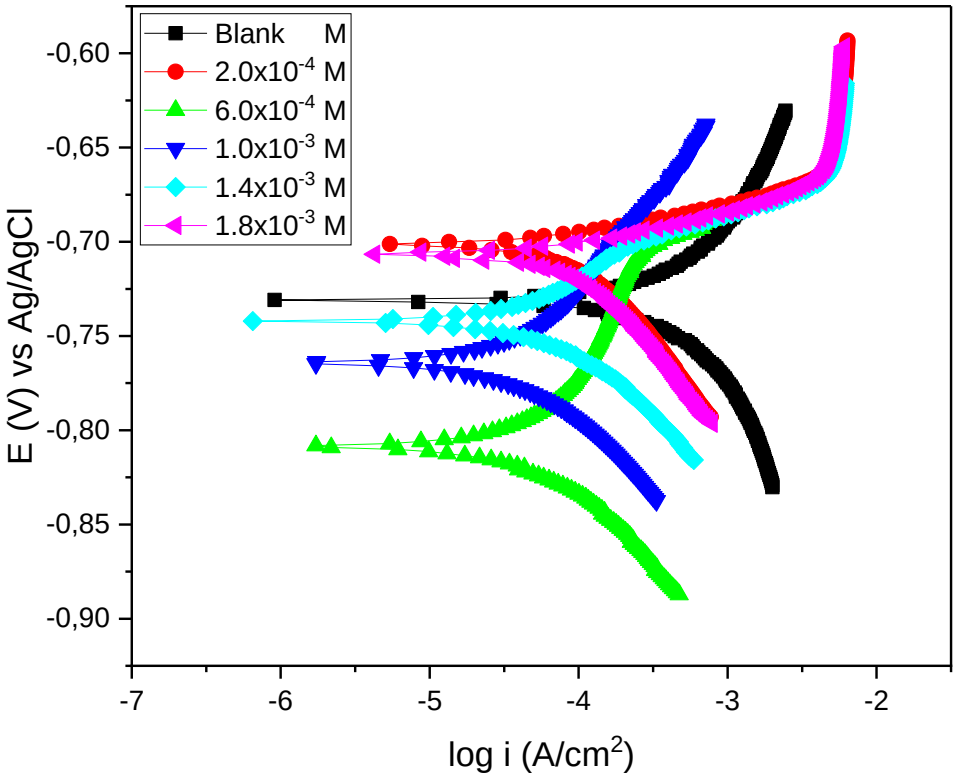

Figure 4.88: Tafel plots for aluminium in 0.5 M HCl in the absence and presence of different concentrations of 6-HFN inhibitor compound.

As can be observed from the plots, the anodic and cathodic half reactions where all affected by the presence of the three inhibitors used. A clear picture of this can be obtained by comparing the anodic and cathodic half reaction of the blank solution and that of the inhibited solution. The presence of the inhibitors in the acid solutions can possibly have several effects on the shape of polarization curve, based on how it is affecting the anodic and cathodic corrosion reaction. For instance, if the inhibitor used was an anodic inhibitor, the current densities of the anodic branch would decrease equivalenting to the inhibition of anodic reaction rates [156]. The same will be the case when considering the cathodic inhibitor. The inhibitors corrosion current densities for both the anodic and cathodic branch in figures 4.80 – 4.88 did not show any particular trend and in some instance, they were even much higher than that of their corresponding blank solution. With that said, it can therefore be concluded that the three compounds adsorb through a mixed type of inhibition process actively involving both the anodic and cathodic inhibition reaction rates. In cases where the cathodic and anodic current densities were lower than that of the blank solution, it can be suggested that the inhibitors were able to retard both the cathodic evolution of H_2 and anodic dissolution of metal reaction [157]. The corrosion current densities (I_{corr}), corrosion potential (E_{corr}), polarization resistance (R_P), anodic Tafel slope (b_a) and cathodic Tafel slope (b_c) were all obtained from the polarization curves by Tafel's

extrapolation using both cathodic and anodic branches of the polarization curves. The corrosion potential (E_{corr}) is the point where the anodic and cathodic current densities are approximately equal [156]. All above mentioned parameters were recorded in Tables 4.23 – 4.25, including the $\%IE_{PDP}$ calculated using equation (43) and $\%IE_{Grav}$ calculated from gravimetric results.

Table 4.23: Potentiodynamic Polarization (PDP) parameters such as corrosion potential (E_{corr}), corrosion current density (i_{corr}), polarization resistance (R_p) and anodic and cathodic Tafel slopes (b_a and b_c) using different inhibitors in 1.5 M sulphuric acid.

Inhibitor	Inhibitor Conc. (M)	$-E_{corr}$ (mV) With Ag/AgCl	i_{corr} (mA.cm^{-2})	R_p (10^{-1}) (Omh)	b_a (mV.dec^{-1})	b_c (mV.dec^{-1})	% IE_{PDP}	% IE_{WL}
Blank	0.00	419.62	0.79825	0.6551	23.405	24.800	-	-
NRNG	2.0x10^{-4}	421.98	0.22477	1.0387	10.285	11.262	71.84	72.32
	6.0x10^{-4}	418.89	0.20117	1.3051	11.138	13.222	74.80	75.57
	1.0x10^{-3}	416.89	0.18076	1.2154	09.210	00.011	77.36	78.43
	1.4x10^{-3}	416.68	0.17556	1.3394	09.819	12.072	78.01	79.73
	1.8x10^{-3}	411.81	0.17505	1.7150	11.928	16.441	78.07	79.69
MNHD	2.0x10^{-4}	427.34	0.28297	0.8737	11.090	11.675	64.55	64.65
	6.0x10^{-4}	429.55	0.20376	1.3405	11.849	13.403	74.47	75.47
	1.0x10^{-3}	426.30	0.16053	1.3135	09.704	9.7166	79.89	81.09
	1.4x10^{-3}	423.97	0.15340	1.4530	09.251	11.527	80.78	81.97
	1.8x10^{-3}	419.31	0.14874	1.7900	11.507	13.220	81.37	82.73
6-HFN	2.0x10^{-4}	416.55	0.27605	0.8458	09.551	12.299	65.41	85.16
	6.0x10^{-4}	417.48	0.11992	1.3629	06.842	08.362	84.98	85.72
	1.0x10^{-3}	416.88	0.11742	1.7826	08.576	11.004	85.29	86.38
	1.4x10^{-3}	409.65	0.11005	1.4269	06.469	08.199	86.21	86.41
	1.8x10^{-3}	415.26	0.10746	1.8372	08.290	10.066	86.54	86.33

Table 4.24: Potentiodynamic Polarization (PDP) parameters such as corrosion potential (E_{corr}), corrosion current density (i_{corr}), polarization resistance (R_P) and anodic and cathodic Tafel slopes (b_a and b_c) using different inhibitors in 1.5 M hydrochloric acid.

Inhibitor	Inhibitor Conc. (M)	-E_{corr} (mV) With Ag/AgCl	i_{corr} (mA.cm^{-2})	R_P (10^{-1}) (Omh)	b_a (mV.dec^{-1})	b_c (mV.dec^{-1})	% IE_{PDP}	% IE_{WL}
Blank	0.00	435.99	0.37298	1.4874	23.406	28.121	-	-
NRNG	2.0x10^{-4}	441.53	0.11934	1.6626	8.1660	10.370	69.01	67.18
	6.0x10^{-4}	446.32	0.11851	7.1173	35.024	43.595	68.23	68.74
	1.0x10^{-3}	432.95	0.11845	3.3185	16.262	20.409	68.24	69.73
	1.4x10^{-3}	443.46	0.10492	4.1630	19.523	20.785	71.87	69.90
	1.8x10^{-3}	440.55	0.10269	2.8930	12.664	14.875	72.47	70.46
MNHD	2.0x10^{-4}	442.14	0.12950	2.4213	13.703	15.259	65.28	61.834
	6.0x10^{-4}	432.25	0.11950	4.6002	24.077	26.678	67.96	69.346
	1.0x10^{-3}	435.73	0.11710	4.4046	22.832	24.740	68.60	70.440
	1.4x10^{-3}	436.25	0.11096	7.0966	36.372	36.155	70.25	71.558
	1.8x10^{-3}	428.76	0.09960	6.6523	28.448	32.888	73.30	73.576
6-HFN	2.0x10^{-4}	421.17	0.09372	0.8433	3.6447	03.634	74.87	72.482
	6.0x10^{-4}	449.33	0.09082	10.687	45.665	43.780	75.65	75.131
	1.0x10^{-3}	431.71	0.08890	5.2204	19.820	23.169	76.16	75.398
	1.4x10^{-3}	463.60	0.08759	16.474	79.153	57.259	76.63	76.590
	1.8x10^{-3}	439.77	0.08490	5.6052	20.522	23.500	77.24	77.538

Table 4.25: Potentiodynamic Polarization (PDP) parameters such as corrosion potential (E_{corr}), corrosion current density (i_{corr}), polarization resistance (R_p) and anodic and cathodic Tafel slopes (b_a and b_c) using different inhibitors in 0.5 M hydrochloric acid.

Inhibitor	Inhibitor Conc. (M)	$-E_{corr}$ (mV) With Ag/AgCl	i_{corr} (mA.cm^{-2})	R_p (10^{-1}) (Omhs)	b_a (mV.dec^{-1})	b_c (mV.dec^{-1})	% IE_{PDP}	% IE_{WL}
Blank	0.00	731.34	0.03613	07.0923	11.984	11.624	-	-
NRNG	2.0x10^{-4}	710.36	0.01193	22.3320	01.209	12.448	66.98	68.98
	6.0x10^{-4}	722.86	0.01010	16.1200	07.342	07.656	72.05	71.12
	1.0x10^{-3}	795.73	0.00806	36.4480	14.291	12.839	77.70	77.01
	1.4x10^{-3}	724.26	0.00798	294.660	107.07	109.44	77.92	78.61
	1.8x10^{-3}	748.85	0.00308	491.740	69.185	70.230	91.48	90.37
MNHD	2.0x10^{-4}	715.29	0.00984	10.9410	05.673	04.401	72.77	73.80
	6.0x10^{-4}	684.81	0.00955	5.3632	02.329	02.391	73.56	74.87
	1.0x10^{-3}	707.61	0.00857	12.3380	03.505	07.970	76.29	75.94
	1.4x10^{-3}	737.78	0.00768	14.8380	05.108	05.394	78.75	78.61
	1.8x10^{-3}	749.61	0.00665	14.8760	04.721	04.402	81.59	82.35
6-HFN	2.0x10^{-4}	701.54	0.00476	13.6500	02.682	03.377	86.84	88.24
	6.0x10^{-4}	808.58	0.00405	53.6110	11.488	08.860	88.79	91.98
	1.0x10^{-3}	764.24	0.00380	65.0420	12.504	10.434	89.49	93.05
	1.4x10^{-3}	722.71	0.00372	37.1570	05.674	07.234	89.71	93.58
	1.8x10^{-3}	706.28	0.00357	13.9600	02.318	02.272	90.12	95.19

Figures 4.80 - 4.88 and Tables 4.23 – 4.25 above clearly shows that the addition of the inhibitors in the acid solutions of 0.5 M and 1.5 M HCl, and 1.5 M H_2SO_4 managed to reduce the corrosion current densities to some extent. This can be seen by comparing the i_{corr} values for the uninhibited process to that of the inhibited process. In Table 4.23, the i_{corr} for the uninhibited process is 0.79825 mA and that of the inhibited ranged between 0.10746 – 0.28297 mA. Similarly, in Tables 4.24 and 4.25, the i_{corr} for the uninhibited process is 0.37298 and 0.03613 mA and that of the inhibited solution ranged between 0.0849 – 0.1295 mA and 0.0030782 – 0.01193 mA, respectively. The corrosion potential values in all three tables are close to each other and shows no particular trend based on the type of metal used (zinc ranged from 409.65 – 429.55 mV for H_2SO_4 and 421.17 – 463.60 mV for HCl and aluminium in HCl ranged from 701.54 – 808.58 mV). This type of behaviour is very common for a mixed type of inhibitors [25]. The percentage inhibition efficiency PDP is found to increase with the increase in the concentration of the inhibitors and they are very close to the percentage inhibition efficiency obtained in the gravimetric analysis. When sulphuric and hydrochloric acids were used as corrosive media in zinc metal, 6-HFN inhibitor amongst others showed maximum efficiency of 86.538% in H_2SO_4 and 77.2374% in HCl in Tables 4.23 and 4.24, respectively. However, when hydrochloric acid was used in the presence of aluminium metal, NRNG compound showed maximum efficiency of 91.4802 % in Table 4.25. The values of both the anodic and cathodic Tafel slopes for the inhibited process show some difference compared to those of the blank process. This signify that both the anodic and cathodic half reactions are affected by the presence of the inhibitor molecules. Other studies revealed that an inhibitor which works as either cathodic or anodic inhibitor, should have an E_{Corr} difference between the blank and the inhibited solution which is > 85 mV, while for a mixed type inhibitor, the difference should be either = or < 85 mV [157, 158]. Examination of E_{Corr} values in Tables 4.23 – 4.25, shows that the difference between the E_{Corr} values for the blank and the inhibited solution are < 85 mV, which suggest that the three flavonoid derivatives (NRNG, MNHD and 6-HFN) used could be classified as a mixed type inhibitor.

4.6 Electrochemical Impedance Spectroscopy

Electrochemical Impedance Spectroscopy has been intensively used as a very strong technique to characterise the corrosion processes and the performance of protective organic coatings. It is used in the corrosion studies to monitor the inhibitor film persistency, and it is also used in the study of inhibitors and scale analysis to provide information about corrosion and the protection mechanism [138]. In this study, EIS was performed in order to better navigate and study the behaviour and adsorption process of corrosion in the absence and presence of different concentration of three flavonoid derivatives. This procedure was performed on a scan rate with final frequency of 100,000 KHz and initial frequency of 0.100 Hz and sinus amplitude of 50.0 mV. The open circuit voltage was allowed to stabilize within 30 minutes to ensure better and reliable results for EIS and PDP. Figures 4.89 – 4.109 represent the Nyquist impedance plots and their corresponding bode impedance plots together with the electrical circuit equal to the electrode electrolyte system for the three inhibitors in two different acids concentration and two metals namely zinc and aluminium at 30° C.

4.6.1 Zinc in sulphuric acid

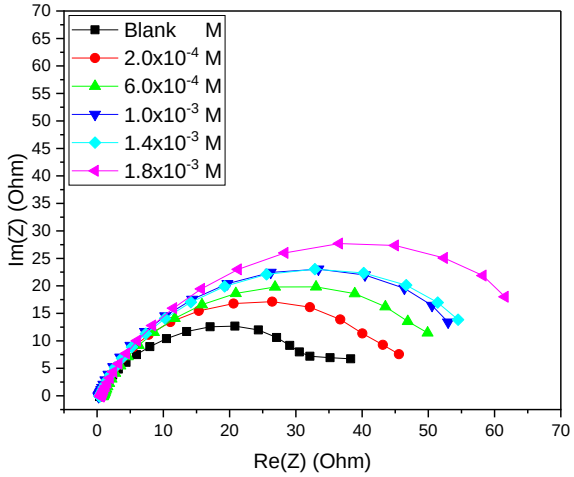

Figure 4.89: Nyquist plot of zinc metal in 1.5 M sulphuric acid in the absence and presence of different concentration of NRNG inhibitor compounds.

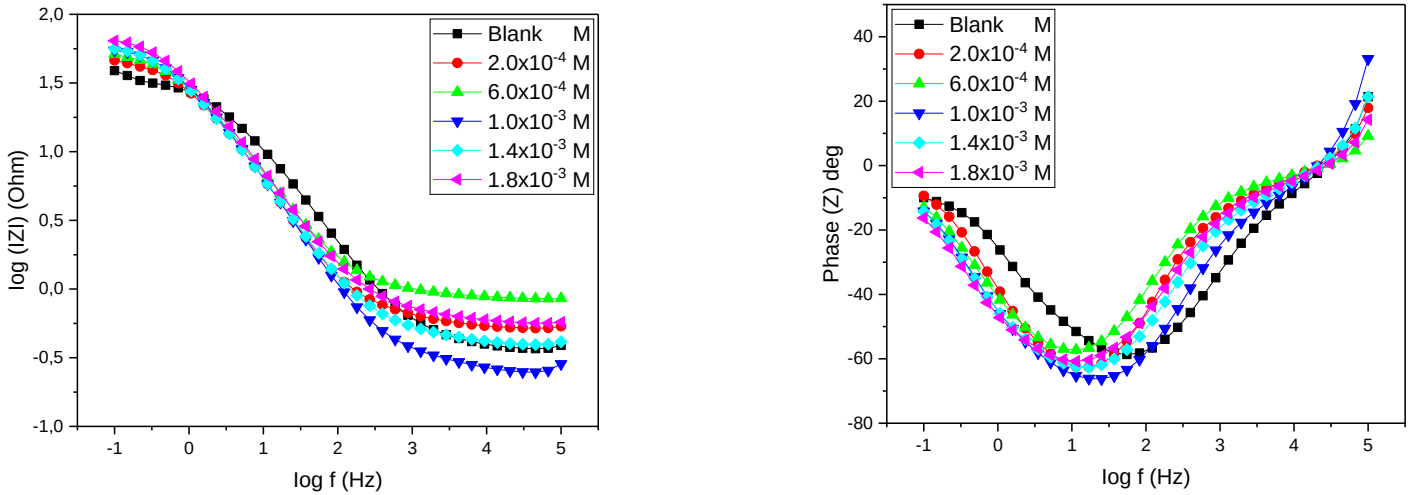

Figure 4.90: Bode plots of zinc metal in 1.5 M sulphuric acid in the absence and presence of different concentrations of NRNG inhibitor compound.

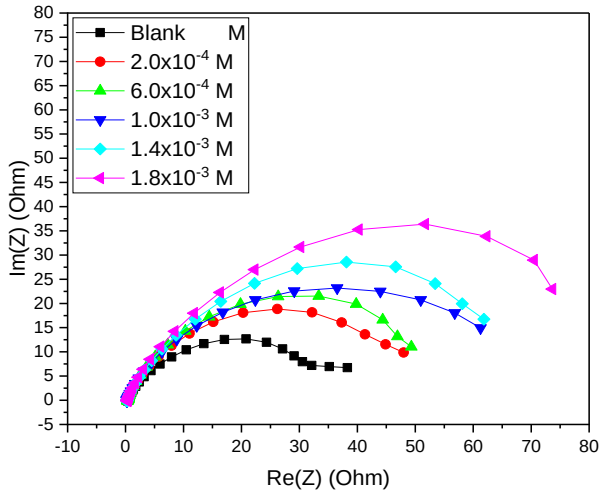

Figure 4.91: Nyquist plot of zinc metal in 1.5 M sulphuric acid in the absence and presence of different concentration of MNHD inhibitor compounds.

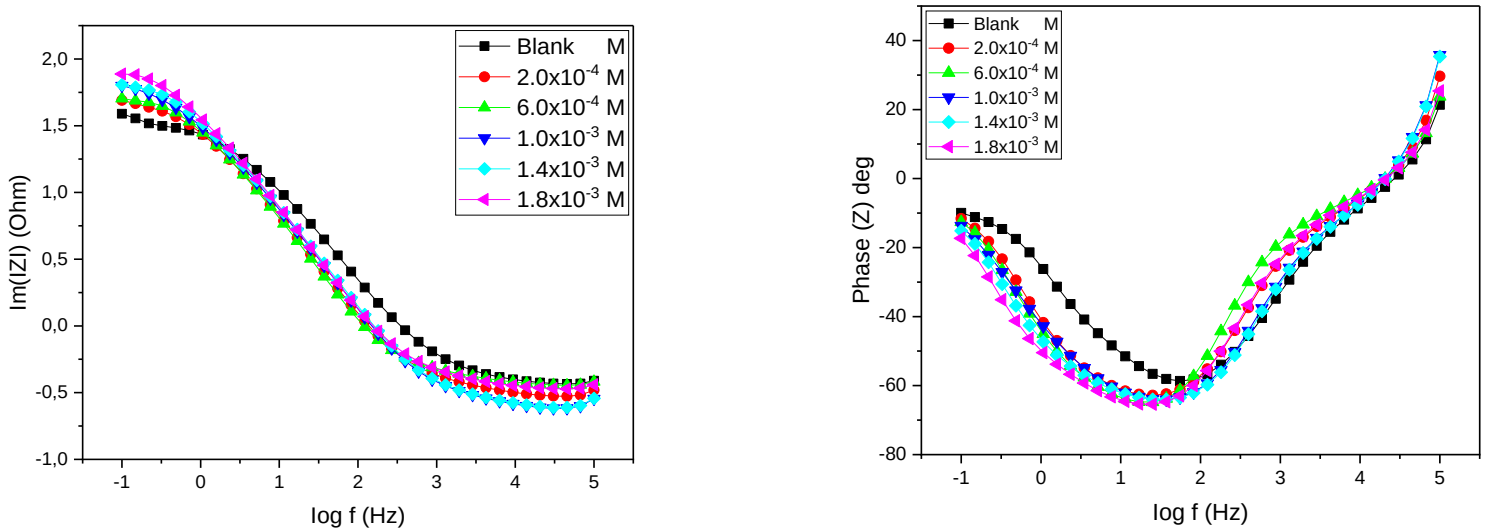

Figure 4.92: Bode plots of zinc metal in 1.5 M sulphuric acid in the absence and presence of different concentrations of MNHD inhibitor compound.

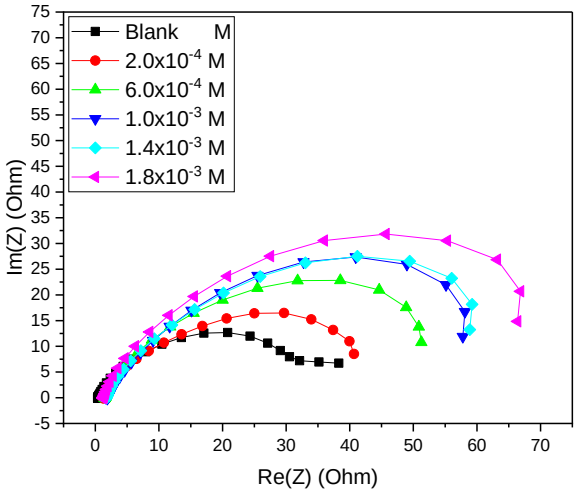

Figure 4.93: Nyquist plot of zinc metal in 1.5 M sulphuric acid in the absence and presence of different concentration of 6-HFN inhibitor compounds.

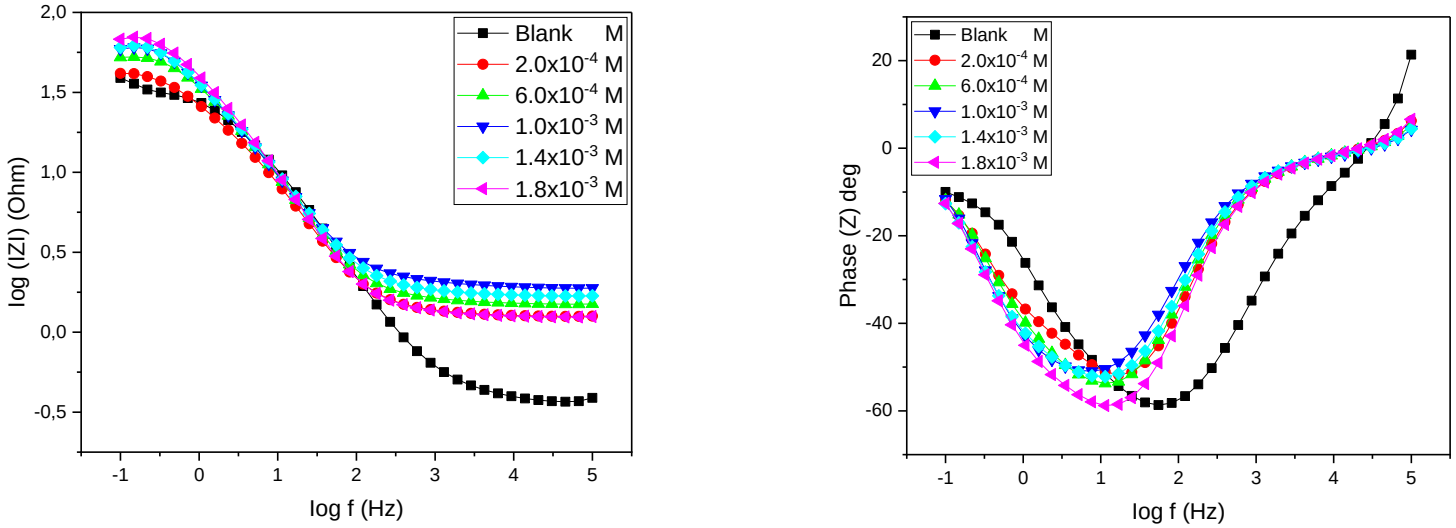

Figure 4.94: Bode plots of zinc metal in 1.5 M sulphuric acid in the absence and presence of different concentrations of 6-HFN inhibitor compound.

4.6.3. Aluminium in hydrochloric acid.

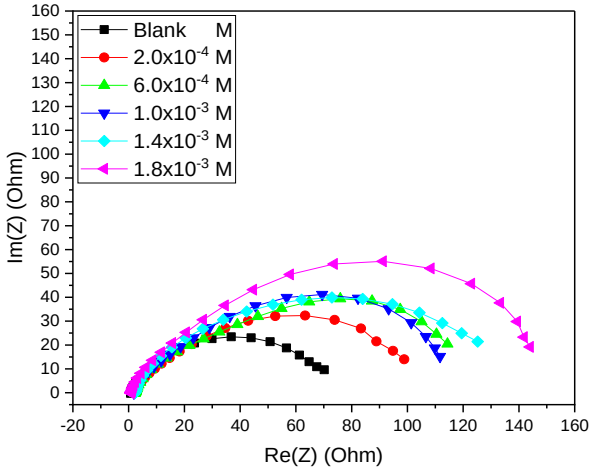

Figure 4.95: Nyquist plot of zinc metal in 0.5 M hydrochloric acid in the absence and presence of different concentration of NRNG inhibitor compounds.

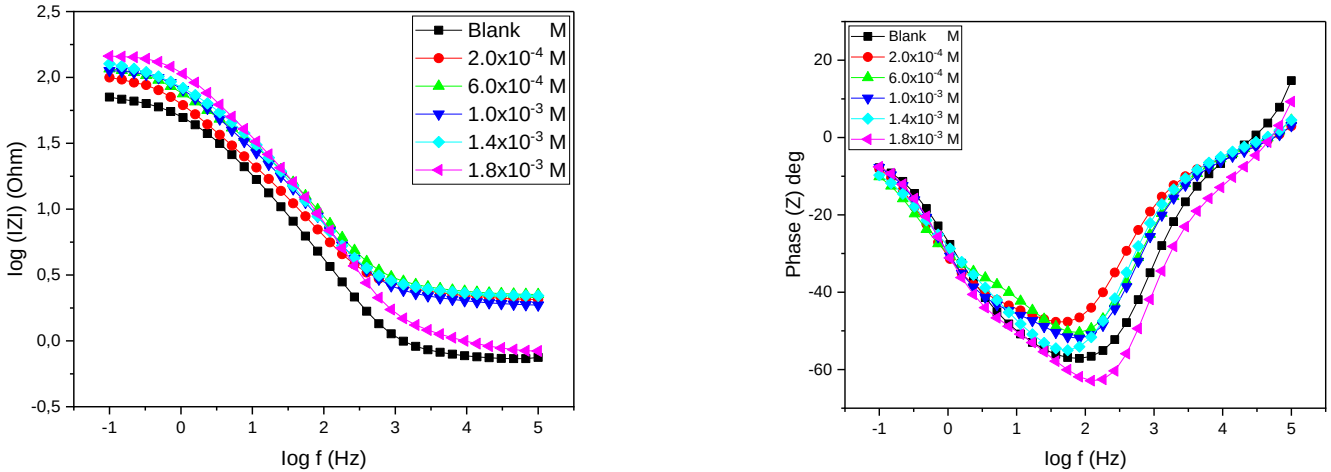

Figure 4.96: Bode plots of zinc metal in 0.5 M hydrochloric acid in the absence and presence of different concentrations of NRNG inhibitor compound.

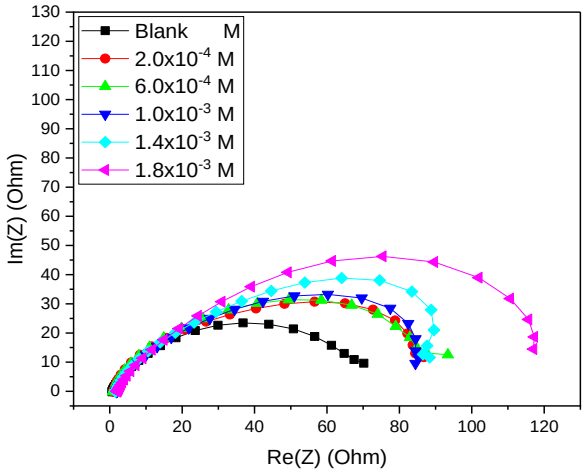

Figure 4.97: Nyquist plot of zinc metal in 0.5 M hydrochloric acid in the absence and presence of different concentration of MNHD inhibitor compounds.

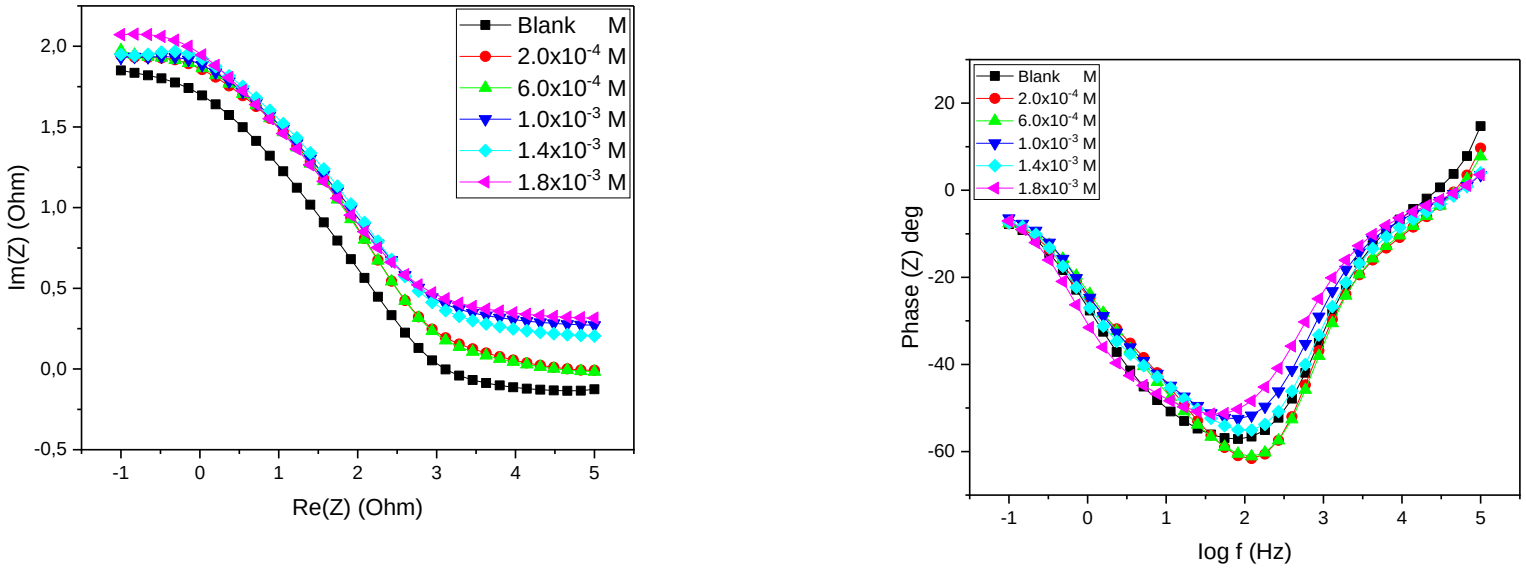

Figure 4.98: Bode plots of zinc metal in 0.5 M hydrochloric acid in the absence and presence of different concentrations of NRNG inhibitor compound.

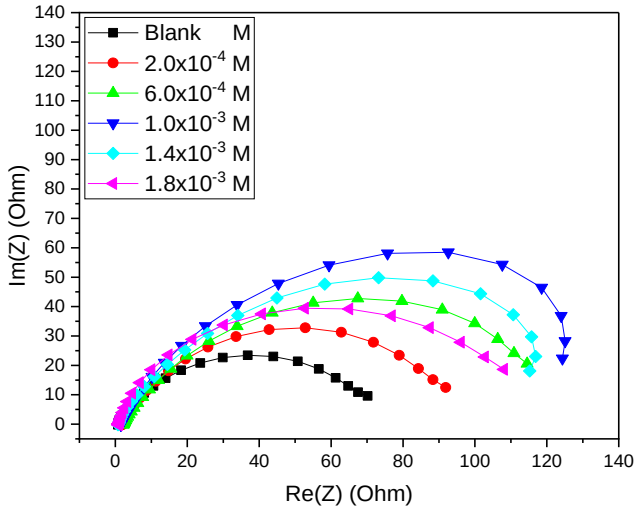

Figure 4.99: Nyquist plot of zinc metal in 0.5 M hydrochloric acid in the absence and presence of different concentration of 6-HFN inhibitor compounds.

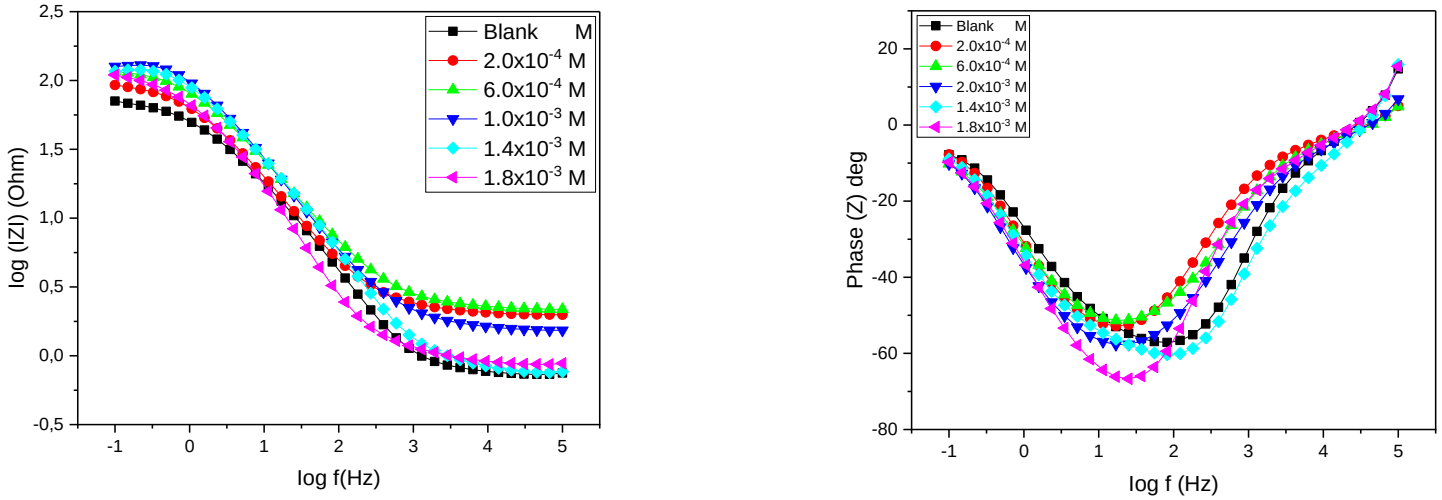

Figure 4.100: Bode plots of zinc metal in 0.5 M hydrochloric acid in the absence and presence of different concentrations of 6-HFN inhibitor compound.

From Figures 4.89 - 4.94, a different shape was observed in the Nyquist plots when the inhibitors were introduced into the sulphuric acid solution as compared to uninhibited sulphuric acid solution. This suggests that the presence of the inhibitors caused a change in the corrosion process mechanism. However, in Figures 4.95 – 4.100 for aluminium metal, the opposite is the case since the introduction of the inhibitors did not alter the shape of the Nyquist plots [159]. The Nyquist plots semicircle diameter and the magnitude of the impedance at low frequency in the bode plots indicate the general performance of the flavonoid derivatives [160]. The Nyquist plots obtained are imperfect semicircles which increases in diameter as the inhibitor concentration increases. This is caused by the formation of a film on the zinc and aluminium metal surface by the inhibitors, since as the concentration of the inhibitors increases more molecules are available in the solution providing more coverage on the metals surface. The imperfect semicircles of Nyquist plots are evidence of a charge transfer process which regulate the corrosion of zinc and aluminium metals [25]. The Nyquist plots presented in this study consists of an inductive loop in the low frequency region and a capacitive loop in the high frequency regions. The capacitive loop in the high frequency represents the charge transfer resistance of the corrosion process and the double layer capacitance.

The electrical circuit equal to the electrode electrolyte system used to fit the experimental data of NRNG, MNHD and 6-HFN is presented in Figures 4.101 and 4.102, for the three inhibitors in the absence and presence of sulphuric and hydrochloric acid in zinc and aluminium metal, respectively. The circuit used to fit the inhibited data was different from the circuit used in the uninhibited solution data as outlined below in the circuits. In the case of sulphuric acid in zinc of uninhibited solution, the circuit used was minimised several times before a perfect fit was obtained. The blank circuit comprises of R1 which correspond to R_s which is the solution resistance, R2 which correspond to charge transfer resistance R_{ct} in the phase interface, R3 is the charge transfer after the formation of the film layer, Q1 and Q2 represent the constant phase element (CPE). The Constant phase element was used in place of double-layer capacitance (C_{dl}) to reflect an ideal capacitor to describe the inhomogeneities in the system. The parameters used in the inhibited circuit have the same meaning as the above for the blank circuit.

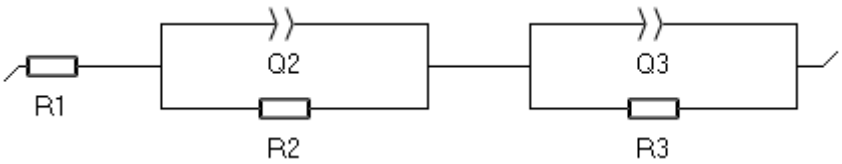

Figure 4.101: Electrical circuit equal to the electrode electrolyte system used to fit the impedance spectra obtained for zinc and aluminium metal corrosion in the presence of 1.5 M sulphuric and 0.5 M hydrochloric acid.

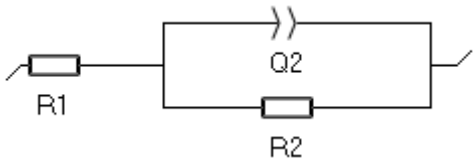

Figure 4.102: Electrical circuit equal to the electrode electrolyte system used to fit the impedance spectra obtained for zinc and aluminium metal corrosion in 1.5 M sulphuric and 0.5 M hydrochloric acid in the presence of three inhibitors NRNG, MNHD and 6-HFN.

Tables 4.26 and 4.27 represent the parameters such as resistance of electrolyte (R_s), resistance of charge transfer (R_{ct}), constant phase element (CPE) and the CPE exponent (n) obtained after fitting the circuit. The value of n describes the corrosion process on the surface of the metal, and it is a flexible value which ranges from -1 to 1, where the value of 1 corresponds to capacitor, the value of -1 corresponds to inductance and 0 corresponds to resistor [161]. $\%IE_{EIS}$ was obtained through (42) equation.

$$\%IE_{EIS} = \left(1 - \frac{R^0 ct}{Rct}\right) \times 100 \quad (42)$$

where R^0_{ct} and R_{ct} are charge resistance in the absence and presence of the three inhibitors compounds NRNG, MNHD and 6-HFN.

Table 4.26: Electrochemical impedance (EIS) parameters such as the resistance of charge transfer (R_{ct}), constant phase element (CPE) and the CPE exponent (n) using different inhibitors in 1.5 M sulphuric acid in zinc metal.

Inhibitor	Inhibitors Cons (M)	R_S (Ω)	R_{ct1} (Ω)	R3 (Ω)	n	n	Q1 ($F.s^{(a-1)}x10^{-3}$)	Q2 ($F.s^{(a-1)}x10^{-3}$)	$\%IE_{EIS}$	$\%IE_{WL}$
Blank	0.00	0.37	14.16	31.79	0.7371	0.7297	0.1189x10	3.747		
NRNG	$2.0x10^{-4}$	0.54	47.86	-	0.8034	-	5.646	-	70.41	72.32
	$6.0x10^{-4}$	0.87	57.36	-	0.7615	-	6.187	-	75.31	75.57
	$1.0x10^{-3}$	0.26	62.25	-	0.7941	-	5.904	-	77.25	78.43
	$1.4x10^{-3}$	0.41	65.07	-	0.7724	-	6.439	-	78.24	79.73
	$1.8x10^{-3}$	0.58	78.66	-	0.7559	-	6.068	-	82.00	79.69
MNHD	$2.0x10^{-4}$	0.30	52.51	-	0.7806	-	5.825	-	73.03	64.65
	$6.0x10^{-4}$	0.37	56.53	-	0.8050	-	5.663	-	74.95	75.47
	$1.0x10^{-3}$	0.24	67.35	-	0.7772	-	5.376	-	78.98	81.09
	$1.4x10^{-3}$	0.25	75.37	-	0.7750	-	5.256	-	81.21	81.97
	$1.8x10^{-3}$	0.34	94.75	-	0.7861	-	5.125	-	84.94	82.73
6-HFN	$2.0x10^{-4}$	1.24	46.44	-	0.7345	-	6.120	-	69.51	85.16
	$6.0x10^{-4}$	1.50	60.72	-	0.7618	-	4.852	-	76.68	85.72
	$1.0x10^{-3}$	1.90	73.07	-	0.7393	-	5.333	-	80.62	86.38
	$1.4x10^{-3}$	1.68	73.81	-	0.7440	-	5.104	-	80.82	86.41
	$1.8x10^{-3}$	1.24	81.13	-	0.7870	-	4.215	-	82.55	86.33

Table 4.27: Electrochemical impedance (EIS) parameters such as the resistance of charge transfer (R_{ct}), constant phase element (CPE) and the CPE exponent (n) using different inhibitors in 0.5 M hydrochloric acid in aluminium metal.

Inhibitor	Inhibitors Cons (M)	R_S (Ω)	R_{ct1} (Ω)	R3 (Ω)	n	n	Q1 ($F.s^{(a-1)}x10^{-3}$)	Q2 ($F.s^{(a-1)}x10^{-3}$)	$\%IE_{EIS}$	$\%IE_{WL}$
Blank	0.00	0.72	34.20	34.44	0.7772	1	1.874	5.38	-	-
NRNG	$2.0x10^{-4}$	2.05	108.0	-	0.6714	-	2.679	-	68.33	68.98
	$6.0x10^{-4}$	2.14	123.1	-	0.6694	-	1.885	-	72.22	71.12
	$1.0x10^{-3}$	1.83	123.4	-	0.6977	-	1.755	-	72.29	77.01
	$1.4x10^{-3}$	2.15	125.1	-	0.7277	-	1.423	-	72.66	78.61
	$1.8x10^{-3}$	0.84	154.7	-	0.7505	-	1.135	-	77.89	90.37
MNHD	$2.0x10^{-4}$	0.99	88.43	-	0.7583	-	1.144	-	61.33	73.80
	$6.0x10^{-4}$	0.97	90.88	-	0.7623	-	1.134	-	62.37	74.87
	$1.0x10^{-3}$	1.84	93.40	-	0.7208	-	1.287	-	63.57	75.94
	$1.4x10^{-3}$	1.58	99.59	-	0.7272	-	1.154	-	65.66	78.61
	$1.8x10^{-3}$	2.06	134.6	-	0.7006	-	1.636	-	74.59	82.35
6-HFN	$2.0x10^{-4}$	2.00	98.29	-	0.7322	-	2.342	-	65.21	88.24
	$6.0x10^{-4}$	0.90	110.0	-	0.8202	-	1.977	-	68.91	91.98
	$1.0x10^{-3}$	2.16	131.0	-	0.7006	-	1.985	-	73.89	93.05
	$1.4x10^{-3}$	0.75	134.2	-	0.7517	-	1.512	-	74.52	93.58
	$1.8x10^{-3}$	1.55	153.9	-	0.7406	-	1.643	-	77.77	95.19

Form Tables 4.26 and 4.27, it can be observed that when the concentration of the inhibitors increases, the charge transfer also increases which is an indication of the formation of the inhibitors film on the surface of the zinc and aluminium metals. This is due to the increasing availability of inhibitors molecules on the solution as the inhibitor concentration increases, providing more protection on the metal. The values of n are close to unity which indicate that the interface is of a capacitive nature. The high values of n are an indication that the inhibitors formed a layer on the zinc metal surface and improve their homogeneity. The values of the constant phase element do not have a stable proper trend but in most cases are found to be decreasing with an increase in the concentration of the inhibitors. This behaviour can be attributed to the adsorption of the inhibitors on the metal surface preventing corrosion cells on the metal surface and hostile corrosion [157]. This kind of behaviour can also be due to the increase in the thickness of the electrical double layer or the reduction in the dielectric constant [162]. The percentage inhibition efficiency for EIS ($\%IE_{EIS}$) calculated in this result increases with an increase in the inhibitors concentration and they are in agreement with the %IE obtained in the gravimetric analysis, AAS and Potentiodynamic polarisation.

Figures 4.103 – 4.108, represent the Nyquist impedance plots of the three inhibitors NRNG, MNHD and 6-HFN, and their corresponding bode impedance plots in the presence of 1.5 M hydrochloric acid in zinc metal.

4.6.4. Zinc in hydrochloric acid.

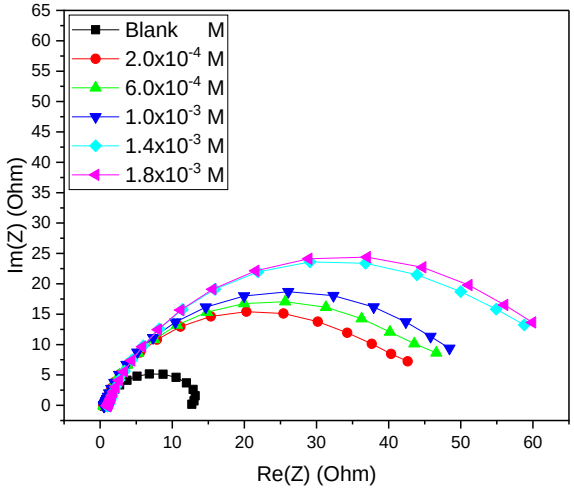

Figure 4.103: Nyquist plot of zinc metal in 1.5 M hydrochloric acid in the absence and presence of different concentration of NRNG inhibitor compounds.

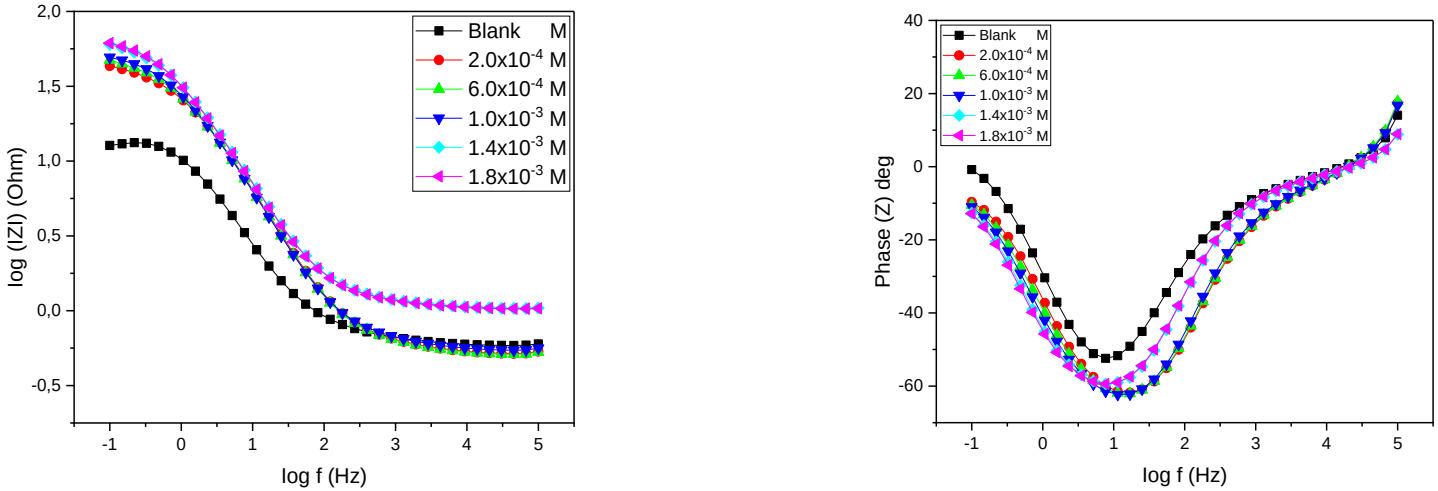

Figure 4.104: Bode plots of zinc metal in 1.5 M hydrochloric acid in the absence and presence of different concentrations of NRNG inhibitor compound.

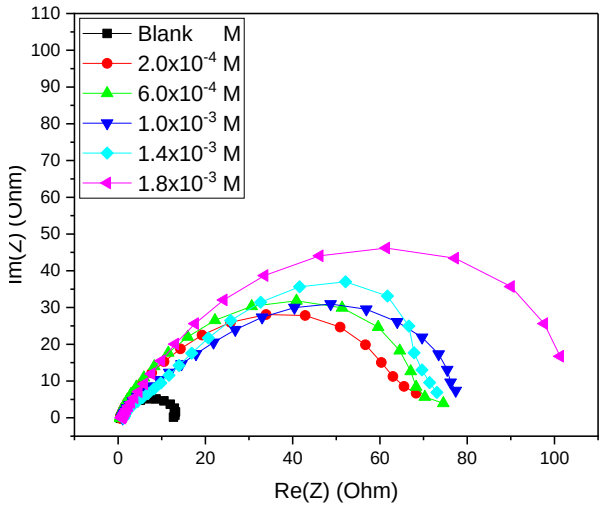

Figure 4.105: Nyquist plot of zinc metal in 1.5 M hydrochloric acid in the absence and presence of different concentration of MNHD inhibitor compounds.

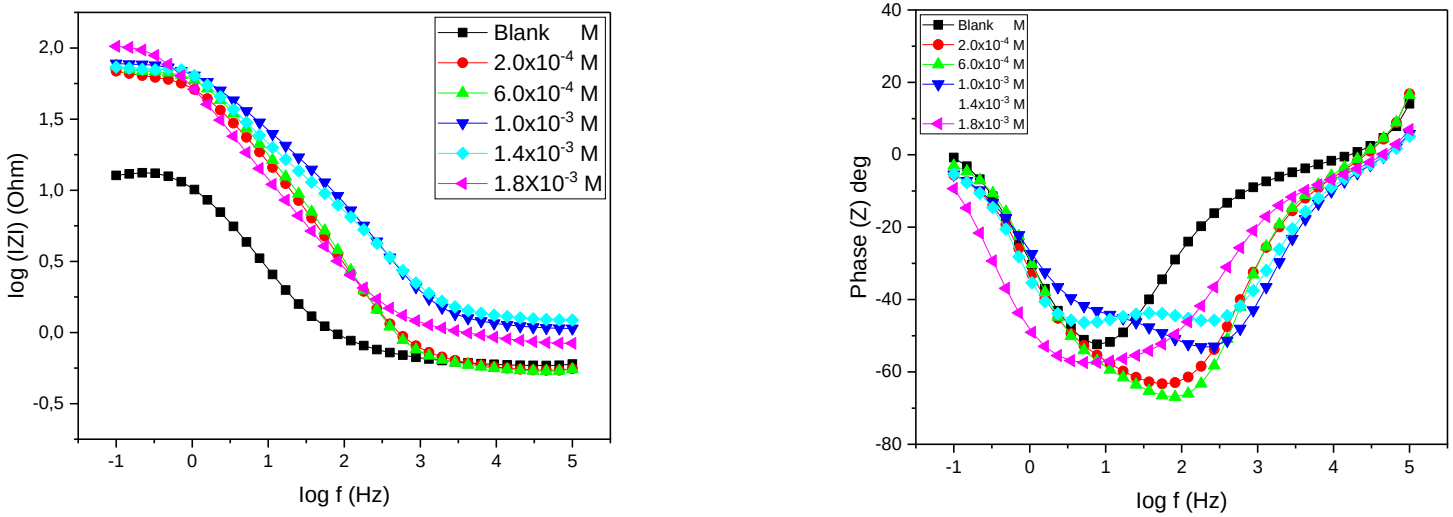

Figure 4.106: Bode plots of zinc metal in 1.5 M hydrochloric acid in the absence and presence of different concentrations of MNHD inhibitor compound.

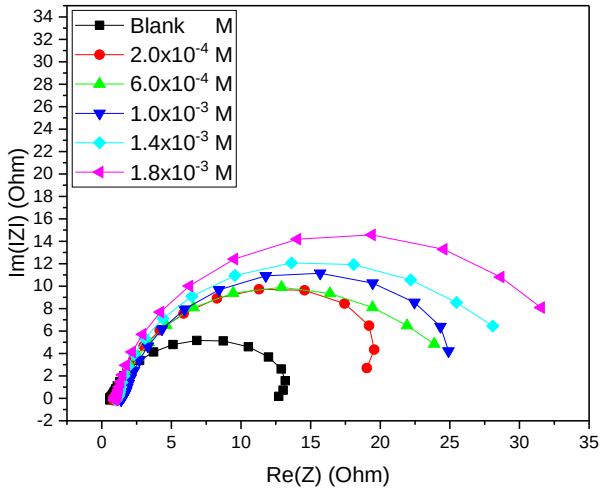

Figure 4.107: Nyquist plot of zinc metal in 1.5 M hydrochloric acid in the absence and presence of different concentration of 6-HFN inhibitor compounds.

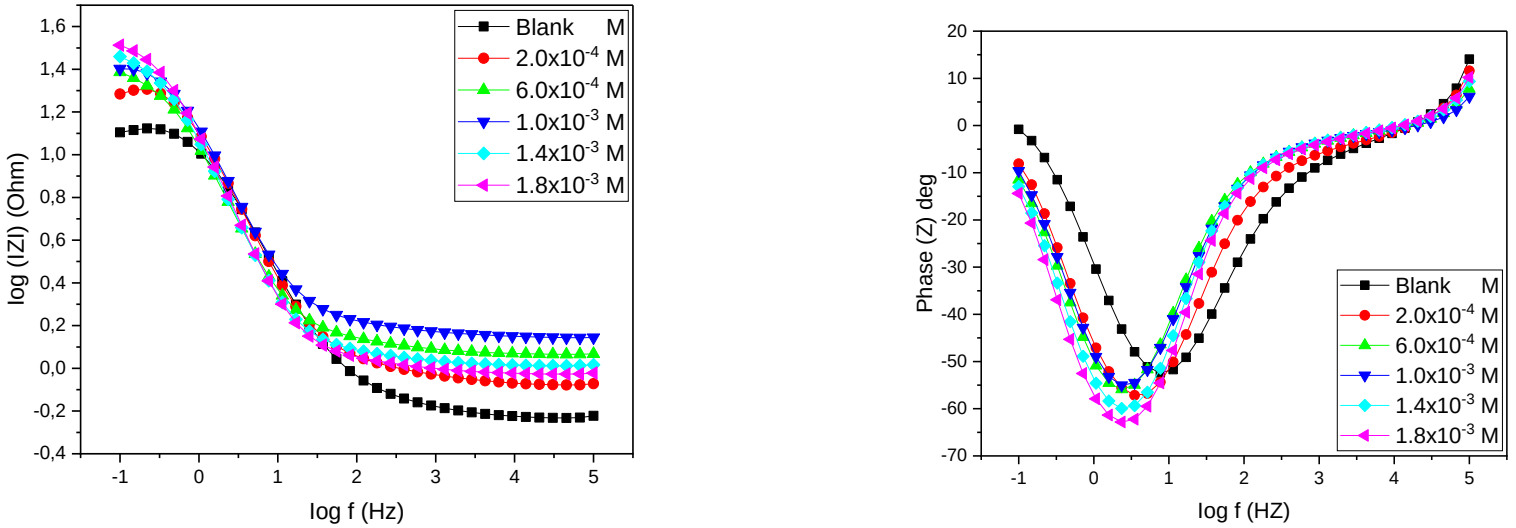

Figure 4.108: Bode plots of zinc metal in 1.5 M hydrochloric acid in the absence and presence of different concentrations of 6-HFN inhibitor compound.

A close examination of the Nyquist plots shows that, the shape is the same in the absence and presence of the inhibitors, which is an indication that the introduction of the inhibitors did not alter the corrosion mechanism. The Nyquist plots semicircle diameter and the magnitude of the impedance at low frequency in the bode plots indicate the general performance of the flavonoid's derivatives [160]. The Nyquist impedance plots obtained are imperfect semicircles which increases in diameter as the inhibitor's concentration increases. This is caused by the formation of a film on the zinc surface by the inhibitors, since as the concentration of the inhibitors increases, more molecules are available in the solution providing more coverage on the metal surface. The imperfect semicircles of Nyquist plots are evidence of a charge transfer process which regulate the corrosion of zinc metal [25].

All the experimental data both in the absence and presence of the inhibitors were fitted with the electrical circuit equal to the electrodes electrolyte system shown in figure 4.102. The circuit comprises of R1 which represent the solution resistance (R_s), R2 represent charge transfer resistance (R_{ct}) and it is related to the magnitude of the electron transfer between the inhibitor and the metal and it is also related to the inhibition efficiency [25]. Q1 is the constant phase element (CPE). Instead of using double layer capacitance (C_{dl}), the constant phase element was used to reflect an ideal capacitor to explain the inhomogeneities in the corrosion system.

Table 4.28 represent the parameters such as solution resistance of electrolyte (R_s), resistance of charge transfer (R_{ct}), constant phase element (CPE) and the CPE exponent (n) obtained after fitting the circuit. The value of n describes the corrosion process on the surface of the metal, and it is an adjustable value which ranges from -1 to 1, where the value of 1 corresponds to capacitor, the value of -1 corresponds to inductance and 0 corresponds to resistor [161].

Table 4.28: Electrochemical impedance (EIS) parameters such as the resistance of charge transfer (R_{ct}), constant phase element (CPE) and the CPE exponent (n) using different inhibitors in 1.5 M hydrochloric acid in zinc metal.

Inhibitor	Inhibitors Cons (M)	R_S (Ω)	R_{ct} (Ω)	N	Q1 ($F.s^{(a-1)}x10^{-3}$)	$\%IE_{EIS}$	$\%IE_{GRAV}$
Blank	0.00	0.612	13.65	0.7988	0.013		
NRNG	$2.0x10^{-4}$	0.533	44.05	0.7975	5.696	69.01	67.18
	$6.0x10^{-4}$	0.529	48.08	0.7957	5.913	71.59	68.74
	$1.0x10^{-3}$	0.563	52.37	0.7984	5.886	73.94	69.73
	$1.4x10^{-3}$	1.065	65.84	0.7901	5.519	79.27	69.90
	$1.8x10^{-3}$	1.061	67.96	0.7898	5.608	79.91	70.46
MNHD	$2.0x10^{-4}$	0.537	70.86	0.7956	2.199	80.73	61.834
	$6.0x10^{-4}$	0.531	74.54	0.8371	1.601	81.69	69.346
	$1.0x10^{-3}$	0.980	85.33	0.6847	1.769	84.00	70.440
	$1.4x10^{-3}$	1.128	90.41	0.6400	2.751	84.90	71.558
	$1.8x10^{-3}$	0.881	130.7	0.7294	3.937	89.56	73.576
6-HFN	$2.0x10^{-4}$	0.886	22.70	0.8256	$0.014x10^{-3}$	39.87	72.482
	$6.0x10^{-4}$	1.214	25.30	0.8479	$0.017x10^{-3}$	46.05	75.131
	$1.0x10^{-3}$	1.455	27.52	0.8443	$0.014x10^{-3}$	50.40	75.398
	$1.4x10^{-3}$	1.070	30.02	0.8739	$0.016x10^{-3}$	54.53	76.590
	$1.8x10^{-3}$	0.983	35.20	0.8820	$0.015x10^{-3}$	61.22	77.538

From Table 4.28, it is observed that the values of R_S do not show a stable trend as the concentration of the inhibitors increases, and this can be accounted for by the geometry variation of the areas which helps in the flowing of the current in the system [25]. From the results above, it is evidence that the charge transfer resistance (R_{ct}) increases with an increase in the concentration of the inhibitors. This is because of the formation of film on the surface of the metal as the concentration of the inhibitors increases. This is largely attributed to the fact that more inhibitors molecules become available in the solution to enhance the formation of the protective film when increasing the concentration of the inhibitors. The values of n are close to unity, which as an indication that the interface is of a capacitive nature. The high values of n are an indication that the inhibitors formed a layer on the zinc metal surface and improve their homogeneity [157]. The values of the constant phase element do not show a stable proper trend but in most cases are found to be decreasing with an increase in the concentration of the inhibitors. This behaviour can be attributed to the adsorption of the inhibitors on the metal surface preventing corrosion cells on the metal surface and hostile corrosion [157]. The percentage inhibition efficiency of EIS is increasing with an increase in the concentration of the inhibitors and correlate very well to the %IE obtained in Potentiodynamic polarisation, atomic absorption spectroscopy and gravimetric analysis.

Chapter 5: Conclusions and Future Work

5.1 Conclusions

In this study, the corrosion inhibition potentials of three flavonoid derivatives namely Naringenin (NRNG), Morin hydrate (MNHD) and 6-Hydroxyflavone (6-HFN) for zinc and aluminium metals were investigated using gravimetric analysis, Atomic Absorption Spectroscopy (AAS), surface characterization [Fourier Transform Infrared Spectroscopy (FTIR) and 2D and 3D microscopy and electrochemical studies [Potentiodynamic Polarization (PDP) and Electrochemical Impedance Spectroscopy (EIS)] in three aggressive acidic environment of 0.5 M and 1.5 M hydrochloric acid, and 1.5 M sulphuric acid at a temperature range of 30 – 60°C.

Therefore, the following conclusions are based on the outcome of the work in this project.

- Gravimetric analysis showed that, the three inhibitors NRNG, MNHD and 6-HFN were able to inhibit the corrosion of zinc and aluminium metals as can be seen by the maximum percentage inhibition efficiency of 90.37, 82.35 and 95.19 % for aluminium in hydrochloric acid, 79.69, 82.73 and 86.33 % for zinc in sulphuric acid and 70.46, 71.56 and 77.54 % for zinc in hydrochloric acid, respectively.
- The adsorption process of the three inhibitors on the metal surface was found to obey the Langmuir adsorption isotherm. In the presence of aluminium metal, the inhibitors were found to adsorb through physisorption. However, in the presence of zinc metal the inhibitors showed a mixed type of inhibition mechanism which means that both electrostatic interaction between the charged molecules of the inhibitors and the metal surface (physisorption), and the charge transfer or sharing of the inhibitors molecules to the metal surface to form a coordinated bond (chemisorption) were all represented. This type of mechanism is supported by the activation energy (E_a) results, in which an increase at low inhibitors concentration (E_a inhibited > E_a uninhibited) was observed which is associated with physisorption and the decrease in higher concentration (E_a inhibited < E_a uninhibited), which is associated with chemisorption, hence a mixed type of inhibition. This type of mechanism was also further supported by the change in Gibbs energy (ΔG°) values.
- The change in enthalpy (ΔH^*) values were obtained as positive which entails that the dissolution process of the zinc and aluminium metals were endothermic.

- The change in entropy (ΔS^*) values were obtained as negative, which suggest that before adsorption process, the inhibitors molecules were very chaotic and once the adsorption process took place the molecules were adsorbed orderly into the metal surface.
- The atomic absorption spectroscopy (AAS) was used to determine the concentration of the metals that was left in the solution after gravimetric analysis. In the presence of sulphuric acid in zinc, the inhibitors managed to reduce the amount of metals specimens left in the solution after gravimetric analysis by the high percentage inhibition efficiency obtained of 82.642 and 81.548 % for MNHD and 6-HFN.
- Fourier transform infrared spectroscopy (FTIR) was utilised to understand the functional groups that disappeared or formed during the adsorption process of the inhibitor molecules on the metals surface. The Ar - OH functional group was the worst affected since no inhibitor was able to retain it after gravimetric analysis in the presence of sulphuric acid. The C=C functional group of the aromatic ring was retained by all the inhibitors in all the metals studied.
- 2D and 3D microscope was also used to study the extent to which the metals were damaged by the acids and the type of corrosion that resulted thereafter, in the absence and presence of the three inhibitors. The aluminium metal in the presence of the inhibitors showed a uniform type of corrosion and its metal in blank solution showed a localised type of corrosion. When the zinc metal was used, the sulphuric blank solution showed uniform corrosion and the hydrochloric acid blank solution showed localised type of corrosion, but in the presence of the inhibitors, the zinc metal showed localised type of corrosion irrespective of the acid used.
- The results obtained from Potentiodynamic Polarization (PDP) and electrochemical impedance spectroscopy (EIS) indicated that the compounds are a mixed type of inhibitor. The results from PDP also indicated that the use of three flavonoids derivatives compounds as corrosion inhibitors managed to significantly reduce the corrosion current densities for the cathodic and anodic half reactions, which indicate that, the dissolution and cathodic reduction of the hydrogen ions were inhibited.
- The order of the inhibition efficiency at $1.8x10^{-3}$ M for the maximum temperature (60°C) was 6-HFN > MNHD > NRNG for zinc metal and NRNG > 6-HFN > MNHD for aluminium metal. The charge transfer resistance R_{ct} was found to be increasing with an increase in the concentration of the inhibitors, signifying the adsorption of the inhibitors onto the metal surface thereby forming a film. The constant phase element values were decreasing with an increase in the

concentration of the inhibitors, further supporting the formation of the film on the metal surface.

- The percentage inhibition efficiency EIS (%EI_{EIS}) was also calculated and found to be correlating very well with the IE results obtained in PDP, AAS and gravimetric analysis.

5.2. Future Work

From this study, there are other several topics that can be explored in future work to support the inhibition potential of NRNG, MNHD and 6-HFN inhibitors. Such includes Scanning electron microscope (SEM) connected to energy dispersive spectroscopy (EDS), and quantum chemical studies. The inhibitors can also be tested on different combinations of aggressive environments and metals, such acetic acids, sea water and other alkaline solutions with mild steel and copper metals.

Chapter 6: References

1. Z. Ahmad, Principles of corrosion engineering and corrosion control, Elsevier (2006): 1 – 130
2. R. Sharma, A. Chaturvedi and R.K. Upadhyay, Corrosion inhibition effect of flower of euphorbia caducifolia for iron in acid media, IOSR Journal of Pharmacy, 7 (2017): 30 – 37.
3. V.M. Abbasov, H.M. Abd El-Lateef, L.I Aliyeva, I.T. Ismayilov, E.E. Qasimov and M.M. Narmin, Efficient Complex Surfactants from the type of fatty acids as corrosion inhibitors for mild steel C1018 in CO_2 - environments, Journal of the Korean Chemical Society, 57.1 (2013): 25 – 34.
4. M.A.A. Ali, Inhibition of mild steel corrosion in cooling systems by low- and non-toxic corrosion inhibitors, the university of Manchester, (2016): 34.
5. V.S. Sastri, Green corrosion inhibitors: theory and practice. Vol. 10. John Wiley & Sons Inc., Hoboken, New Jersey. (2012) 1 – 11.
6. J. Floruo and D.J. Miller D, Handbook of coating additives, 2nd Ed, (2004): 136.
7. G.H. Koch, M.P. Brongers, N.G. Thompson, Y.P. Virmani and J.H. Payer, Cost of corrosion in the United States. In Handbook of environmental degradation of materials. William Andrew Publishing, (2005): 3 – 24.
8. D.M. Bastidas, E. Cano, and E. M. Mora. Volatile corrosion inhibitors: A review. Anti-Corrosion Methods and Materials, 52.2 (2005): 71 – 77.
9. G.F. Hays, Corrosion process and advanced materials in industry, Now is the time. In Elizer, A. (Ed) Switzerland: Tech publications Ltd (2010): 1 – 6.
10. D. Parker, Skills transfer, capacity building imperative in corrosion control industry, Engineering News, 28 May 2009: Web. 15 July 2016.
11. V.S. Saji. Contemporary developments in corrosion inhibitors-Review of patents. Recent Patents on Corrosion Science, 1.1 (2011): 63 – 71.
12. K. Myles and Associates, Corrosion control: Principles and practice, Randburg South Africa: Myles publication, (1995): 1.
13. N.O. Obi-Egbedi, I.B. Obot, Adsorption behavior and corrosion inhibitive potential of xanthenes on mild steel/sulphuric acid interface, Arabian Journal of Chemistry, 5. 1 (2012): 121 – 133.
14. C.V. Patil and K.B. Ghanedra, An investigation into the environmental impacts of atmospheric of building materials, International journal of chemistry sciences and applications, (2013): 1 – 6.
15. J.R. Davis, (Ed.). (2000). Corrosion: Understanding the basics. Asm International. Chapter 1, (2000) pg 2.

16. D. Landolt, Corrosion and surface chemistry of metals, Engineering Science, Materials, EPFL press, (2007): 1 – 3
17. A.P.I. Popoola, O.E. Olorunniwo, and O.O Ige, Corrosion resistance through the application of anti-corrosion coatings. In Developments in corrosion protection. IntechOpen. (2014): 242 – 261.
18. K.E. Heusler, D. Landolt, and S. Trasatti, Electrochemical corrosion nomenclature (Recommendations 1988). Pure and applied chemistry, 61.1 (1989): 19 – 22.
19. W.D. Callister, Materials Science and Engineering: An Introduction, 7th Ed, New York: John Wiley & Sons, Inc. 7 (2007): 665 – 715.
20. N. K. Frank and M. C. John, The Nalco Water Handbook (1979): 143 – 147.
21. A. De la Rive, Bulleting for the history of chemistry. Chemistry of Electrochemical and Physics., 45 (1930) 28.
22. AWWA Stuff, Ductile-iron pipe and fittings, American water works association. (2011): 166.
23. W. Hill John and K. Kolb Doris, Chemistry for Changing Times, 9th Ed., (No. QD33 H54 2001). Prentice Hall., (2001): 1 – 103.
24. A. Kamis, Cost of corrosion, Bullet. FKKKSA, 6 (1992): 12 – 15.
25. L.C. Murulana, Adsorption, thermodynamic and density functional theory investigation of some sulphonamides as corrosion inhibitors for selected metals in acidic medium, North West University: Faculty of Agriculture, Doctoral dissertation, Science and Technology, (2015): 9, 149.
26. S.A. Umoren, I.B. Obot, E.E. Ebenso, P.C. Okafor, O. Ogbobe, E.E. Oguzie, Gum arabic as a potential corrosion inhibitor for aluminium in alkaline medium and its adsorption characteristic, Anti-Corrosion Methods and Material, 53 (2006): 277 – 282.
27. S. Chihi, N. Gherraf, B. Alabed and S. Hameurlain, Inhibition effects of flavonoids extract of euphoria guyoniana on the corrosion of mild steel in H_2SO_4 medium, Journal of Fundamental and Applied Sciences, 1. 2 (2009): 31 – 39.
28. N. O. Eddy, S. R. Stoyanov, E. E. Ebenso, Fluoroquinolones as corrosion inhibitors for Mild steel in acidic medium; experimental and theoretical studies, International Journal of Electrochemical Science, 5 (2010): 1127 – 1150.
29. I. Dehri, M. Ozcan, The effect of temperature on the corrosion of mild steel in acidic media in the presence of some sulphur-containing organic compounds, Materials Chemistry and Physics, 98.2-3 (2006): 316 – 323.
30. F.M. Donahue and K. Nobe, Amaides derivatives as corrosion inhibitors, Electrochemical Society, 112 (1965): 886.

31. E. Khamis, F. Bellucci, R. M. Latanision, and E. S. H. El-Ashry, Acid corrosion inhibition of nickel by 2-(triphenosphoranylidene) succinic anhydride, Corrosion 47. 9 (1991): 677 – 686.

32. A. Sadaqat, Types of corrosion and rates of corrosion SlideShare 13CH26. Mehran university of engineering and technology, Sind, Parkistan, (2014): 23 – 24.

33. R. Dutton, Problems with volatile corrosion in the metal finishing industry pollution control, Met. Finish 102.11 (2004): 12.

34. M.G. Fontana, Corrosion Engineering, 3rd Ed, Tata McGraw Hill Education Private Limited, New Delhi, (2005): 45.

35. V. Hluchan, B.L. Wheeler and N. Hackerman, Amino acids as corrosion inhibitors in hydrochloric acid solutions. Materials and Corrosion, 39.11 (1988): 512 – 517.

36. P.R. Roberge, Corrosion Engineering Principles and Practice, 2nd Ed. McGraw Hill, New York, USA (2008): 708 – 754.

37. U. R. Evans, and A. B. Winterbottom. Metallic corrosion, passivity, and protection, (1948)

38. K. James and P. E. Rice, Consulting Engineer, Drew Principles of industrial Water Treatment, Olney, Maryland (1977).

39. N. Mora, E. Cano, E.M. Mora and J.M. Bastidas, Influence of pH and oxygen on copper corrosion in simulated urine fluid, Biomaterials, 23.3 (2002): 667 – 671.

40. H. R. Copson, Effects of velocity on corrosion by water, Industrial and engineering chemistry, 44. 8 (1952): 1745 – 1752.

41. M.A. Quraishi, M.Z.A. Rafiguee, S. Khan and N. Saxena, Corrosion inhibition of aluminium in acidic solution by some imdazoline derivatives, Journal of Applied Electrochemistry, 37. 10 (2007): 1153 – 1162.

42. A.K. Singh, M.A. Quraishi, Piroxicam; A novel corrosion inhibitor for mild steel corrosion in HCl acid solution, Journal of Material and Environmental science, 1. 2 (2010): 101 – 110.

43. C. Arya, P.R.W. Vassie, Influence of cathode-to-anode ratio and separation distance on galvanic corrosion currents of steel in concrete containing chlorides, Cement and Concrete Research, 25.5 (1995): 989 – 998.

44. K. Denpo, H. Ogawa, Fluid flow effects on CO_2 corrosion resistance of oil well materials, NACE International, Corrosion, 49.6 (1993): 442 – 449.

45. P.R. Roberge, Corrosion books: handbook of corrosion engineering. Material and Corrosion, 54 (2002): 175 – 284.

46. M. Schneider, K. krimmer, C. Lammel, K. Sempf and M. Hermann, Galvanic corrosion of metal/Ceramic coupling, Corrosion Science, 80 (2014): 191 – 196.
47. Techniques of monitoring corrosion and related parameters in filed applications. NHCE 3T199. Houston, Tex.: NHCE International. (1990): 1 – 41.
48. R. Davis Joseph, ed. Alloying: understanding the basics. ASM international, (2001): 100 – 150.
49. M.L. Free, Understanding the effect of surfactant segregation on corrosion inhibition of mild steel in acidic medium, Corrosion Science, 44.12 (2002): 2865 – 2870.
50. A. Philip and P.E. Schweitzer, Encyclopedia of corrosion technology, 2nd Ed. CRC press, (2004): 2004.
51. M. Ramakrishna, N. Srdjan and D. A. Gulino, Erosion corrosion and synergistic effects in distrurbed liquid-particle flow, In CORROSION 2006, NACE International, (2006): 1 – 2.
52. M.M. Salama, Influence of sand production on design and operations of piping systems, In CORROSION 2000, NACE International, (2000): 80.
53. B.A. McLaury, S.A. Shirazi, J.R. Shadley, E.F. Rybicki, Parameters affecting flow accelerated erosion and erosion-corrosion, CORROSION, (No. CONF-950304-). NACE International, Houston, TX (United States), (1995): 120.
54. A. Neville, T. Hodgkiess, and J.T. Dallas, A study of the erosion-corrosion behavior of engineering steels for marine pumping applications, Wear 186 (1995): 497 – 507.
55. G.T. Burstein, K. Sasaki, Effect of impact angle on the erosion-corrosion of 304L stainless steel, Wear, 240.1-2 (2000): 80 – 94.
56. S. Zhou, M.M. Stack and R.C. Newman, Characterization of synergistic effects between erosion and corrosion in an aqueous environment using electrochemical techniques, Corrosion, 52.12 (1996): 934 – 946.
57. Z. Xinyan and G.S. Frankel, Quantitative study of exfoliation corrosion: exfoliation of slices in humidity technique, Corrosion Science, 49.2 (2007): 920 – 938.
58. I.B. Beech, J. Sunner, Biocorrosion: Towards Understanding Interactions Between Biofilms and Metals. Current Opinion in Biotechnology, 15.3 (2004): 181 – 186.
59. A. Heyer, F. D'Souza, C.F. Leon Morales, G. Ferrari, J.M.C. Mol, J.H.W de Wit, Ship ballast tanks a review from microbial corrosion and electrochemical point of view, Elsevier Ocean Engineering, 70 (2013): 188 – 200.
60. W.P. Iverson, Microbial Corrosion of Metals. Advances in Applied Microbiology, Academic Press, 32 (1987): 1 – 36.

61. I. Beech, A. Bergel, A. Mollica, H. Flemming, V. Scotto and W. Sand, Microbially influenced corrosion of industrial materials, Brite-Euram III Thematic Network, (2000): 3.
62. H. Kumar and V. Yadav, Corrosion characteristic of mild steel under different atmospheric conditions by vapour phase corrosion inhibitors, American Journal of Materials Science and Engineering, 1.3 (2013): 34 – 39.
63. H.H. Uhlig and R.W. Revie, Corrosion and corrosion control: An Introduction to Corrosion Science and Engineering. (Book), John Wiley & Sons, Inc., 441 (1985): 1985.
64. M. Yasmashita, H. Konishi, T. Kozakura, J. Mizuki and H. Uchida, In situ observation of initial rust formation process on carbon steel under Na_2SO_4 and NaCl solution films with wet/dry cycles using synchrotron radiation x-rays, Corrosion Science, 47 (2000): 2492 – 2498.
65. M.G. Fontana, Corrosion Engineering, 3rd Ed. McGraw-Hill, New York (1986) 51 – 376.
66. S. Alka, C. Guddi, S. Arpita and Y. Swati, Inhibitive and adsorption properties of ethanolic extract of fruit of azadirach indica on the corrosion of copper in HCl, 3. 9 (2014): 798.
67. J. Kruger, Electrochemistry of corrosion, The Electrochemical Society: Electrochemistry encyclopedia, (2001).
68. ASM International: The effect and economic impact of corrosion, in: Corrosion: Understanding the basics, www.asminternational.org/content/ASM/StoreFiles/06691G_Chapter_1.pdf. (2000).
69. P.G. Sheasby and R. pimner, the surface treatment and finishing of aluminium and its alloys, ASM international,2 (2001): 2 – 3.
70. Z. Szklarska-Smialowska, Pitting corrosion of Aluminium, Corrosion Science, 41.9 (1999): 1743 – 1767.
71. K. Mutombo and M. Du Toit, Corrosion fatigue behaviour of aluminium 5083-H111 welded using gas metal arc welding method, CSIR, University of Pretoria South Africa, Arc Welding. BoD–Books on Demand, (2011): 185 – 643.
72. R.A. Prabhu, T.V. Venkatesha and B.M. Praveen, Electrochemical study of the corrosion behaviour of zinc surface treated with a new organic chelating inhibitor, Internal Scholarly Research Network, (2012): 1.
73. M.E. Weeks. The discovery of the elements. III. Some eighteenth-century metals. Journal of chemical education, 9.1 (1932) 22.
74. B.R.W. Hinton and L. Wilson, The corrosion inhibition of zinc with cerous chloride, Corrosion Science, 29.8 (1989): 967 – 985.
75. C.O. Beale, Copper in South Africa-part 1, Journal of the Southern African Institute of Mining and Metallurgy, 85.3 (1985): 73 – 80.

76. C. Leygraf, I Odnevall Wallinder, J. Tidblad and T. Graedel, Atmospheric Corrosion, 2nd Ed. John Wiley & Sons: Hoboken, NJ, USA, (2016): 1 – 374.
77. T.E. Graedel, J.P. Franey, R. Baboian, B.I. Bellante, E.B. Cliver The Statue of Liberty Restoration, Eds.; NACE: Houston, TX, USA, (1990).
78. T.E. Graedel, K. Nassau and J.P. Franey, Copper patinas formed in the atmosphere—I. Introduction, Corrosion Science, 27.7 (1987): 639 – 657.
79. K.P. Fitzgerald, J. Nairn and A. Atrens, The chemistry of copper patination. Corrosion Science, 40.12 (1998): 2029 – 2050.
80. K.P. Fitzgerald, J. Nairn, G. Skennerton and A. Atrens, Atmospheric corrosion of copper and the colour, structure and composition of natural patinas on copper, Corrosion Science, 48.9 (2006): 2480 – 2509.
81. T. Chang, I. Odnevall Wallinder,D. de la Fuente, B. Chico, M. Morcillo, J.M. Welter and C. Leygraf, Analysis of Historic Copper Patinas. Influence of Inclusions on Patina Uniformity, Materials 10.3 (2017): 298.
82. M. Morcillo, T. Chang, B. Chico, D. de la Fuente, I. Odnevall Wallinder, J.A. Jiménez and C. Leygraf, Characterisation of a centuries-old patinated copper roof tile from Queen Anne's Summer Palace in Prague, Materials Characterization, 133 (2017): 146 – 155.
83. I.O. Wallinder, T. Korpinen, R. Sundberg, C. Leygraf, Atmospheric corrosion of naturally and pre-patinated copper roofs in Singapore and Stockholm—Runoff rates and corrosion product formation. Outdoor atmospheric corrosion. Townsend, H.E., Ed. ASTM International, (2002): 230 – 244.
84. P. Lopesino, J Alcanta, D. de la Fuente, B. Chico, J.A. Jimenez and M. Murcilo, Corrosion of copper in unpolluted chloride-rich atmosphere, national centre for metallurgical research, Metals, 8.11 (2018): 1 – 866.
85. E. Mattsson and R. Holm, Copper and Copper alloys. In ASTM STP 435; ASTM International: West Conshohocken, PA, USA, (1968:) 187–210.
86. D.W. Rice, P. Peterson, E.B. Rigby, P.B.P. Phipps, R.J. Cappell and R. Tremoureux, Atmospheric Corrosion of Copper and Silver, Journal of the Electrochemical Society, 128.2 (1981): 275 – 284.
87. O. Kubaschewski and B.E. Hopkins, Oxidation of Metals and Alloys; Butterworths Scientific Publications: London, UK, (1953): 3 – 12.
88. T.E. Graedel, Copper patinas formed in the atmosphere—II. A qualitative assessment of mechanisms, Corrosion Science, 27.7 (1987): 721 – 740.

89. L. Veleva, P. Quintana, R. Ramanauskas, R. Pomes, L. Maldonado, Mechanism of copper patina formation in marine environments, Electrochimica Acta, 41.10 (1996): 1641 – 1645.
90. S.H. Suh, Y. Suh, H.G. Yoon, J.H Oh, Y. Kim, K. Jung, H. Kwon, Analysis of pitting corrosion failure of copper tubes in an apartment fire prinkler system, engineering failure analysis: Engineering Failure Analysis, 64 (2016): 111 – 125.
91. W. D. Callister, Material Science and Engineering and Introduction, John Willy and sons Inc. 4th Ed, (1997): 550 – 554.
92. E.C. Chinwko, B.O. Odio, J.L. Chukwuneke and J.E. Sinebe, Investigation of the effects of corrosion on mild steel in five different environments, International Journal of Scientific and Technology Research, 3.7 (2014): 306 – 310.
93. D. Brondel, R. Edwards, A. Hayman, F. Clamart, D. Hill, S. Mehta and T. Semerad, Corrosion in the oil industry. Oilfield Review, 6.2 (1994): 4 – 18.
94. M.M. Stack, Mapping tribo-corrosion processes: some new directions for the new millennium, Tribology International, 35.10 (2002): 681 – 689.
95. D. Yang, Corrosion inhibition performance of imidazolium ionic liquids and their influence on surface ferrous carbonate layer formation. Doctoral dissertation, The graduate faculty of the university of Akron, (2016): 1 – 23.
96. Zavenir-bolg, Different method of corrosion prevention method, February 23,2018.
97. B. Donnelly, T.C. Downie, R. Grzeskowiak, H.R. Hamburg and D. Short. A study of the inhibiting properties of some derivatives of thiourea, Corrosion Science, 14.10 (1974): 109 – 606.
98. B.G. Clubley, Chemical inhibitors for corrosion control: the proceedings of an international symposium, 2nd Ed. Royal Society of Chemistry and the institution of corrosion science and technology, University of Manchester (1998): 12 – 122.
99. K. L. Vasanth. Corrosion inhibition in naval vessels. CORROSION/96, paper 233 (1996).
100. S.A. Umoren, U.F. Ekane, Inhibition of mild steel corrosion in H_2SO_4 using exudate gum from Pachylobus Edulis and synergistic potassium halides additives. Chemical Engineering Communications, 197.10 (2010): 1339 – 1356.
101. R.W. Revie and H.H. Uhlig, Corrosion handbook, New York: John Wiley and Sons. (2000): 320 – 533.
102. R.W. Revie, ed. Uhlig's corrosion handbook (Vol. 57). John Wiley & Sons (2011): 1022 – 1089.

103. S.A. Yaro, A.A. Khadom, K.R. Wael, Apricot juice as green corrosion inhibitor of mild steel in phosphoric acid, Alexandria Engineering Journal, 52.1 (2013): 129 – 135.

104. V. Gentil. Corrosão. edição-Rio de Janeiro. RJ-LTC-Livros técnicos e. (1996).

105. N.M. El-Haddad, Chitosan as a green inhibitor for copper corrosion in acidic medium, International Journal of Biological Macromolecules, 55 (2013): 142 – 149.

106. B. Sanyal, Organic compounds as corrosion inhibitors in different environments A review, Progress in Organic Coatings, 9.2 (1981): 165 – 236.

107. T.A Söylev, and M.G. Richardson, Corrosion inhibitors for steel in concrete: State-of-the-art report. Construction and Building Materials, 22.4 (2008): 609 – 622.

108. L.C. Murulana, M.M. Kabanda and E.E. Ebenso, Experimental and theoretical studies on the corrosion inhibition of mild steel by some sulphonamides in aqueous HCl. Royal Society of Chemistry Advances, 5 (2015): 28743 – 28761.

109. A. Chokshi, Kunal. Study of Inhibitor-Scale Interaction in Carbon dioxide Corrosion of Mild Steel, Doctoral dissertation, Ohio University, (2004): 22

110. N. Nontete Suzan. TGA-FTIR study of the vapours released by volatile corrosion inhibitor model systems, Doctoral dissertation, University of Pretoria, (2013): 1.

111. I.L. Rosenfeld, B. P. Persiantseva, and P. B. Terentiev. "Mechanism of metal protection by volatile inhibitors." Corrosion, 20.7 (1964): 222 – 234.

112. P.K. Agrawal, Carbon-13NMR of flavonoids. Elseiver science publishers, Amsterdam, (1989): 2 – 5.

113. M.A. Al-Qudah, Inhibition of copper corrosion by flavonoids in nitric acid. Department of chemistry faculty of science Yamouk University, Irbid 21163, Journal of Chemistry, 8.1 (2011): 326-332.

114. A.N. Panche, A.D. Diwan and S.R. Chandra, Flavonoids: An overview, Journal of Nutritional Science, 5 (2016): 47.

115. S.P Rusznyák, St, and A. Szent-Gyorgyi. Vitamin P: flavonols as vitamins. Nature, 27 (1936) 138.

116. J.A. Ross, and C.M. Kasum. Dietary flavonoids: bioavailability, metabolic effects, and safety, Annual Review of Nutrition, 22.1 (2002), 19 – 34.

117. A. I. Ikeuba, B. I. Ita, R.A. Etiuma, V.M. Bassey, B. U. Ugi and E. B. Kporokpo, Green Corrosion Inhibitors for mild steel in H_2SO_4 Solution: Flavonoids of Gongronema latifolium, Corrosion and Electrochemistry Research Group Department of Pure and Applied Chemistry, University of Calabar, Calabar, Chemical and Process Engineering Research, 34 (2015): 1 – 10.

118. N.C. Michael, and J.A. Olubunmi. The corrosion inhibition of mild steel in sulphuric acid solution by flavonoid (catechin) separated from Nypa fruticans Wurmb leaves extract. Science Journal of Chemistry, 2(4), (2014) 27-32.
119. M. Gopiraman, C. Sathya, S. Vivekananthan, D. Kesavan, and N. Sulochana, Influence of 2,3-Dihydroxyflavanone on Corrosion Inhibition of Mild Steel in Acidic Medium, Journal of Materials Engineering and Performance, 21.2 (2012): 240 – 246.
120. G. James, Speight in environmental inorganic chemistry for engineers, Industrial Inorganic Chemistry, (2017): 140.
121. C. Sharma, S. Bhattacharya, Emissions of Reactive Nitrogen from Energy and Industry Sectors in India. The Indian Nitrogen Assessment, Elsevier, (2017): 483 – 488.
122. D.A. Skoog, D.M. West and F.A. Holler. *Fundamentals of analytical chemistry*. Nelson Education, 2013.
123. G. Scrates, Infrared characteristic group frequencies, Chichester: willey, 2. J. Coates, Interpretation of infrared spectra, A practical approach. In: Meyers, R.A. (Ed.). Encylopedia of analytical chemistry, Chichester; Willey, (2000): 10815 – 10837.
124. H. Uhlig, Corrosion Handbook, New York: Wiley Publications (1948): 527 – 528.
125. B. I. Ita and O. E. Offiong. The study of the inhibitory properties of benzoin, benzil, benzoin-(4-phenylthiosemicarbazone) and benzil-(4-phenylthiosemicarbazone) on the corrosion of mild steel in hydrochloric acid. Materials chemistry and physics, 70. 3 (2001): 330 – 335.
126. M.A. Quraishi, V. Bharadwaj and D. Jamal. Inhibition of corrosion of mild steel in well water by phenolic compounds Materials Chemistry and Physics, 77 (2003): 665.
127. H.L. Wang, H.B. Fan and H.S. Zheng. Recent advances in Camellia oleifera Abel: A review of nutritional constituents, biofunctional properties, and potential industrial applications. Bulletin of Electrochemistry, 19 (2003): 295.
128. F. Blin, S.G Leary, K. Wilson, G.B. Deacon, P.C. Junk and M. Forsyth. Corrosion mitigation of mild steel by new rare earth cinnamate compounds, Journal of Applied Electrochemistry, 34.6 (2004): 591 – 599.
129. K. Tebbji, H. Oudda, B. Hammouti, M. Benkaddour, M. Elkodadi, F. Malek and A. Ramdani, Inhibitive action of two bipyrazolic isomers towards corrosion of steel in 1 M HCl solution. Applied Surface Science, 241.3-4 (2005): 326 – 334.
130. B. Fernandez, L. Labo and R. Pereiro, Atomic adsorption spectrometry/ fundamental, instrumentation and capabilities, Encyclopedia of analytical science 3rd Ed: Elseivier, (2019): 137 – 143.

131. M. Sperling. Flame and graphite furnace atomic absorption spectrometry in environmental analysis. Encyclopedia of Analytical Chemistry: Applications, Theory and Instrumentation (2006).

132. A. l. Onen. Kinetic studies of selected corrosion inhibitors of aluminium and mild steel in acid medium. Doctoral Dissertation. University of Jos. (2010) 79.

133. I.B. Obot, and N.O. Obi-Egbedi. "Fluconazole as an inhibitor for aluminium corrosion in 0.1 M HCl." Colloids and Surfaces A: Physicochemical and Engineering Aspects 330.2-3 (2008): 207 – 212.

134. N.A. Negm, and M.F. Zaki. Corrosion inhibition efficiency of nonionic Schiff base amphiphiles of p-aminobenzoic acid for aluminum in 4N HCL. Colloids and Surfaces A: Physicochemical and Engineering Aspects 322.1-3 (2008): 97 – 102.

135. M.N. Al-Qasmi. Natural products as corrosion inhibitors of some metals in aqueous media. A Thesis, Umm Al-Qura University, Faculty of Applied Science for Girls, Chemistry Department. (2010) 70.

136. D.U.Omoduda and N.C.Oforka**.** Evaluation of sulphanoamides as corrosion inhibitors. Journal of Physics, 2, 148. (1999).

137. A. Zarrouk, B. Hamouti, H. Zrrouk, S.S. Al-Deyab, M. Messail. Temperature effect, activation energies and thermodynamic adsorption studies of L-cysteine methyl ester hydrochloride as copper corrosion inhibitor in nitric acid 2M." International Journal of. Electrochemistry. Sci 6.12 (2011): 6261 – 6274.

138. E.E. Gomes. Green inhibition of mild steel corrosion in a CO2 saturated saline solution. Doctoral Dissertation. American University of Sharjah. 2015.

139. S. Alpha, Studies of hydroxytriazenes as corrosion inhibitors for mild steel, Doctoral dissertation, Mohanaal Sukhadia University. (2016) 126 – 145.

140. M. Elachouri, M.S. Hajji, M. Salem, S. Kertit, J. Aride, R. Coudert,E. Essassi, Inhibition of pitting corrosion by surfactants as a function of temperature Corrosion. 52 (1996).

141. H.K. Dhaif, E. Q. Jasim, Z. A. Muhajjar, and A. Shanta. Corrosion Inhibition of Mild-Steel in 0.5 M HCl using some prepared 1, 2, 3-Triazoles Derivatives. Mediterranean Journal of Chemistry 9.4 (2019): 290 – 304.

142. F.M. Donahue and K. Nobe. Theory of organic corrosion inhibitors: adsorption and linear free energy relationships. Journal of the Electrochemical Society 112.9 (1965): 886.

143. E. Khamis, F. Bellucci, R.M. Latanision and E.S.H. El-Ashry. Acid corrosion inhibition of nickel by 2-(triphenosphoranylidene) succinic anhydride. Corrosion 47.9 (1991): 677 – 686.

144. A.J.A., Nasser and M.A., Sathiq. Comparative study of N-[(4-methoxyphenyl)(morpholin-4-yl) methyl] acetamide (MMPA) and N-[morpholin-4-yl (phenyl) methyl] acetamide (MPA) as corrosion inhibitors for mild steel in sulfuric acid solution." Arabian Journal of Chemistry 10 (2017): S261 – S273.

145. X. Li, S. Deng, H. Fu and G. Mu, G. Inhibition effect of 6-benzylaminopurine on the corrosion of cold rolled steel in H2SO4 solution. Corrosion Science 51.3 (2009): 620 – 634.

146. I.L. Rosenfeld, Corrosion Inhibitors, Chimia, Moscow, 1977. Page 13

147. Z.A. Foroulis, in: Proceedings of the sixth European Symposium on Corrosion Inhibitors, Ferrara, Annali dell' Università di Ferrara, 1985, p. 48 – 130.

148. A. Popova, E. Sokolova, S. Raicheva, and M. Christov. AC and DC study of the temperature effect on mild steel corrosion in acid media in the presence of benzimidazole derivatives. Corrosion science 45.1 (2003): 33 – 58.

149. G.N. Mu, X. Li, and F. Li. Synergistic inhibition between o-phenanthroline and chloride ion on cold rolled steel corrosion in phosphoric acid. Materials Chemistry and Physics 86.1 (2004): 59 – 68.

150. E.A. Noor. Temperature effects on the corrosion inhibition of mild steel in acidic solutions by aqueous extract of fenugreek leaves. International Journal of Electrochemical Science 2.12 (2007).

151. A. Zarrouk, B. Hammouti, T. Lakhlifi, M. Traisnel, H. Vezin, and F Bentiss. New 1H-pyrrole-2, 5-dione derivatives as efficient organic inhibitors of carbon steel corrosion in hydrochloric acid medium: electrochemical, XPS and DFT studies.Corrosion Science 90 (2015): 572 – 584.

152. M. Bouklah, B. Hammouti, M. Lagrenee, and F. Bentis. Thermodynamic properties of 2, 5-bis (4-methoxyphenyl)-1, 3, 4-oxadiazole as a corrosion inhibitor for mild steel in normal sulfuric acid medium. Corrosion science 48.9 (2006): 2831 – 2842.

153. X. Li, L. Tang, L. Li, G. Mu, and G. Liu. Synergistic inhibition between o-phenanthroline and chloride ion for steel corrosion in sulphuric acid. Corrosion science 48.2 (2006): 308 – 321.

154. Q. Wu, F. Merchant, and K. Castleman, eds. Microscope image processing, Elseiver. (2010).

155. U. Carragher. An Electrochemical Investigation into the Corrosion Protection Properties of Coatings for the Active Metal Copper. Diss. National University of Ireland Maynooth, 2013, Page 126

156. R. Catubig. Investigation of corrosion inhibition mechanisms of rare-earth mercaptoacetate inhibitors on AA2024-T3. No. Ph. Dissertation. Deakin University, 2014. Page 59.

157. H.M. Abd El-Lateef, Z. A. Abdallah, and M. S. M. Ahmed. Solvent-free synthesis and corrosion inhibition performance of Ethyl 2-(1, 2, 3, 6-tetrahydro-6-oxo-2-thioxopyrimidin-4-yl) ethanoate on carbon steel in pickling acids: Experimental, quantum chemical and Monte Carlo simulation studies. Journal of Molecular Liquids 296 (2019): 111800.
158. A.R. Sayed, M.M. Saleh, M.A. Al-Omair and H.M. Abd Al-Lateef. Efficient route synthesis of new polythiazoles and their inhibition characteristics of mild steel corrosion in acidic chloride medium, Journal of molecular Structure 1184 (2019) 452 – 461.
159. H. Lgaz, K.S. Bhat, R. Salghi, S. Jodeh, M. Algarra, B. Hammouti, and A Essamri. Insights into corrosion inhibition behavior of three chalcone derivatives for mild steel in hydrochloric acid solution. Journal of Molecular Liquids, 238, (2017) 71 – 83.
160. M. Mahdavian, and R. Naderi. Corrosion inhibition of mild steel in sodium chloride solution by some zinc complexes. Corrosion Science, 53(4), (2011): 1194 – 1200.
161. O. G. Mofu. Corrosion inhibition of mild steel in 1 M HCl using synthesized eco-friendly polymer composites. MSc Dissertation. University of Johannesburg. 2017.
162. T. Nesane. Corrosion inhibition exploration of synthesized carboxylic acid and amino esters on selected metals in acid medium. MSc Dissertation. University of Venda. 2020.